Stochastic and deterministic kinetic equations in the context of mathematics applied to biology

Nils Caillerie

Institut Camille Jordan
UMR 5208 du CNRS

Équations cinétiques stochastiques et déterministes dans le contexte des mathématiques appliquées à la biologie

Nils Caillerie

Thèse de doctorat

Université Claude Bernard Lyon 1

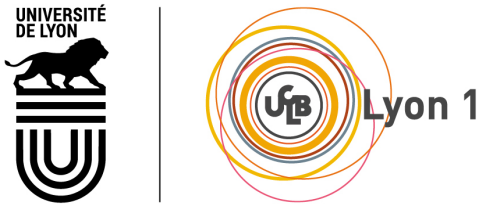

N° d'ordre NNT : 2017LYSE1117

THÈSE DE DOCTORAT DE L'UNIVERSITÉ DE LYON
opérée au sein de
l'Université Claude Bernard Lyon 1

École Doctorale ED512
Infomaths

Discipline : Mathématiques

Soutenue publiquement le 5 juillet 2017, par :
Nils Caillerie

Équations cinétiques stochastiques et déterministes dans le contexte des mathématiques appliquées à la biologie

---

Devant le jury composé de :

Nicolas Champagnat, Chargé de recherches INRIA, INRIA Nancy Grand-Est	Rapporteur
Jérôme Coville, Chargé de recherches INRA, INRA Avignon	Rapporteur
Sylvie Benzoni-Gavage, Professeure, Université Lyon 1	Examinatrice
Anne de Bouard, Directrice de recherches CNRS, École Polytechnique	Examinatrice
Sepideh Mirrahimi, Chargée de recherches CNRS, Université Toulouse III	Examinatrice
Élisabeth Mironescu, Professeure, École Centrale de Lyon	Examinatrice
Vincent Calvez, Directeur de recherches CNRS, Université Lyon 1	Directeur de thèse
Julien Vovelle, Chargé de recherches CNRS, Université Lyon 1 (Invité)	Directeur de thèse

Mis en page avec la classe thesul.

Remerciements

Rédiger une thèse est un exercice troublant pour la personnalité. À force de se nommer soi-même "Nous", "on" ou encore "l'auteur", on finirait par en oublier que l'auteur en question, c'est moi. Avant de me conformer à l'usage de la première personne du pluriel, j'aimerais utiliser le "je" afin de remercier toutes les personnes qui m'ont accompagné au cours de ces trois riches années.

Pour commencer, j'aimerais remercier les membres de mon jury pour avoir accepté de juger mon travail. Je remercie mes rapporteurs MM. Champagnat et Coville pour avoir accepté ce rôle et pour avoir relu mon travail avec attention. Cette nouvelle version a tenu compte du mieux possible de leurs éventuelles remarques.

Je tenais aussi à remercier mes deux directeurs de thèse, Julien et Vincent. S'il me fallait qualifier Julien par un seul mot, je choisirais celui-ci : "positif". Julien a toujours été disponible et souriant avec moi. Lorsque je lui apportais le compte-rendu de mon travail, il préférait toujours aborder les aspect positifs en premier, avant d'émettre des critiques constructives sur les erreurs et les imprécisions. Je considère que c'est une qualité très rare et je le remercie pour cela. J'ai eu également beaucoup de chance de rencontrer Vincent à mon arrivée à Lyon, alors que je ne connaissais presque personne. Son cours de Master est celui qui m'a motivé à poursuivre en thèse et à m'intéresser aux maths-bio, et je lui en suis éternellement reconnaissant.

Au début de cette aventure, Christelle était ma petite amie. Au cours de la thèse, elle est tout à tour devenue ma partenaire de PACS, ma fiancée, puis mon épouse. Merci à elle de m'avoir accompagné et d'avoir su supporter ma mauvaise humeur lorsque je rencontrais un lemme qui ne voulait pas se laisser démontrer !

J'adresse également ma plus grande sympathie et ma tristesse à l'idée de quitter (momentanément, j'espère) les membres du "club du traquenard" : Colin, Tanya, Maxime et Maxime. Je sais gré à Colin de m'avoir toujours donné ses conseils avisés en matière de relooking et de coupe de cheveux. Je remercie Tanya pour sa bonne humeur et son énergie constante, du bureau jusqu'aux confins du Canada. De Maxime et Maxime, je dirais que l'un est très intelligent et que l'autre est très sympathique. J'espère que nous aurons de nouveau l'occasion, un soir, de laisser filer le temps autour d'un apéro qui s'éternise, quite à le regretter le lendemain...

Mes pensées vont aussi à Emeric qui m'a proposé de travailler avec lui et qui m'a permis de découvrir la ville de Cambridge. Merci à lui pour ses conseils et sa disponibilité. Merci également à Samuel pour avoir mis à ma disposition ses connaissances et ses algorithmes de statistiques. Merci enfin à Serge pour le temps qu'il m'a consacré en fin de première année. En espérant que nos collaborations continuent à l'avenir, je les salue.

Je remercie également les membres du comité d'organisation d'Inter'Actions16 avec qui j'ai vécu d'intenses moments... d'organisation : Coline, Álvaro, Lucie, Mohamed et Nacho.

Je salue chaleureusement toutes les personnes qui ont partagé l'un de mes innombrables bureaux, à l'ENS, à l'ICJ ou bien au sous-sol du bâtiment Braconnier : Xiaolin, Maxime, Samuel, Anass, Mélina, Mélina, Ignacio, Benoît, Qiong Qiong, Bin, Jean-Cyrille, Vagelis, Mélanie, Clément... Je remercie aussi tous les doctorants et les doctorantes de l'ICJ qui ont supporté mes passages intempestifs dans leur bureau, à la recherche d'un(e) exposant(e) pour le séminaire : Hugo, Ariane, Simon, Gwladys, Benjamin, Jian, Simon, Mathias, Marion, Luigia, Michele, Quentin, Antoine, Yannick, Agathe, François, encore un Simon, François et les autres...

Merci à Aurélie, Céline et Laurent à l'ICJ et à Magalie, Sandy et Virginia à l'ENS pour leur disponibilité.

Je voudrais remercier aussi les membres de mes deux clubs de foot. À l'ENS : Loïc, Samuel, Alexandre, Bastien, Emmanuel, Nathalie, Chris, Bruno, Pedro, Florian. À l'ICJ : Cap'tain Léon, Vincent, Francesco, Arnaud, Frédéric...

Je salue tous ceux qui, à Lyon, sont responsables de la communication des mathématiques et grâce à qui j'ai pu parfaire mon CV de vulgarisateur : l'équipe MathαLyon, notamment Thomas et Régis, l'équipe du séminaire de la détente mathématique Marie, Olga et Valentin et enfin, Eric Leroux pour avoir tiré le portrait de ma thèse.

Plus personnellement, je remercie ma famille, Papa, Maman, Isabelle, Christine et Florence pour m'avoir soutenu tout au long de ces années.

Cette liste ne saurait être exhaustive et il est statistiquement impossible que parmi toutes les personnes qui m'ont aidé au cours de ma thèse, je n'en oublie pas une poignée au passage. Si c'est le cas, je saurai leur exprimer ma gratitude par un autre moyen.

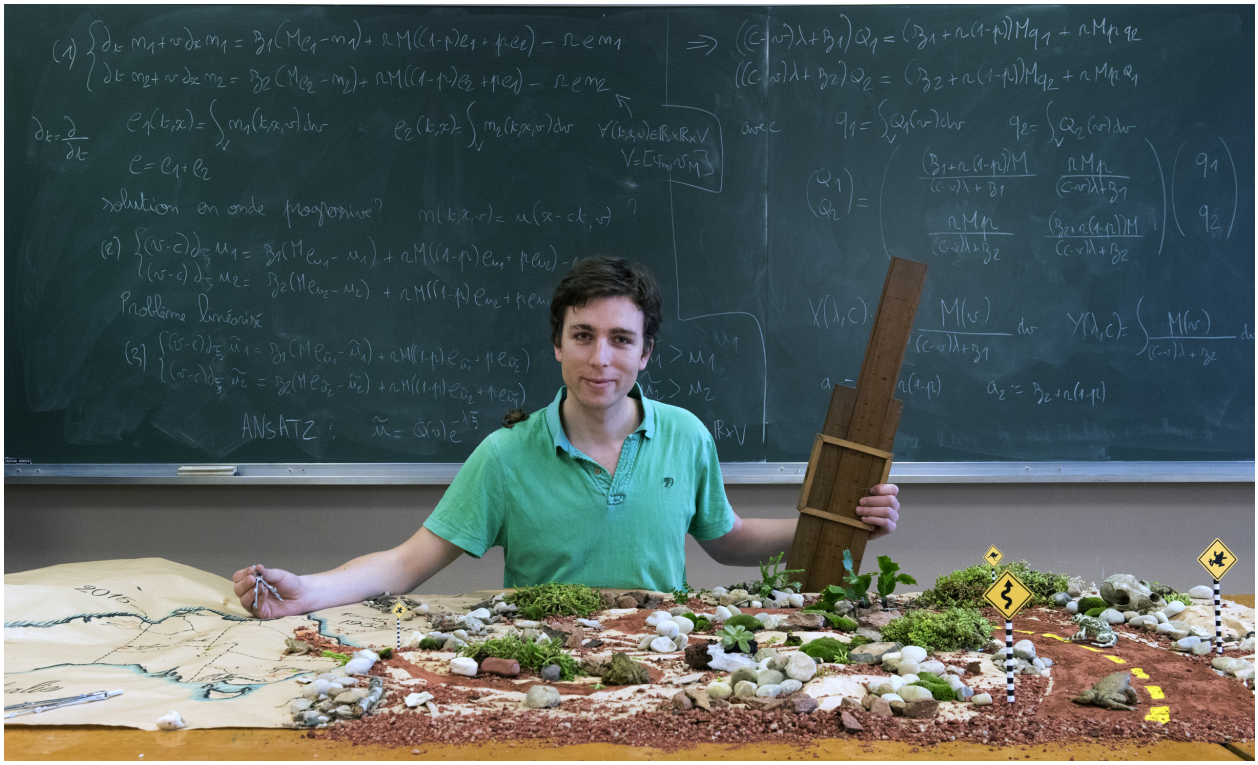

Crédits photo : Eric Le Roux, Alexandre Watson *These's art*

Je dédicace cette thèse à tous mes "Papas" et "Mamans" mathématiques, tous ces professeurs qui m'ont donné, tour à tour, l'envie de faire des mathématiques ma profession :
À mon vrai Papa, donc, qui m'aura aidé à faire mes devoirs de maths du CP jusqu'au doctorat,
À Vincent Obaton, qui m'a donné pour la première fois l'envie de faire des maths,
À Eric Labeye-Voisin qui m'a appris que la créativité en maths ne saurait se passer de rigueur,
À Catherine Labeye-Voisin, pour son grand dévouement lorsque je passais l'agrégation et enfin,
À Vincent Calvez et Julien Vovelle pour avoir été, tout au long de ces trois années, bien plus que des directeurs de thèse.
Sans vous, cette thèse n'existerait probablement pas.

Sommaire

Introduction

1 Motivations et cadre de la thèse

Cette thèse est une contribution aux domaines des mathématiques et de la biologie. Du point de vue mathématique, les travaux présentés proposent l'étude de phénomènes de propagation dans des modèles mathématiques de dynamique spatiale inspirés par la biologie. Du point de vue de la biologie, les travaux présentés proposent une modélisation mathématique de la propagation d'une espèce invasive de crapauds (*Rhinella marina*) en Australie, s'appuyant sur des données recueillies par des biologistes australiens.

Deux motivations principales sont à l'origine d'une telle étude. La première concerne la préservation de la biodiversité en Australie ; la seconde concerne la validation d'hypothèses théoriques formulées par les biologistes pour expliquer l'accélération du front de propagation chez certaines espèces invasives. Nous détaillons ces deux motivations ci-après.

1.1 L'invasion du crapaud buffle

Le crapaud buffle a été introduit en Australie dans les années 1930 dans l'État du Queensland en Australie pour lutter contre un parasite de la canne à sucre. Non seulement le crapaud n'a pas vraiment rempli sa mission, mais depuis, le problème du parasite a été réglé et le crapaud, quant à lui, a commencé à envahir l'Australie en suivant la côte est. Nous renvoyons à [110] et aux Figures 1 et 3 à l'intérieur (que nous reproduisons ici en Figure 1) pour plus de détails sur cette propagation.

La propagation de cette espèce est très suivie par les biologistes car le crapaud met en danger la biodiversité locale. En effet, il constitue un prédateur pour de nombreux insectes et rongeurs mais il a en revanche peu de prédateurs à cause de sa forte toxicité. Son invasion est d'autant plus préoccupante qu'elle est en constante accélération depuis plusieurs années, comme le montre bien la Figure 1.

Une telle accélération du front a déjà été observée chez d'autres espèces, comme les papillons, les mouches et les criquets [74, 101, 106], mais aussi dans la propagation de tumeurs [88].

Parmi les hypothèses proposées par les biologistes, l'une d'entre elles a retenu l'attention de la communauté math-bio : celle d'un "processus d'évolution qui concentre les phénotypes spatialement plutôt que temporellement" [102].

FIGURE 1 – **Propagation du crapaud buffle en Australie depuis les années 30**

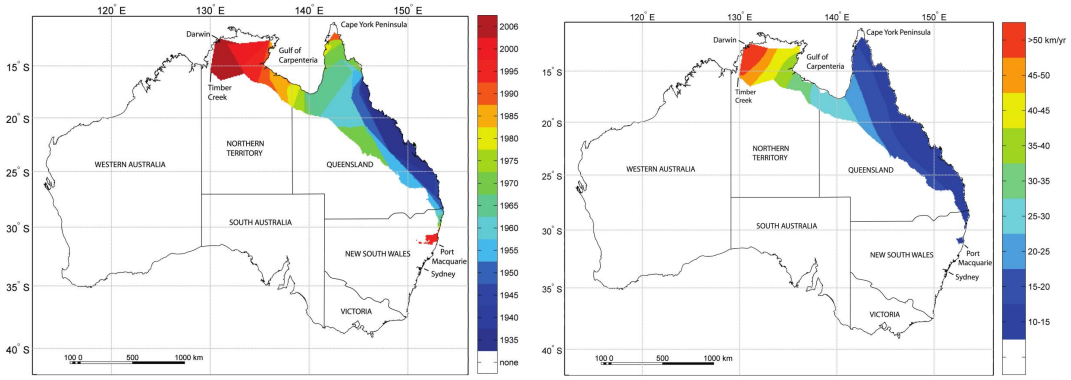

Première carte : propagation du crapaud buffle en fonction du temps. Le crapaud était par exemple présent dans toute la zone colorée en 2006. En revanche, il n'était pas présent dans la zone rouge brique lors de l'année 2000.
Seconde carte : vitesse d'expansion du crapaud buffle en fonction de sa position. Lorsqu'elle a démarré depuis le Queensland, la colonie de crapauds se propageait à une vitesse comprise entre 10 et 15 kilomètres par an. Lorsqu'elle a atteint la ville de Darwin, cette vitesse était supérieure à 50 kilomètres par an.
Source : [110] M. Urban, B. Phillips, D. Skelly, and R. Shine (2008). A toad more traveled : the heterogeneous invasion dynamics of cane toads in Australia. The American Naturalist.

1.2 Évolution darwinienne *versus* Tri spatial

L'évolution darwinienne : un processus d'évolution qui concentre les phénotypes temporellement

Nous présentons ici ce que nous entendons par "un processus d'évolution qui concentre les phénotypes temporellement", c'est à dire la théorie introduite par Darwin [48]. En aucun cas, nous ne souhaitons exposer complètement cette théorie, ni être exhaustif dans la présentation de ses exemples ; nous la présentons brièvement pour mieux comprendre ce qui la différencie de l'hypothèse du tri spatial.

Pour commencer, il convient de préciser ce que nous entendons par phénotype. Il s'agit de l'ensemble des caractères observables d'un individu donné, qu'ils soient macroscopiques (tailles des membres, couleur du pelage...), microscopiques (flore intestinale, code sanguin...) ou comportementaux (sociabilité, mode de reproduction...).

La théorie darwinienne propose une explication au phénomène de sélection naturelle qui repose sur trois principes :

1. Plusieurs phénotypes sont présents au sein d'une même espèce
2. Les phénotypes sont transmis d'une génération à l'autre
3. Lors de cette transmission, une modification aléatoire du phénotype peut avoir lieu

Dans le cas d'une espèce à reproduction sexuée par exemple, un nouveau-né reçoit la moitié du matériel génétique de son père et la moitié du matériel génétique de sa mère. Au cours de ce processus, un nouveau phénotype peut apparaître par association des deux codes

FIGURE 2 – **La phalène du bouleau**

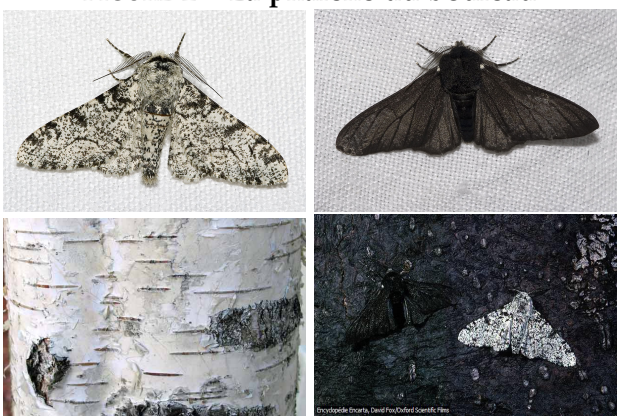

En haut : phalène du bouleau de couleurs blanche et noire.
En bas à gauche : écorce de bouleau blanche, à droite : deux phalènes sur un tronc d'arbre de couleur noire.
Sources : Wikipedia et Encyclopédie Encarta.

génétiques des parents (métissage) ou par des erreurs lors de la transmission de l'ADN d'un des parents aux gamètes (spermatozoïde ou ovule).

La théorie de Darwin prédit *la survie du plus adapté*. Dans un environnement donné, si un phénotype présente un avantage significatif par rapport aux autres, l'ensemble des phénotypes présents au sein de la population va se concentrer au fil des générations autour du phénotype le mieux adapté.

Depuis l'exposition de cette théorie, une très grande quantité d'exemples est venue corroborer cette hypothèse. Nous présentons un cas d'école : la phallène du bouleau [108], qui est une espèce de papillons. Nous tenons à faire remarquer avant d'expliquer cet exemple, que des critiques ont été adressées à juste titre sur l'apparente simplicité des mécanismes évolutifs mis en jeu. Nous nous contenterons ici de présenter une version très simple, malgré ses imprécisions.

En 1896, James Tutt observe que la majorité des phalènes de la région de Manchester est de couleur noire, alors que le premier spécimen de couleur noire a été observé en 1848. Il fait alors l'hypothèse que l'environnement industriel de la région de Manchester, en particulier la haute teneur en suie qui noircit l'écorce des bouleaux, est responsable de cette évolution. En 1955, Bernard Kettlewell valide expérimentalement cette hypothèse. L'explication est que le phénotype "être de couleur noire" offre un avantage sélectif puisqu'il permet à la phalène de mieux se camoufler contre les bouleaux et donc d'échapper aux oiseaux qui la chassent. Puisque les phalènes blanches sont facilement repérables par leurs prédateurs, elles s'éteignent très vite. À l'inverse, dans des zones moins industralisées où les bouleaux conservent leur couleur blanche naturelle, les phalènes sont majoritairement blanches.

FIGURE 3 – **Modèle simpliste d'évolution darwinienne**

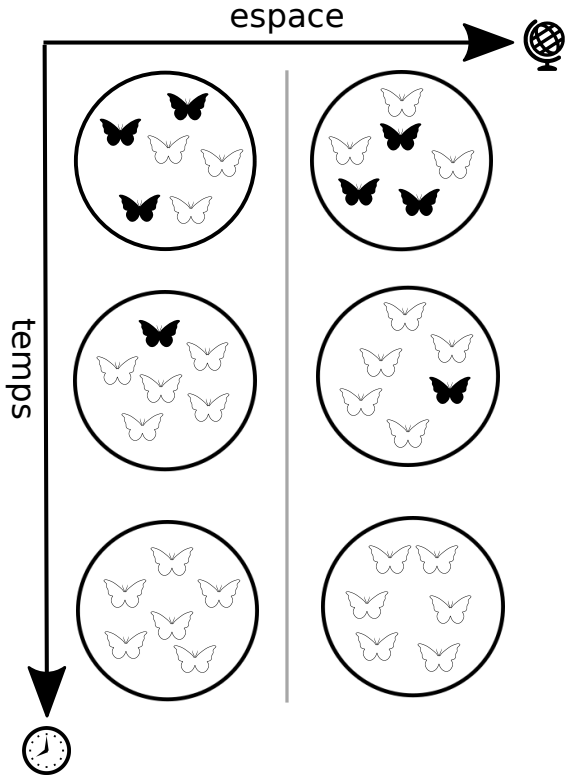

Le processus d'évolution darwinienne est un processus qui concentre les phénotypes dans le temps. À qualité d'environnement égale, l'espace n'a pas d'influence sur la répartition des phénotypes. Ici, nous supposons que le phénotype "être de couleur blanche" est le plus avantageux.

Cet exemple nous permet de caricaturer grossièrement la théorie de Darwin comme un processus évolutif qui concentre les phénotypes temporellement. En effet, on peut se représenter ce phénomène comme suit. Supposons qu'on libère, dans une zone avec des bouleaux blancs, une colonie de phalènes composée pour moitié d'individus blancs et pour moitié d'individus noirs. On ne change jamais d'emplacement et on note à différents temps la proportion des phalènes. On observera alors une augmentation de la population blanche. Supposons qu'une autre personne ait conduit la même expérience à une centaine de kilomètres de notre emplacement, mais dans un environnement où les bouleaux sont également de couleur blanche. Alors, ses résultats seront identiques. Ainsi, ce n'est pas en se déplaçant d'un site à l'autre qu'on observera une proportion différente de phallènes, mais en en restant immobile et en laissant le temps s'écouler. Le phenomène de concentration autour du pénotype "être de couleur blanche" est donc temporel.

Nous donnons une illustrations graphique de ce phénomène de concentration temporelle en Figure 3.

L'hypothèse du tri spatial

Nous reprenons ici des idées contenues dans [102]. Imaginons une population envahissant un nouvel environnement. On suppose que chaque individu a un phénotype différent ayant une influence sur ses déplacements. On peut par exemple penser à des différences morphologiques (comme la taille des pieds [63] ou des pattes [93]), physiologique (comme l'endurance [84]), mais aussi comportementales (comme le mode de déplacement utilisé : nombre de pauses, forme des trajectoires etc. [2, 33]).

Lorsque cette population va se propager dans son environnement, un tri spatial évident va avoir lieu : les plus véloces (que ce soit morphologiquement, physiologiquement ou comportementalement) seront à l'avant du front de propagation, les moins véloces derrière. Si l'on laisse la population se propager suffisamment longtemps, le tri sera d'autant plus clair. Au moment de se reproduire, les individus seront donc déjà triés en fonction de leur phénotype de dispersion. La génération suivante héritera du phénotype de dispersion de la génération en cours. Cependant, avec des aléas dans la transmission des phénotypes, les individus nés à l'avant du front pourront éventuellement bénéficier des meilleurs gènes, en laissant de côté les moins bons gènes. Si une telle "amélioration" a lieu, cela a alors pour effet d'accélérer la propagation du front, puisqu'elle est portée à présent par des individus plus dispersifs qu'à la génération précédente. Cela a également pour effet de perpétuer le tri spatial, et donc d'entretenir encore plus le phénomène.

Nous illustrons cette hypothèse avec une analogie que nous empruntons à [102]. Imaginons une course de bateaux un peu spéciale. Il s'agit d'une course en ligne où chaque équipage est composé de huit matelots. Chaque matelot est, soit un matelot aguerri, soit un matelot débutant. Au départ de la course, chaque bateau est rempli par un équipage dont la répartition entre matelots aguerris et débutants est aléatoire (cf Figure 4).

Pour simplifier, nous supposons que la vitesse des bateaux est directement proportionnelle aux nombres de matelots aguerris qui compose son équipage. Ainsi, un bateau avec n matelots aguerris navigue à la vitesse nautique de n noeuds.

Au bout d'une heure, la répartition des bateaux est donnée en Figure 5. On suppose alors que des nouveaux bateaux sont créés et entrent dans la course avec une condition bien particulière, que nous exposons ci-après.

Pour créer un nouvel équipage, il faut que deux bateaux soient à la même distance de la ligne de départ. Si une telle condition est vérifiée, on crée un nouvel équipage en prenant au hasard quatre matelots du premier bateau et quatre matelots du second bateau. Ces matelots sont alors remplacés sur leur bateau d'origine par des matelots de qualité égale (cf Figure 6).

On laisse alors la course reprendre. Par ce procédé, les échanges ont évidemment été effectués entre bateaux de velocité égale. Les nouveaux bateaux auront donc une vélocité proche de celle des bateaux "parents" et, grâce à l'aléa dans la sélection de son équipage, cette vitesse peut aussi être plus forte ou plus faible. Si elle est plus forte, comme cela arrive dans la deuxième ligne (cf. Figure 6 et 7), on fait deux observations : le tri spatial a été renforcé, mais surtout, le front de propagation des bateaux s'est accéléré, il avance désormais à la vitesse instantanée de 8 noeuds pour une vitesse de 6 noeuds au début de la course.

FIGURE 4 – **La course de bateaux évolutive, étape 1**

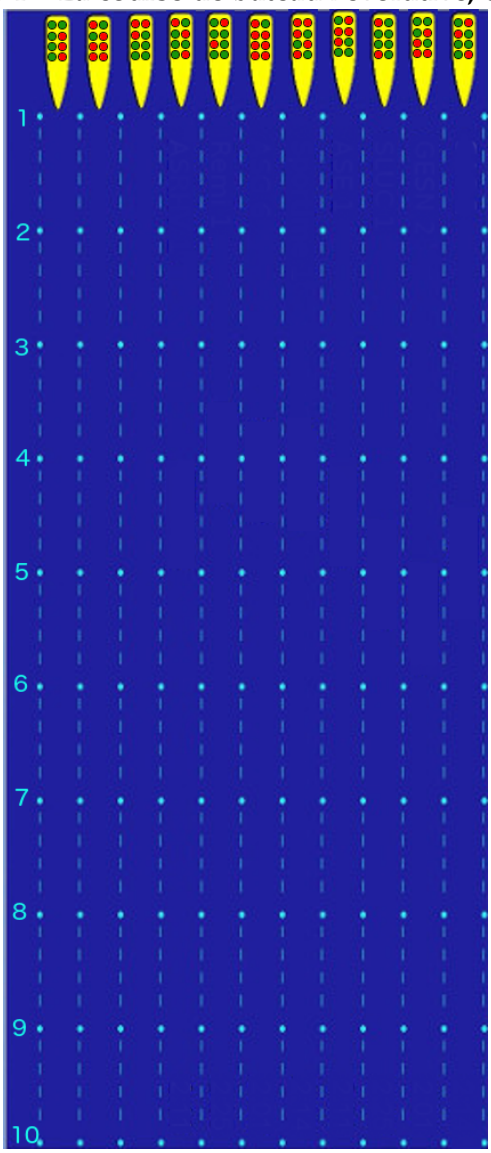

Au départ, la répartition entre matelots aguerris (en vert) et débutants (en rouge) est aléatoire.

FIGURE 5 – **La course de bateaux évolutive, étape 2**

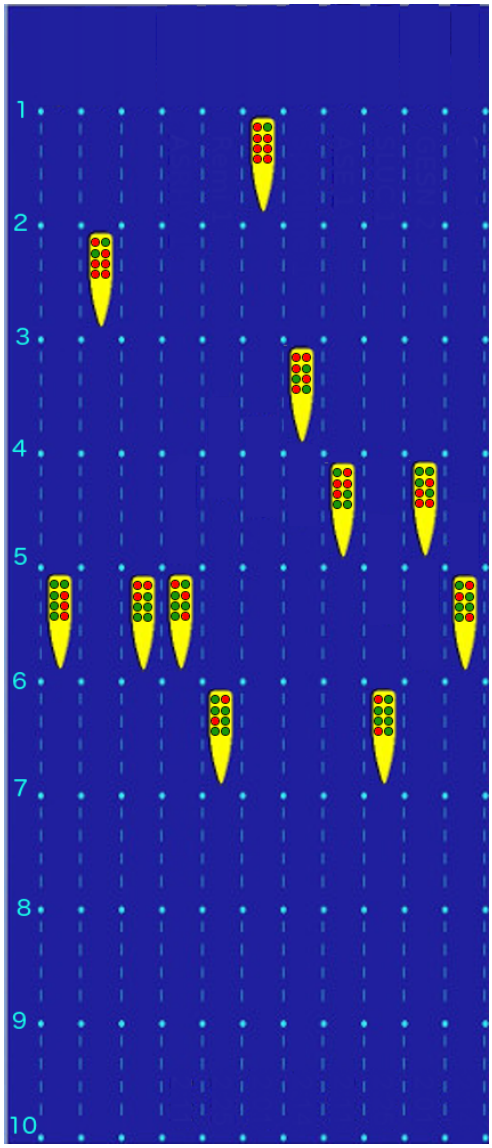

Au bout d'une heure, un bateau avec n matelots aguerris aura parcouru n milles : il a donc une vitesse moyenne de n noeuds. Le front de propagation est porté par les bateaux les plus véloces : il avance à la vitesse de 6 noeuds.
NB : ici, la vitesse est calculée en fonction de la poupe (l'arrière) du bateau.

FIGURE 6 – **La course de bateaux évolutive, étape 3**

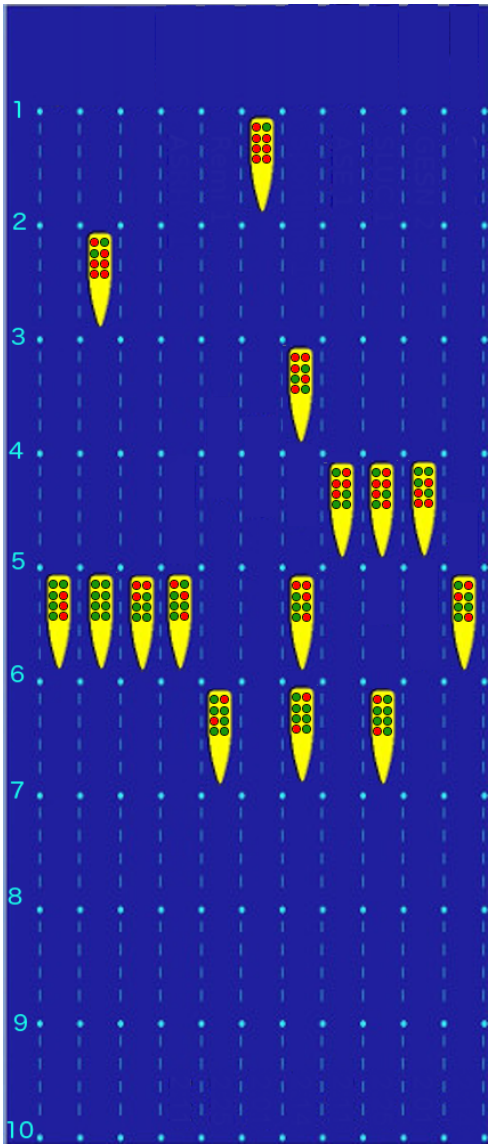

Création de bateaux : à l'étape 2, il y avait 2 bateaux à 4 milles de la ligne de départ, 4 bateaux à 5 milles et 2 bateaux à 6 milles. On crée donc 1 bateau à 4 milles du départ, 2 bateaux à 5 milles et 1 bateau à 6 milles. Quatre matelots provenant de chacun des 2 bateaux "parents" forment le nouvel équipage et sont remplacés sur leur bateau d'origine par des matelots de même qualité.

FIGURE 7 – **La course de bateaux évolutive, étape 4**

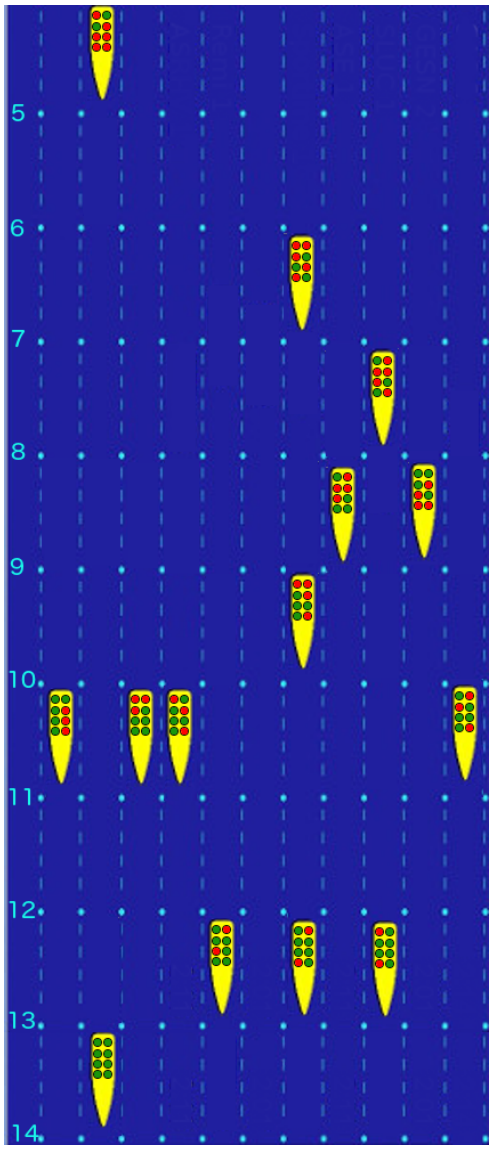

Le front est désormais porté par le bateau dans la deuxième ligne qui a hérité de 8 matelots aguerris de la part des bateaux de la première et de la troisième ligne. Le front de propagation avance désormais avec une vitesse instantanée de 8 noeuds.

Dans cette analogie, il faut interpréter les bateaux comme les individus de l'espèce invasive et les matelots comme les gènes responsables du phénotype "être véloce". L'échange des matelots est interprété comme la transmission à la naissance de 50% du patrimoine génétique de la mère et de 50% de celui du père.

Dans ce modèle, la variation des phénotypes en fonction du temps n'a pas de pertinence, celle en fonction de l'espace, beaucoup plus. En effet, on retrouve à l'avant du front une majorité de phénotypes à forte vélocité et l'inverse à l'arrière, mais ce tri ne risque pas de changer au cours du temps. C'est pourquoi on parle d'"un processus d'évolution qui concentre les phenotypes spatialement plutôt que temporellement".

Bien entendu, en l'état, ce qui précède n'est qu'un modèle nécessitant que l'on fournisse des preuves scientifiques à son application. Pour trouver des exemples d'une telle propagation chez une espèce, il faut, conformément à ce qui a été précédemment expliqué, chercher des espèces pour lesquelles le tri spatial est explicitement observé. C'est le cas par exemple de *Tettigoniidae*, une famille de criquets présents en Grande-Bretagne [103] qui présente des différence de taille d'ailes, mais aussi de *Pinus contorta*, une espèce de pin en Amérique du Nord [47] qui dissémine, selon les specimens, des quantités de graines différentes. C'est également le cas d'une espèce de fourmis [82] mais aussi et surtout, de *Rhinella marina*, le crapaud buffle qui nous intéresse.

Comme pour la théorie de Darwin en son temps, les mathématiques pourraient fournir des arguments supplémentaires pour étayer cette hypothèse. Un effort significatif a éte fait dans ce sens depuis quelques années et des résultats théoriques confirment la validité de cette théorie du point de vue des mathématiques. Nous citerons l'équation du crapaud buffle [25] comme exemple de modèle mathématique inspiré de la biologie qui présente les caractéristiques recherchées par les biologistes. Du point de vue des biologistes cependant, ce résultat n'est vraiment satisfaisant que si l'équation du crapaud buffle est validée par une comparaison avec des données statistiques. Or, comme nous allons le voir dans la prochaine section, des doutes peuvent être formulés en la matière.

Dans cette thèse, nous proposerons d'une part des modèles mathématiques qui modélisent mieux la propagation du crapaud buffle, à l'aide de données statistiques collectées sur le terrain par les biologistes. Nous proposerons d'autre part une étude de ces modèles mathématiques déterministes et enfin, nous proposerons des résultats similaires dans un cadre aléatoire beaucoup plus abstrait.

2 État de l'art

2.1 L'équation du crapaud buffle

Cette équation a pour but, entre autres, d'apporter une modélisation mathématique de l'hypothèse du tri spatial pour expliquer l'accélération d'une espèce invasive dont le comportment dispersif évolue. Étant donné le cadre biologique sous-tendu par cette problématique, l'équation a naturellement pris le nom "cane toad equation".

Avant de présenter cette équation, présentons les deux briques élémentaires dont elle est composée. Comme indiqué plus tôt, l'équation décrit la dynamique spatiale d'une espèce invasive pour laquelle le comportement dispersif est sujet à une évolution génétique. Il faut donc modéliser d'une part la dynamique spatiale et d'autre part, la dynamique évolutive de

cette espèce.

Concernant la dynamique spatiale, la brique élémentaire provient des travaux du statisticien et biologiste Fisher [61] et des mathématiciens Kolmogorov, Petrovsky et Piskunov [78]. L'équation de Fisher-KPP est donnée par :

$$\frac{\partial n}{\partial t}(t,x) - \theta \frac{\partial^2 n}{\partial x^2}(t,x) = rn(t,x))(1-n(t,x)), \quad (t,x) \in \mathbb{R}_+ \times \mathbb{R}, \tag{1}$$

où $r, \theta > 0$ sont fixés. Cette équation décrit la propagation d'une espèce dont la densité macroscopique est donnée par la fonction n. On suppose que la population se propage dans son environnement selon une diffusion caractérisée par le coefficient θ. Avec un taux de reproduction r, les individus se reproduisent, mais une compétition inter-spécifique au sein de la population limite la densité de sorte que $n \leq 1$. Dans ce modèle, aucune évolution génétique n'est observée et la propagation de l'espèce se fait à vitesse constante. En effet, on peut montrer que, dans ce cadre, la vitesse d'expansion de l'espèce est constante et égale à $2\sqrt{r\theta}$. Nous renvoyons à [5, 6, 30, 60, 72] pour des résultats plus précis à ce sujet.

Concernant la dynamique évolutive, l'aléa dans la transmission des phénotypes est modélisé par une équation de diffusion :

$$\frac{\partial n}{\partial t}(t,\theta) - \alpha \frac{\partial^2 n}{\partial \theta^2}(t,\theta) = 0, \quad (t,\theta) \in \mathbb{R}_+ \times \Theta, \tag{2}$$

Cette fois, $\theta \in \Theta \subset \mathbb{R}$ est interprété comme un trait génétique. Il est important de ne considérer aucun avantage adaptatif si l'on veut rester dans l'hypothèse du tri spatial. Cela se traduit dans le modèle par le fait que le taux de reproduction r ne dépend pas du trait θ.

L'équation du crapaud buffle est une combinaison de ces deux équations :

$$\frac{\partial n}{\partial t}(t,x,\theta) - \theta \frac{\partial^2 n}{\partial x^2}(t,x,\theta) - \alpha \frac{\partial^2 n}{\partial \theta^2}(t,x,\theta) = rn(t,x,\theta)(1-\rho(t,x)), \quad (t,x,\theta) \in \mathbb{R}_+ \times \mathbb{R} \times \Theta, \tag{3}$$

où $\rho(t,x) := \int_\Theta n(t,x,\theta)d\theta$.

Dans cette équation, on considère le coefficient de diffusion comme un trait phénotypique qui est différent selon les individus et qui évolue. Plusieurs travaux ont traité de l'équation du crapaud buffle. Citons en priorité [12, 25, 36, 37, 38, 94] ainsi que la thèse de Bouin [19] puisque la présente thèse s'inscrit dans sa continuité. Dans [23, 107] est traité le cas de traits bornés, on suppose donc que $\Theta = [\theta_{min}, \theta_{max}]$. Dans ce cas, la propagation de l'espèce se fait à vitesse constante. Pour montrer cela, on recherche des solutions dites en "ondes progressives", c'est-à-dire des solutions de (3) de la forme $n(t,x,v) = h(x \cdot e - ct, \theta)$ vérifiant $h(z,\theta) \to 0$ quand $z \to +\infty$ et $h(z,\theta) \to 1$ quand $z \to -\infty$. La fonction h est interprétée comme le profil de l'onde, le vecteur $e \in \mathbb{S}^1$ comme la direction et $c \in \mathbb{R}$ comme la vitesse de l'onde dans la direction e. Pour rechercher de telles solutions, on s'inspire de la structure de propagation vérifiée par les espèces modélisées. De telles propagation sont dites "à front tiré" : le front de propagation est conduit par des faibles populations à la frontière du front, contrairement aux fronts "poussés" conduits par des grandes populations. Cette constatation conduit à considérer la vitesse d'expansion de populations pour lesquelles la compétition entre individus a peu d'influence, mais qui sont en tout petit nombre, ce qui mène à chercher des solutions de la forme $h(z,\theta) = Q(\theta)e^{-\lambda z}$ pour l'équation sans le terme quadratique. La fonction Q est alors solution de

$$\lambda c Q - \theta \lambda^2 Q - \alpha \partial^2_{\theta\theta} Q = rQ, \tag{4}$$

que l'on interprète comme un problème spectral de valeur propre λc associé au vecteur propre Q. Dans [23], les auteur montrent qu'un tel problème spectral admet des solutions pour tout λ et que la fonction $\lambda \mapsto c(\lambda)$ admet un minimum que l'on note c^*. De plus, ils montrent que des solutions en ondes progressives existent pour tout $c \geq c^*$. Cette valeur est essentielle pour comprendre la propagation de l'espèce modélisée [107]. On peut en effet montrer que, si l'on suit la propagation en se déplaçant moins vite que c^* dans la direction e, on finira dans une zone saturée d'individus. À l'inverse, si l'on va plus vite, on finira dans une zone vide.

Ce résultat n'est pas satisfaisant dans la perspective de valider l'hypothèse du tri spatial. En effet, il ne prédit aucune accélération de la propagation. Cependant, une sur-représentation des individus à fort coefficient θ est observée à l'avant du front. Le problème de l'absense d' accélération été levé dans [13, 28] où a été démontrée une propagation d'ordre $3/2$ en temps (c'est-à-dire une accélération), dans le cas d'un espace des traits Θ non borné.

Ces résultats sont autant d'arguments qui renforcent l'hypothèse du tri spatial. Une population invasive soumise à une évolution des traits phénotypiques de dispersion peut, en effet, voir sa propagation s'accélérer au cours du temps et ce, uniquement grâce à une évolution du comportement dispersif au sein des individus. Toutefois, l'équation du crapaud buffle repose très fortement sur l'hypothèse d'une propagation diffusive de l'espèce, hypothèse remise en cause par les observations sur le terrain. Nous détaillons cela dans le prochain paragraphe. Loin de limiter l'impact de l'équation du crapaud, ces remises en cause nous invitent toutefois à chercher des modèles plus adéquats pour renforcer le poids de l'hypothèse du tri spatial.

2.2 Études statistiques sur la propagation du crapaud

Le crapaud buffle est l'objet d'une vaste littérature en biologie qui a notamment montré sa remarquable adaptation à son nouvel environnement australien. Une description exhaustive de cette littérature est impossible, aussi nous contenterons nous de détailler les références qui seront les plus utilisées dans cette thèse. Nous nous servirons de plusieurs études statistiques portant sur deux phénomènes différents : la dynamique démographique et le comportement dispersif.

Pour le premier, nous nous appuierons sur [80] et les références contenues à l'intérieur. Ce papier démontre la bonne adaptation du crapaud à l'Australie en comparant les données démographiques du crapaud relevées en Amérique du sud et en Australie. Parmi ces données, nous nous servirons notamment de celles sur les taux de fécondité des oeufs, et sur les taux de survie du crapaud d'une étape de son développement à une autre : têtard, métamorphe, juvénile puis adulte.

Concernant la dynamique spatiale, nous distinguons à nouveau deux subdivisions. La première, que nous avons déjà évoquée traite la propagation du crapaud à l'échelle du continent et fait état d'une vitesse d'expansion supérieure à 50 kilomètres par an en 2005 [91, 110]. Nous reproduisons en Figure 1 deux cartes particulièrement éloquentes à ce sujet.

La seconde étude statistique en la matière se place à l'échelle de l'individu. Pour comprendre la dispersion de l'espèce, une étude statistique longue de dix ans a été conduite notamment par Brown, Phillips et Shine. L'étude a été menée sur un site fixe, dans la plaine de la rivière Adelaide, non loin de la ville de Darwin dans la zone UTM 52L (voir Figure 8). Chaque année, durant la saison humide, des crapauds ont été capturés, puis relâchés après qu'une ceinture GPS a été placée autour de leur taille. Par la suite, leur position a été relevée quotidiennement pendant des périodes allant de 5 à 65 jours. L'étude a commencé pendant

FIGURE 8 – Zone d'étude de la dispersion des crapauds

Source : Google Earth.

la saison humide de 2005 (de novembre 2004 à avril 2005) et a été reproduite chaque année jusqu'en 2014. Il est important de noter que l'année 2005 correspond à la première apparition du crapaud dans la zone. Cela signifie que cette date correspond au passage du front de propagation, c'est-à-dire, théoriquement, au passage des crapauds les plus dispersifs. En 2014, les biologistes supposent que le front est passé depuis suffisamment longtemps pour que se trouvent, dans la zone, des crapauds qui ne présentent pas de phénotype dispersif particulier. Ainsi, cet étude devrait en théorie faire le constat de différences significatives entre les crapauds de 2005 et ceux de 2014.

Cette étude a été traitée dans de nombreux papiers parmi lesquels [33, 83, 91], ainsi que le premier chapitre de la présente thèse. Nous reproduisons en Annexe A une partie des données citées plus haut, c'est-à-dire les trajectoires des 22 crapauds relevées pendant la saison humide 2005. Présentons à présent les conclusions que les biologistes ont tiré de leur étude statistique.

Les modèles diffusifs sous-estiment la vitesse d'expansion des crapauds

Pour commencer, il est à noter que les modèles diffusifs classiquement utilisés sous-estiment la vitesse de propagation lorsqu'on les confronte aux données statistiques. Dans [91] est proposé un modèle discret basé sur deux phases bien distinctes. Conformément aux observations faites sur le terrain, les auteurs séparent l'année en deux saisons : une saison de reproduction (correspondant à la saison sèche) et une saison de dispersion (correspondant à la

saison humide). Ils considèrent également deux populations : les adultes qui se déplacent durant la saison de dispersion et qui, durant la saison de reproduction, engendrent la deuxième population, les juvéniles. Cette population ne prend pas part à la saison de dispersion aussitôt. Une année plus tard, on considère que les juvéniles sont devenus adultes et qu'ils prennent alors part à la saison de dispersion. Dans le modèle, la saison dite de reproduction sert également à prendre en compte la mortalité des crapauds (conformément aux données fournies dans [80]) pour modéliser la croissance démographique de la population. En résumé, partant d'une population J_0 de juvéniles et d'une population A_0 d'adultes, le nombres d'individus (J, A) à la fin de la saison de reproduction est donné par :

$$\begin{pmatrix} J \\ A \end{pmatrix} = \begin{pmatrix} 0 & F \\ \sigma_j & \sigma_a \end{pmatrix} \begin{pmatrix} J_0 \\ A_0 \end{pmatrix} \tag{5}$$

où σ_a et σ_j sont les taux de survie respectivement des adultes et des juvéniles et F le taux de reproduction.

Pour la phase de dispersion, un modèle diffusif est considéré. Ainsi, à partir d'une population structurée en espace $J_0(x)$, $A_0(x)$, la répartition de la population au bout d'un temps T est donnée par :

$$\begin{pmatrix} J_T(x) \\ A_T(x) \end{pmatrix} = \begin{pmatrix} J_0(x) \\ (k_\sigma * A_0)(x) \end{pmatrix},$$

où k_σ est le noyau de la chaleur :

$$k_\sigma(x) := \frac{1}{\sqrt{2\pi\sigma^2 T}} \exp\left(-\frac{x^2}{2T\sigma^2}\right),$$

et σ est le coefficient de diffusion, dont les valeurs numériques sont tirées de l'étude trajectorielle précédemment mentionnée.

Afin d'observer une accélération, les auteurs ont également pris en compte une évolution des traits phénotypiques. Deux évolutions sont prises en compte : l'évolution des traits reproductifs (L) qui engendre une variation des quantités σ_a, σ_j et F et une évolution des traits dispersifs (D) qui engendre une variation du trait σ. Finalement, quatre sous-modèles sont considérés : celui où aucune évolution n'est prise en compte (L_0D_0), celui où la variation d'un seul trait est considérée (L_0D_+) et (L_+D_0) et celui où les deux évolutions sont possibles (L_+D_+). Ces modèles prédisent une accélération du front mais, confrontés aux données de propagation à l'échelle du pays, on constate qu'ils sous-estiment la vitesse d'invasion, comme le montre la Figure 3 dans [91] que nous reproduisons ici en Figure 9.

En conclusion de leur article, les auteurs mettent en cause leur modèle d'évolution pour expliquer cette mésestimation de la vitesse d'invasion. Nous proposons dans cette thèse une autre explication qui remet plutôt en cause la validité de la phase de dispersion considérée. Cette remise en cause prend sa source dans deux papiers, à savoir [83] et [33].

Les crapauds ont des trajectoires à direction persistante

Dans [83], l'étendue des données trajectorielles est utilisée. Les auteurs comparent les comportements dispersifs des crapauds en analysant leurs trajectoires au moment de leur arrivée

FIGURE 9 – **Modèles diffusifs confrontés aux données**

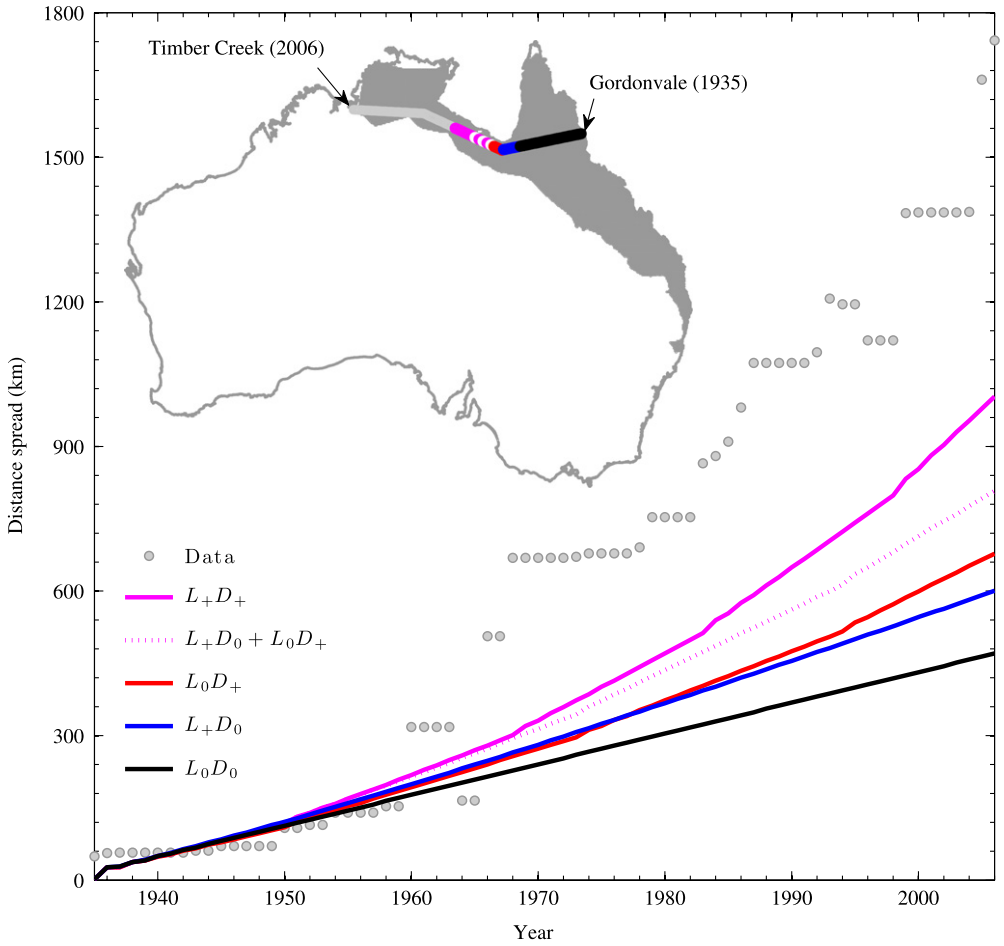

Lignes pleines : prédictions des modèles diffusifs. Points gris : données sur la propagation du crapaud buffle.
Source : [91] T. Perkins, B. Phillips, M. Baskett, and A. Hastings (2013). Evolution of dispersal and life history interact to drive accelerating spread of an invasive species. Ecology Letters.

FIGURE 10 – **Illustration de l'angle de virage**

Nous illustrons ici ce que nous entendons par persistance directionnelle. L'angle formé par la trajectoire entre le jour 1 et 2 puis entre le jour 2 et 3 est plus grand sur la première trajectoire que sur la deuxième. On dit que la persistance directionnelle de la première trajectoire est plus faible.

dans la zone d'observation avec celles relevées quelques années plus tard, lorsque la population s'est vraiment installée dans les lieux. Leur étude démontre que les crapauds observés lors du passage du front ont une tendance à garder une direction de marche persistante, c'est-à-dire que, d'un jour à l'autre, l'angle du virage formé par la trajectoire est faible en moyenne (voir Figure 10). Nous donnons en Figure 11 deux exemples de trajectoires de crapauds : l'une, relevée en 2005, qui présente une forte persistance directionnelle et l'autre, relevée en 2014, qui en présente une faible. On comprend assez bien qu'une grande persistance permet à un crapaud de parcourir des distances plus longues en moyenne puisque peu de retours en arrière sont alors effectués.

Dans la même zone d'observation, quelques années plus tard, les crapauds n'ont plus du tout le même comportement et les angles formés par les virages sont plus grands en moyenne [83].

La persistance directionnelle est transmise d'une génération à l'autre

Cette persistance directionnelle est un comportement qui varie d'un individu à l'autre. Comme une grande persistance favorise des voyages à longue distance, il n'est pas surprenant de retrouver ces comportements chez les individus à l'avant du front de propagation. Cependant, pour entrer dans le cadre du tri spatial, il faut que ce comportement puisse être interprété comme un trait phénotypique inhérent à l'individu, ce qui n'est pas évident à première vue. Cette question a été abordée dans [33]. Dans cet article, les observations de [83] sur la persistance directionnelle ont été confirmées sur des crapauds en captivité, mais surtout, il a été constaté que les parents ayant un tel comportement le transmettaient partiellement à leur descendance.

FIGURE 11 – **Deux trajectoires à persistances différentes**

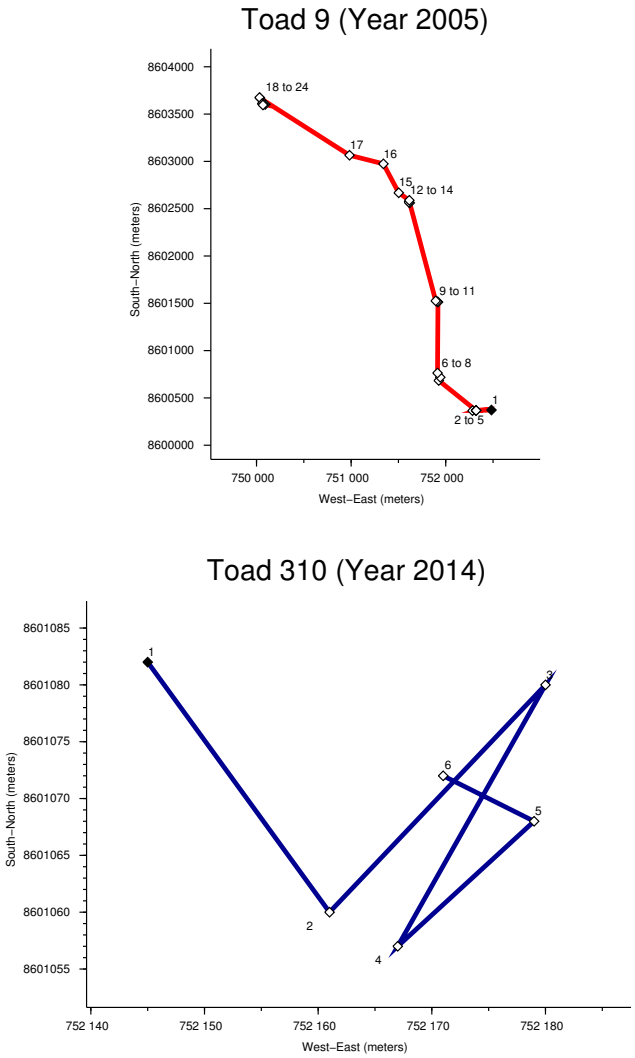

Ligne rouge : trajectoire d'un crapaud relevée en 2005 qui présente une forte persistance directionnelle. Ligne bleue : trajectoire d'un crapaud relevée en 2014 qui présente une faible persistance directionnelle. Abcisses : coordonnées UTM Ouest-Est (en mètres). Ordonnées : coordonnées Sud-Nord (en mètres). Données fournies par MM. Brown, Phillips et Shine.

Conclusion

Si l'on résume : les modèles diffusifs considérés sous-estiment la vitesse d'invasion des crapauds. Les crapauds les plus dispersifs sont ceux qui présentent une forte persistance directionnelle et pour lesquels l'approximation de diffusion peut être fausse. Cette persistance directionnelle est transmise d'une génération à l'autre et peut donc être interprétée comme un trait phénotypique, sujet à évolution. Nous pouvons alors faire l'hypothèse suivante : ce trait phénotypique serait le trait évolutif qui, dans le cadre de l'hypothèse du tri spatial, serait responsable de l'accélération de l'invasion. Les modèles de propagation du crapaud doivent donc être orientés dans ce sens. Pour des espèces qui présentent des fortes persistances directionnelles, l'approximation de diffusion n'est pas pertinente, comme cela a par exemple été montré dans le cas de la bactérie *Escherichia coli* [98]. Dans ces cas-là, il faut rester à une échelle d'observation plus fine et conserver notamment la structure en vitesse des populations. Ceci nous oriente donc vers des modèles de dispersion basés sur des équations cinétiques. Par ailleurs, la structure des données trajectorielles dont nous disposons se prête bien à ce type de modèle.

2.3 Les équations cinétiques et la dynamique spatiale

Les équations cinétiques ont été introduites à l'origine pour l'étude de vastes systèmes de particules en interaction, issus de la physique statistique. Citons comme exemple de telles particules, les particules d'un gaz confiné ou d'un plasma. Isolée, on suppose qu'une de ces particules se déplace en ligne droite selon une direction et une vitesse donnée par un vecteur v. Si jamais elle rencontre une autre particule avec une vitesse v', une collision va avoir lieu et les deux particules vont changer de vecteur vitesse selon une fonction de v et v'. Avec un très grand nombre de particules, l'approche microscopique (à l'échelle des particules) est bien trop complexe à appréhender mais, à l'inverse, l'échelle macroscopique (à l'oeil nu) est trop grossière puisqu'on perd l'information sur les vitesses des particules. La bonne échelle est une échelle intermédiaire, qu'on appelle mésoscopique, où on ne considère plus les particules une par une mais une densité de particules présente en un temps donné, à une position de l'espace donnée et se déplaçant avec une vitesse donnée. Ainsi, la solution d'une équation cinétique est une fonction $f(t, x, v)$ où t représente le temps, x l'espace et v la vitesse. Les deux exemples fondamentaux issus de la physique sont l'équation de Boltzmann [17] qui traite d'interactions matérielles entre particules lors de collisions (modèles de type "sphères dures" par exemple) et l'équation de Vlasov [112] qui traite d'interactions à distance (entre particules chargées électriquement par exemple). Nous renvoyons à [111] pour plus de détails sur ce sujet.

Les modèles cinétiques ont été adaptés avec succès pour des problèmes, entre autres, de dynamique spatiale de populations. L'hypothèse fondamentale dans ces modèles est que les populations considérées ne conservent pas la mémoire de leurs déplacements passés et ajustent leurs futurs déplacements en fonction seulement de l'observation du présent. Cette hypothèse permet de rester à l'échelle microscopique dans le cadre de marches aléatoires markoviennes dont la densité d'individus est décrite par les équations de Chapman-Kolmogorov forward.

L'adaptation des modèles de la physique peut se faire naturellement. Par exemple, des équations de type Boltzmann ont été récemment étudiées dans le cadre de la fourmi *Lasius niger* [16]. Dans cet exemple, les interactions entre les fourmis ont lieu lorsque l'une d'elle

trouve sur son chemin une phéromone laissée par une autre fourmi, ce qui la pousse alors à aller dans la direction indiquée par la phéromone. On a là une interaction qu'on peut interpréter comme une collision puisqu'un changement de vitesse a lieu lors de la rencontre de deux agents (en l'occurence une fourmi et une phéromone). Des interactions à distance, de type Vlasov, peuvent également être prises en compte. Les modèles cinétiques ont par exemple été utilisés pour modéliser l'apparition de vols en formation pour les oiseaux migrateurs [39, 52]. Dans ce cas, les interactions entre oiseaux ont lieu par le biais d'observations mutuelles des individus entre eux qu'on peut interpréter comme une force d'interaction à distance.

Les équations cinétiques ont également été utilisées pour l'étude de phénomènes de propagation. Deux approches peuvent alors être envisagées :

Ondes progressives

Nous présentons ici le principe de solutions en ondes progressives sur une équation cinétique issue de [26, 46, 71, 99] dont la motivation provient de l'étude de la propagation d'*Escherichia coli*. L'équation considérée est :

$$\begin{cases} \partial_t g + v\partial_x g = z(M(v)\rho - g) + r\rho(M(v) - g), \quad (t,x,v) \in \mathbb{R}_+ \times \mathbb{R} \times V \\ \rho(t,x) = \int_V g(t,x,v)dv. \end{cases} \tag{6}$$

Cette équation donne l'évolution en fonction du temps de la densité g d'une colonie d'individus dont la dynamique spatiale et démographique est donnée comme suit : un individu donné alterne des phases de déplacements rectilignes uniformes de vecteur $v \in V \subset \mathbb{R}$ (d'où le terme $v\partial_x$) et de changements de direction. Ces changements de direction ont lieu à chaque fois après un temps aléatoire de loi exponentielle de paramètre z. Lors de ces changements de vitesse, l'individu choisit une nouvelle vitesse v' selon la loi de probabilité sur V donnée par la densité M (*ergo* le terme $M(v)\rho - g$). Avec un taux de reproduction r, la population est renouvelée proportionnellement à sa capacité actuelle (d'où le terme $r\rho$) mais une capacité d'accueil de l'environnement limite la densité d'individus de sorte que $g \leq M$, d'où le terme $(M - g)$.

Pour étudier la propagation de cette espèce, on peut chercher des solutions en ondes progressives, c'est-à-dire des solutions de (6) sous la forme $g(t,x,v) = h(x - ct, v)$ avec $\lim_{z\to+\infty} h(z,v) = 0$ et $\lim_{z\to-\infty} h(z,v) = M(v)$. Une telle solution se comporte de la manière suivante : on observe le déplacement de la forme de la fonction h se déplacer vers la droite avec une vitesse donnée par c. On peut donc interpréter la solution g comme une onde de profil h se déplaçant à vitesse constante c.

Pour trouver de telles solutions, on se sert d'un principe de comparaison. Il faut pour cela trouver une fonction $\overline{g}$ (appelée sur-solution) et $\underline{g}$ (appelée sous-solution) qui sont en permanence respectivement au dessus et en dessous de la solution g. On se référera à [26] pour plus de détails sur la construction de sous et sur-solutions.

Le résultat démontré dans [26] est le suivant :

Theorem 0.1. *(Bouin-Calvez-Nadin) On suppose* $\inf M > 0$. *Il existe un* $c^* < \sup V$ *tel que, pour tout* $c \in [c^*, \sup V]$, *il existe une solution de (6) en onde progressive et tel que, pour tout* $c \in [0, c^*)$, *il n'en existe pas.*

De plus, la solution g de (6) vérifie (sous des conditions précisées dans [26]) :

$$c < c^* \quad \Longrightarrow \quad \forall v \in V, \quad \lim_{t\to+\infty} \left(\sup_{x\leq ct} |M(v) - g(t, x + ct, v)| \right) = 0 \tag{7}$$

$$c > c^* \quad \Longrightarrow \quad \forall v \in V, \quad \lim_{t\to+\infty} \left(\sup_{x\leq ct} g(t, x + ct, v) \right) = 0 \tag{8}$$

Ceci permet d'interpréter c^* comme la vitesse de propagation de l'espèce. En effet, si l'on se place en un point initialement et que l'on avance avec une vitesse plus forte que c^*, on se retrouvera en temps long dans une zone vide d'individus. À l'inverse, si l'on ne va pas suffisamment vite, on se retrouvera dans une zone envahie.

Nous relevons deux hypothèses techniques qui limitent le champ d'application de ce résultat. Tout d'abord, on suppose que V est compact et que $\inf M > 0$. Ensuite, le théorème est valable uniquement pour une dimension en espace et en vitesse égale à 1. L'un des résultats de cette thèse est d'étendre ce résultat aux dimensions supérieures et dans la cas où M peut s'annuler.

Point de vue de l'optique géométrique

Nous présentons cette approche sur l'équation de transport avec un opérateur de collision BGK linéarisé, issue de [22]. L'équation considérée est (6) pour $r = 0$ (c'est-à-dire sans reproduction) :

$$\partial_t f + v\partial_x f = M\rho - f \tag{9}$$

Une manière plus faible de caractériser la propagation est d'utiliser le méthode dite de l'approximation de l'optique géométrique [58, 66]. Pour la comprendre, on peut l'interpréter de la manière suivante : supposons qu'on observe une population animale. Pour observer sa propagation, on se place à très grande hauteur, dans un satellite par exemple. Ceci engendre deux soucis : le premier, c'est qu'à cette hauteur, on n'observe des phénomènes significatifs qu'à partir d'un temps long, c'est pourquoi il faut également modifier l'échelle des temps d'observation. Du point de vue mathématique, ces deux changements d'échelle se caractérisent par l'étude, non plus de la fonction f, mais de la fonction $f^\varepsilon(t, x, v) = f(t/\varepsilon, x/\varepsilon, v)$, solution de :

$$\partial_t f^\varepsilon + v\partial_x f^\varepsilon = \frac{1}{\varepsilon}(M\rho^\varepsilon - f^\varepsilon) \tag{10}$$

Le second problème est que, à cette hauteur, la zone envahie d'animaux n'est séparée de la zone vide que par une ligne, ce qui crée des singularités. Suivant [58, 65], il faut effectuer la transformée de Hopf-Cole $f^\varepsilon = M(v)e^{-\frac{\varphi^\varepsilon(t,x,v)}{\varepsilon}}$. La fonction φ^ε est alors solution de

$$\partial_t \varphi^\varepsilon + v\partial_x \varphi^\varepsilon = \int_V M' \left(1 - e^{\frac{\varphi^\varepsilon - \varphi'^\varepsilon}{\varepsilon}} \right) dv'. \tag{11}$$

La quantité φ^ε est mathématiquement très intéressante. En effet, on peut montrer que φ^ε converge en un sens (voir [20, 22] pour plus de détails) vers une fonction φ^0, qui ne dépend pas de v. Cette fonction φ^0 nous donne des informations sur la propagation de notre espèce. En effet, on peut montrer que, là où $\varphi^0 > 0$, la population est absente et que, là où $\varphi^0 = 0$,

la population est présente. Si l'on dispose de surcroît d'une équation qui décrit l'évolution de φ^0, on peut donc suivre la propagation de la population modélisée par (9).

Justement, dans [22] est démontré le théorème suivant :

Theorem 0.2. *(Bouin-Calvez) Si* $\inf M > 0$ *et la condition initiale est bien préparée* i.e. $\varphi^\varepsilon(0,x,v) = \varphi_0(x)$*, alors la fonction* φ^ε *converge uniformément localement vers une fonction* φ^0*, indépendante de* v*, qui est la solution au sens des viscosités de l'équation de Hamilton-Jacobi*

$$\begin{cases} \partial_t \varphi^0 + H(\partial_x \varphi^0) = 0, & (t,x) \in \mathbb{R}_+ \times \mathbb{R}, \\ \varphi^0(0,x) = \varphi_0(x), & x \in \mathbb{R}. \end{cases}$$

où H *est implicitement donné par : pour tout* $p \in \mathbb{R}$*, le réel* $H(p)$ *est l'unique réel vérifiant*

$$\int_V \frac{M(v)}{1 + H(p) - v \cdot p} dv = 1. \tag{12}$$

Ce résultat a été utilisé et étendu dans [20] au cas de l'équation (6) avec un terme de croissance et de saturation $r\rho(M(v) - f)$. Dans ce cas là aussi, l'approximation de l'optique géométrique permet d'obtenir des résultats de propagation. Mathématiquement, tout se passe comme dans le cas $r = 0$. Ainsi le résultat mentionné permet d'établir des résultats de propagation dans des équations issues de la biologie.

Il est à noter que dans l'article original [22], l'hypothèse $\inf M > 0$ n'est pas mentionnée, pas plus que le fait qu'on se place en dimension d'espace et de vitesse égale à un. Pourtant, les conclusions du théorème sont conservées telles quelles. Au cours de cette thèse, nous démontrerons que le théorème 0.2 est faux si ces deux conditions ne sont pas vérifiées et nous le corrigerons.

Afin de passer à la limite $\varepsilon \to 0$ pour φ^ε, on se sert de la méthode de la fonction test perturbée introduite par Evans [57]. Plus récemment, cette méthode a été adaptée dans le cadre des EDP stochastiques, nous la présentons ci-après dans le cadre déterministe et dans le cadre stochastique.

2.4 La méthode de la fonction test perturbée

La méthode de la fonction test perturbée est une méthode employée pour démontrer des résultats de convergence pour des solutions d'EDP. Plus précisément, si on dispose d'une suite de fonctions $(f^\varepsilon)_\varepsilon$ solutions d'une suite d'EDP indexée par ε, la méthode permet de démontrer des résultats de convergence de $f^\varepsilon \to f^0$, où f^0 est solution d'une EDP "limite" de la suite d'EDP indexée par ε.

On notera au passage les termes "fonction test". Cette méthode s'applique en effet dans le cas où l'EDP limite est considérée dans un sens faible, qui implique des fonctions test. Il y a plusieurs exemples de telles formulations qui impliquent des fonctions tests, comme la formulation au sens des distributions, la formulation au sens des viscosités pour les équations déterministes et la formulation avec des générateurs infinitésimaux pour les EDP stochastiques. La méthode n'est pas appliquée dans le premier cas car il est plus simple de procéder différemment. Nous traiterons ici les deux derniers cas.

Fonction test perturbée et solutions de viscosité

Cette application est à l'origine de la méthode de la fonction test perturbée. On rappelle ici la définition de formulation au sens des viscosités [44].

Definition 0.3. *Soit φ uniformément continue de $\mathbb{R}_+ \times \mathbb{R}^d$ dans $\mathbb{R}$.*

On dit que φ est une sous-solution au sens des viscosités de l'équation de Hamilton-Jacobi $\partial_t f + H(\nabla_x f) = 0$ si, pour toute fonction test $\psi \in C^1(\mathbb{R}_+ \times \mathbb{R}^d)$ telle que $\varphi - \psi$ admet un maximum local en un point (t^0, x^0), ψ vérifie :

$$\partial_t \psi(t^0, x^0) + H(\nabla_x \psi(t^0, x^0)) \leq 0$$

On dit que φ est une sur-solution au sens des viscosités de l'équation de Hamilton-Jacobi $\partial_t f + H(\nabla_x f) = 0$ si, pour toute fonction test $\psi \in C^1(\mathbb{R}_+ \times \mathbb{R})$ telle que $\varphi - \psi$ admet un minimum local en un point (t^0, x^0), ψ vérifie :

$$\partial_t \psi(t^0, x^0) + H(\nabla_x \psi(t^0, x^0)) \geq 0$$

On dit que φ est une solution au sens des viscosités si c'est à la fois une sous et une sur-solution de viscosité.

La méthode de la fonction test perturbée nous permet à la fois d'exhiber un candidat pour la limite de φ^ε mais aussi de montrer que ce candidat est en effet la limite de φ^ε. Nous illustrons la méthode sur l'équation (11).

Pour commencer, on vérifie que φ^ε possède bien une limite. Cela peut se faire en établissant des estimations *a priori* vérifiées par l'équation (11) par exemple (voir [22]). Grâce au théorème d'Arzelà-Ascoli, on extrait alors de $(\varphi^\varepsilon)_\varepsilon$ une sous-suite qui converge uniformément vers une fonction φ^0, qu'on essaie d'identifier.

L'identification de la limite se fait de manière formelle. L'idée est de supposer que φ^ε converge "gentillement", c'est-à-dire que $\varphi^\varepsilon(t, x, v) = \varphi^0(t, x) + \varepsilon\eta(t, x, v)$. Cela n'est pas si simple *a priori* , mais ce n'est pas grave. Si l'on place cette expression dans (11), on obtient après passage à la limite (formelle) :

$$\partial_t \varphi^0 + v \cdot \nabla_x \varphi^0 = 1 - \int_V M' e^{\eta - \eta'} dv'. \tag{13}$$

Pour que cette équation puisse être vérifiée, il faut que φ^0 soit solution d'une équation de Hamilton-Jacobi (voir [22] pour plus de détails). La fonction η est également uniquement déterminée par cette équation, à une constante près qui dépend de t et de x. On retient alors φ^0 comme candidat pour la limite de $(\varphi^\varepsilon)_\varepsilon$.

Toute cette manipulation est formelle et rien n'indique, par exemple, que la fonction φ^0 a la régularité nécessaire pour être solution d'une EDP de Hamilton-Jacobi. C'est donc une solution au sens faible qu'il faut chercher, une solution au sens des viscosités. On considère donc une fonction ψ telle que $\varphi^0 - \psi^0$ admette un minimum (resp. un maximum) local en un point (t^0, x^0).

L'idée finale est de perturber la fonction test ψ^0 comme effectué précédemment, c'est-à-dire en posant $\psi^\varepsilon = \psi^0 + \varepsilon\eta$, où η est la même fonction que celle considérée précédemment (en replaçant φ^0 par ψ^0). Par convergence uniforme de ψ^ε vers ψ^0 et de φ^ε vers φ^0, la fonction $\varphi^\varepsilon - \psi^\varepsilon$ admet un minimum (resp un maximum) local en un point $(t^\varepsilon, x^\varepsilon, v^\varepsilon)$ tel que $(t^\varepsilon, x^\varepsilon) \to (t^0, x^0)$, ce qui nous permettra en passant à la limite de conclure que $\partial_t \psi(t^0, x^0) + H(\nabla_x \psi(t^0, x^0)) \geq 0$ (resp $\leq$).

Fonction test perturbée en stochastique

Il y a plusieurs manières d'interpréter la solution d'une équation différentielle stochastique. Prenons par exemple le processus d'Ornstein-Uhlenbeck [89] qui vérifie l'EDS suivante :

$$\begin{cases} df_t = \theta(\mu - f_t)dt + \sigma dW_t, \\ f_0 = x. \end{cases} \tag{14}$$

où $(W_t)_t$ est un processus de Wiener. La première consiste à partir de la définition de la solution d'une EDS :

$$f_t = x + \theta \int_0^t (\mu - f_s)ds + \sigma \int_0^t dW_s.$$

La seconde est de considérer une formulation en terme de générateur infinitésimal. Par définition, le générateur infinitésimal $\mathscr{L}$ de f_t est donné par

Definition 0.4. *Soit $(\Omega, \mathcal{F}, \mathbb{P})$ un espace de probabilité, $(X, \|\cdot|)$ un espace de Banach et $(f_t)_t$ un processus stochastique à valeurs dans X. On définit le générateur infinitésimal $\mathscr{L} : \mathcal{D}(\mathscr{L}) \to C_b^0(X, \mathbb{R})$ de $(f_t)_t$ par*

$$\mathscr{L}\varphi(x) = \lim_{t \searrow 0} \frac{1}{t} \mathbb{E}_g[\varphi(f_t) - \varphi(g)],$$

où, $\mathcal{D}(\mathscr{L}) \subset C_b^0(X)$ est le domaine où une telle expression est définie et $\mathbb{E}_{f_0}$ est l'espérance pour la loi de probabilité $\mathbb{P}(\cdot \mid f_0 = g)$.

Cet opérateur $\mathscr{L}$ agit sur l'espace des fonctions continues bornées qui est donc interprété comme notre espace de fonctions test. Le résulat fondamental est que ce générateur infinitésimal caractérise le processus. Ainsi, on peut formuler la solution d'une EDS en partant de la définition ou bien en donnant son générateur infinitésimal. Dans le cas du processus d'Ornstein-Uhlenbeck, le générateur infinitésimal est donné par :

$$\mathscr{L}\varphi(x) = \theta(\mu - x)\varphi'(x) + \frac{\sigma^2}{2}\varphi''(x).$$

De même, toute EDP stochastique est associée de manière unique à un générateur infinitésimal et donc à une formulation en terme de fonctions test. Nous présentons cette notion sur un exemple tiré de [51] : l'équation considérée est

$$\partial_t f^\varepsilon + \frac{1}{\varepsilon} v \nabla_x f^\varepsilon = \frac{1}{\varepsilon^2}(M\rho^\varepsilon - f^\varepsilon) + \frac{1}{\varepsilon} f^\varepsilon m^\varepsilon, \tag{15}$$

où $m^\varepsilon = m(t/\varepsilon^2, x)$ et m est un processus de Markov stationnaire et $\rho^\varepsilon = \int f^\varepsilon dv$. Les auteurs démontrent que ρ^ε converge en un certain sens (voir [51]) vers ρ^0 la solution d'une équation de diffusion de la forme

$$d\rho = \operatorname{div}(K\nabla\rho)dt + \frac{1}{2}F\rho + \rho Q^{1/2} dW(t), \tag{16}$$

où $(W_t)_t$ est un processus de Wiener. Nous renvoyons à [51] pour plus de détails quant à la définition de F, Q et K. Ce qui nous intéresse ici, c'est l'adaptation de la méthode de la fonction test perturbée à ce cadre.

Pour ce faire, on commence comme dans le cas déterministe par obtenir un résultat de convergence pour f^ε. Dans le cadre précédent, on établissait des estimations lipschitz *a priori*

pour utiliser le théorème d'Arzelà-Ascoli. Ici, on doit établir des estimations uniformes en ε en norme L^2 ainsi qu'un résultat de tension pour la loi de ρ^ε. La tension d'un espace de probabilités est une sorte d'équivalent de la notion de compacité dans un espace métrique [14]. Par le théorème de Prokhorov, ρ^ε converge en loi, à extraction d'une sous-suite près, vers une fonction ρ^0. La limite ρ^0 est identifiée grâce à la méthode de la fonction test perturbée. Pour cela, on identifie le générateur infinitésimal $\mathscr{L}^\varepsilon$ associé à $(f^\varepsilon, m^\varepsilon)$:

$$\mathscr{L}^\varepsilon\varphi(f,n) = -\frac{1}{\varepsilon}(v\nabla_x f, D\varphi(f,n)) + \frac{1}{\varepsilon^2}(M\rho - f, D\varphi(f,n)) + \frac{1}{\varepsilon}(fn, D\varphi(f,n)) + \frac{1}{\varepsilon^2}A\varphi(f,n), \tag{17}$$

où A est le générateur infinitésimal de m et $D\varphi$ représente la dérivée de φ par rapport à la variable f.

On souhaite identifier ρ^0 grâce à l'opérateur limite $\mathscr{L} = \lim_{\varepsilon\to 0}\mathscr{L}^\varepsilon$. Pour cela, comme précédemment, on regarde ce qui se passe lorsqu'on considère une fonction test perturbée, c'est-à-dire $\varphi^\varepsilon = \varphi + \varepsilon\varphi_1 + \varepsilon^2\varphi_2$. Placée dans l'équation (17), cette décomposition donne des conditions nécessaires vérifiées par $\mathscr{L}$ qui permettent de l'identifier comme le générateur de l'équation (16). On présentera dans cette thèse un résultat de convergence similaire en s'appuyant sur les techniques employées dans [51].

Les contributions de cette thèse ont été évoquées à plusieurs reprises, prenons à présent le temps de les détailler.

3 Principaux résultats obtenus

3.1 Vers des modèles cinétiques pour la propagation du crapaud buffle

Le but de ce travail est de trouver un modèle mathématique pour lequel une invasion accélérée est observée et qui, de surcroît, propose des vitesses d'expansion du front proches de la réalité.

Dans cette optique, nous proposons un travail moins ambitieux. Nous étudions deux modèles sans évolution des traits de dispersion et nous les confrontons à des données relevées sur le terrain par des biologistes.

Pour ce faire, nous adoptons la même méthode que [91]. Ainsi, nous séparons nos modèles en deux phases : une phase dite de dispersion et une phase de reproduction. Nos deux modèles sont semi-discrets. Pendant la phase de dispersion, nous supposons que les individus se déplacent suivant un processus à sauts de vitesse. Pour la phase de reproduction, nous considérons que la population totale est simplement augmentée par un coefficient multiplicateur (voir formule (5)).

Nos deux modèles ne diffèrent que par leur phase de dispersion, la phase de reproduction est identique. Les modèles de dispersion sont inspirés par notre observation des données trajectorielles de 22 crapauds observés au cours de la saison humide de 2005. Ces données ont été relevées par Gregory Brown, Benjamin Phillips et Richard Shine. 22 crapauds ont été suivis au cours de la saison humide de 2005 (de novembre 2004 à avril 2005). Pour relever la position journalière d'un crapaud la méthode employée sur le terrain est la suivante : on capture le crapaud, on l'équipe d'une ceinture contenant une balise GPS et on le libère ensuite. La balise GPS émet un signal chaque jour à la même heure donnant la position du crapaud.

Les deux processus à sauts de vitesse que nous considérons sont tirés de nos observations des données trajectorielles fournies par les biologistes. Pour chacun des deux modèles,

nous supposons qu'un individu se déplace suivant le processus aléatoire suivant : l'individu alterne des phases de déplacements rectilignes uniformes et des phases (instantanées) de redistribution de vitesse. Nous supposons que les phases de déplacements durent pendant un temps aléatoire de loi exponentielle de paramètre $z > 0$, après quoi l'individu change de vitesse. Lorsqu'un tel changement a lieu l'individu doit alors choisir une nouvelle direction et une nouvelle vitesse. C'est principalement dans cette redistribution en vitesse que nos deux modèles se distinguent l'un de l'autre.

Le modèle EWR

Ce modèle se fie sur l'observation de l'histogramme donné en Figure 12. Cet histogramme représente tous les déplacements journaliers des 22 crapauds observés. Comme nous pouvons le voir, les données présentent une majorité de crapauds ayant des déplacements courts (de 0 à 100 mètres), mais également une petite quantité d'individus ayant des déplacements très grands (de 600 à 1700 mètres). Nous pouvons tirer de cet histogramme une loi de répartition empirique des vitesses.

Dans ce modèle, nous supposons que, lors d'un saut de vitesse, un individu choisit une nouvelle vitesse selon la loi empirique tirée de l'histogramme 12. Le modèle tire son nom de l'existence de trois modes de déplacements : le mode "en campement" où le crapaud ne bouge pas du tout (cf. le bâton bleu dans l'histogramme), le mode "en marche" (*walking* en anglais) correspondant aux vitesses comprises entre 0 et 600 mètres par jour et le mode "en course" (*running* en anglais) pour les vitesse supérieures à 600 mètres par jour.

Le modèle ER

Pour ce modèle, nous considérons 5 paramètres : z, d_m, d_e, γ et v_M. Nous supposons que les individus marchent pendant un temps aléatoire de loi exponentielle d'espérance d_m puis font une pause pendant un temps de loi exponentielle d'espérance d_e. Durant la phase de marche, les individus changent de direction après des temps aléatoires de loi exponentielle d'espérance $\frac{1}{z}$. Lors de la redistribution de leur vitesse, les individus choisissent une nouvelle vitesse uniformément sur $[0, v_M]$ et une nouvelle direction choisie en fonction de leur précédente direction de marche. Si cette dernière direction est donnée par l'angle θ qu'elle fait avec l'axe Nord-Sud, nous supposons que la nouvelle direction est donnée par une loi de wrapped Cauchy de moyenne θ et de paramètre γ. La loi de wrapped Cauchy est une loi de probabilité sur $[-\pi, \pi]$ qui correspond à la loi de Cauchy sur $\mathbb{R}$ modulo 2π. Plus γ est grand, plus la variance de la loi est grande. Nous représentons la densité de probabilité de la loi de wrapped Cauchy en Figure 13. Ce coefficient γ est interprété dans notre modèle comme la directionnalité. En effet, plus γ est faible, plus la nouvelle direction choisie est proche de la précédente. De même, z est interprété comme la persistance puisque, plus z est faible, moins l'individu change de direction.

Estimation des paramètres et calcul de la vitesse d'invasion

Pour étudier la pertinence de nos modèles, nous comparons leur vitesse de propagation théorique avec celle constatée en Australie au cours de l'année 2005 (légèrement supérieure à

FIGURE 12 – **Histogramme des déplacements journaliers des crapauds**

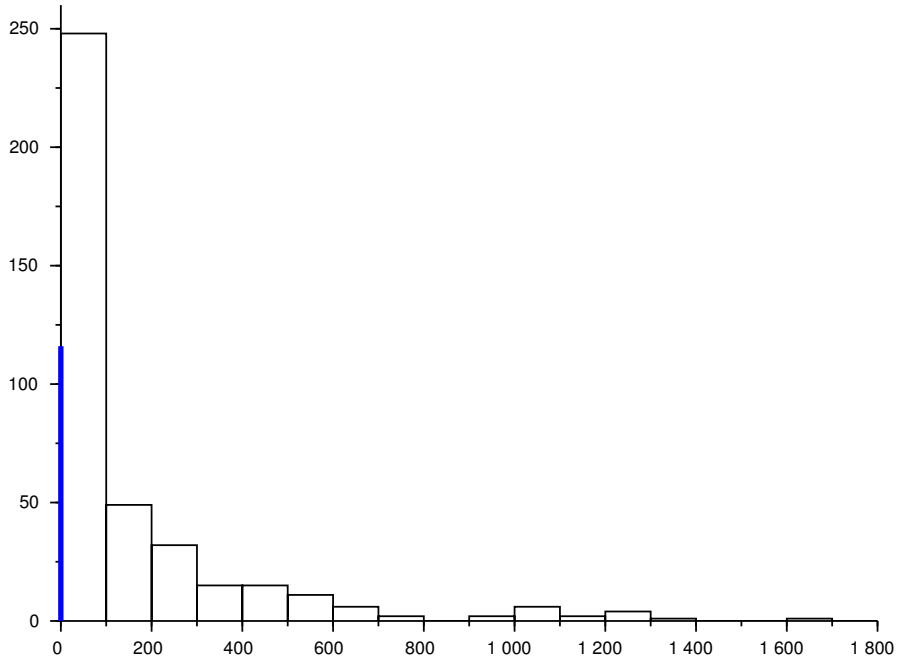

L'échantillon de données dont nous disposons sont les positions journalières de 22 crapauds relevées pour chaque crapaud pendant plusieurs jours. De ces données, nous tirons le déplacement journalier en calculant la distance entre les positions successives des crapauds. Nous obtenons ainsi 510 déplacements journaliers représentés dans l'histogramme ci-dessus. Nous représentons l'histogramme obtenu pour les classes $]100n, 100(n+1)]$*, où* $n \in 0, \ldots, 1.6$*. Nous représentons également la classe* $\{0\}$ *par un bâton bleu.*

FIGURE 13 – **Densité de probabilité de la loi de wrapped Cauchy**

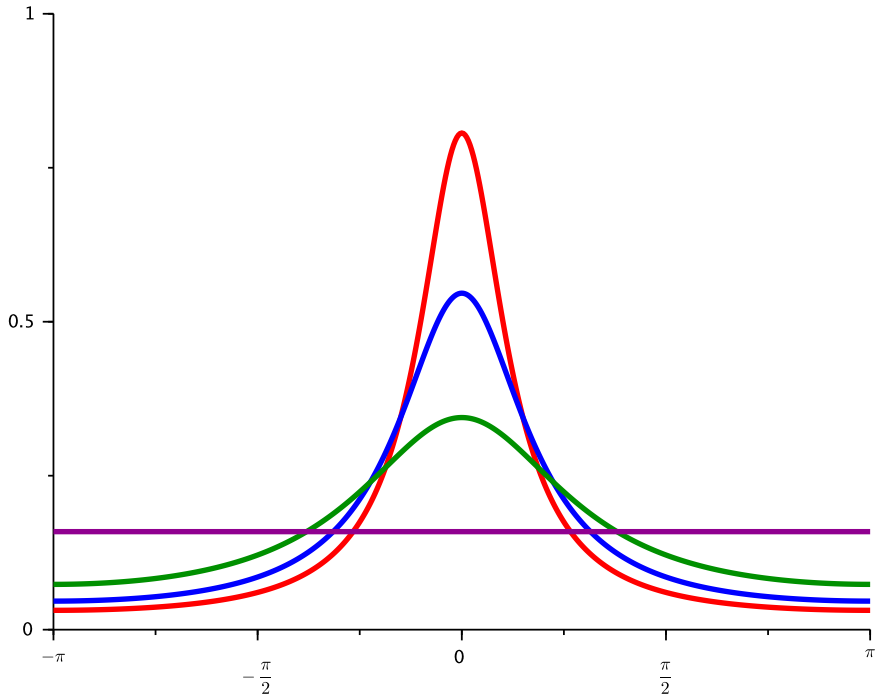

Densité de la loi de wrapped Cauchy d'espérance 0 pour $\gamma = 0.4$ (en rouge) $\gamma = 0.6$ (en bleu), $\gamma = 1$ (en vert) et $\gamma = 100$ (en mauve).
La densité est donnée par la fonction

$$f(\theta) = \frac{1}{2\pi} \cdot \frac{\sinh(\gamma)}{\cosh(\gamma) - \cos(\theta - \theta_0)},$$

où θ_0 est l'espérance (ici, $\theta_0 = 0$). Plus γ est grande, plus la fonction a tendance à s'écraser vers la distribution de la loi uniforme.

50km/an, cf. Figure 1). Deux problèmes se posent alors.

Le premier problème est d'arriver à établir une vitesse théorique de propagation pour les modèles. Pour ce faire, nous nous inspirons des méthode employées dans [26] pour trouver des solutions en ondes progressives à l'équation (6) et nous utilisons un calcul numérique pour trouver la vitesse.

Le second problème concerne les paramètres du modèle. Naturellement, la vitesse d'invasion théorique des deux modèles est une fonction de ces paramètres, que nous devons estimer à l'aide des données.

Pour les paramètres dans la phase de reproduction, nous nous fions aux données communiquées dans [80] et les références contenues à l'intérieur. Cet article donne des données sur la survie du crapaud aux différentes phases de son développment et sur le taux de fécondité des femelles. Expliquons à présent comment nous estimons les paramètres dans la phase de dispersion.

Pour le modèle EWR, nous avons déjà expliqué comment notre étude de l'histogramme 12 nous permet de sélectionner une loi empirique pour la redistribution de vitesses.

Pour le modèle ER, nous estimons les paramètres d_m, d_e, v_M, γ et z par un calcul bayesien approché sur les trajectoires. Cette méthode consiste à simuler une grande quantité de trajectoires du processus ER pour une multitude de coefficients d_m, d_e, v_M, γ et z et, par un algorithme de rejet (appelé algorithme ABC), à ne garder que celles qui sont les plus proches des véritables trajectoires des crapauds. À présent, présentons rapidement nos résultats.

La vitesse calculée pour le modèle EWR ($\approx$ 15km/an) est trop faible comparée aux 50km/an constatés. Pour le modèle ER, un nombre non-négligeables de paramètres sélectionnés sont associés à une vitesse de propagation proche de 50km/an, mais la majorité sous-estime la vitesse de propagation. Nous donnons en Figure 14 l'histogramme des vitesses d'expansion du front calculées pour les paramètres retenues par l'algorithme ABC.

En plus de ce résultat, nous faisons une analyse de la dépendance de nos modèles aux paramètres. Cette étude démontre que nos modèles sont très sensibles à une variation même faible du nombre d'individus ayant des grandes vitesses de déplacements journaliers. Cela signifie qu'il faut faire preuve d'une grande précision statistique pour manipuler ces modèles.

La conclusion de ce travail tend à confirmer que les modèles cinétiques sont à privilégier pour la modélisation de l'invasion du crapaud buffle, même si nos modèles sont perfectibles.

3.2 Effet de la dimension dans la limite d'échelle des équations cinétiques vers les équations de Hamilton-Jacobi

Dans cette partie, nous nous intéressons à l'équation cinétique (9) que nous rappelons ci-dessous :

$$\partial_t \varphi^\varepsilon + v \cdot \nabla_x \varphi^\varepsilon = \int_V M' \left(1 - e^{\frac{\varphi^\varepsilon - \varphi'^\varepsilon}{\varepsilon}}\right) dv', \quad (t,x,v) \in \mathbb{R}_+ \times \mathbb{R}^n \times V, \tag{18}$$

où $V \subset \mathbb{R}^n$. Nous rappelons que cette équation a déjà été traitée par Bouin et Calvez dans [22] mais que leur résultat nécessitait quelques corrections. Par ailleurs, nous nous placerons dans un cadre plus général. Ainsi, contrairement à [22], nous ne supposerons pas que V est symétrique. Nous supposerons seulement que 0 appartient à l'intérieur de l'enveloppe

FIGURE 14 – **Histogramme des vitesses de propagation calculées pour le modèle ER**

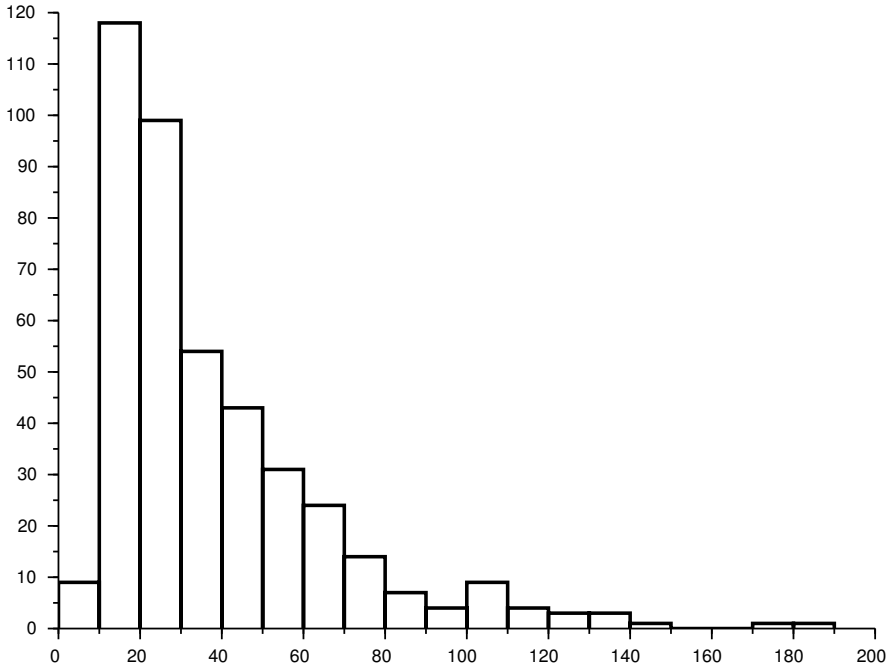

Notre algorithme ABC retient une quantité de 425 jeu de paramètres γ, d_m, d_e, v_M et z. Pour chacun, nous calculons la vitesse d'expansion théorique par une méthode s'inspirant de la recherche de solutions en ondes progressives conduite dans [26]. Nous représentons l'histogramme des 425 vitesses de propagation calculées ci-dessus. Parmi les paramètres retenus, une majorité donne une vitesse trop faible (<50km/an) mais un nombre non négligeable (31, en tout) est dans le bon ordre de grandeur (entre 50 et 60 km/an).

convexe de V. Dans ce qui suit, on ne considérera que le cas où V est convexe et on se référera au Chapitre 2 de cette thèse pour le cas général.

Comme rappelé dans la description de la méthode de la fonction test perturbée (voir l'équation (13)), notre recherche d'une limite φ^0 nous conduit à l'équation suivante :

$$(1 - \partial_t \varphi^0 - v \cdot \nabla_x \varphi^0) e^{-\eta} = \int_V M' e^{-\eta'} dv'. \tag{19}$$

En posant $Q = e^{-\eta}$, $p = \nabla_x \varphi^0$ et $H = -\partial_t \varphi^0$ on se ramène finalement à un problème spectral formulé par :

$$\text{Trouver un couple} (H, Q) \in \mathbb{R} \times L^1(V) \text{ tel que } (1 + H - v \cdot p) Q = \int_V M' Q' dv'.$$

Alors, nécessairement,

$$Q(v) = \frac{\int_V M' Q' dv'}{1 + H - v \cdot p},$$

et donc

$$1 = \int_V \frac{M(v')}{1 + H - v' \cdot p} dv'. \tag{20}$$

Si l'on suppose en plus que

$$\int_V \frac{M(v')}{\max\limits_{v \in V} v \cdot p - v' \cdot p} dv' > 1, \tag{21}$$

alors, on a par convergence monotone,

$$\begin{aligned} \lim_{H \to -1 + \max\limits_{v \in V} v \cdot p} \int_V \frac{M(v')}{1 + H - v' \cdot p} dv' &> 1, \\ \lim_{H \to +\infty} \int_V \frac{M(v')}{1 + H - v' \cdot p} dv' &= 0, \end{aligned}$$

et il existe donc un unique $H(p) \in \mathbb{R}$ vérifiant (20). Cependant, la condition (21) peut ne pas être vérifiée et dans ce cas, (20) n'a pas de solution puisque

$$\begin{cases} \int_V \frac{M(v')}{1 + H - v' \cdot p} dv' \leq 1, & \text{si } H < \max\limits_{v \in V} v \cdot p, \\ \int_V \frac{M(v')}{1 + H - v' \cdot p} dv' = +\infty, & \text{sinon.} \end{cases}$$

Il faut alors chercher des solutions du problème spectral dans l'espace des mesures positives. On trouve alors des solutions sous la forme

$$H(p) = -1 + \max_{v \in V} v \cdot p, \quad Q = \int_V \frac{M}{\max\limits_{v \in V} v \cdot p} dv + \alpha \delta_w, \tag{22}$$

où $\alpha > 0$ et δ_w est la masse de Dirac en w avec w tel que $w \cdot p = \max_{v \in V} v \cdot p$. Cette formulation de Q complique la méthode de la fonction test perturbée puisque Q est alors singulière au point w.

Dans le chapitre 2, nous nous placerons dans le cas général, nous poserons $\mu(p) = \max\limits_{v \in \text{Conv}(V)} \{v \cdot p\}$ et nous démontrerons le théorème suivant :

Theorem 0.5. *On suppose que φ^ε vérifie (18) et que la condition initiale est bien préparée, c'est-à-dire $\varphi^\varepsilon(0,x,v) = \varphi_0(x)$. Alors φ^ε converge uniformément localement vers φ^0, indépendante de v, qui est l'unique solution de viscosité de l'équation de Hamilton-Jacobi*

$$\begin{cases} \partial_t \varphi^0 + H(\nabla_x \varphi^0) = 0, \\ \varphi(0,x) = \varphi_0(x). \end{cases}$$

où H est donné implicitement par la formule (20) quand cela est possible, et $H(p) = \mu(p) - 1$ sinon.

Notre résultat est très intéressant, et ce pour plusieurs raisons. Tout d'abord, nous avons établi qu'une singularité apparaissait lors du passage de la dimension 1 aux dimensions supérieures. Cela est assez surprenant et, à notre connaissance, il n'y a pas encore d'interprétation de ce phénomène pour le processus à saut de vitesse associé à l'équation (18). Par ailleurs, le hamiltonien H que nous exhibons peut présenter une singularité C^1, ce qui est inédit dans ce type d'étude. Enfin, notre résultat généralise le travail de [22] à un espace des vitesses V non-symétrique. Cela pourrait se révéler utile, dans l'optique d'utiliser notre résultat en modélisation.

3.3 Une approche Hamilton-Jacobi pour un processus à sauts de vitesse forcé

Dans le Chapitre 3, nous traitons de l'équation cinétique suivante :

$$\partial_t u^\varepsilon + v(\theta,\varphi)\cdot\nabla_x u^\varepsilon + \frac{\alpha}{\varepsilon}\partial_\theta u^\varepsilon = \int_V M(\varphi')\left(1 - e^{\frac{u^\varepsilon - u'^\varepsilon}{\varepsilon}}\right) d\nu', \tag{23}$$

pour $\alpha = 1$, $V = \{(\theta,\varphi) \in [0,2\pi]\times[0,\pi]\}$, $d\nu(\theta,\varphi) = \sin\varphi.d\varphi.d\theta$ et

$$v(\theta,\varphi) = (\sin\varphi.\cos\theta, \sin\varphi.\sin\theta, \cos\varphi).$$

Cette équation modélise la dispersion de particules dont les vitesses sont situées sur la sphère 2-dimensionnelle et qui respectent un processus à sauts de vitesse comme celui décrit précédemment mais qui, en plus, subit en permanence une force extérieure au système qui dévie les trajectoires des particules.

Nous utilisons à nouveau la méthode de la fonction test perturbée pour démontrer un résultat de convergence pour u^ε. Plus précisément,

Theorem 0.6. *On suppose que u^ε vérifie (23) et que la condition initiale est bien préparée, c'est-à-dire $u^\varepsilon(0,x,\theta,\varphi) = u_0(x)$. Alors u^ε converge uniformément localement vers u^0 indépendante de (θ,φ) qui est l'unique solution de viscosité de l'équation de Hamilton-Jacobi*

$$\begin{cases} \partial_t u^0 + H(\nabla_x u^0) = 0, \\ u(0,x) = u_0(x). \end{cases}$$

où $H(p)$ pour $p \in \mathbb{R}^3$ est donné implicitement par la formule

$$\int_V M' \int_0^{+\infty} \exp\left(-\int_0^t (1 + H(p) - v(\theta' - \alpha s, \varphi')\cdot p) ds\right) dt d\nu' = 1. \tag{24}$$

quand cela est possible, et $H(p) = |p_3| - 1$ sinon.

Il est à noter que ce travail est une première tentative d'étude de propagation dans une équation de Vlasov avec un terme de scattering (réorientation) :

$$\partial_t f + v \cdot \nabla_x f + \mathrm{div}_v(\Gamma(v) f) = M\rho - f, \quad (t, x, v) \in \mathbb{R}_+ \times \mathbb{R}^n \times V, \tag{25}$$

où $\Gamma(v) \in \mathbb{R}^n$ est un terme de force. Jusqu'à présent le cas $V = \mathbb{S}^2$ décrit en (23) est le seul pour lequel nous avons un résultat. De ce fait, le Théorème 0.6 est quelque peu décevant car peu général. Nous tenons toutefois à justifier sa présence dans la présente thèse. Pour commencer, nous tenons à noter que, si les hypothèses ont été affaiblies, elles l'ont été pour établir des estimations *a priori* pour l'équation (23) et ainsi utiliser le théorème d'Arzelà-Ascoli. La preuve que la limite de $(\varphi^\varepsilon)_\varepsilon$ vérifie l'équation de Hamilton-Jacobi utilise peu les hypothèses qui affaiblissent la généralité de notre Théorème 0.6. Ainsi, si l'on arrive à justifier que $(\varphi^\varepsilon)_\varepsilon$ converge par une autre méthode que le théorème d'Arzelà-Ascoli, nous prétendons qu'il sera alors facile d'adapter notre preuve pour généraliser notre théorème.

Par ailleurs, nous voudrions souligner que notre résultat a exhibé un résultat très intéressant. En effet, si l'on considère (23) sans terme de force, on se retrouve dans le cas de [22, 34] traité dans cette thèse en Chapitre 2. Examinons la différence entre les deux résultats. Nous commençons par observer que la formule (24) est cohérente avec (20). En effet, sans terme de force ($\alpha = 0$), les deux formules sont équivalentes. Par contre, lorsque ces deux formules n'admettent pas de solution, on se rend compte que le hamiltonien $H(p) = \mu(p) - 1$ et celui donné par $H(p) = |p_3| - 1$ sont différents. Ainsi, malgré son manque de généralité, notre théorème a un intérêt certain.

3.4 Ondes progressives pour un modèle de transport-réaction en multi-D

Nous nous intéressons ici à l'existence de solutions en ondes progressives pour l'équation cinétique de transport-réaction

$$\partial_t f + v\nabla_x f = M(v)\rho - f + r\rho(M(v) - f), \quad \mathbb{R}_+ \times \mathbb{R}^n \times V \tag{26}$$

où $V \subset \mathbb{R}^n$ est symétrique, $\rho(t, x) = \int f(t, x, v)dv$ et M est une densité de probabilité. Comme indiqué plus tôt, l'existence de solutions en ondes progressives a été démontrée dans [26], mais seulement pour le cas unidimensionnel et pour $\inf M > 0$. Dans le chapitre 4 de cette thèse, nous étendrons ce résultat au cas multi-dimensionnel. Dans ce cadre, une solution en onde progressive est une fonction de la forme $f(t, x, v) = h(x \cdot e - ct, v)$ où $\lim_{z\to+\infty} h(z, v) = 0$ et $\lim_{z\to-\infty} h(z, v) = M(v)$. La fonction h est associée à une vitesse $c > 0$ mais aussi à une direction de propagation $e \in \mathbb{S}^{n-1}$.

Comme dans [26], cette recherche nous conduit à la résolution du problème spectral

$$\lambda c Q = (\lambda v \cdot e - 1)Q + (1 + r) \int M' Q' dv'. \tag{27}$$

La ressemblance avec le problème spectral évoqué dans le chapitre 2 est frappante et, à nouveau, le passage à la dimension supérieure ne se fait pas sans heurt. À vrai dire, il est toujours possible de définir un $c(\lambda, e)$ tel que (27) admette une solution $L^1(V)$ et la fonction $\lambda \mapsto c(\lambda, e)$ admet également un minimum c^*. On peut donc reprendre la preuve de [26] pour construire des sur-solutions et sous-solutions se déplaçant à vitesse $c > c^*$. Ce qui change dans le cas multi-D, c'est la preuve que c^* est bien la vitesse minimale, c'est-à-dire qu'aucune solution en onde progressives n'existe pour $c < c^*$.

Pour démontrer ce résultat, nous nous servirons des techniques employées dans le chapitre 2 pour généraliser les résultats de [20] pour le modèle 1-D. Plus précisément, nous obtiendrons un résultat de convergence pour le potentiel $\varphi^\varepsilon = -\varepsilon \ln\left(\frac{f(t/\varepsilon,x/\varepsilon,v)}{M(v)}\right)$. Puis, nous utiliserons l'approche de l'optique géométrique : nous démontrerons que φ^ε converge vers φ^0 solution d'une équation de Hamilton-Jacobi. Nous démontrerons ensuite que le domaine $\left\{(t,x) \in \mathbb{R}_+ \times \mathbb{R}^d \mid \varphi^0(t,x) = 0\right\}$ se propage à vitesse c^* et enfin, nous démontrerons l'égalité $\left\{\varphi^0 = 0\right\} = \{f > 0\}$ pour

$$\varphi^0(0,x) = \begin{cases} +\infty & \rho(0,x) = 0 \\ 0 & \rho(0,x) > 0 \end{cases}.$$

Enfin, nous démontrerons deux résultats de propagation pour des données initiales de f différentes, à savoir une donnéee initiale à support compact et une donnée initiale à support dans une bande.

3.5 Méthode de la fonction test perturbée pour une EDP avec terme aléatoire

Dans ce travail, nous nous intéressons à l'EDP suivante qui comporte un terme aléatoire :

$$\partial_t f^\varepsilon + \frac{v}{\varepsilon} \cdot \nabla_x f^\varepsilon = \frac{\lambda}{\varepsilon^2}\left(M\rho^\varepsilon - f^\varepsilon\right) + \frac{1}{\varepsilon^2}\rho^\varepsilon v \cdot \nabla_x \overline{m}_t^\varepsilon, \quad (t,x,v) \in \mathbb{R}_+ \times \mathbb{T}^d \times V, \tag{28}$$

où $\mathbb{T}^d$ est le tore en dimension d, $\rho^\varepsilon = \int_V f^\varepsilon dv$ et $\overline{m}_t^\varepsilon(x) := \overline{m}_{t/\varepsilon^2}(x)$ avec $(\overline{m}_t)_t$ un processus de Markov stationnaire. L'équation (28) est obtenue après le réechelonnement $(t,x,v) \to (t/\varepsilon^2, x, v)$ dans l'équation

$$\partial_t f + \varepsilon v \cdot \nabla_x f = \lambda\left(M\rho - f\right) + \rho v \cdot \nabla_x \overline{m}_t, \quad (t,x,v) \in \mathbb{R}_+ \times \mathbb{T}^d \times V.$$

La motivation de travail, une nouvelle fois, provient de problèmes de modélisation issus de la biologie. Considérons

$$\partial_t f + v \cdot \nabla_x f = \lambda\left(M\rho - f\right) + \rho\left(v \cdot \nabla_x \overline{m}_t\right)_+, \quad (t,x,v) \in \mathbb{R}_+ \times \mathbb{T}^d \times V, \tag{29}$$

où g_+ est la partie positive de la fonction g. L'équation (29) modélise la densité mésoscopique d'un système de particules qui suit un processus à sauts de vitesse avec des sauts de fréquence λ. Par ailleurs, les particules sont sensibles aux variations d'un agent attractif dont la densité est donnée par la quantité $\overline{m}_t(x)$. Pour s'orienter, les particules privilégient les directions vers lesquelles la quantité de l'agent attractif augmente. On peut par exemple interpréter cet agent attractif comme un nutriment et les particules comme des cellules qui cherchent à consommer ce nutriment. Notons toutefois que, dans ce modèle, la quantité de nutriment n'est pas dégradée par les particules.

Dans notre travail, nous considérons que la densité des nutriments est un processus aléatoire donné par le processus $\overline{m}$. Nous considérons également l'équation sans la partie positive considérée dans (29). En conséquence, notre équation ne vérifie pas de conservation de la positivité. Cela signifie que, même avec une condition initiale positive, une solution de l'équation peut devenir négative. Cette hypothèse a pour effet de simplifier notre étude mais elle limite son intérêt du point de la modélisation bio. Ainsi, une perspective que nous souhaitons poursuivre par la suite, serait de démontrer le même type de résultat en gardant la partie positive dans l'équation.

Comme dans [51], nous démontrons un résultat de convergence pour la suite $(\rho^\varepsilon)_\varepsilon$. Plus précisément, nous démontrons que ρ^ε converge en loi dans $C([0,\tau], H^{-\delta}(\mathbb{R}^d))$ vers la solution ρ de l'EDP stochastique

$$\begin{aligned} d\rho &= \frac{1}{\lambda^2}\mathrm{div}\left(\left(\lambda K(M) - \mathbb{E}K\nabla_x\eta_0' K\nabla_x\eta_0\right)\nabla_x\rho\right)dt && (30)\\ &- \frac{1}{\lambda^2}\mathrm{div}\left(\rho\mathbb{E}K\nabla_x\eta_0'\mathrm{div}\left(K\nabla_x\eta_0\right)\right)dt && (31)\\ &+ P(\rho)\Sigma^{1/2}\circ dW_t, \quad \text{in } \mathbb{R}_+\times\mathbb{R}^d. && (32)\end{aligned}$$

Nous spécifierons toutes les notations utilisées dans cette formule ansi que les hypothèse que nous utilisons dans le Chapitre 5. Pour démontrer ce résultat, nous utiliserons la méthode de la fonction test perturbée en nous inspirant de [51].

Nous souhaitons souligner une spécificité intéressante dans notre résultat. En examinant (30), nous pouvons nous rendre compte que le terme de diffusion

$$\mathrm{div}\left(\left(\lambda K(M) - \mathbb{E}K\nabla_x\eta_0 K\nabla\eta_0'\right)\nabla_x\rho\right),$$

comporte une partie négative. Si l'on se place dans la cas déterministe, on a alors $\eta_0 \equiv \eta_0' \equiv 0$. Cela signifie que, dans notre cadre, ce sont les termes stochastiques qui diminuent la diffusion dans l'équation limite. Cela est plutôt inattendu et nous voudrions nous pencher sur ce résultat plus en avant à l'avenir.

4 Perspectives

À présent que nous avons détaillé les contributions apportées par cette thèse, nous voudrions proposer quelques pistes de réflexion pour compléter ou poursuivre ces résultats.

4.1 Modélisation du crapaud buffle

Après notre étude statistique, nous nous proposons de conduire plusieurs travaux pour poursuivre notre réflexion. Pour commencer, il convient de rendre nos modèles plus précis. Pour ce faire, nous proposons d'affiner notre étude statistique. En effet, dans nos deux modèles, nous avons supposé que le comportement de tous les individus étaient les mêmes. Or, comme nous indiquons en conclusion de notre Chapitre 1, cette hypothèse a tendance à ralentir la propagation dans notre modèle et elle est contredite par les données. En effet, ces dernières montrent que, parmi les 22 crapauds suivis, seuls 11 ont eu au moins un déplacement de plus de 600 mètres d'un jour sur l'autre. Pour nous en convaincre, nous renvoyons à notre Annexe A où nous présentons les données dont nous nous sommes servis.

Comme indiqué plus tôt, notre travail sur les crapauds est une première étape avant d'étudier un modèle plus ambitieux. Ainsi, nous proposons de nous inspirer de l'équation du crapaud buffle pour bâtir un modèle cinétique qui incluent un phénotype hétérogène au sein de la population. Comme exemple, nous pouvons penser à l'équation suivante :

$$\frac{\partial f}{\partial t} + v\cdot\nabla_x f - \alpha\frac{\partial^2 f}{\partial z^2} = z(M(v)\rho - f) + r\rho(M(v) - f), \quad (t,x,v,z)\in\mathbb{R}_+\times\mathbb{R}^d\times V\times Z, \quad (33)$$

où $\rho(t,x,z) = \int f(t,x,v,z)dv$, $V \subset \mathbb{R}^d$ et $Z \subset \mathbb{R}_+$. Cette équation reprend l'équation (6) et s'inspire de l'équation du crapaud buffle pour la prise en compte de mutations génétiques. L'équation (33) modélise la propagation d'une espèce qui suit un processus à sauts de vitesse dont la fréquence z de changement de direction est un trait phénotypique hétérogène au sein de la population.

De manière similaire aux travaux sur l'équation du crapaud buffle, nous proposons d'étudier des résultats de propagation dans cette équation. Nous pensons que la présente thèse facilite le travail, puisque nous avons généralisé les résultats de [26] au cas multi-dimensionnel. Enfin, si cette étude présente des résultats satisfaisants (c'est à dire une propagation accélérée ainsi qu'un tri spatial), nous pourrons envisager de confronter le modèle aux données statistiques dans le même esprit que notre Chapitre 1.

4.2 Formalisme Hamilton-Jacobi dans les équations cinétiques avec terme de force

Revenons sur l'équation (23). Après réechelonnement hyperbolique $(t,x,v) \to (t/\varepsilon, x/\varepsilon, v)$, l'équation devient :

$$\partial_t f^\varepsilon + v \cdot \nabla_x f^\varepsilon + \frac{1}{\varepsilon}\mathrm{div}_v(\Gamma(v) f^\varepsilon) = \frac{1}{\varepsilon}\left(M\rho^\varepsilon - f^\varepsilon\right), \quad (t,x,v) \in \mathbb{R}_+ \times \mathbb{R}^n \times V.$$

Ici, le bon ansatz WKB est le suivant : $f^\varepsilon = \overline{M} e^{-\frac{\varphi^\varepsilon}{\varepsilon}}$, où $\overline{M}$ est une solution de $\mathrm{div}_v(\Gamma \overline{M}) = M\int_V \overline{M} dv - \overline{M}$. La fonction $(\varphi^\varepsilon)_\varepsilon$ est alors solution de :

$$\partial_t \varphi^\varepsilon + v \cdot \nabla_x \varphi^\varepsilon = \frac{\Gamma(v)}{\varepsilon} \cdot \nabla_v \varphi^\varepsilon = \frac{M}{\overline{M}} \int_V \overline{M}' \left(1 - e^{-\frac{\varphi^\varepsilon - \varphi'^\varepsilon}{\varepsilon}}\right) dv'.$$

Nous proposons d'étudier la limite $\varepsilon \to 0$ de φ^ε. Comme annoncé plus tôt, nous pensons que l'identification de l'équation de Hamilton-Jacobi limite faite dans notre Chapitre 3 peut être facilement adaptée à ce cas plus général. Toutefois, il faudra changer de méthode pour démontrer le résultat de convergence par rapport à notre approche car nous pensons que les estimations *a priori* sont impossbiles à établir en toute généralité. Nous proposons de nous inspirer de la méthode des semi-limites relaxées mise en place au Chapitre 4 pour parvenir à nos fins.

4.3 Application de notre limite de diffusion stochastique en biologie

Comme annoncé plus tôt, notre résultat de limite de diffusion dans le contexte stochastique ne peut pas être directement appliquée en modélisation biologique, car notre équation ne préserve pas la positivité. Nous proposerons dans un travail futur de nous intéresser à l'équation

$$\partial_t f^\varepsilon + \frac{v}{\varepsilon} \cdot \nabla_x f^\varepsilon = \frac{\lambda}{\varepsilon^2}\left(M\rho^\varepsilon - f^\varepsilon\right) + \frac{1}{\varepsilon^2}\rho^\varepsilon \left(v \cdot \nabla_x \overline{m}_t^\varepsilon\right)_+, \quad (t,x,v) \in \mathbb{R}_+ \times \mathbb{T}^d \times V, \tag{34}$$

et de démontrer un résultat de convergence similaire à celui du Chapitre 5. Enfin, nous voudrions comprendre comment expliquer la diminution de la diffusion dûe au terme stochastique dans l'équation (30).

Première partie

Étude statistique d'une invasion biologique : le cas du crapaud buffle en Australie

Chapitre 1

L'expansion du crapaud buffle avec des modèles à sauts de vitesse

Dans ce travail en commun avec Vincent Calvez et Samuel Soubeyrand, nous développons deux modèles mathématiques pour la propagation d'une espèce invasive, motivés par le problème de l'invasion du crapaud buffle en Australie. En nous référant à la littérature existante, nous séparons notre modèle en deux phases : une phase dite de dispersion, où les crapauds envahissent leur environnement et une phase de reproduction, où ils sont immobiles mais où la population augmente. Pour les deux modèles, nous considérons le même modèle de reproduction, qui provient de la littérature biologique. Pour la phase de dispersion, nous considérons deux modèles à sauts de vitesse. Ces modèles se basent sur des observations sur le terrain, montrant que les crapauds ont une tendance à avoir des directions de déplacement persistantes. Pour les deux modèles, nous dérivons une formule théorique pour la vitesse de propagation des crapauds, obtenue depuis l'équation cinétique satisfaite par la densité mésoscopique du processus à sauts de vitesse. Cette vitesse dépend naturellement des paramètres du modèle, qui ont des interprétations biologiques. Nous estimons les paramètres dispersifs par le biais de statistiques sur les déplacements journaliers de crapauds buffle (*Rhinella marina*) en Australie. Enfin, nous comparons les vitesses de propagation calculées par ces estimations avec la véritable vitesse de propagation des crapauds.

Contents

1.1 Introduction

The cane toad's invasion in Australia has recently raised a lot of interest from both the biology and the mathematics community. Since the first introduction in 1935 in Queensland, Australia of one hundred individuals, the population has raised to two hundred millions and is now present overall the North-eastern coast of Australia [110]. This propagation has dramatic ecological effects since the cane toad has a large variety of preys but not so many predators, thanks to their toxic skin [109]. This issue has naturally drawn interest from the biology community. Various sources have confirmed the well adaptedness of the species to its new environment, in comparison to the species' native South America [3, 10, 73, 80, 81]. Not only has the toad well adapted to its environment but its propagation has accelerated from 10km/year to more than 50km/year [93, 110]. Similar accelerated expansion has already been reported for different species, among which the bush cricket in Britain [106].

One possible explanation to this acceleration is that spatial sorting is driven by evolutionary processes [93, 96, 102, 103] : the most dispersive toads have the ability to move farther away. Reproduction and genetical transmission favor the rise of the most dispersive individuals at the propagation front. Thanks to the randomness of the genetical processes, the new generation can have individuals with even better dispersive abilities, causing the front to accelerate.

This hypothesis has raised the interest of the mathematical community. The classical framework for the modeling of population spatial dynamics relies on diffusion equations. The so-called cane toad equation [23] was built from the famous Fisher-KPP equation [61, 78]. This equation describes the density of a population of individuals which propagation is a diffusion process with heterogeneous diffusion coefficient within the population. This coefficient is interpreted as a phenotypical trait which, itself, follows a diffusion process. The reaction term is a non-local mono-stable operator similar to the one from the Fisher-KPP equation.

When the set Θ of admissible traits is bounded, travelling waves exist [23], and one can show that the propagation front has a constant speed [107]. When Θ is infinite, one observes an accelerating front [13, 25, 28]. Superlinear spreadings have also been established on the cane toad equation for a different kind of reaction term, namely a bistable reaction term [27] and a local reaction term [28].

Recently, the validity of diffusion models for the propagation of the toads was challenged. Indeed, diffusive dispersal models have constantly underestimated the speed of invasion, when confronted to data, despite taking reproduction and dispersive behavior evolution into account [91]. Individual observations of captive toads showed that some individuals have a tendency to walk in persistent directions and that this behavior is transmitted from one generation to the next [33]. Moreover, it was established that the toads who show more persistence (ability to keep a compass direction for a long time) and more directionality (small variance of the turning angle when choosing a new compass direction) are the ones found at the vanguard of the invasion [83].

This new information could explain why diffusion models have failed to provide an accurate speed of propagation since the invasion front is led by toads who have a superdiffusive dispersive behavior. Such an issue has already been faced and dealt with in the modeling of the propagation of the *Escherichia coli* bacterium. A set of experiments has shown that the diffusion approximation was not valid and that one has to stick to a kinetic equation at the mesoscopic scale to accurately describe the propagation of the bacteria [98].

Kinetic equations, such as the well-known Boltzmann equation, have originally been defined to study the behavior of huge systems of interacting particles, such as a confined gas. They have also been successfully adapted for biological means, such as the modeling of *Escherichia coli* [98], the Cucker-Smale model for bird flocking [39], alignement interactions for self-propelled particles [52] or the formation of pheromone trails for the common ant [16], among many other examples. A kinetic equation is a mesoscopic description of a large set of small particles that we can describe at the microscopic scale through very simple interactions. The main difference with diffusion equations is that we keep the information about the velocity of individuals while studying the density of particles (thus, the "mesoscopic" term). We pay this by the addition of a new variable : while macroscopic densities in diffusion equations are functions of the time t and the space x, mesoscopic densities are functions of t, x but also of the velocity variable v.

In this paper, we build two models that match more accurately the range expansion of the toads than diffusion models. Those models are inspired by [91] for the reproduction process but we change the dispersal process of the toads following fields observations made in [33, 83]. We test the validity of both models on their capacity to accurately describe the propagation of the cane toad in Australia during the year 2005. The theoretical speed of propagation is obtained by looking for travelling wave solutions in the same spirit as [21, 23]. Naturally, this theoretical speed of propagation is a function of the dispersal parameters of the models. We estimate those parameters thanks to data on daily trajectories of the toad during the wet season 2005. Finally, we check whether the estimated parameters provide a theoretical speed of invasion that is close to the actual range expansion of that time.

Considering our relatively short time scale, we consider in our models that the population does not evolve, such that our models provide a constant theoretical speed of invasion, hence no acceleration arises. Thus, our models do not accurately describe the propagation of the

toads for a time scale of 80 years. However, one of our models provides satisfactory results in our small time scale. It may be adapted for a longer time scale with addition of an evolutionary process. Thus, this paper is a validation of the well-adaptedness of kinetic equations for the cane toads' modeling and a preliminary work before adding evolutionary changes to this framework.

We detail what we mean by travelling wave solutions, how to find them and how to obtain the speed formula in Section 1.2. We describe our two models in Section 1.3 and explain how the theoretical speed of propagation of the model is obtained via an implicit formula. In Section 1.4, we detail how we estimate the reproduction and dispersal parameters, thanks to data. To estimate the dispersal parameters of our first model, we summarize the data with the help of the so-called "Time averaged mean-square displacement", we use approximate bayesian computation to select the parameters that best matches the daily displacements of the toads and we finally compute the theoretical speed of propagation with the estimated parameters. For the second model, we use more standard statistical tools. The Section 1.5 is devoted to the presentation and a discussion of our results, as well as a sensitivity (with respect to the parameters) analysis and some perspectives to adapt our model to a larger time scale.

1.2 Travelling waves

One way to capture the speed of propagation of a system of interacting particles, *e.g.* a colony of living individuals, is to look for traveling wave solutions. The idea behind this notion comes from the observation that some invasive species tend to invade their environment at a constant speed, with their density forming a constant shape, or profile, moving with this speed.

The search for travelling wave solutions of kinetic equations has already been investigated in [46, 71, 99]. We illustrate this notion on an example of a velocity-jump process modeled at the mesoscopic scale by the following kinetic equation :

$$\partial_t f + v \cdot \nabla_x f = M(v)\rho - f + r\rho(M(v) - f), \quad (t, x, v) \in \mathbb{R}_+ \times \mathbb{R}^d \times V, \tag{1.1}$$

where, $V \subset \mathbb{R}^d$ is compact and symmetric, $\rho(t,x) := \int_V f(t,x,v)dv$, $M \in L^1(V)$ is a probability density function and $r > 0$. This equation models the mesoscopic density of a population structured with respect to its space variable x and its velocity variable v. Starting from its initial condition, the population moves according to the following mechanism : every individual moves in straight lines with velocity v and after an exponential random time, chooses randomly a new velocity with probability density function M on V, independently from its last velocity. With a reproductive rate $r > 0$, new individuals are created proportionaly to the density ρ. They move with a velocity chosen randomly with the same law and finally, a carrying capacity of the environment limits the density such that $0 \leq f \leq M$.

A travelling wave solution of (1.1) is a solution of the form $f(t,x,v) = h(x \cdot e - ct, v)$, where $e \in \mathbb{S}^{d-1}$ and $c > 0$ are fixed parameters. Moreover, we ask that h has the following limits

$$\lim_{z \to -\infty} h(z,v) = M(v), \quad \lim_{z \to +\infty} h(z,v) = 0. \tag{1.2}$$

If one represents the function $h(x \cdot e - ct, v)$ as a function of x and v for consecutive times t, one sees the shape of function h being dragged with velocity c towards the direction $e \in \mathbb{S}^{d-1}$.

Therefore, we understand h as the profile, e as the direction and c as the speed of the travelling wave.

The function $h(z,v)$ necessarily satisfies :

$$(-c+v\cdot e)\frac{\partial h}{\partial z} = M(v)\int_V h(v')dv' - h + r\int_V h(v')dv'\,(M(v)-h)\,, \quad (z,v)\in\mathbb{R}\times V. \tag{1.3}$$

We expect a so-called *pulled* front, that is, we expect the propagation of the population to be driven by small population at the edge of the front. That's why we suppose that the propagation is driven by individuals which are not subject to the inter-specific competition and we study the linearized problem

$$(-c+v\cdot e)\frac{\partial \tilde{h}}{\partial z} = M(v)\int_V \tilde{h}(v')dv' - h + rM(v)\int_V \tilde{h}(v')dv', \quad (z,v)\in\mathbb{R}\times V. \tag{1.4}$$

We look for solution of (1.4) using separation of variables, that is solutions of the form $\tilde{h} = e^{-\lambda z}Q \geq 0$ which gives the following spectral problem :

$$\lambda(c-v\cdot e)Q = M(v)\int_V Qdv - Q + rM(v)\int_V Qdv, \quad v\in V. \tag{1.5}$$

In [21, 26], the authors have shown that, for all $\lambda > 0$, the spectral problem (1.5) has a solution $(c(\lambda), Q)$ and that the function $\lambda \mapsto c(\lambda)$ has a global minimum $c^* > 0$. Moreover, they proved that travelling wave solutions (c,h) exists for all $c \geq c^*$.

The previously defined c^* is a crucial tool to understand the propagation of the modeled process. One can indeed prove (see [23]) that, starting from a biologically relevant initial condition, that is, a compactly supported initial condition satisfying $0 \leq f \leq M$, the solution of the equation will satisfy

$$\begin{cases} \lim\limits_{t\to+\infty} f(t, x\cdot e + ct, v) = 0, & \text{if } c > c^* \\ \lim\limits_{t\to+\infty} |M(v) - f(t, x\cdot e + ct, v) = 0|\,, & \text{if } 0 \leq c < c^* \end{cases}.$$

The interpretation is straight-forward : if one is following the population with a velocity greater than c^*, then one will eventually end up in an empty zone. In the opposite case, one will end up in a saturated zone, *i.e.* a zone where f is equal to the carrying capacity M.

From a biological point of view, this means that the population will expand with velocity c^*. To evaluate the speed of propagation of our two models, we will also look for travelling wave solutions and keep the minimal speed as our theoretical speed of propagation.

1.3 The two models

The following models are designed to fit as accurately as possible the dispersal behavior of *Rhinella marina*. On the matter, the tropical Australian year can be split into two seasons. During the dry season, the toads barely move and stay close to water sources. This is when toads mate and female toads lay eggs. During one dry season, a fertile egg will evolve through a tadpole stage and a metamorph stage to a juvenile toad. Only at the next dry season will it be an adult, ready to move away from its pond.

The wet season runs from November to April. This is when the propagation of the adult toads is observed. Toads tend to walk with a persistent direction for several days and make pauses that can also last several days.

The Figures 1.1, 1.2, 1.3 and 1.4 show examples of trajectories of toads that were radio tracked for several days during the wet season 2005 (November 2004- April 2005) at a location between the city of Darwin and the Adelaide river (UTM zone : 52L). One can also find in the Annex A all the trajectories of the toads that were tracked during wet season 2005.

Similar to [91] and according to the behavior of the cane toads, we build a model based on two different phases.

The first phase is the dispersal phase. During this phase, we suppose that the overall number of toads does not change. We emphasize that this means that no toads are born (which is biologically relevant), but mostly that no toads die during the dispersal seasons. The only time where we consider death events is during the dry season, where we consider an adult survival rate $\sigma_a < 1$.

The second phase is the reproductive phase and it is the same for both models. It describes the number of adult and juvenile toads at the end of the dry season, given their number at the beginning of the season. This process will be parametrized by biologically relevant parameters, such as the number of eggs a female can lay or the survival rate of the young toads through their developmental process.

We consider that the two phases succeed each other indefinitely and last both for a time $T > 0$. Since the wet season extends from November to April and the dry season from May to October, T can be interpreted as the duration of a season, *ergo* T are six months and $2T$ is one year. The Figure 1.5 illustrates this succession of phases.

The two models we consider only differ on the dispersive phase and are based on kinetic equations, *i.e* velocity structured equations. In the first model, we will consider two dispersal modes : an encamped (E) mode, where the individuals do not move and a running (R) mode where they move. This model will be referred as the ER model. In the second model, we will consider intermediate walking (W) modes and, once again, an encamped (E) and a running (R) mode. This model will hence be referred as the EWR model.

1.3.1 The reproduction phase

The reproduction phase is common to both models.

We refer to [80] and the references therein for details about the biological relevance of the model. Our model is the following. We consider three populations : the adults, that is, individuals which are 1 year old or older, among which the moving toads and the encamped toads, and the juveniles which are between 1 month and 1 year old. We denote by m the total amount of moving adults, by E the total number of encamped adults and by J the total amounts of juveniles. At the end of every dry season, the number of adults is the number of adults which survived the year plus the number of juveniles which survived the year and are

FIGURE 1.1 – **Trajectory of toad 8**

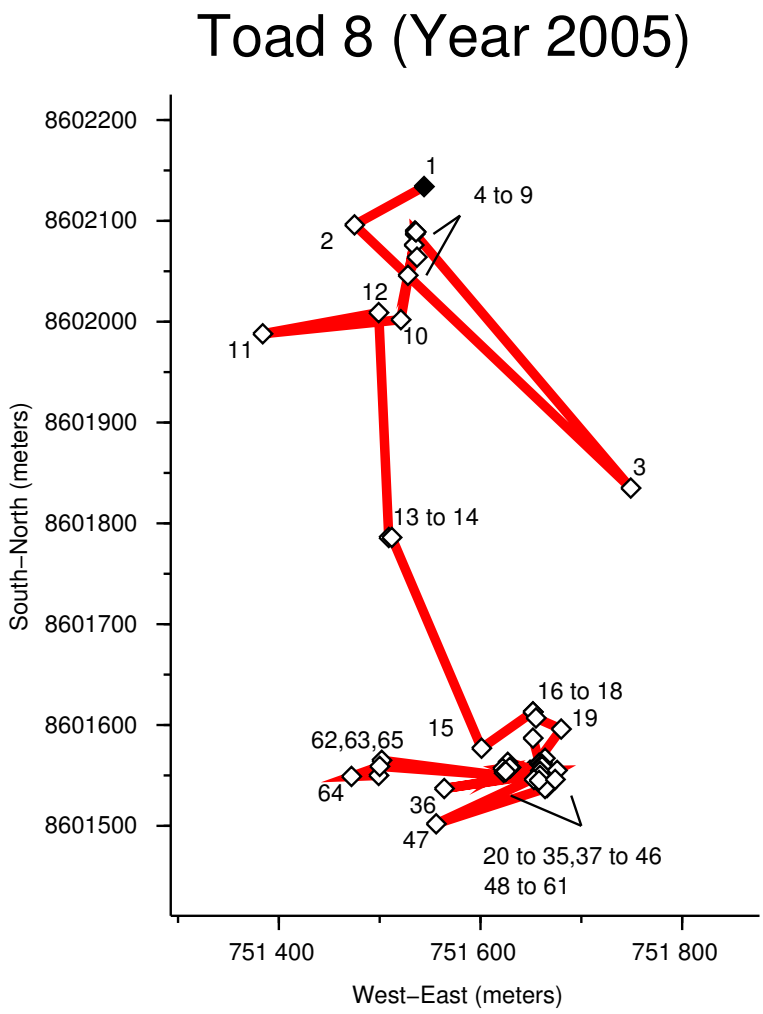

Trajectory of Toad number 8, radio tracked between 02/04 and 04/30 of year 2005.
Black diamond : original position of the toad.
White diamonds : daily position of the toad after the release.
x-axis : West-Eastern UTM coordinates.
y-axis : South-Northern UTM coordinates.
Courtesy of G. Brown, B. Phillips and R. Shine.

FIGURE 1.2 – **Trajectory of toad 9**

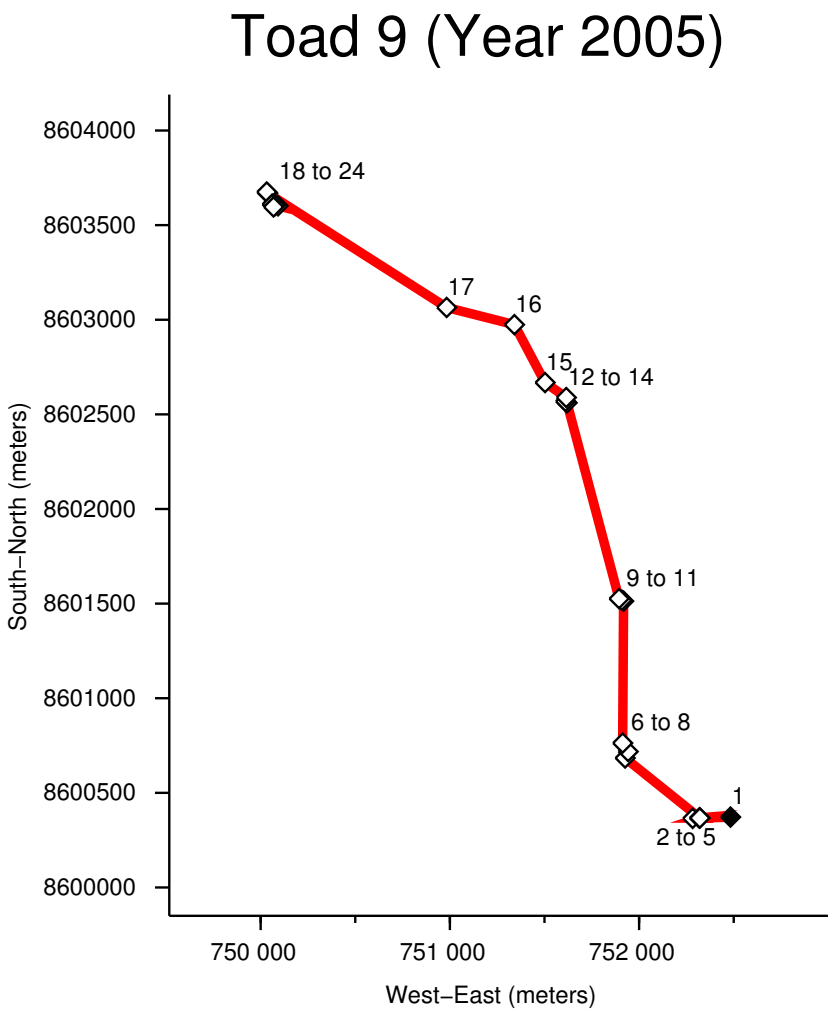

Trajectory of Toad number 9, radio tracked between 03/02 and 03/25 of year 2005
Black diamond : original position of the toad.
White diamonds : daily position of the toad after the release.
x-axis : West-Eastern UTM coordinates.
y-axis : South-Northern UTM coordinates.
Courtesy of G. Brown, B. Phillips and R. Shine.

FIGURE 1.3 – **Trajectory of toad 16**

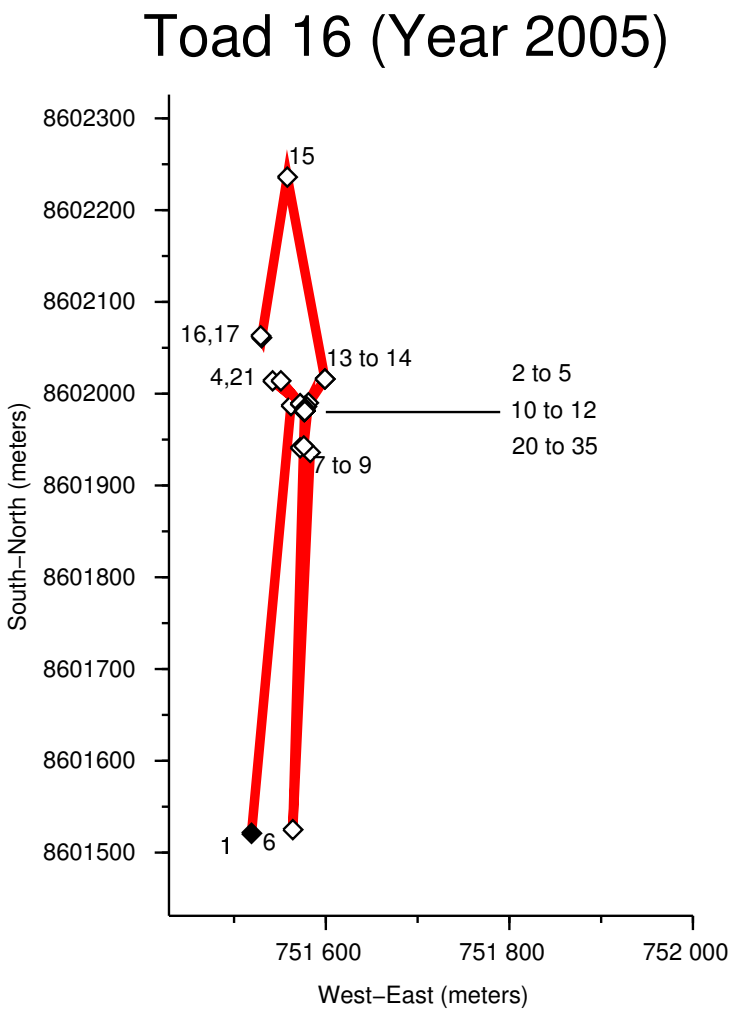

Trajectory of Toad number 16, radio tracked between 03/27 and 04/30 of year 2005.
Black diamond : original position of the toad.
White diamonds : daily position of the toad after the release.
x-axis : West-Eastern UTM coordinates.
y-axis : South-Northern UTM coordinates.
Courtesy of G. Brown, B. Phillips and R. Shine.

FIGURE 1.4 – **Trajectory of toad 21**

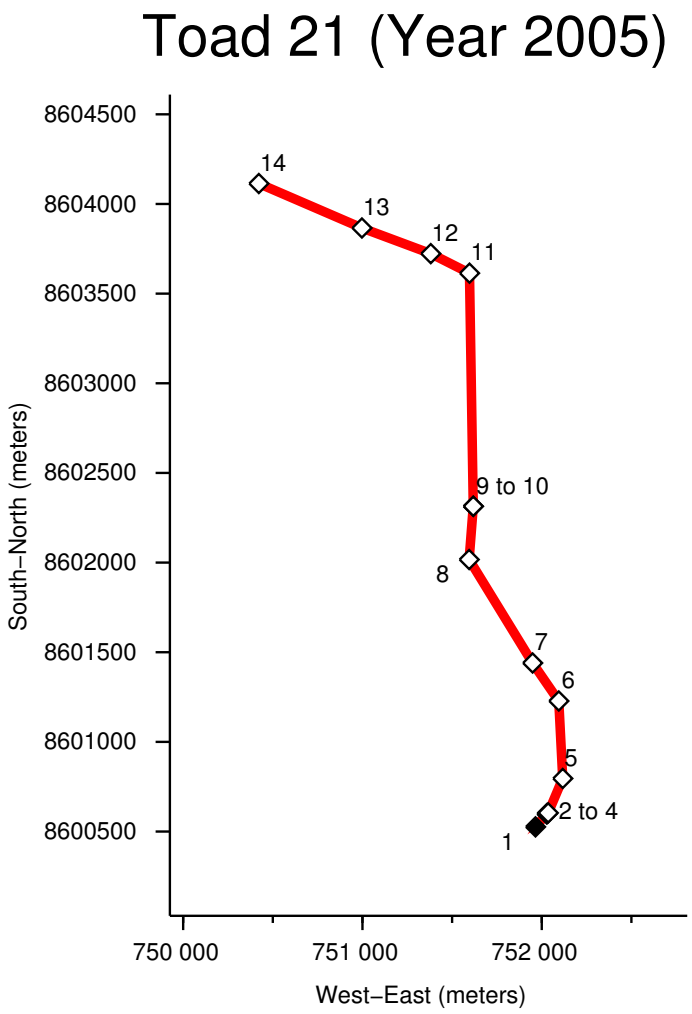

Trajectory of Toad number 21, radio tracked between 04/17 and 04/30 of year 2005.
Black diamond : original position of the toad.
White diamonds : daily position of the toad after the release.
x-axis : West-Eastern UTM coordinates.
y-axis : South-Northern UTM coordinates.
Courtesy of G. Brown, B. Phillips and R. Shine.

FIGURE 1.5 – **The two phases of our models**

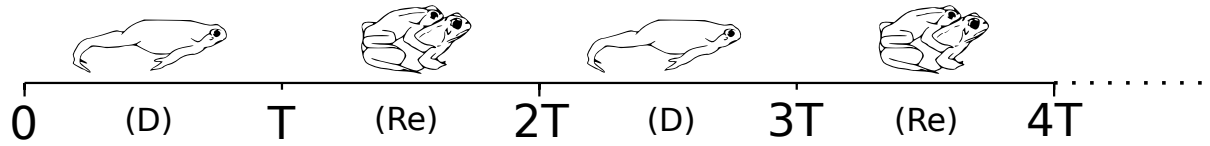

In both our models, we consider a succession of a dispersive phase between time $2nT$ *and* $(2n+1)T$ *(wet season) and a reproduction phase between time* $(2n+1)T$ *and* $(2n+2)T$ *(dry season). Drawings : courtesy of Margo Perkins.*

now adults. The new number of adults is therefore :

$$\sigma_a m + \sigma_a E + \sigma_j J, \tag{1.6}$$

where $0 \leq \sigma_a \leq 1$ is the adults' survival rate and $0 \leq \sigma_j \leq 1$ the survival juveniles' rate. We consider that every juvenile becomes an adult after one year such that the only juveniles present at the end of a the reproduction season are the ones who were born at the beginning of the season.

We suppose that as many females as males are born from a clutch and that their survival and dispersal rates are the same. Therefore, we consider that the females' population represents 50% of the total population repartition regardless of geographical or environmental considerations. Following [80] and references therein, we suppose that every adult female lays one clutch of size ϕ every year. Every fertilized egg must go through a developmental process that will finally turn it into a juvenile.

Within two to four days, a tadpole hatches from the egg [80, 109]. After 14 to 28 days, the tadpole metamorphoses into a juvenile [10, 73] through a metamorph phase.

At every step, a death event may occur such that every evolution is associated with a survival rate : we denote by σ_{egg} the egg survival rate, by σ_t the tadpole survival rate and by σ_m the metamorphe survival rate. Through this process, the recruitment success ratio is given by

$$F = \frac{1}{2}\phi\sigma_{egg}\sigma_t\sigma_m.$$

We suppose that a proportion p of the juveniles will start the dispersal phase encamped and that $1-p$ will start as moving toads. Finally, the reproduction operator we consider is given by

$$(J, m, E) \mapsto \begin{pmatrix} 0 & F & F \\ (1-p)\sigma_j & \sigma_a & 0 \\ p\sigma_j & 0 & \sigma_a \end{pmatrix} \begin{pmatrix} J \\ m \\ E \end{pmatrix} \tag{1.7}$$

Let us mention here that our model slightly differs from Lampo and de Leo's model, where the tadpole survival rate is given by

$$\sigma_t(\mathcal{T}) = \frac{\sigma_{t\,\max}}{1 + d\mathcal{T}},$$

where $d > 0$, $\sigma_{t\,\max} > 0$ and $\mathcal{T}$ is the tadpole density. Through the earlier exposed process, the tadpole density is given by :

$$\mathcal{T} = \frac{1}{2}\phi\sigma_{egg}(m + E).$$

The propagation of the cane toad being pulled by small populations at the edge of the front, the theoretical speed of propagation of our model will be computed in areas where $m \ll 1$ and $E \ll 1$, so we will consider that $\mathcal{T} \ll 1$, such that no intra-specific competition is involved and

$$\sigma_t(\mathcal{T}) = \sigma_t = \sigma_{t\,\max}.$$

The Figure 1.6 illustrates our reproduction model.

1.3.2 The ER model

We develop here a model based on fields observations compiled in [33, 83]. The process has two different behavior depending if it is the dispersal (D) phase or the reproduction (Re) phase. During the reproduction phase, we consider the model described earlier. During the dispersal phase, we consider all individuals to follow the same piecewise deterministic Markov process (PDMP) on $\mathbb{R}^2$: an individual can be either in a "running" or in a "encamped" mode. When it is in encamped mode, the individual does not move, when it is in running mode, it moves. We suppose that those two phases succeed each other. The encamped mode lasts for an exponential time with mean d_e and the running mode lasts for an exponential time with mean d_m. At the end of the encamped mode, the individual starts to run again with the velocity it had during the last running mode. Moreover, we suppose that a proportion $\frac{d_e}{d_m+d_e}$ of juveniles will start the dispersal season encamped and a proportion $\frac{d_m}{d_m+d_e}$ will be moving.

We consider that the toads are physically equal, so they can all walk at various speeds, up to a maximal speed $v_M > 0$. Starting at a position x, an individual in running mode has a velocity v chosen uniformly randomly on the disc $D_{v_M} := \left\{v \in \mathbb{R}^2 \mid |v| \leq v_M\right\}$. Hereafter, we parametrize the vectors in D_{v_M} with their polar coordinates $(r, \theta) \in [0, v_M] \times [0, 2\pi)$ and set $v(r, \theta) := (r\cos\theta, r\sin\theta)$. The position of an individual at time $t > 0$ is therefore given by :

$$X_t = x + r \begin{pmatrix} \cos\theta \\ \sin\theta \end{pmatrix} t. \tag{1.8}$$

After a random exponential time with mean $\frac{1}{z} > 0$, the individual changes its velocity. When such a change occur, the individual changes its velocity, with a memory of its last direction. Given its last orientation θ, the new one θ' is chosen randomly such that $\theta' - \theta$ is a wrapped Cauchy distributed random variable with mean 0 and parameter γ. The probability density function of the wrapped Cauchy distribution with mean μ and parameter γ is :

$$f_\gamma(\theta) = \frac{1}{2\pi} \cdot \frac{\sinh(\gamma)}{\cosh(\gamma) - \cos(\theta - \mu)},$$

FIGURE 1.6 – **The toad life-cycle**

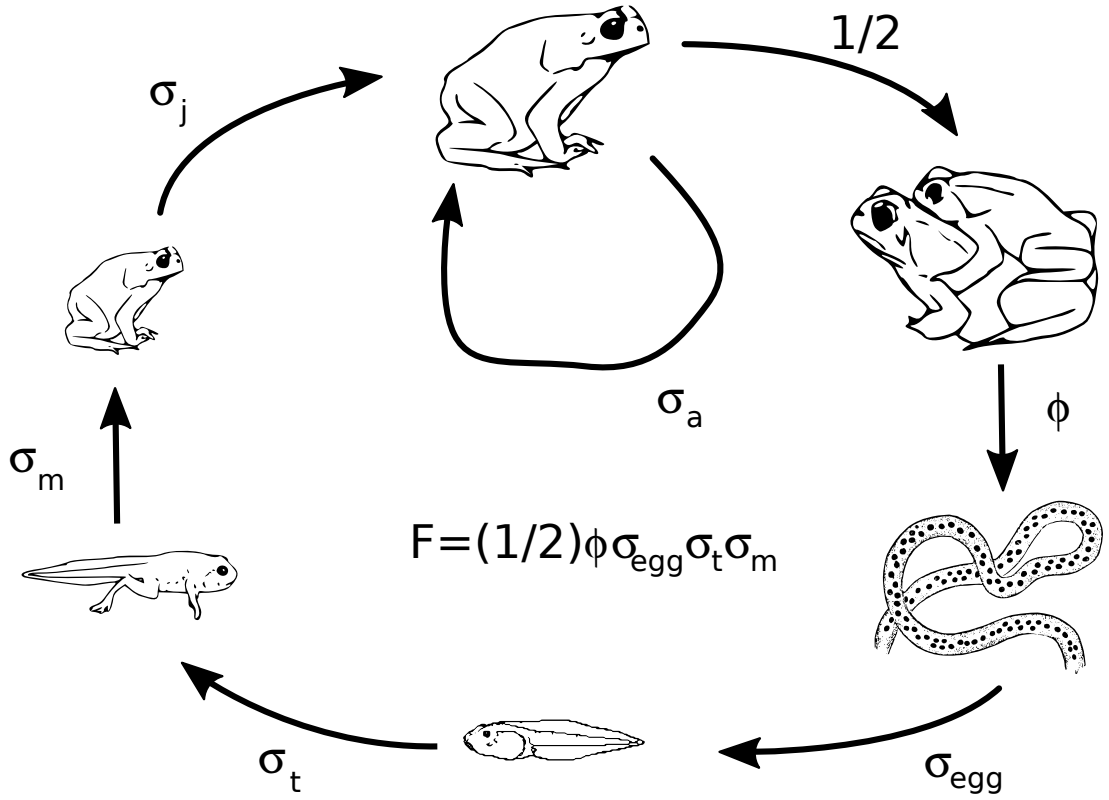

Schematic cane toad's life-cycle illustrating our choice of parameters.
$1/2$ *: proportion of females within the population.*
ϕ *: clutch-size.*
σ_{egg} *: fertility rate of an egg.*
σ_t *: survival rate of a tadpole.*
σ_m *: survival rate of a metamorph.*
σ_j *: survival rate of a juvenile.*
σ_a *: survival rate of an adult.*
Drawings : courtesy of Margo Perkins (adult, juvenile and mating toads), Clipart courtesy FTIC (eggs), Nils Caillerie (tadpole and metamorph).

FIGURE 1.7 – **Heat map of the velocity probability density functions**

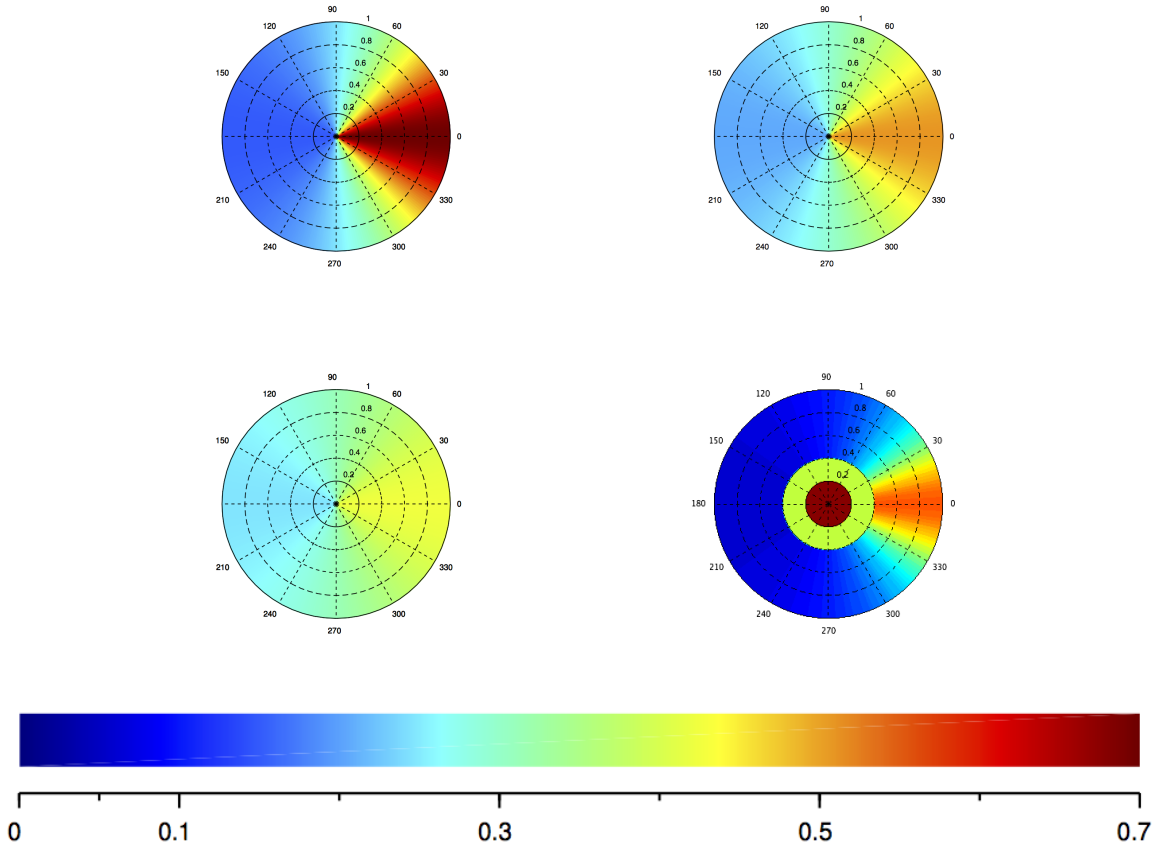

Heat maps of the velocity probability distribution function.
First line : wrapped Cauchy distribution for $\gamma = 1,\ 1.5$.
Second line : wrapped Cauchy distribution for $\gamma = 2$ *and composition of two uniform and one wrapped Cauchy distribution.*

FIGURE 1.8 – **The directionality dispersal model for high γ**

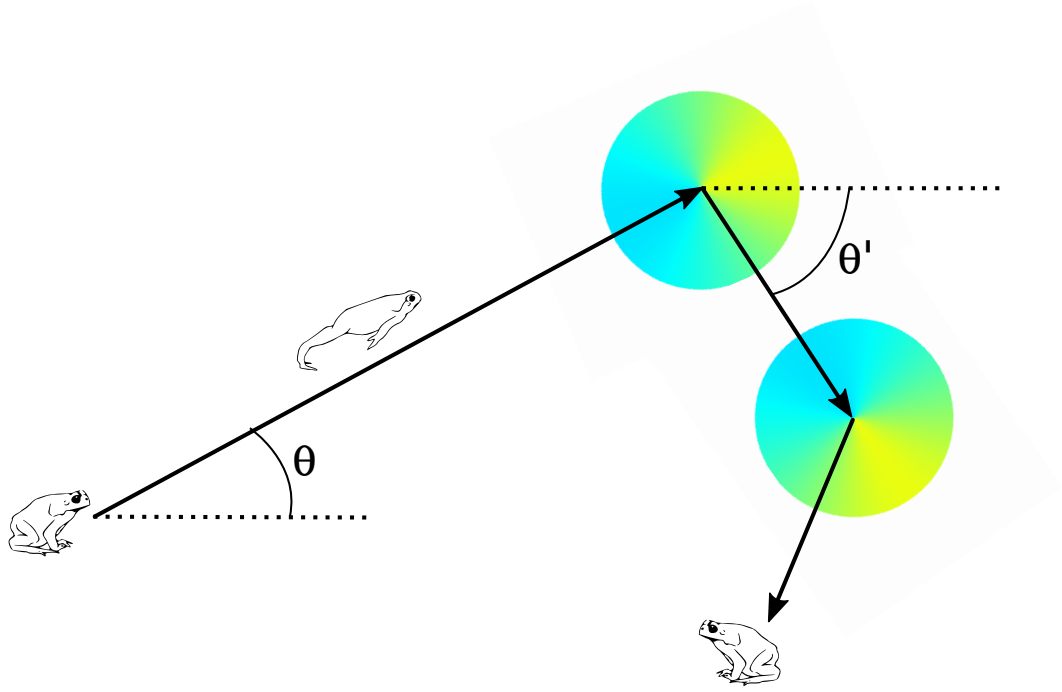

The running mode lasts for an exponential time of mean d_m. An individual walks following a straight line of compass direction θ. After a random exponential time of mean $\frac{1}{z}$, it choses a next compass direction θ', such that $\theta' - \theta$ is a wrapped Cauchy distribution of parameter γ. The process goes on until the individual sets to encamped mode. Then, it waits for an exponential time of mean d_e and then carries on. Here, we consider $\gamma = 2$.
Drawings : courtesy of Margo Perkins.

The new intensity r is chosen independently from the last one and the velocity distribution is constant with respect to the radius variable. The so-called collision kernel associated to this process is therefore

$$T_\gamma^{v_M}(r,\theta) = \frac{2}{v_M^2} \cdot \frac{1}{2\pi} \cdot \frac{\sinh(\gamma)}{\cosh(\gamma) - \cos(\theta)}.$$

The Figure 1.7 gives the so-called heat maps of the wrapped Cauchy distribution for various parameters γ. We illustrate in Figure 1.8 our dispersal model for a high variance of the wrapped Cauchy distribution and in Figure 1.9 for a small variance.

From kinetic theory, this random walk can be modeled at the mesoscopic scale by the mesoscopic density $m(t,x,r,\theta)$ of the moving individuals, the density $E(t,x,\theta)$ of the encamped

FIGURE 1.9 – **The directionality dispersal model for small γ**

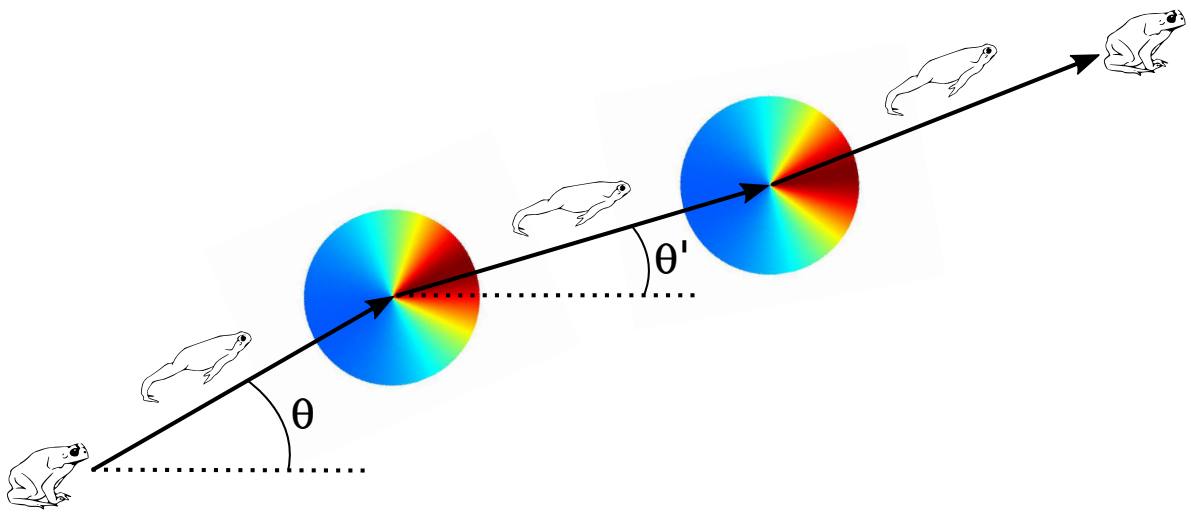

The process is the same as in Figure 1.8, only its variance is smaller. As a consequence, an individual is more likely to end further from its original position than the one with a high variance. Here, $\gamma = 1$. Drawings : courtesy of Margo Perkins.

individuals and the density $J(t,x)$ of the juveniles, such that the model finally reads :

$$\text{(IC)} \quad \begin{cases} m(0,x,r,\theta) \\ E(0,x,\theta) \\ J(0,x) \end{cases}, \tag{1.9}$$

$$\text{(D)} \quad \begin{cases} \frac{\partial m}{\partial t} + v(r,\theta)\cdot\nabla_x m = z\left(T_\gamma^{v_M} *_\theta M - m\right) - \frac{1}{d_m} m + \frac{2}{d_e \cdot v_M^2} E, \\ \frac{\partial E}{\partial t} = \frac{1}{d_m} M - \frac{1}{d_e} E, \\ M(t,x,\theta) = \int_0^{v_M} m(t,x,r,\theta) r.dr \\ \frac{\partial J_t}{\partial t} = 0. \end{cases} \qquad 2nT \le t \le (2n+1)T, \tag{1.10}$$

$$\text{(Re)} \quad \begin{pmatrix} J((2n+2)T) \\ m((2n+2)T) \\ E((2n+2)T) \end{pmatrix} = \begin{pmatrix} 0 & F & F \\ \frac{d_m}{d_m+d_e}\sigma_j & \sigma_a & 0 \\ \frac{d_e}{d_m+d_e}\sigma_j & 0 & \sigma_a \end{pmatrix} \begin{pmatrix} J((2n+1)T) \\ m((2n+1)T) \\ E((2n+1)T) \end{pmatrix}. \tag{1.11}$$

We look for travelling wave solutions of the complete model, *i.e.* solutions of the form

$$\begin{pmatrix} J(2nT,x) \\ m(2nT,x,r,\theta) \\ E(2nT,x,\theta) \end{pmatrix} = e^{-\lambda(x\cdot e - 2cnT)} \begin{pmatrix} \mathcal{J} \\ \mathcal{Q}(r,\theta) \\ \mathcal{E}(\theta) \end{pmatrix}, \tag{1.12}$$

Let us look for travelling waves of speed $\tilde{c}$ in the dispersal phase. Without loss generality, we consider $e = \begin{pmatrix} 1 & 0 \end{pmatrix}$. The dispersal phase forces

$$\begin{cases} \lambda(\tilde{c} - r.\cos(\theta))\mathcal{Q}(r,\theta) = z\left(T_\gamma^{v_M} *_\theta \int \mathcal{Q} r.dr - \mathcal{Q}\right) - \frac{1}{d_m}.\mathcal{Q} + \frac{2}{d_e \cdot v_M^2}\mathcal{E}, \\ \lambda\tilde{c}\mathcal{E} = \frac{1}{d_m}.\int \mathcal{Q} r.dr - \frac{1}{d_e}\mathcal{E}. \end{cases} \tag{1.13}$$

As for the Equation (1.5), we expect that, for all λ there exists a $\tilde{c}_{ER}(\lambda)$ solving the eigenvalue problem (1.13), associated to the eigenvector $Q_\lambda, \mathcal{E}_\lambda$. We refer to [26] and to the Chapter 4 of the present thesis for examples of the resolution of such a spectral problem. Those examples, however, are easier to solve than ours since only one equation is involved. We will investigate the resolution of such a spectral problem in a future work.

Finally, the search for traveling wave solutions boils down to solving the eigenvalue problem

$$e^{2\lambda cT} \begin{pmatrix} \mathcal{J}_\ge \\ \mathcal{Q}_\ge \\ \mathcal{E}_\ge \end{pmatrix} = \begin{pmatrix} 0 & Fe^{\lambda\tilde{c}_{ER}(\lambda)T} & Fe^{\lambda\tilde{c}_{ER}(\lambda)T} \\ \frac{d_m}{d_m+d_e}\sigma_j & \sigma_a e^{\lambda\tilde{c}_{ER}(\lambda)T} & 0 \\ \frac{d_e}{d_m+d_e}\sigma_j & 0 & \sigma_a e^{\lambda\tilde{c}_{ER}(\lambda)T} \end{pmatrix} \begin{pmatrix} \mathcal{J}_\ge \\ \mathcal{Q}_\ge \\ \mathcal{E}_\ge \end{pmatrix}. \tag{1.14}$$

From Perron-Frobenius theorem, for all $\lambda > 0$, there exists a unique $c_{ER}(\lambda)$ solving the eigenvalue problem (1.14). We define $c_{ER}^* := \inf_{\lambda>0} c_{ER}(\lambda)$.

1.3.3 The EWR model

The model is based on a closer look at the tracking data. As previously, we consider a reproduction phase and a dispersal phase. Within the dispersal phase, we consider a running and an encamped mode. However, we also consider a set of n different "walking" modes. We consider all individuals capable of running up to a maximal speed $v_M > 0$. We parametrize D_{v_M} with respect to the polar coordinates and consider all individuals to walk in straight lines such that the position X_t of an individual is given by the ordinary differential equation (1.8).

After a random exponential time with mean $\frac{1}{z} > 0$, the individual changes its velocity. Then, it can set to the encamped mode with probability p or, with probability $1-p$, remain in a moving mode and choose a new velocity. In the second case, with probability $(\alpha_i)_{1\leq i\leq n}$, it chooses the i-th walking mode and then choses a new velocity uniformly on the set $\{v_{i-1} < r \leq v_i\}$ independently from its last velocity, where $0 =: v_0 < v_1 \cdots < v_n < v_{n+1} := v_M$. In particular, when it chooses a walking mode, an individual keeps no memory of its last orientation. With probability α_{n+1}, it chooses the running mode *i.e.* it chooses a new orientation with memory of the previous one with the previously explained wrapped Cauchy distribution. It also chooses a new speed r such that the velocity redistribution function is constant with respect to the radius variable. When an individual sets from the encamped mode to the running mode, it chooses its velocity uniformly in $\{v_n < r \leq v_M\}$ regardless of its past velocities.

As they are defined, the parameters α satisfy $\alpha_1 + \ldots + \alpha_{n+1} = 1$.The transition kernel of the velocity redistribution is then given by

$$\forall \theta \in [0,2\pi), \quad T^{\alpha}_{\gamma} m(r,\theta) := \begin{cases} \frac{\alpha_1}{\pi v_1^2} \int_0^{v_M} \int_0^{2\pi} m r'.dr'.d\theta' & 0 < r \leq v_1 \\ \vdots & \\ \frac{\alpha_n}{\pi(v_n^2 - v_{n-1}^2)} \int_0^{v_M} \int_0^{2\pi} m r'.dr'.d\theta' & v_{n-1} < r \leq v_n \\ \frac{2\alpha_{n+1}}{v_M^2 - v_n^2} \int_0^{2\pi} \frac{1}{2\pi} \cdot \frac{\mathrm{sh}(\gamma)}{\mathrm{ch}(\gamma) - \cos(\theta - \theta')} \int_0^{v_M} m(\theta', r') r'.dr'.d\theta' & v_n < r \leq v_M \end{cases}$$

$$\forall \theta \in [0,2\pi), \quad T^{\alpha} E(r,\theta) := \begin{cases} \frac{\alpha_1}{\pi v_1^2} E & 0 < r \leq v_1 \\ \vdots & \\ \frac{\alpha_n}{\pi(v_n^2 - v_{n-1}^2)} E & v_{n-1} < r \leq v_n \\ \frac{\alpha_{n+1}}{v_M^2 - v_n^2} E & v_n < r \leq v_M \end{cases}$$

In Figure 1.7, we give an example of a heat map for an EWR model with two walking modes. An individual keeps its velocity until the next ringing of the exponential clock and then, choses a new velocity with the same random process. This process goes on until the end of the dispersal phase. As earlier, we consider that a juvenile will start encamped with probability p and that it will move with probability $1-p$. We illustrate our model in Figure 1.10.

FIGURE 1.10 – **The EWR model for $n = 2$**

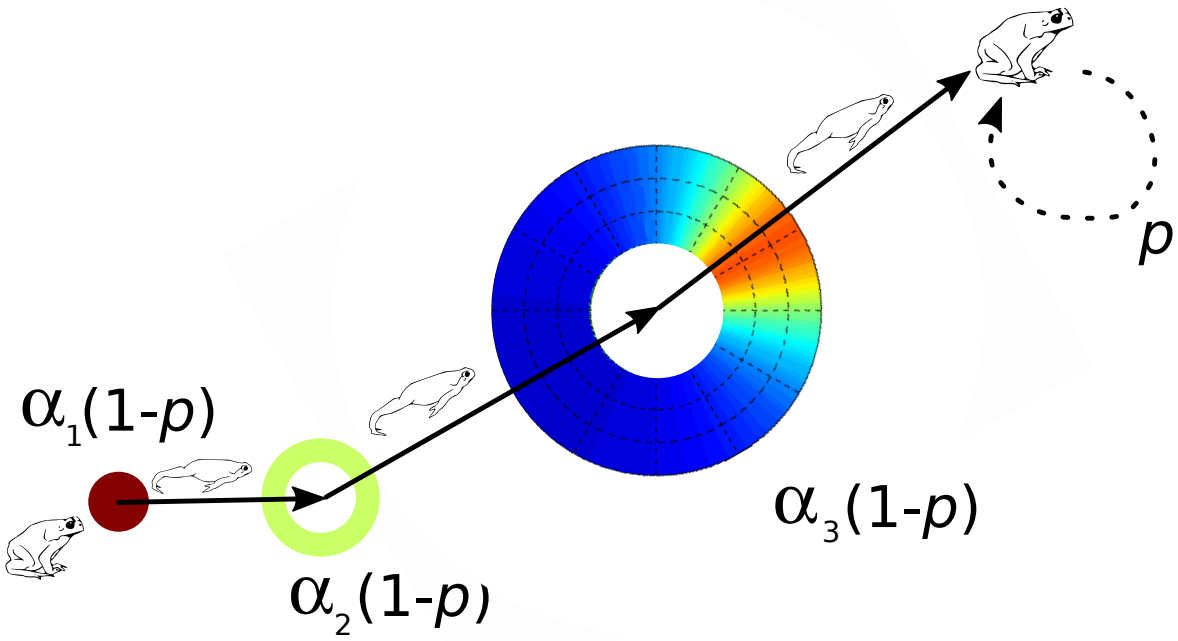

With probability $\alpha_1(1-p)$, an individual walks following a straight line with velocity chosen randomly on the disc D_{v_1} (walking mode 1). After a random a exponential time of mean z, with probability $\alpha_2(1-p)$, it chooses a new velocity uniformly in the set $\{v_1 < r \leq v_2\}$ (walking mode 2). With probability $\alpha_3(1-p)$ it choses a new orientation with a wrapped Cauchy distribution centered on its last orientation and a new speed uniformly in $\{v_2 < r \leq v_M\}$. With probability p, it choses to remain encamped and does not move until the next ticking of the exponential clock.
Drawings : courtesy of Margo Perkins.

From a mathematical point of view, this process can be modeled at the mesoscopic scale with a kinetic equation satisfied by the mesoscopic density $m(t,x,r,\theta)$ of moving individuals at time $t>0$, geographical position $x\in\mathbb{R}^2$ moving with velocity $v\in D_{v_M}\setminus\{0\}=:V$, $E(t,x)$ the density of encamped individuals and $J(t,x)$ the density of juveniles at time t and position x. Our model reads :

$$\text{(IC)}\quad \begin{cases} m(0,x,r,\theta) \\ E(0,x) \\ J(0,x) \end{cases}, \tag{1.15}$$

$$\text{(D)}\quad \begin{cases} \frac{\partial m}{\partial t}+v(r,\theta)\cdot\nabla_x m = z\left(T_\gamma^\alpha m - m\right) - zp.m + z(1-p)T^\alpha E, \\ \frac{\partial E}{\partial t} = zp.M - z(1-p)E, \\ M(t,x) := \int_0^{v_M}\int_0^{2\pi} m(t,x,r,\theta)r.dr.d\theta, \\ \frac{\partial J}{\partial t}=0. \end{cases} \qquad 2nT\le t\le (2n+1)T, \tag{1.16}$$

$$\text{(R)}\quad \begin{pmatrix} J((2n+2)T) \\ m((2n+2)T) \\ E((2n+2)T) \end{pmatrix} = \begin{pmatrix} 0 & F & F \\ (1-p)\sigma_j & \sigma_a & 0 \\ p\sigma_j & 0 & \sigma_a \end{pmatrix} \begin{pmatrix} J((2n+1)T) \\ m((2n+1)T) \\ E((2n+1)T) \end{pmatrix}. \tag{1.17}$$

As earlier, We look for solutions of the form

$$\begin{pmatrix} J(2nT,x) \\ m(2nT,x,r,\theta) \\ E(2nT,x) \end{pmatrix} = e^{-\lambda(x\cdot e-2cnT)} \begin{pmatrix} \mathcal{J} \\ \mathcal{Q}(r,\theta) \\ \mathcal{E} \end{pmatrix}, \tag{1.18}$$

We use the dispersal phase to identify $\mathcal{Q}$, and $\mathcal{E}$. From earlier considerations, we look for solutions of (1.16) the form $m(t,x,v)=e^{-\lambda(x_1-ct)}\mathcal{Q}(v)$ and $E(t,x)=e^{-\lambda(x_1-ct)}\mathcal{E}$, where

$$\begin{cases} \lambda(c-r\cos\theta)\mathcal{Q} = z\left(T_\gamma^\alpha\mathcal{Q}-\mathcal{Q}\right) - zp.\mathcal{Q} + z(1-p)T^\alpha\mathcal{E}, \\ \lambda c\mathcal{E} = zp.\int \mathcal{Q}r.dr.d\theta - z(1-p)\mathcal{E}. \end{cases} \tag{1.19}$$

As earlier, we expect that, for all $\lambda>0$ there exists a $\tilde{c}_{EWR}(\lambda)$ solving the eigenvalue problem (1.19), associated to the eigenvector $(\mathcal{Q}_\lambda,\mathcal{E}_\lambda)$. Hence, the solution given by (1.18) must follow the post-dispersal relation

$$\begin{cases} J(T,x)=J(0,x), \\ m(T,x,v)=e^{-\lambda(x_1-\tilde{c}_{EWR}(\lambda)T)}\mathcal{Q}_\lambda(v) \\ E(t,x)=e^{-\lambda(x_1-\tilde{c}_{EWR}(\lambda)T)}\mathcal{E}_\lambda \end{cases}. \tag{1.20}$$

The reproduction phase gives

$$\begin{pmatrix} J(2T,x) \\ m(2T,x,v) \\ E(2T,x) \end{pmatrix} = \begin{pmatrix} 0 & F & F \\ (1-p)\sigma_j & \sigma_a & 0 \\ p\sigma_j & 0 & \sigma_a \end{pmatrix} \begin{pmatrix} J(0,x) \\ e^{-\lambda(x_1-\tilde{c}_{EWR}(\lambda)T)}\mathcal{Q}_\lambda(v) \\ e^{-\lambda(x_1-\tilde{c}_{EWR}(\lambda)T)}\mathcal{E}_\lambda \end{pmatrix},$$

Plugging ansatz (1.18), it finally all boils down to solving the following eigenvalue problem :

$$e^{2\lambda cT}\begin{pmatrix}\mathcal{J}\\ \mathcal{Q}\\ \mathcal{E}\end{pmatrix}=\begin{pmatrix}0 & Fe^{\lambda\tilde{c}_{EWR}(\lambda)T} & Fe^{\lambda\tilde{c}_{EWR}(\lambda)T}\\ (1-p)\sigma_j & \sigma_a e^{\lambda\tilde{c}_{EWR}(\lambda)T} & 0\\ p\sigma_j & 0 & \sigma_a e^{\lambda\tilde{c}_{EWR}(\lambda)T}\end{pmatrix}\begin{pmatrix}\mathcal{J}\\ \mathcal{Q}_\lambda\\ \mathcal{E}_\lambda\end{pmatrix}. \tag{1.21}$$

From Perron-Frobenius theorem, for all $\lambda > 0$, there exists a unique $c_{EWR}(\lambda)$ solving the eigenvalue problem (1.21). We define $c^*_{EWR} := \inf_{\lambda>0} c_{EWR}(\lambda)$.

1.4 Statistics

1.4.1 Data

We use the same set of data as in [83, 33].The data were communicated by Brown, Phillips, Shine. We gratefully acknowledge them for providing us with data and subsequent informations about their use.

Cane toads were radio tracked on a daily basis on the Adelaide River flood plain in tropical Australia during wet season (November to March) 2005, just when the first toads arrived in the area. This guarantees that the radio tracked toads are the one who were pulling the front at that time. The dataset we are using is the daily position in UTM coordinates (UTM zone 52L) of 22 toads tracked for a period of time that lasted between 6 and 65 days. All telemetry procedures were carried out under approval of the University of Sydney Animal Ethics Committee (permit L04/11-2005/3/4252).

1.4.2 Time averaged mean-square displacement

To analyze the trajectory of the radio tracked toads, we use the so-called "time averaged mean square displacement", (TAMSD) : consider a toad i which was radio tracked for T_i days and the position of which are given by the East-West UTM coordinates $x_i(t)$ and the South-North coordinates $y_i(t)$ for $1 \le t \le T_i$, we set for all $1 \le \delta \le T_i - 1$,

$$TAMSD^i(\delta) := \frac{1}{T_i-\delta}\sum_{t=1}^{T_i-\delta}\left(x_i(t+\delta)-x_i(t)\right)^2+\left(y_i(t+\delta)-y_i(t)\right)^2. \tag{1.22}$$

The mean square displacement is a well-known tool to characterize a random walk. For the Brownian motion, it has been shown that the mean value of the mean-square displacement is the diffusion coefficient of the process. This result provides a good statistical tool to estimate the diffusion coefficient of a set of particles, assuming they have the same diffusion coefficient. When several diffusion coefficients exist, one must track single particles separately. If each trajectory has not enough data to conduct a statically relevant study, one way to overcome this issue is to use the TAMSD.

For a diffusive motion, it has been shown that for the continuous version of (1.22), that the TAMSD's expectation is a linear function of t which slope is the diffusion coefficient [4, 70, 69]. For biophysical applications, the discrete version of the TAMSD has shown similar properties [95].

FIGURE 1.11 – **TAMSD of toad 8**

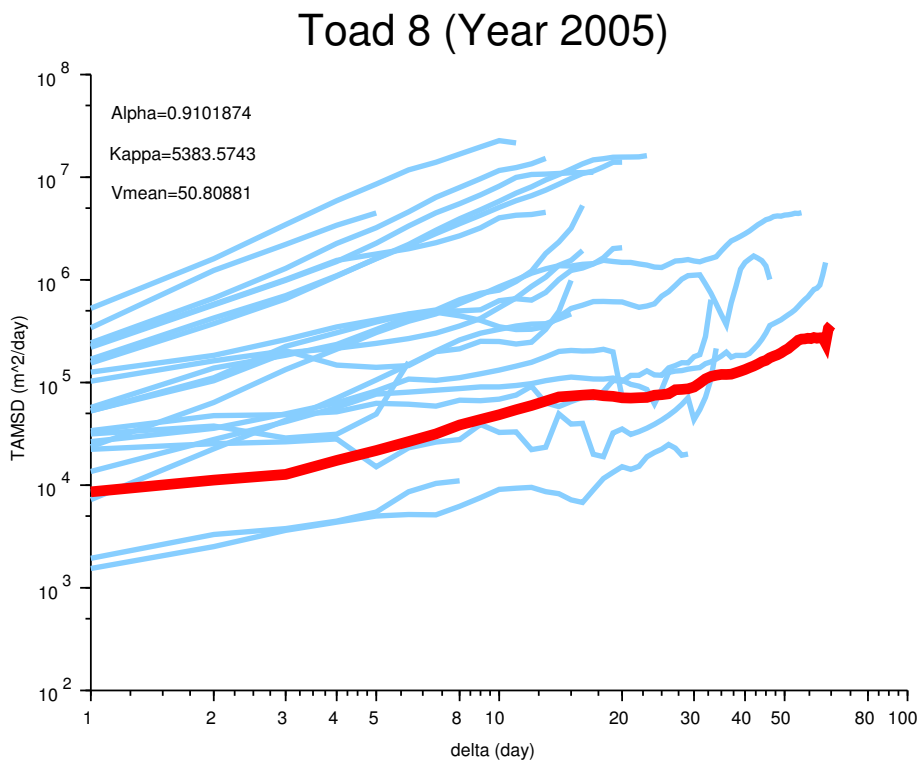

Red line : function $\delta \mapsto \ln(TAMSD(\delta))$ of Toad number 8, radio tracked between 02/04 and 04/30 of year 2005.
Light-blue lines : TAMSD of all the other radio tracked toads.
Units : δ (days), $TAMSD(\delta)$ (m^2/day).

In our framework, the value of the TAMSD is expected to be of the form $TAMSD(\delta) = \kappa.\delta^{\alpha}$. If the individuals walk according to a diffusive process, we expect $\alpha = 1$ and we will use κ to estimate the diffusion coefficient. When $\alpha = 2$, the behavior of the motion is said to be "ballistic" (*i.e*its trajectory is a straight line). Between $\alpha = 1$ and $\alpha = 2$ we say that the motion is superdiffusive. Between $\alpha = 0$ and $\alpha = 1$, the motion is said to be subdiffusive. We represent in Figures 1.11, 1.12, 1.13 and 1.14 the TAMSD of four radio tracked toads. We represent the TAMSD in log-log scale and use linear regression to estimate α and κ. We represent the estimated coefficients with a point cloud in Figure 1.15. We can see quite clearly that the hypothesis of a diffusion process has to be challenged since the dots do not gather around the line $\{\alpha = 1\}$.

FIGURE 1.12 – **TAMSD of toad 9**

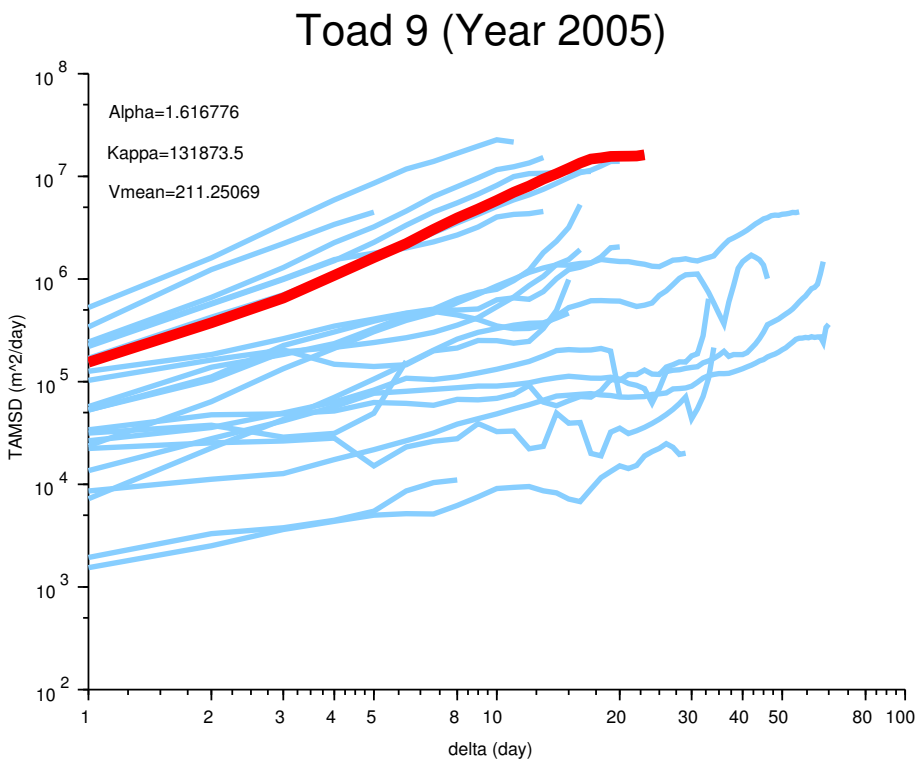

Red line : function $\delta \mapsto \ln(TAMSD(\delta))$ *of Toad number 9, radio tracked between 03/02 and 03/25 of year 2005.*
Light-blue : lines are the TAMSD of all the other radio tracked toads.
Units : δ *(days),* $TAMSD(\delta)$ (m^2/day).

FIGURE 1.13 – **TAMSD of toad 16**

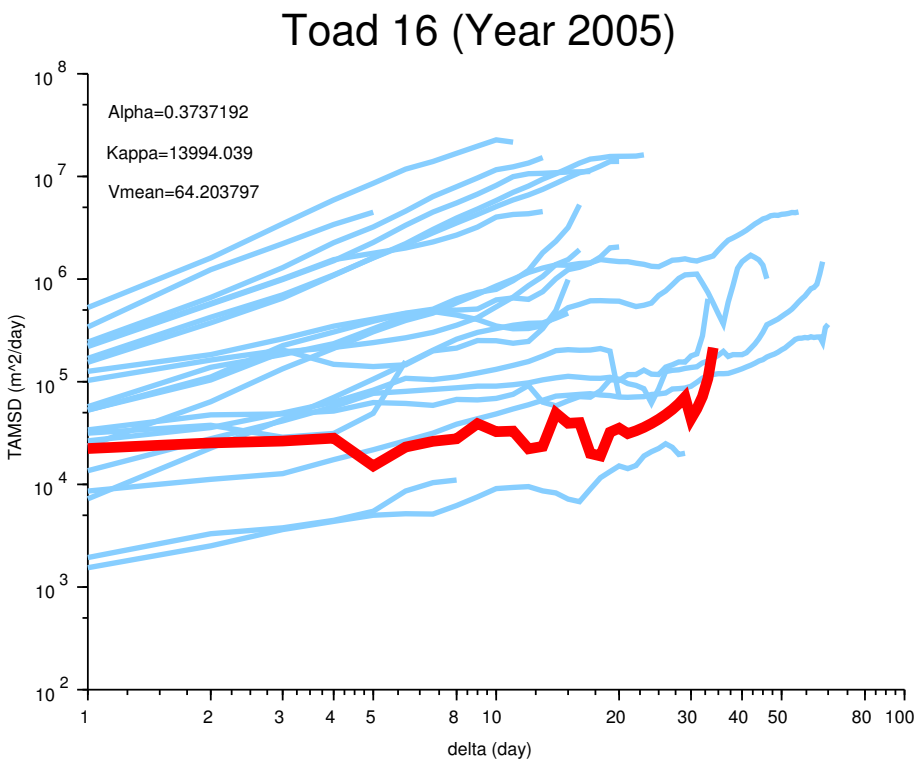

Red line : function $\delta \mapsto \ln(TAMSD(\delta))$ of Toad number 16, radio tracked between 03/27 and 04/30 of year 2005.
Light-blue lines : TAMSD of all the other radio tracked toads.
Units : δ (days), $TAMSD(\delta)$ (m^2/day).

FIGURE 1.14 – **TAMSD of toad 21**

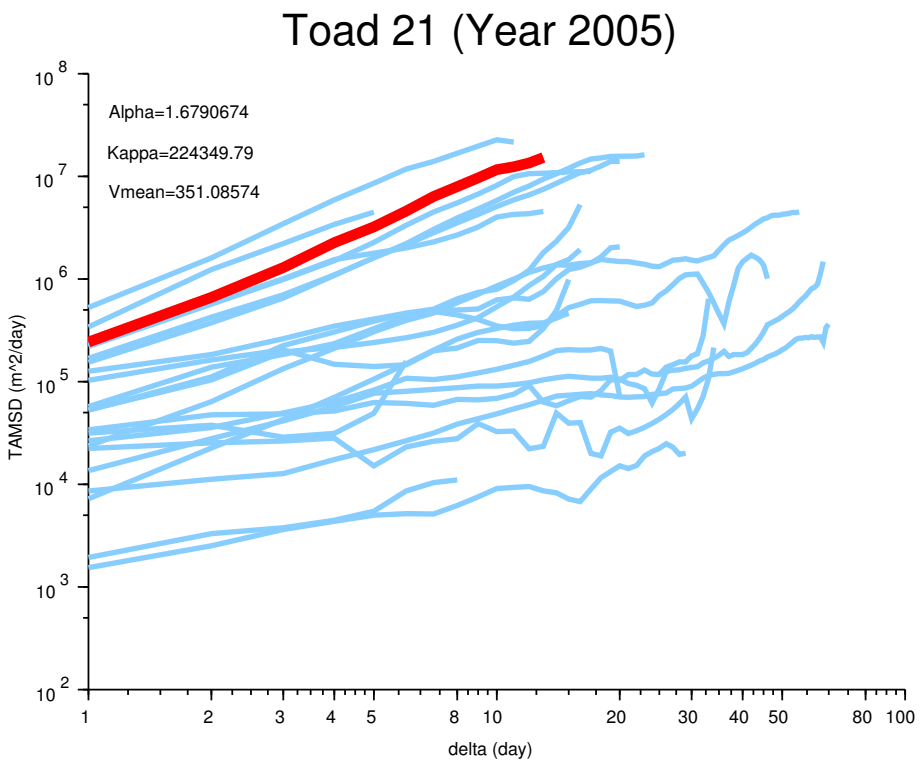

Red line : function $\delta \mapsto \ln(TAMSD(\delta))$ *of Toad number 21, radio tracked between 04/17 and 04/30 of year 2005.*
Light-blue lines : TAMSD of all the other radio tracked toads.
Units : δ *(days),* $TAMSD(\delta)$ (m^2/day).

FIGURE 1.15 – **Estimated κ and α of the radio tracked toads**

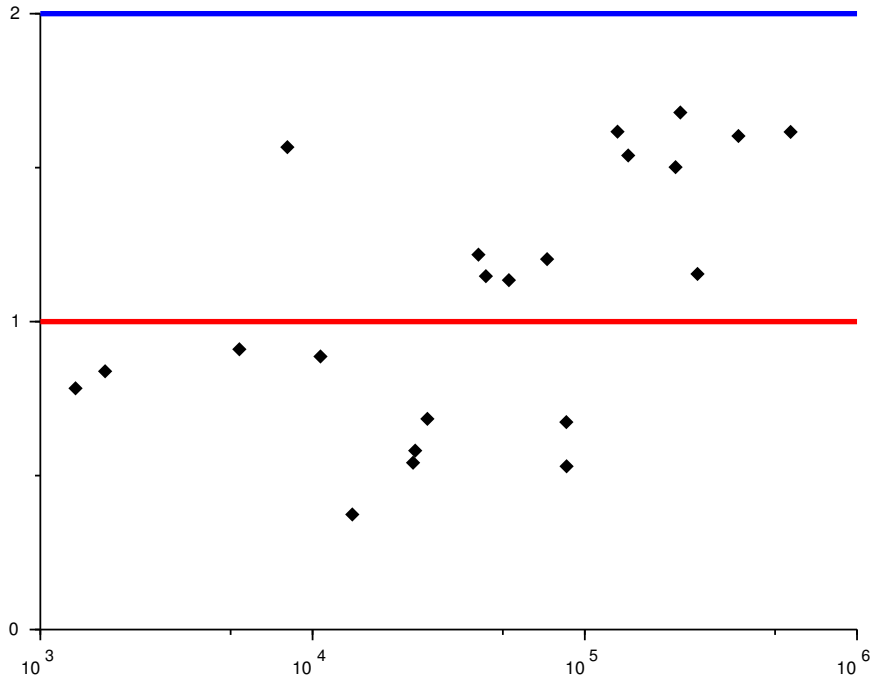

Black dots : estimated (κ, α) of the 22 radio tracked toads.
Units : κ-axis (m^2/day), α-axis (none).
Red line : $\{\alpha = 1\}$.
Blue line $\{\alpha = 2\}$.
We expect a diffusion process to gather along the red line and a ballistic process to gather along the blue one.

1.4.3 Approximate bayesian computation

Principle of approximate Bayesian computation (ABC)

Suppose that we have at disposal a parametric model allowing us to simulate, conditionally on parameter values, data with the same structure than observed data. The basic ABC procedure (ABC-rejection) for estimating model parameters is carried out as follows : (i) sets of parameters are independently simulated under a prior distribution ; (ii) for each set of parameters a data set with the same structure than the observed data set is simulated under the implicit model ; then, (iii) the simulated parameters corresponding to simulated data sets which are *close* to the observed data set are used to build the posterior distribution. More sophisticated versions of ABC, including iterative algorithms, have been proposed (see reviews by [11, 45, 86, 87]). For our application, we applied one of these approaches, in which the closeness between the observed and simulated data sets is measured by an optimal distance.

In any ABC procedure, the closeness of the data sets is quantified with a distance that has to be defined. Classically in ABC, the distance between data sets is defined as a mean square distance between summary statistics whose dimension is much lower than the dimension of raw data, and the closeness is defined with a *tolerance threshold*. Obviously, the choice of the summary statistics, the distance between the summary statistics and the tolerance threshold influence the accuracy of the inference. For our application, we used an improved version of ABC–rejection proposed by [104], in which (i) the distance is defined as a weighted sum of squares of some pre-defined summary statistics and (ii) the weights are optimized together with the tolerance threshold. The sections below briefly describe the methodological background.

ABC–rejection

Consider observed data $\mathcal{D} \in \mathbb{D}$ which are assumed to be generated under the stochastic model $\mathcal{M}_\theta$ parametrized by $\theta \in \Theta$ with prior density π. The data space $\mathbb{D}$ and the parameter space Θ are both included in multidimensional sets of real vectors.

The posterior distribution $p(\theta \mid \mathcal{D})$ can be estimated using the following ABC–rejection algorithm :

A1. Carry out the next two steps, independently for i in $\{1, \ldots, I\}$,
- Generate θ_i from π and simulate $\mathcal{D}_i$ from $\mathcal{M}_{\theta_i}$.
- Accept θ_i if $\mathcal{D}_i = \mathcal{D}$, reject it otherwise.

The set of accepted θ_i form a sample from the posterior distribution

$$p(\theta \mid \mathcal{D}) = \frac{f(\mathcal{D} \mid \theta)\pi(\theta)}{\int_\Theta f(\mathcal{D} \mid \alpha)\pi(\alpha)d\alpha},$$

where $f(\mathcal{D} \mid \theta)$ is the conditional probability distribution function of $\mathcal{D}$ given θ, i.e. the likelihood corresponding to the model $\mathcal{M}_\theta$.

In practice, this algorithm is rarely usable : the probability of generating $\mathcal{D}_i$ equal to $\mathcal{D}$ is very low when the dimensionality of the data space $\mathbb{D}$ is large and this probability is even zero for continuous data. To circumvent this difficulty two ideas have been applied : the introduction of a tolerance threshold and the replacement of the raw data by statistics. This leads to the following ABC–rejection algorithm :

A2. Carry out the next three steps, independently for i in $\{1,\dots,I\}$,
- Generate θ_i from π and simulate $\mathcal{D}_i$ from $\mathcal{M}_{\theta_i}$.
- Compute the statistics $S_i = s(\mathcal{D}_i)$, where s is a function from $\mathbb{D}$ to the space $\mathbb{S}$ of statistics.
- Accept θ_i if $d(S_i, S) \leq \varepsilon$, where d is a distance over $\mathbb{S}$ and ε is a tolerance threshold for the distance between the observed statistics $S = s(\mathcal{D})$ and the simulated ones.

The set of accepted parameters, say $\Theta_{\varepsilon,I} = \{\theta_i : d(S_i, S) \leq \varepsilon, i = 1,\dots,I\}$, form a sample from the posterior distribution

$$p_\varepsilon(\theta \mid S) = \frac{\left(\int_{B(S,\varepsilon)} g(z \mid \theta)dz\right)\pi(\theta)}{\int_\Theta \left(\int_{B(S,\varepsilon)} g(z \mid \alpha)dz\right)\pi(\alpha)d\alpha},$$

where $g(S \mid \theta)$ is the conditional probability distribution function of S given θ.

When ε tends to zero, $p_\varepsilon(\theta \mid S)$ may be a good approximation of the posterior distribution conditional on the statistics, i.e.

$$p(\theta \mid S) = \frac{g(S \mid \theta)\pi(\theta)}{\int_\Theta g(S \mid \alpha)\pi(\alpha)d\alpha},$$

and the sample $\Theta_{\varepsilon,I}$ of accepted parameters is approximately distributed under this posterior distribution. If, in addition, the statistics are sufficient, then $g(S \mid \theta) = f(\mathcal{D} \mid \theta)$ and $\Theta_{\varepsilon,I}$ is approximately a sample from the classical posterior distribution $p(\theta \mid \mathcal{D})$ conditional on the data.

In practice, instead of the tolerance threshold ε, the analyst selects a proportion $\tau \in (0,1]$ of accepted parameters and obtain ε as a function of $\tau : \varepsilon = \varepsilon(\tau)$. A small value is generally chosen for the acceptance rate τ because of the reason explained in the previous paragraph; Typically, τ is 0.001 (e.g. 10^3 accepted parameters among $I = 10^6$ simulations).

In many applications, when the statistics are quantitative variables, the distance $d(S_i, S)$ is the Euclidean distance up to a standardization of the components of the statistics (i.e. each component of S_i and S is divided by the corresponding empirical standard deviation calculated by using the I simulations).

ABC–rejection with optimal weighted distance and acceptance rate

In [104], the authors proposed to use a weighted distance between S_i and S whose weights w are optimized together with the acceptance rate τ. Thereafter, we adapt the specifications of the problem to our case study. Suppose that S_i and S have dimension $J \times K$ ($J, K \in \mathbb{N}^*$) : $S_i = \{S_{ijk} : j = 1,\dots,J; k = 1,\dots,K\}$ and $S = \{S_{jk} : j = 1,\dots,J; k = 1,\dots,K\}$; in our application, J is the number of different statistics and K is the number of toads. The weighted distance is defined as :

$$d(S_i, S; w) = \sum_{j=1}^{J}\sum_{k=1}^{K} w_j\sqrt{(S_{ijk} - S_{jk})^2},$$

where $0 \leq w_J \leq 1$ and $\sum_{j=1}^{J} w_j = 1$. Following [104], $w = (w_1,\dots,w_J)$ and τ are selected by minimizing a mean square error criterion computed for the posterior median of the parameter vector θ (heuristically, we select w and τ such that the posterior median of θ minimizes a specific combination bias/variance). The minimization is carried out with the Nelder-Mead algorithm modified to take into account the constraints on w and τ.

Application for the toad

To select which parameters are relevant in the ER model, we use the previously described rejection algorithm. We simulate the random walk we described in Section 1.3.2 for 10^6 randomly selected values of (z, v_M, γ, d_m). We choose the following *prior* laws :

$$\begin{aligned} z &\sim \text{Exp}(1), \\ \gamma &\sim \text{Exp}(1), \\ d_m &\sim \text{Exp}(4), \\ d_e &= 5, \\ v_M &\sim \text{Unif}([0, 3000]) \end{aligned}$$

The summary statistics of each simulated trajectory are its α coefficient, its κ coefficient, the mean daily displacement (average of the distance between two consecutive locations) and the maximal daily displacement (maximal distance between two consecutive locations). Optimal weights (applied to raw summary statistics $(\alpha, \kappa, v_{\text{mean}}, v_{\max})$, which have significantly different ranges of variation) are $w_{opt} \approx (0.9985, 3 \times 10^{-10}, 0.0009, 0.0006)$ and the optimal tolerance threshold is $\tau_{opt} \approx 4.3 \times 10^{-4}$. This optimum led to a posterior sample of size 425. We will detail our results in Section 1.4.4.

Before moving on, we would like to motivate some of our choices of prior laws. To set down the number of simulations and according to observations from [83], we fixed $d_e = 5$ days. Indeed, the authors have studied a discrete model similar to ours and concluded that the probability that a toad does not relocate from one day to the next (hence remains encamped) is 0.8 (see Figure 2 in [83]). Moreover, they have observed that this typical duration of the encamped does not differentiate the first toads of 2005 from the others. In the continuous framework, this waiting time is modeled by a exponential law of parameter $(1 - 0.8)^{-1} = 5$. Let us notice from [83], Figure 2 that toads have probability 0.6 to remain dispersive from one day to the next. Thus, we expect our approximate bayesian computation to select values of d_m that are close to $(1 - 0.6)^{-1} = 2.5$. We do not take a law of mean 2.5 as our prior since we do not want our choice of prior to be influenced by earlier statistical results. Since we do not have any clue as to how z and γ are distributed, we choose an exponential law of parameter 1, which is supported on $\mathbb{R}_+$.

We chose the uniform law $\text{Unif}([0, 3000])$ for the parameter v_m since the data have shown that no toad can walk a distance longer than 3km/day.

1.4.4 Estimation of parameters

Reproduction parameters

The reproduction parameters are drawn from biology literature. We refer to Table 1 and Figure 2 in [80] and the references therein to motivate our choice of reproduction parameters. Mean values were selected, where available. Where not available, we used the middle point of the range. Finally, as explained in Section 1.3, we consider the maximal survival rate of tadpoles. Our parameters are given by (1.23) :

TABLE 1.1 – **Sample of the selected parameters**

z (day^{-1})	d_m (days)	v_M (m/day)	γ
1.82772	0.91399	1062.4953	0.38317
2.64364	0.81195	972.7258	1.38744
0.62731	0.19239	1839.411	0.27045
0.26056	0.90046	977.5999	3.88819
1.3785	0.65702	1078.097	0.93346
1.22786	0.989	1092.8731	1.31425
⋮	⋮	⋮	⋮

$$\begin{aligned} \phi &= 15000, \\ \sigma_{egg} &= 71.8\%, \\ \sigma_t &= 34.99\%, \\ \sigma_m &= 8.2\%, \\ \sigma_j &= 5\%, \\ \sigma_a &= 50\%, \\ F = \frac{1}{2}\phi\sigma_{egg}\sigma_t\sigma_m &= 154.50534. \end{aligned} \tag{1.23}$$

Here are the key numbers that one should keep in mind : at the end of every reproduction phase, there are approximately 154 times as much juveniles as there are adults and, 50% of the adults and 5% of the juveniles will survive through the year.

Dispersal parameters of the ER model

Our posterior sample is a 425 set of 4 parameters. The Figure 1.16 shows the histogram of the selected parameters and the Figure 1.17 shows the selected parameters projected on the $v_M - d_m$ plane. The Table 1.1 gives a sample of the selected parameters.

Dispersal parameters of the EWR model

The EWR parameters were chosen with a more standard statistical approach. To estimate the number of walking modes and the corresponding velocities, we represent the distribution of the daily displacement by a histogram in Figure 1.18. The histogram shows 5 classes of distinguishable displacements. Out of the 510 recorded daily displacements, 116 correspond to toads that did not move at all. We therefore estimate the parameter p by $116/510 \approx 0.227$. Out of the 394 remaining displacements, 196 correspond to toads which walked a distance

FIGURE 1.16 – **Histogram of the selected parameters**

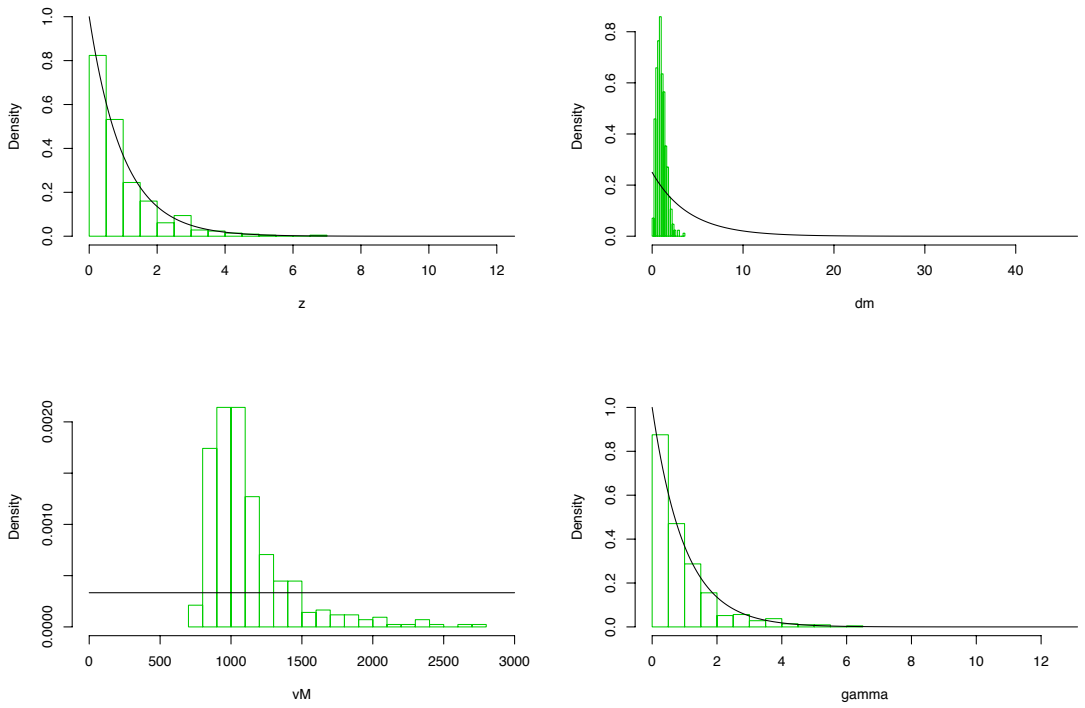

First line, first column : histogram of the selected z.
First line, second column : histogram of the selected d_m.
Second line, first column : histogram of the selected v_M.
Second line, second column : histogram of the selected γ.
Black line : prior *law. Green bars :* posterior *law (selected parameters).*
Units : z (day^{-1}, d_m (days), v_M (meters/day), γ (none).
Graphics computed and drawn by S. Soubeyrand.

FIGURE 1.17 – **Projection of the *posterior* law on the $v_M - d_m$ plane**

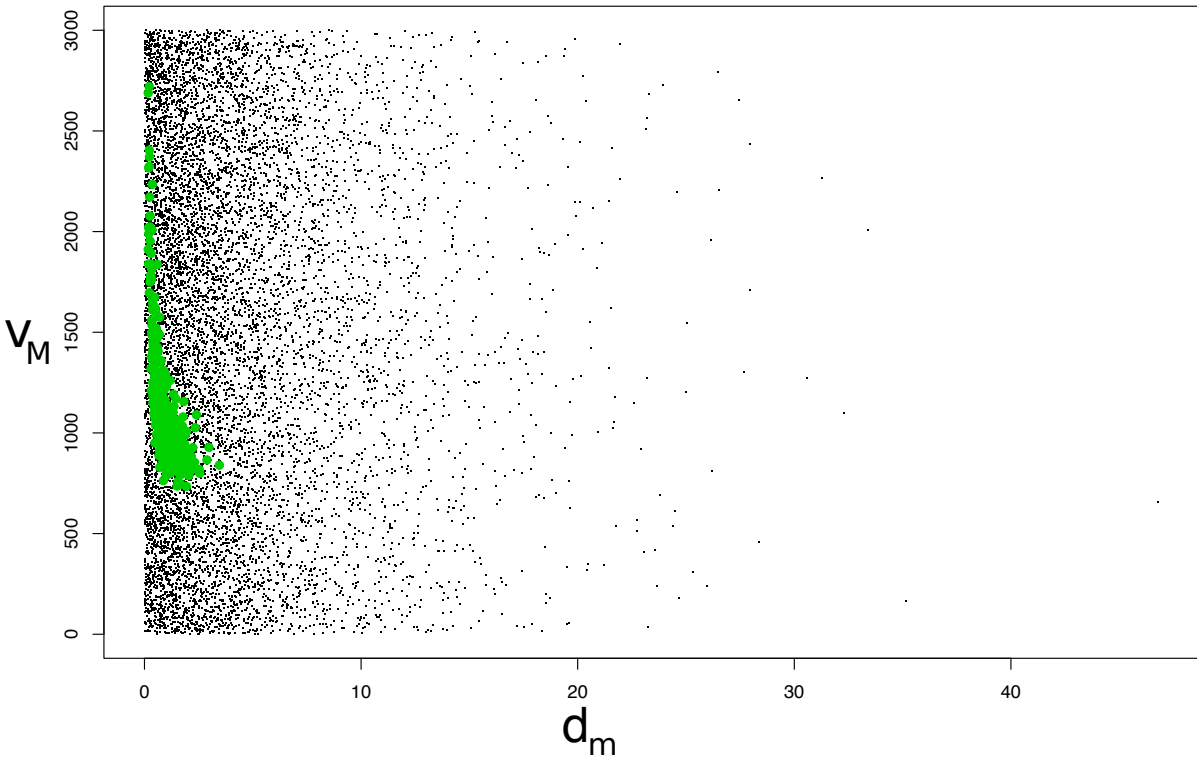

Black dots : simulated trajectories.
Green dots : selected simulated trajectories.
Units : d_m-axis (days), v_M-axis (meters/day).
Graphic computed and drawn by S. Soubeyrand.

FIGURE 1.18 – **Histogram of the daily displacement distribution of the radio tracked toads**

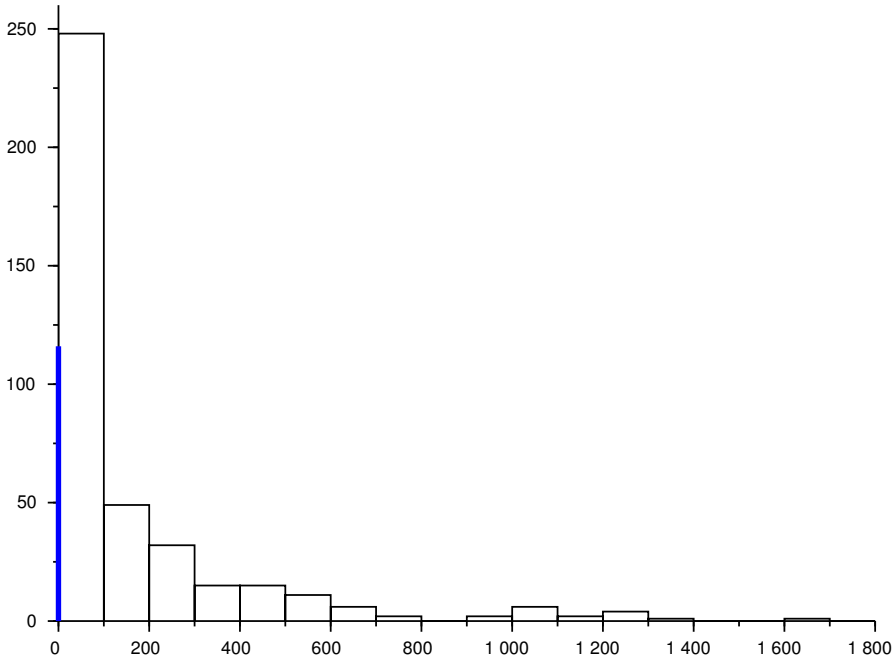

x-axis : daily displacement of the 22 radio tracked toads. y-axis : number of toads in the class. Number of data : 510. Blue stick : number of encamped toads (not relocating).

from 0 to 100 meters during one day, 133 which walked from 100 to 300 meters, 41 which walked from 300 to 600 meters and 24 with walked from 600 to 1700 meters.

This explains the following estimation of parameters :

$$\begin{aligned} p &= \frac{116}{510} \approx 0.227, \\ \alpha_1 &= \frac{196}{394} \approx 0.629, \\ v_1 &= 0.1 \text{ km} \\ \alpha_2 &= \frac{133}{394} \approx 0.206, \\ v_2 &= 300 \text{ km}, \\ \alpha_3 &= \frac{41}{394} \approx 0.104, \\ v_3 &= 600 \text{ km}, \\ \alpha_4 &= \frac{24}{394} \approx 0.061, \\ v_M &= 1.7 \text{ km}. \end{aligned} \tag{1.24}$$

To motivate our introduction of three walking modes,

$$n = 3, \tag{1.25}$$

with a uniform redistribution and one running mode with a wrapped Cauchy distribution, we plot the histogram of the turning angle between two consecutive days for the four observed class of velocities. The Figure 1.20 shows the histogram of the turning angles for our four modes, without normalization. The Figure 1.21 shows the histogram of the turning angles when the next location of the toad is between 0 and 100 meters away of its last location. The Figure 1.22 shows the histogram of the turning angles when the next location of the toad is between 100 and 300 away meters for its last location. The Figure 1.23 shows the histogram of the turning angles when the next location of the toad is between 300 and 600 away meters away from its last location. The Figure 1.24 show the histogram of the turning angles when the toad is 600 to 1700 meters away from its last location. We also represent the estimated probability density function, namely the uniform law on $[-\pi, \pi]$ for the walking modes and, for the running mode, the wrapped Cauchy distribution with parameter

$$\gamma = 0.4, \tag{1.26}$$

which visually fits the histogram. Since the previous parameters were estimated with data on daily displacements only, we choose to select the frequency of velocity change accordingly, such that

$$z = 1. \tag{1.27}$$

FIGURE 1.19 – **Normalized histogram of the daily displacement distribution of the radio tracked toads**

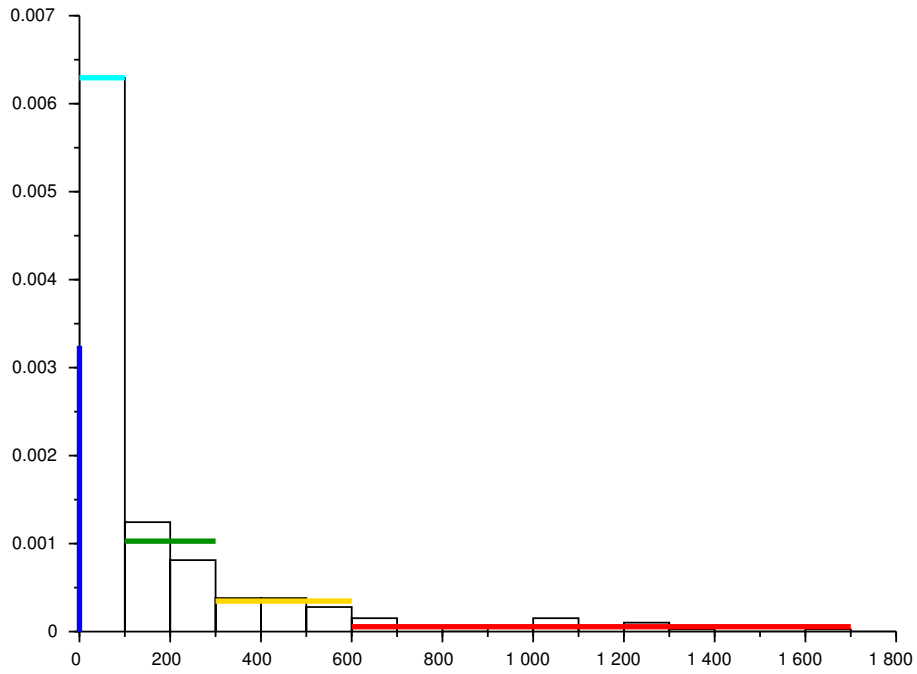

x-axis : daily displacement of the 22 radio tracked toads.
y-axis : frequency of toads in the class.
Blue stick : frequency of encamped toads.
Light-blue line : frequency of the toads in the first walking mode.
Green line : frequency of the toads in the second walking mode.
Yellow line : frequency of the toads in the third walking mode.
Red line : frequency of the toads in running mode.

FIGURE 1.20 – **Non-Normalized histogram of the turning angle for toads in the four dispersal modes**

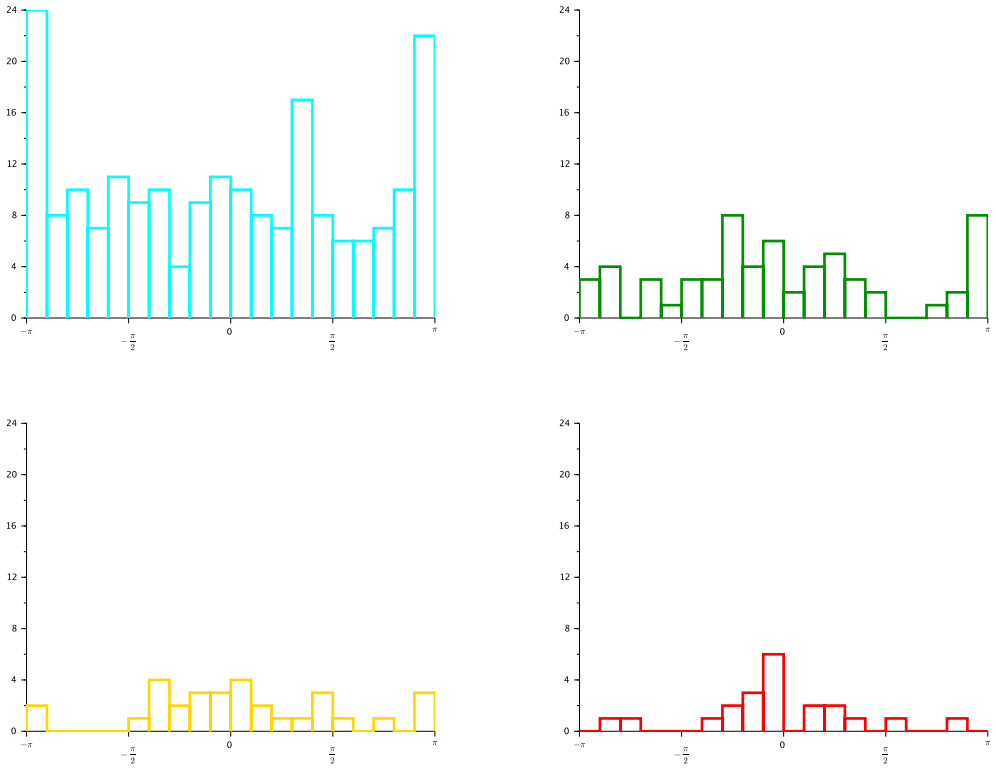

Upper left histogram (light-blue) : first walking mode ($< 100m/day$).
Upper right (green) : second walking mode ($100 < \cdot < 300m/day$).
Lower left histogram (yellow) : third walking mode ($300 < \cdot < 600m/day$).
Lower right (red) : running mode ($600 < \cdot < 1700m/day$).
x-axis : turning angles.
y-axis : number of data in the corresponding class.

FIGURE 1.21 – **Normalized histogram of the turning angle for toads in the first walking mode**

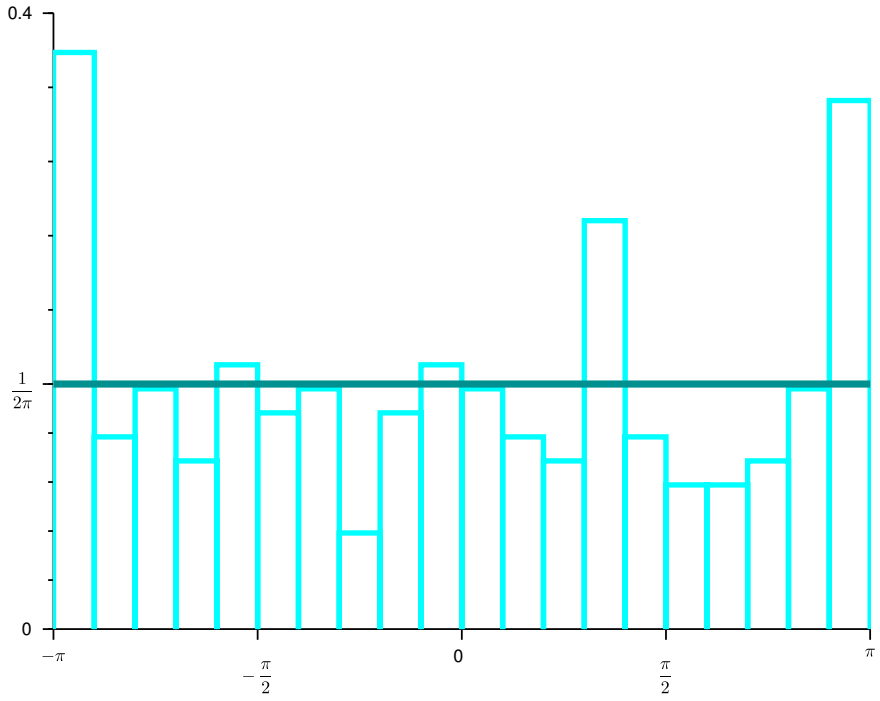

x-axis : turning angles.
y-axis : frequency.
Green-blue line : probability density function of the uniform law on $[-\pi, \pi]$.

FIGURE 1.22 – **Normalized histogram of the turning angle for toads in the second walking mode**

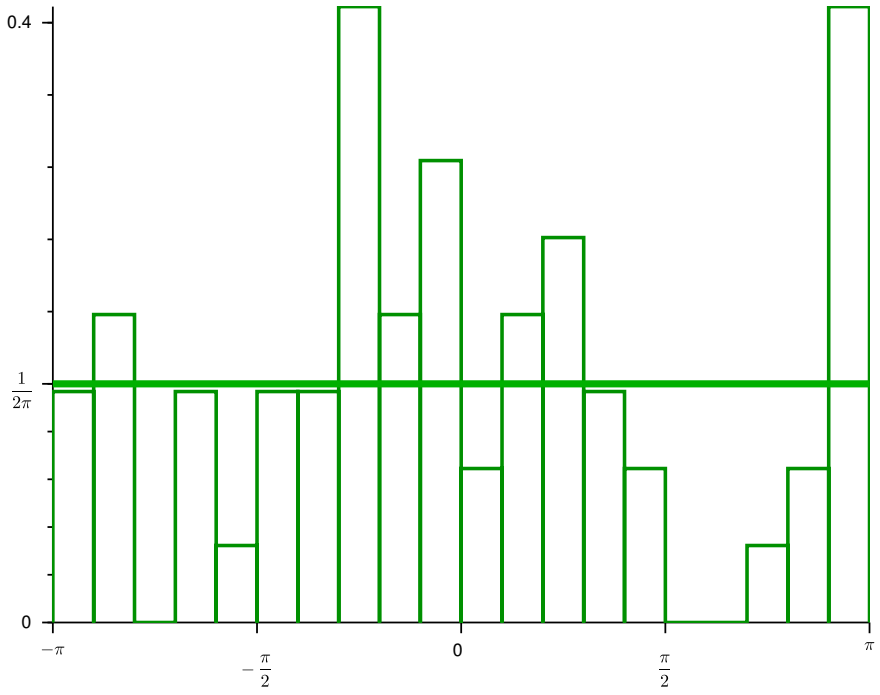

x-axis : turning angles.
y-axis : frequency.
Light-green line : probability density function of the uniform law on $[-\pi, \pi]$.

FIGURE 1.23 – **Normalized histogram of the turning angle for toads in the third walking mode**

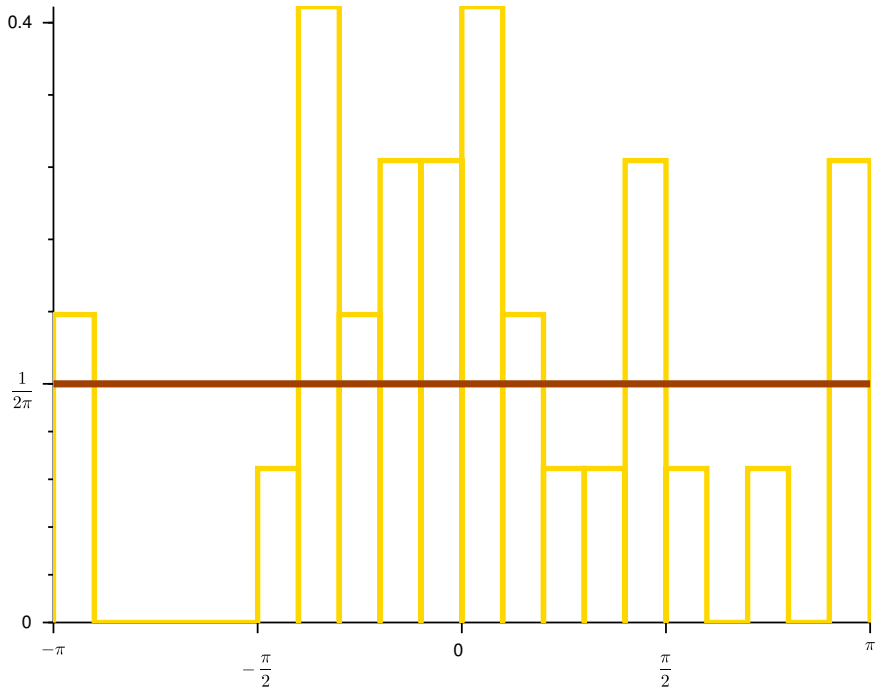

x-axis : turning angles.
y-axis : frequency.
Brown line : probability density function of the uniform law on $[-\pi, \pi]$.

FIGURE 1.24 – **Normalized histogram of the turning angle for toads in running mode**

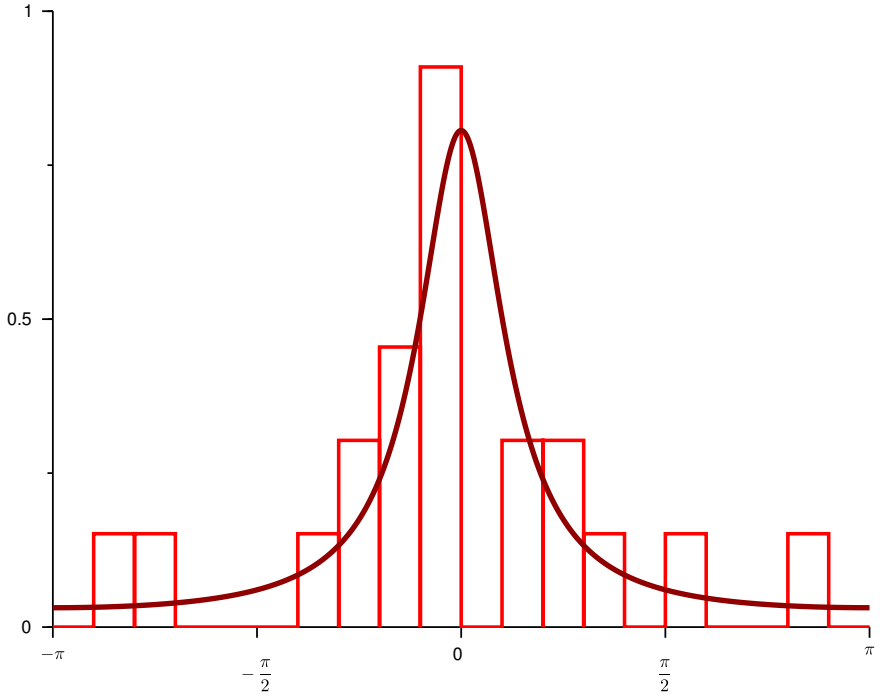

x-axis : turning angles.
y-axis : frequency.
Brick-red line : probability density function of wrapped Cauchy distribution with parameter $\gamma = 0.4$.

The heat map of T^{α}_{γ} for our estimated $(\alpha_i)_{1\leq i\leq 4}$ and γ is given in Figure 1.25.

1.4.5 Numerics

Before stating our results, we shortly describe how we numerically compute the speed c^* for both models. We first need to solve the spectral problem (1.13) and (1.19). We choose to discretize our problem, such that our continuous eigenvalue problem becomes a finite-dimensional spectral problem. From Perron-Frobenius theorem, since we are looking for positive eigenvectors, one needs to find the principle eigenvalue of a finite-dimensional matrix. In order to do so, we need to discretize both the $\int \cdot r.dr$ operator and the $T*_{\theta}$ operator. We discretize both operators using the trapezoidal rule. We then have to numerically solve the spectral problem (1.14) and (1.21), which we do by using standard numerical methods. The minimizer of $c(\lambda)$ was computed with a precision of 10^{-2}.

1.5 Results and discussion

1.5.1 Results

Let us recall the conclusions of our statistical studies. We extracted the so-called reproduction parameters from [80]. For the ER model, based on observations from [83], we fixed $d_e = 5$. Our approximate bayesian computation provided 245 sets of 4 estimates for z, d_m, v_M and γ. For those sets, we numerically compute the speed of propagation c^*_{ER} and represent their histogram in Figure 1.26.

We would like to point out that, among all our computed sets of parameters, 31 give a speed $50 < c^*_{EWR} < 60$, we represent those parameters in Figure 1.27.

For the EWR model, we extracted a single estimate for the parameter p, the parameter γ, the set $(\alpha_i)_i$ and the set $(v_i)_i$ with help of a standard statistical study on the histogram of the speed distributions and the turning angle distributions. We numerically compute c^*_{EWR}, which gives :

$$c^*_{EWR} = 15.877 \text{ km/year}. \tag{1.28}$$

1.5.2 Sensitivity analysis

We discuss here the dependence of our models on the parameters. We split our analysis in two parts. In the first part, we analyse the dependence of the ER model on the reproduction parameters and in the second part, we analyse the dependence on the dispersal parameters of both models.

For this, we will need to fix some parameters while studying the dependence of c^* with respect to the others. We do this accordingly to our statistical study. Thus, unless otherwise stated, we will fix our parameters according to (1.23), (1.25), (1.24), (1.26) and (1.27) for both the EWR and the ER model. For the ER model, we fix $v_M = 1$ km/day.

FIGURE 1.25 – **Heat map of T_γ^α with the estimated parameters**

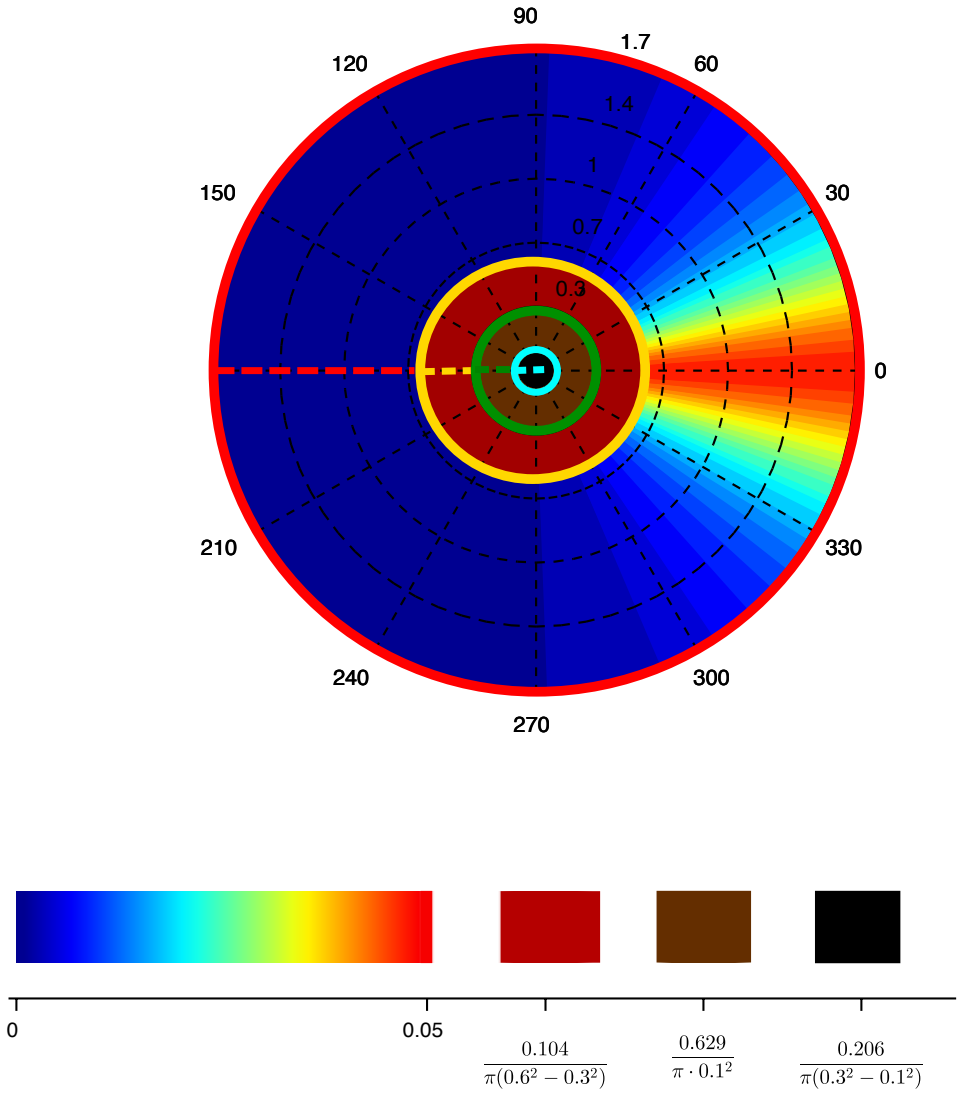

Light-blue circle : $\{r = 0.1\}$ *(maximal speed of the first walking mode).*
Green circle : $\{r = 0.3\}$ *(maximal speed of the second walking mode).*
Yellow circle : $\{r = 0.6\}$ *(maximal speed of the third walking toad).*
Red circle : $\{r = 1.7\}$ *(maximal speed of the running mode).*
Units : radial (km/day), tangential (degrees).

FIGURE 1.26 – **Histogram of c^*_{ER} for the estimated parameters**

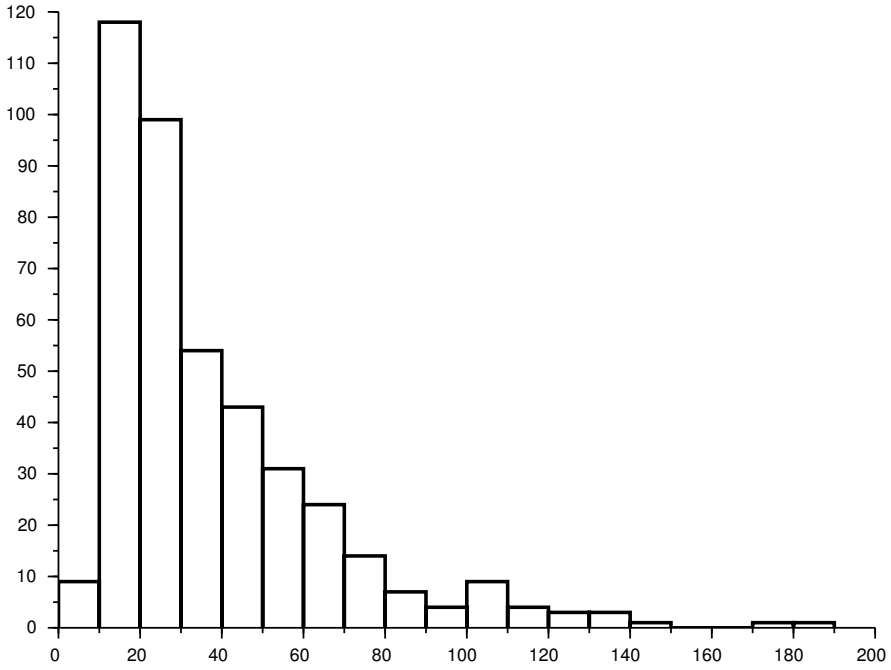

x-axis : c^*_{ER}.
y-axis : number of set in the class.
Total number of data : 245.

FIGURE 1.27 – **Sample of the selected parameters**

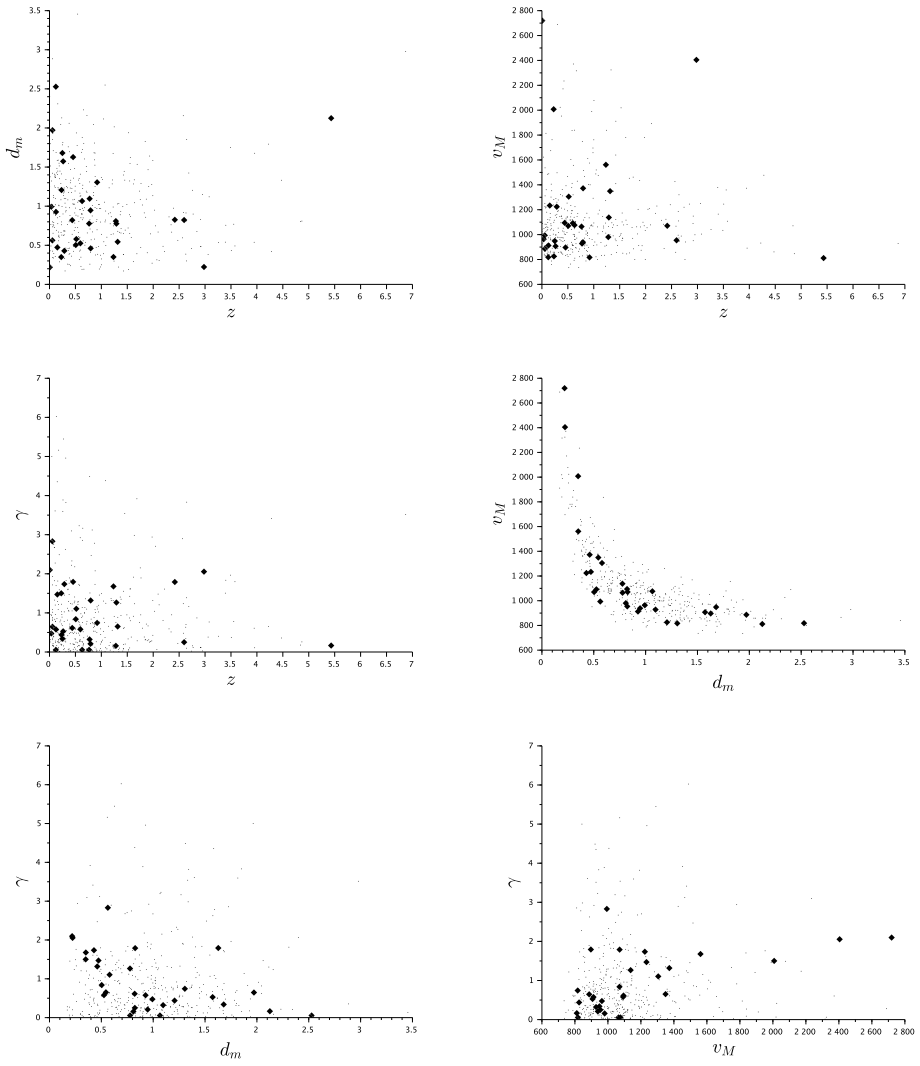

Points : all the selected parameters by our ABC procedure.
Black diamonds : selected parameters which give a speed $50 < c^*_{ER} < 60$.
Units : d_m *(days),* z *day*$^{-1}$, γ *(none),* v_M *(meters/day).*

TABLE 1.2 – **Lowest and highest value of the reproduction parameters**

	Lowest	"Middle"	Highest
ϕ	7500	15000	20000
σ_{egg}	68.8%	71.8%	73.8%
σ_m	1.2%	8.2%	17.6%
σ_a	30%	50%	70%
σ_j	3%	5%	7%
σ_t	34.99%	34.99%	34.99%

Dependance on the reproduction parameters in the ER model

Let us recall that our choice of parameters is motivated by Table 1 in [80]. We have already explained how we picked those parameters. Let us now explore how the speed c^* changes when we pick other parameters. In order to keep our models biologically relevant, we compute c^* three times per coefficients : one for the lowest value given in [80], Table 1, one for the highest value and one for the "middle" value, in the sense that we gave previously. The corresponding values are given in Table 1.2. We compute c^*_{ER} and c^*_{EWR} for those 3^5 sets of parameters and give the results in Figure 1.28 and 1.29.

Dependance to the dispersal parameters

For the ER model, we fix $v_M = 1$ km/day and $d_e = 5$ days, and represent in Figures 1.30, 1.31 and 1.32 the function c^*_{ER} as a function of z and γ for different values of d_m. In Figure 1.33, we dix $d_e = 5$ days, $d_m = 2.5$ days, $\gamma = 0.4$ and $z = 1$ and represent c^*_{ER} as a function of v_M.

For the EWR model, we are interest in the dependence with respect to γ, p and α_4. in Figure 1.34, we represent c^*_{EWR} as a function of γ fand we fix the other parameters, according to our statistical study. Similarly, in Figure 1.35, we represent c^*_{EWR} as a function of p. Finally, in Figure 1.36, we represent c^*_{EWR} as a function of α_4 where we fixed all other parameters but α_3, since the equality $\alpha_4 + \alpha_3 + \alpha_2 + \alpha_1 = 1$ must hold.

Before discussing our result, we would like to emphasize that this sensitivity analysis is satisfactory, as far as monotonicity is concerned. Indeed all the monotonicity that we observed in the last Figures are the one we expected of our models.

– c^*_{EWR} and c^*_{ER} are increasing with respect to γ because a high directionality is induced by a small variance in the wrapped Cauchy distribution.

FIGURE 1.28 – **Dependance on the reproduction parameters in the ER model**

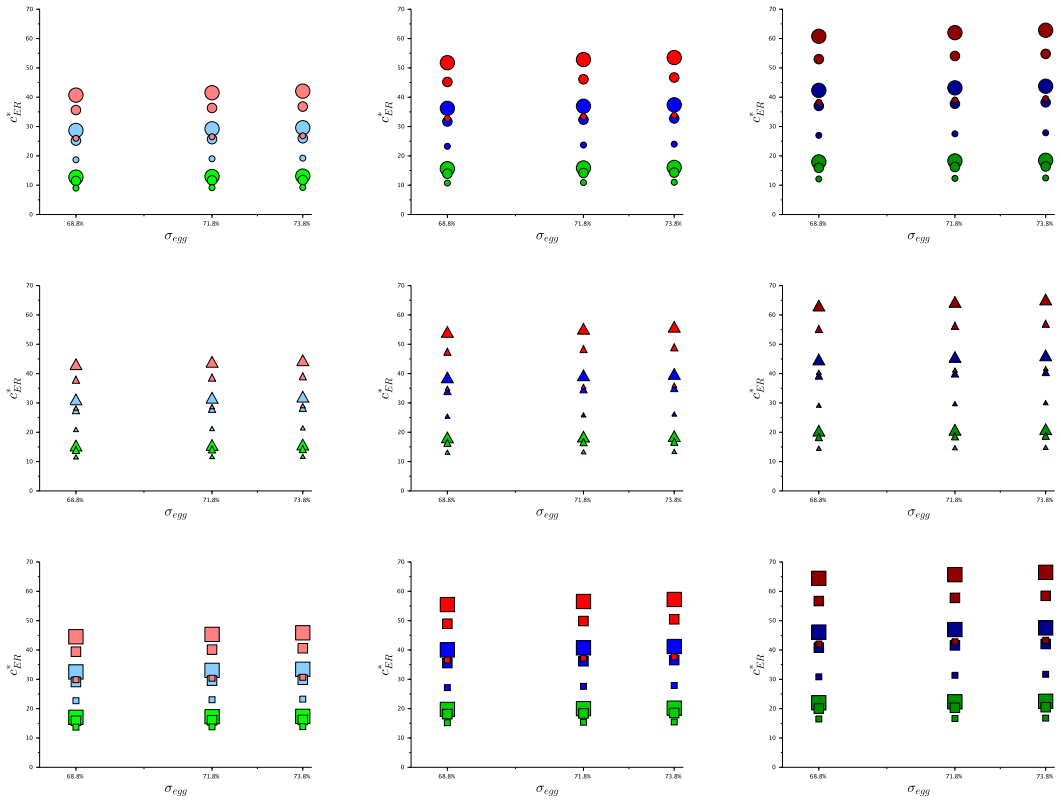

Numerical computation of c^*_{ER} as a function of σ_{egg} for $\sigma_{egg} = 68.8\%$, 71.8% and 73.8% for various parameters ϕ, σ_a, σ_j and σ_m.
Reproduction paremeters :
$\phi = 7500$ (small marks), 15000 (medium marks) and 20000 (large marks).
$\sigma_m = 1.2\%$ (circle marks), 8.2% (triangle marks) and 17.6% (square marks).
$\sigma_j = 3\%$ (light colored marks), 5% (regular colored marks), 7% (dark colored marks).
$\sigma_a = 30\%$ (green marks), 50% (blue marks), 70% (red marks).

FIGURE 1.29 – **Dependance on the reproduction parameters in the EWR model**

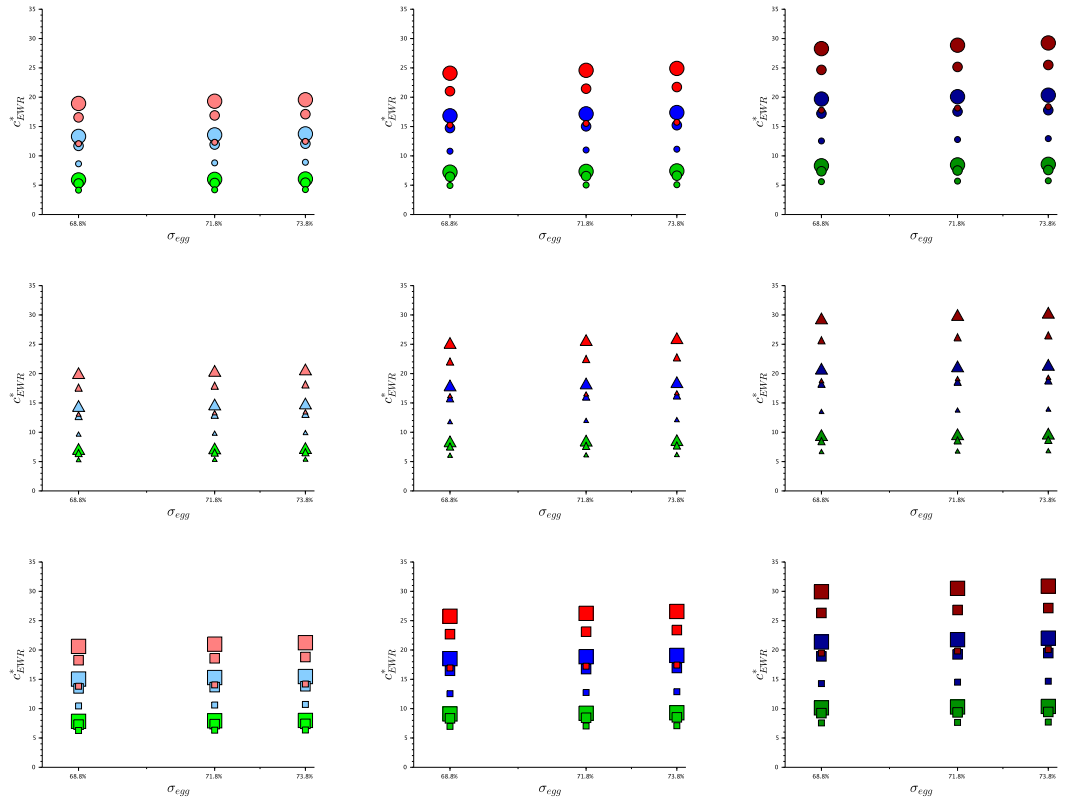

Numerical computation of c^*_{EWR} as a function of σ_{egg} for $\sigma_{egg} = 68.8\%$, 71.8% and 73.8% for various parameters ϕ, σ_a, σ_j and σ_m.
Reproduction paremeters :
$\phi = 7500$ *(small marks),* 15000 *(medium marks) and* 20000 *(large marks).*
$\sigma_m = 1.2\%$ *(circle marks),* 8.2% *(triangle marks) and* 17.6% *(square marks).*
$\sigma_j = 3\%$ *(light colored marks),* 5% *(regular colored marks),* 7% *(dark colored marks).*
$\sigma_a = 30\%$ *(green marks),* 50% *(blue marks),* 70% *(red marks).*

FIGURE 1.30 – **Numerical speed of propagation for the ER model with $d_m = 1$**

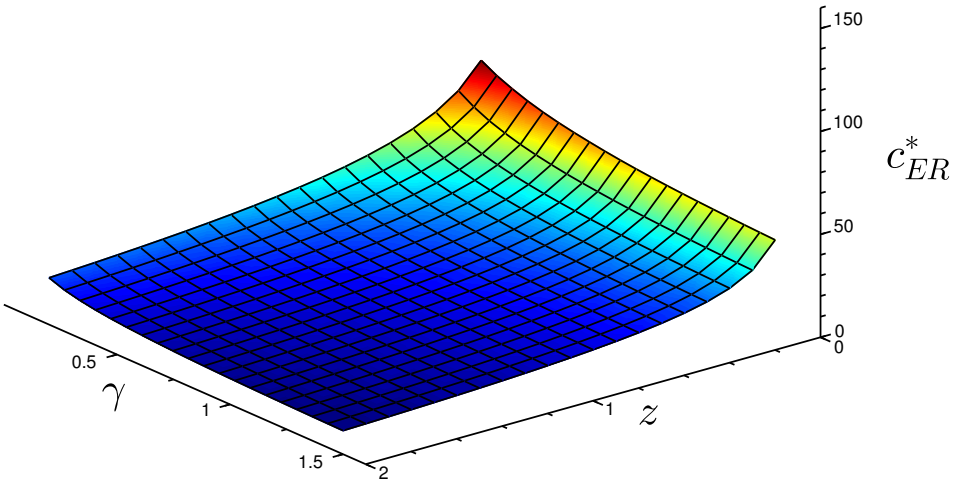

Numerical computation of c^*_{ER} as a function of γ and z.
Dispersal parameters : $d_m = 1$ day, $d_e = 5$ days, $v_M = 1$km/day.
Units : z-axis : $(day)^{-1}$, γ-axis : none, c^*-axis : km/year.
Maximal value : 69.764 km/year.

FIGURE 1.31 – **Numerical speed of propagation for the ER model with $d_m = 2.5$**

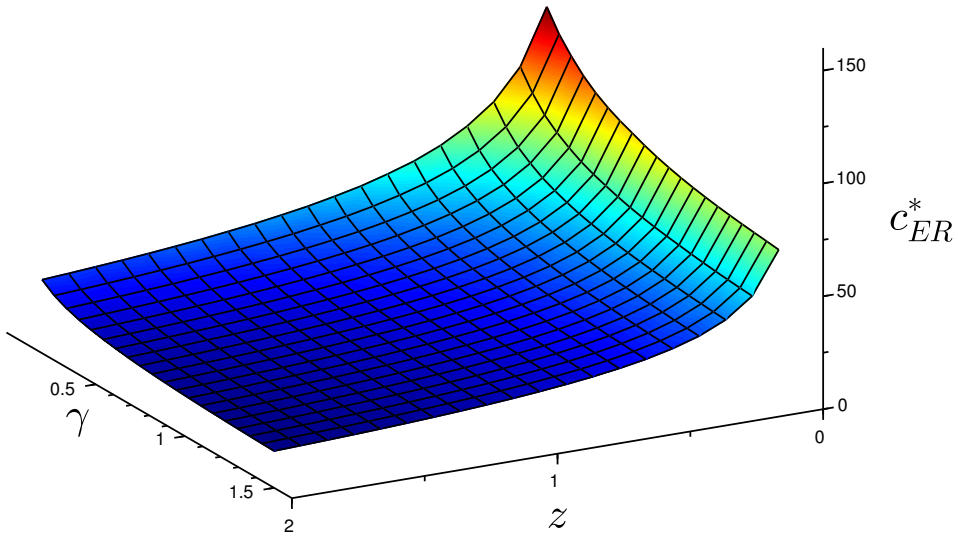

Numerical computation of c^*_{ER} as a function of γ and z.
Dispersal parameters : $d_m = 2.5$ days, $d_e = 5$ days, $v_M = 1$km/day.
Units : z-axis : $(day)^{-1}$, γ-axis : none, c^*-axis : km/year.
Maximal value : 115.968 km/year.

FIGURE 1.32 – **Numerical speed of propagation for the ER model with $d_m = 5$**

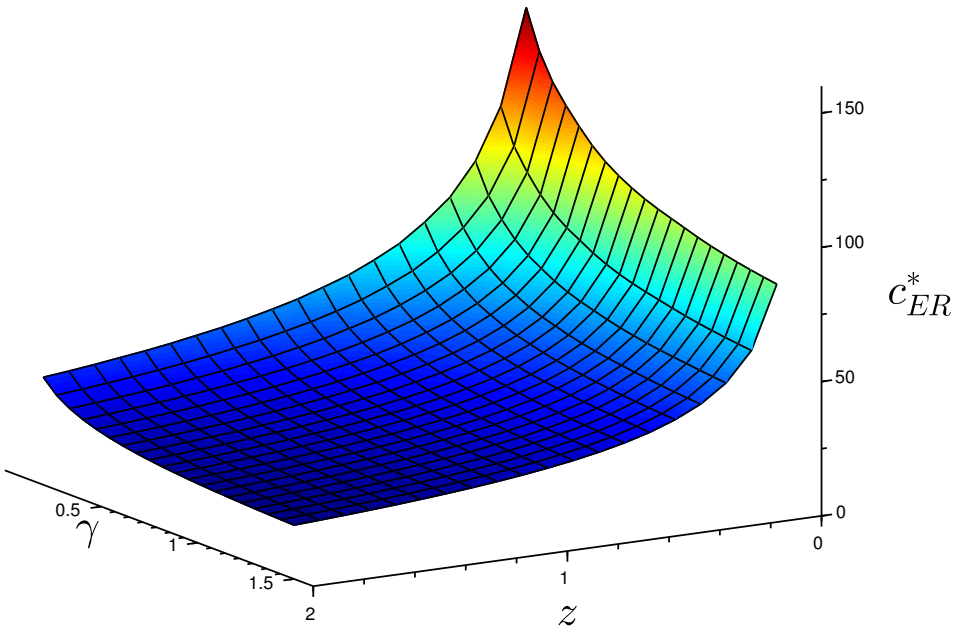

Numerical computation of c^*_{ER} as a function of γ and z.
Dispersal parameters : $d_m = 5$ days, $d_e = 5$ days, $v_M = 1$km/day.
Units : z-axis : $(day)^{-1}$, γ-axis : none, c^*-axis : km/year.
Maximal value : 152.826 km/year.

FIGURE 1.33 – **Numerical speed of propagation for the ER model as a function of v_M**

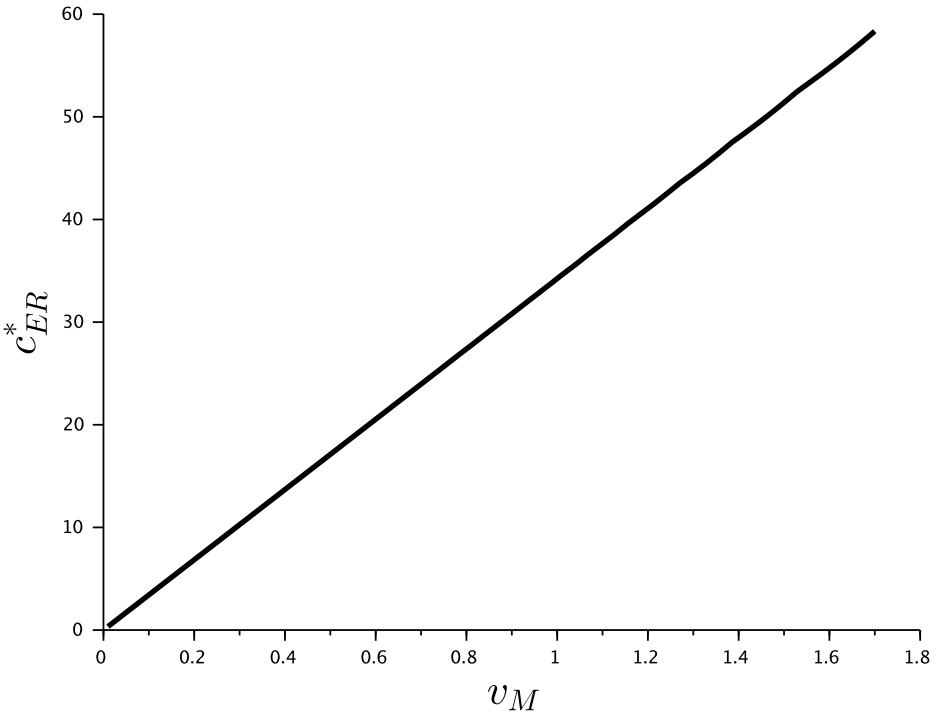

Units : v_M-axis : km/day, c^*-axis : km/year.
Slope : 34.2/365.

FIGURE 1.34 – **Numerical speed of propagation for the EWR model as a function of γ**

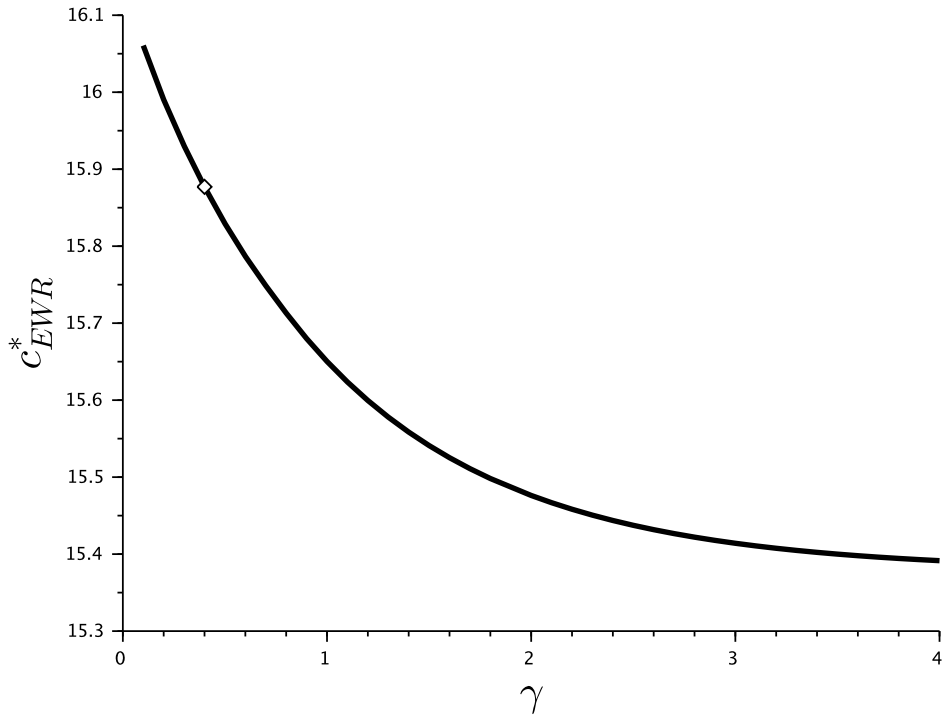

Numerical computation of c^*_{EWR} as a function of $\gamma \in [0.1, 4]$.
Units : γ-axis : none, c^*-axis : km/year.
White diamond : estimated speed of our model
Maximal value : 16.06 km/year.

FIGURE 1.35 – **Numerical speed of propagation for the EWR model as a function of p**

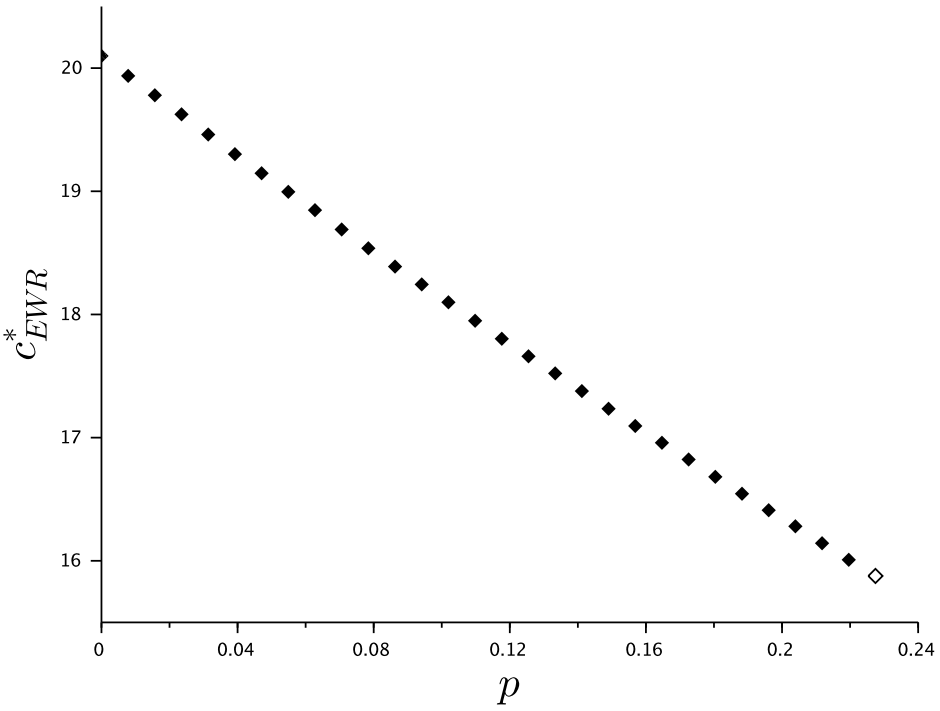

Numerical computation of c^*_{EWR} as a function of $p \in \{0, \frac{4}{510}, \frac{8}{510}, \ldots, \frac{116}{510}\}$.
Units : p-axis : none, c^*-axis : km/year.
White diamond : estimated speed of our model
Slope : -18.5 km/year.

FIGURE 1.36 – **Numerical speed of propagation for the EWR model as a function of α_4**

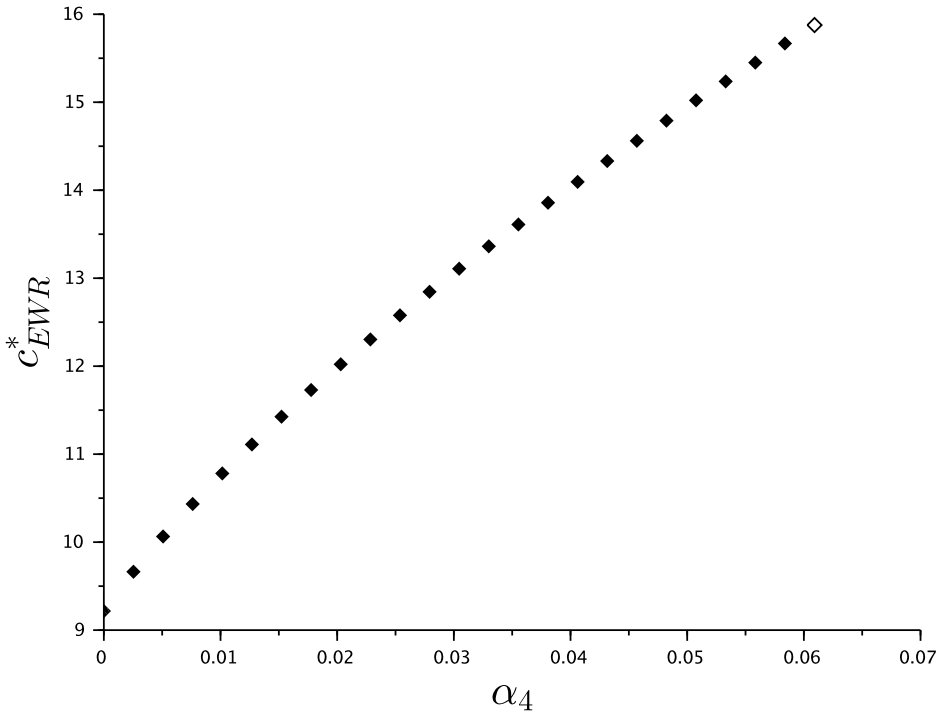

Numerical computation of c^*_{EWR} as a function of α_4.
Variables : $\alpha_4 \in \{0, \frac{1}{394}, \ldots, \frac{24}{394}\}$ and $\alpha_3 = 0.104 + \alpha_4$.
Units : α-axis : none, c^*-axis : km/year.
White diamond : estimated speed of our model
Slope : 106.1 km/year.

- c^*_{EWR} is increasing with respect to v_M since this can be interpreted as a maximal speed. Moreover, it is linear.
- c^*_{EWR} is decreasing with respect to z because high persistance is induced by a small parameter z.
- c^*_{EWR} is decreasing with respect to the reproduction parameters. This is quite understandable.
- c^*_{ER} is decreasing with respect to d_m. This was expected since d_m correspond to the average number of day spent in mobile mode.
- c^*_{EWR} is decreasing with respect to p. This was expected since the higher p is, the more paused the trajectories are.
- c^*_{EWR} is in creasing with respect to α_4. This was expected since α_4 correspond to a so called "running" mode. We would like to point out that the c^*_{EWR} strongly depends on α_4.

1.5.3 Discussion

Let us now discuss our results. In the ER model, the *posterior* law of the parameters v_M and d_m clearly differ from the *prior* laws but those of γ and z show a clear similarity with their *prior* law, which means that those parameters are not significant in the microscopic description of the model. They have however an influence when we compute the speed of propagation. The 31 sets of parameters given by Figure 1.27 are pretty accurate, as far as v_M is concerned. The parameters d_m for which c^*_{ER} is accurate are slightly smaller than the expected value of 2.5 days. The estimated z are close to the value of 1 change per day, which is quite satisfactory. We did not expect any particular value but very small values (*i.e* very persistant trajectories) or very big ones (*i.e.* erratic trajectories) would have been surprising. The parameters γ are also satisfactory for the same reasons. We did not expect them to be close to 0.4 as in the EWR because this value of 0.4 was obtained for toads in running mode, which do not account for the total population.

The ER model is satisfactory in the sens that it gives a large amount of ABC selected parameters which also provide a good speed of propagation. It is perfectible in the sense that the mode of the selected parameters corresponds to a theoretical speed of invasion of $10 < c^*_{ER} < 20$ (check Figure 1.26).

We can try to look for explanations. Our main hypothesis is that our model lacked a walking mode. Indeed, our model only considered two possible modes, *i.e.* an encamped mode, where individuals did move at all and a running mode, where individuals kept a very persistent direction. However, the histograms of the speed distribution showed that the toads which did not relocate between two days were not the majority of the toads, but that many of them walked quite a short distance, indeed, but walked anyway.

The EWR model tried to solve that problem. The statistics of the speed and turning angle distribution clearly showed that several walking modes have to be taken in consideration. The estimated parameters however provided a speed of propagation c^*_{EWR}, which is quite small compared to the current range of invasion. One possible explanation is that our walking modes lacked some directionality. We can indeed see in Figure 1.23 that the uniform law does not fit the histogram best. As we saw, the lack of directionality tends to slow down the propagation. This may not be significant, though. Indeed, one can see from Figure (1.34) that c^*_{EWR} does not depend strongly on γ. It depends strongly on α, however, as the Figure 1.36 clearly

FIGURE 1.37 – $\kappa - \alpha$ **graph**

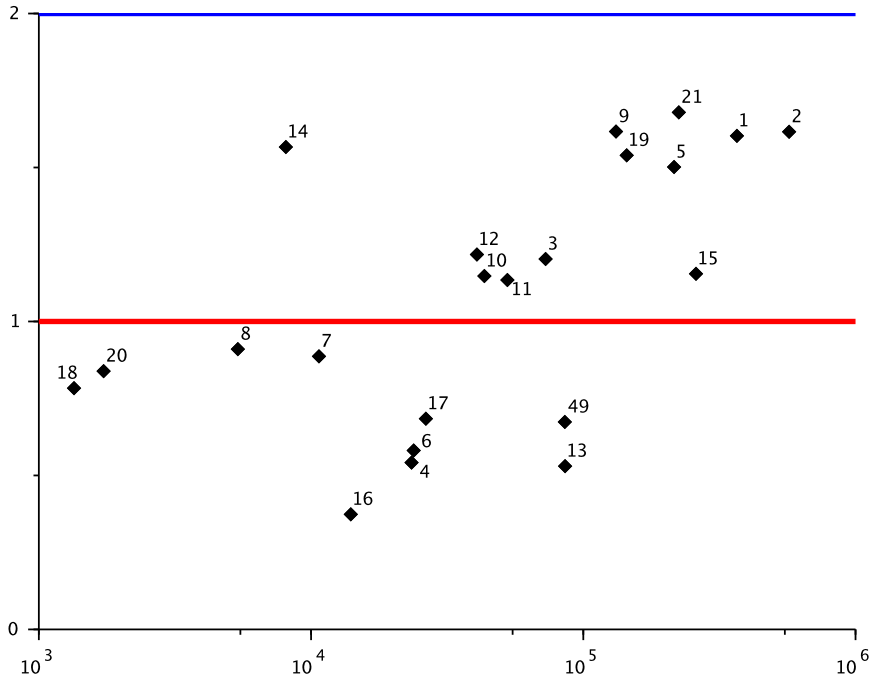

$\kappa - \alpha$ graph with the number of the corresponding toad
Units : α-axis : none, κ-axis : m^2/day.

shows.

This makes us think of an other explanation. Our model considers all toads to be able to walk at the different observed speeds. In reality, only 11 of our 22 toads were ever observed in running phase. We show in Annex A the histogram of daily displacement of each toad. One can see that some toads only stay in the lowest walking modes while other alternate walking and running phases. One can observe that the toads that had daily displacements between 0.6 and 1.7 kilometers are found in majority in the right side of the $\kappa - \alpha$ graph (see Figure 1.37). This means that there exists a significant difference of dispersal behavior even within the population at the vanguard. One of the major assumptions we made in both our models was to consider that all toads had the same dispersal behavior. We think that the limits of our models rely here. We can think that a more accurate model considering a heterogeneity of behaviors within the population could deliver a more precise speed of propagation.

We would also like to point out that the models also depend on the reproduction parameters, which we might adjust a little bit in the future. With our chosen parameters (1.23), the principle eigenvalue μ of the reproduction matrix (1.7) is close to 3, which means that we consider that the population has a growing rate of 300% each year. This is less than other

observations. We refer for example to [55], where a growing rate of 360% was considered. By monotonicity with respect to the reproduction parameters, we expect our theoretical speeds of invasion to be higher if we stick to their numbers.

In conclusion, our models encourage us to keep on studying velocity-jump models for the modeling of the cane toad's invasion. In the EWR model, we can find a set of parameters which are chosen by an approximate bayesian computation on the trajectories and which also predict a good speed of propagation. The ER model does not show satisfactory results yet, but it is perfectible if we consider heterogeneity in the dispersal behavior within the population.

Perspectives

We give here a list of perspectives for future work.

From a mathematical point of view, one still needs to establish propagation results for both our models. More precisely, one must investigate the existence of travelling waves solutions beyond linear analysis and show a spreading result involving the minimal speed c^*_{ER} and c^*_{EWR}.

Assuming that we find a better kinetic model which is accurate at the microscopic scale and which theoretical speed of propagation fits the actual one, one could build a complete kinetic model for which the dispersal parameters are phenotypical variables.

From a biological point of view, one could investigate how to explain this evolution and if those different dispersal behaviors are transmitted from one generation to the next.

Acknowledgment

We thank Gregory Brown, Benjamin Phillips and Richard Shine for sharing their data and Hugues Berry for interesting conversations about the TAMSD.

We thank Margo Perkins for allowing us to use her drawing of the adult toad, the juvenile toad, the walking toad and the mating toads. Drawings of the toads' eggs : Clipart courtesy FCIT. Sources : [40, 91]

This project has received funding from the European Research Council (ERC) under the European Unions Horizon 2020 research and innovation programme (grant agreement No 639638).

Deuxième partie

L'approche Hamilton-Jacobi pour la propagation de processus à sauts de vitesse et le problème de la dimension

Chapitre 2

Grandes déviations pour un processus à sauts de vitesse avec une approche Hamilton-Jacobi

Nous nous intéressons à un processus aléatoire sur $\mathbb{R}^n$ qui alterne des phases de mouvements rectilignes uniformes et change de vitesse à des temps exponentiels. Nous étudions plus précisément l'équation de Kolmogorov après rééchelonnement hyperbolique $(t,x,v) \to \left(\frac{t}{\varepsilon}, \frac{x}{\varepsilon}, v\right)$, $\varepsilon > 0$, puis nous effectuons une transformée de Hopf-Cole qui nous donne une équation cinétique suivie par un potentiel. Nous montrons la convergence pour $\varepsilon \to 0$ de ce potentiel vers la solution de viscosités d'une équation de Hamilton-Jacobi $\partial_t \varphi + H\left(\nabla_x \varphi\right) = 0$ où le hamiltonien peut présenter une singularité $\mathcal{C}^1$, ce qui est assez inédit dans ce type d'études.

Contents

Version française abrégée

Nous nous donnons une densité de probabilité $M \in L^1(\mathbb{R}^n)$ et nous notons V son support. Nous supposons que V est compact et que 0 appartient à l'intérieur de l'enveloppe convexe de V, que l'on note $\mathrm{Conv}(V)$. Pour $p \in \mathbb{R}^n$, nous notons $\mu(p) = \max\{v \cdot p \mid v \in \mathrm{Conv}(V)\}$. Nous étudions le mouvement de particules dans $\mathbb{R}^n$ suivant le processus de Markov déterministe par morceaux défini comme suit : une particule donnée se déplace de manière rectiligne uniforme avec une vitesse $v \in V$ tirée aléatoirement en suivant la loi de probabilité $M(v')\,dv'$. À des temps exponentiels de paramètre 1, la particule change de direction en tirant une nouvelle vitesse tirée selon la loi $M(v')\,dv'$. Afin d'étudier des résultats de grandes déviations du processus similairement aux techniques développées dans [31, 59], nous nous intéressons à l'équation de Chapman-Kolmogorov forward suivie par la densité de particules après un réechelonement hyperbolique $(t,x,v) \to \left(\frac{t}{\varepsilon}, \frac{x}{\varepsilon}, v\right)$, $\varepsilon > 0$:

$$\partial_t f^\varepsilon + v \cdot \nabla_x f^\varepsilon = \frac{1}{\varepsilon}\left(M(v)\,\rho^\varepsilon - f^\varepsilon\right), \quad (t,x,v) \in \mathbb{R}_+ \times \mathbb{R}^n \times V.$$

Nous étudions plus particulièrement l'équation vérifiée par un potentiel φ^ε obtenu après passage par une transformée de Hopf-Cole : $f^\varepsilon(t,x,v) = M(v)\,e^{-\frac{\varphi^\varepsilon(t,x,v)}{\varepsilon}}$. Nous cherchons alors une éventuelle limite pour φ^ε. Nous procédons à un développement WKB : $\varphi^\varepsilon = \varphi + \varepsilon\eta$, ce qui amène, en posant $p = \nabla_x \varphi$ et $H = -\partial_t \varphi$, à la résolution d'un problème spectral dans l'espace des mesures positives : chercher (H, Q) un couple valeur/vecteur propres associé à l'opérateur $Q \mapsto (v \cdot p - 1)\,Q + \int_V M'Q'dv'$. On obtient une équation de Hamilton-Jacobi $\partial_t \varphi + H(\nabla_x \varphi) = 0$. Pour $n = 1$ et $M \geq \delta > 0$ sur son support, le vecteur propre Q a une densité et conduit à un hamiltonien H défini par l'équation implicite

$$\int_V \frac{M(v)}{1 + H(p) - v \cdot p} dv = 1.$$

La positivité de Q garantit que $H(p) \geq \mu(p) - 1$. En dimension supérieure toutefois, et même si $M \geq \delta > 0$, cette équation peut ne pas avoir de solution $H(p)$ lorsque p devient grand. Cela se manifeste pour le vecteur propre par une concentration de la mesure Q autour des valeurs v qui annulent $1 + H(p) - v \cdot p$, ce qui force $H(p) = \mu(p) - 1$. Cette transition entraîne une singularité $\mathcal{C}^1$ du hamiltonien.

Nous démontrons la convergence de φ^ε vers φ, où φ est solution de viscosité [44] de l'équation de Hamilton-Jacobi en utilisant la méthode de la fonction test perturbée [57].

2.1 Introduction

We continue the work initiated in [18, 22]. Let $M \in L^1(\mathbb{R}^n)$ be a probability density function. We suppose that the support of M, which we denote V, is compact and that 0 belongs to the interior of Conv (V), the convex hull of V. We denote by $|\cdot|$ the euclidian norm in $\mathbb{R}^n$ and by $\cdot$ the canonical scalar product. For $p \in \mathbb{R}^n$, we define

$$\mu(p) := \max\{v \cdot p \mid v \in \text{Conv}(V)\}, \tag{2.1}$$

$\text{Arg}\mu(p) := \{v \in \text{Conv}(V) \mid v \cdot p = \mu(p)\}$ and $\text{Sing}(M) := \left\{p \in \mathbb{R}^n, \quad \int_V \frac{M(v)}{\mu(p)-v\cdot p} dv \leq 1\right\}$.

We focus on the motion dynamics in $\mathbb{R}^n$ of particles given by the following piecewise deterministic Markov process : a particle moves successively in straight lines with velocity v, chosen randomly with probability distribution $M(v')\,dv'$. At random exponential times (with parameter 1), the particle changes its velocity, choosing randomly a new velocity with distribution $M(v')\,dv'$. The Chapman-Kolmogorov forward equation associated to the probability density function $f(t,x,v)$ of this process is given by :

$$\partial_t f + v \cdot \nabla_x f = M\rho - f, \quad (t,x,v) \in \mathbb{R}_+ \times \mathbb{R}^n \times V, \tag{2.2}$$

where $\rho(t,x) = \int_V f(t,x,v)\,dv$. In order to investigate large deviation principles for the process, one can study the large scale hyperbolic limit $(t,x) \to \left(\frac{t}{\varepsilon}, \frac{x}{\varepsilon}\right)$ with $\varepsilon > 0$. In this scale, the kinetic equation (5.1) reads :

$$\partial_t f^\varepsilon + v \cdot \nabla_x f^\varepsilon = \frac{1}{\varepsilon}\left(M\rho^\varepsilon - f^\varepsilon\right), \quad (t,x,v) \in \mathbb{R}_+ \times \mathbb{R}^n \times V. \tag{2.3}$$

Then, we perform the following Hopf-Cole transformation : $f^\varepsilon(t,x,v) = M(v)\, e^{-\frac{\varphi^\varepsilon(t,x,v)}{\varepsilon}}$, where we expect the potential φ^ε to become independent of v as $\varepsilon \to 0$. Such techniques have already been studied for a more general case of Markov process with a finite discrete set of states in [31] and, from a probabilistic point of view, in [59].
Here, assume that the initial condition is well-prepared, i.e. it does not depend on v : $\varphi^\varepsilon(0,x,v) = \varphi_0(x)$. We believe that the conclusion of this paper is not dramatically modified if $\varphi^\varepsilon(0,x,v) = \varphi_0(x,v)$. Indeed, the only expected change concerns the initial condition of the Hamilton-Jacobi equation which should be independent of v. This is left for future work. The equation satisfied by φ^ε reads

$$\partial_t \varphi^\varepsilon + v \cdot \nabla_x \varphi^\varepsilon = \int_V M(v')\left(1 - e^{\frac{\varphi^\varepsilon - \varphi'^\varepsilon}{\varepsilon}}\right) dv', \quad (t,x,v) \in \mathbb{R}_+ \times \mathbb{R}^n \times V. \tag{2.4}$$

As in [68], the limit potential satisfies a Hamilton-Jacobi equation. Surprisingly enough, our Hamiltonian may lack $\mathcal{C}^1$ regularity as we will show in Proposition 2.2.

Theorem 2.1. *Under the previous assumptions, φ^ε converges locally uniformly on $\mathbb{R}_+ \times \mathbb{R}^n \times V$ toward φ, where φ does not depend on v. Moreover, φ is the viscosity solution of the following Hamilton-Jacobi equation :*

$$\partial_t \varphi(t,x) + H(\nabla_x \varphi(t,x)) = 0, \quad (t,x) \in \mathbb{R}_+ \times \mathbb{R}^n, \tag{2.5}$$

with initial condition $\varphi(0,\cdot) = \varphi_0$ and a hamiltonian H given as follows : if $p \in \text{Sing}(M)$, then $H(p) = \mu(p) - 1$. Else, $H(p)$ is uniquely determined by the following formula :

$$\int_V \frac{M(v)}{1 + H(p) - v \cdot p} dv = 1. \tag{2.6}$$

A corollary to Theorem 2.1 is that Theorem 1.1 from [22] is only correct when $\mathrm{Sing}(M) = \emptyset$ since there is no solution to (2.6) when $p \in \mathrm{Sing}(M)$. The present result establishes the appropriate statement in the case $\mathrm{Sing}(M) \neq \emptyset$. Interestingly enough, the proof appears quite different due to the apparition of Dirac masses in the velocity variable in the expression of the corrector.

2.2 Identification of the hamiltonian

In order to identify the limit $\varphi := \lim_{\varepsilon \to 0} \varphi^\varepsilon$, we perform the formal expansion $f^\varepsilon = MQe^{-\frac{\varphi}{\varepsilon}}$ where Q is to be determined. Plugging this ansatz into the kinetic formulation (2.3) and writing $p = \nabla_x \varphi$ and $H = -\partial_t \varphi$, we get (at the formal limit $\varepsilon \to 0$) the following spectral problem :

$$(1 + H - v \cdot p)\, Q = \int_V M(v')Q(v')dv'. \tag{2.7}$$

A similar spectral problem has been studied in [41] in a more general case. The positivity of Q yields $H \geq v \cdot p - 1$ for all $v \in V$ hence $H \geq \mu(p) - 1$. Suppose $H > \mu(p) - 1$. Then, $1 + H - vp > 0$ for all $v \in V$ and $Q(v) = \dfrac{\int_V M(v')\, Q(v')\, dv'}{1 + H - v \cdot p}$. Integrating against M with respect to v, we obtain the following problem : find H such that $\int_V \frac{M(v)}{1+H-v\cdot p} dv = 1$. If $p \in \mathrm{Sing}(M)^c$, by monotonicity, such H exists and is unique. Equation (2.6), however, does not have an L^1 solution for $p \in \mathrm{Sing}(M)$. Similarly to [41], we look for solutions in a larger set, namely the set of positive measures. Then, a solution to the spectral problem is the eigenvalue $H = \mu(p) - 1$ associated to the positive measure $Q = \frac{dv}{\mu(p) - v\cdot p} + \alpha(p)\, \delta_w$ where $\alpha(p) = 1 - \int_V \frac{M(v)}{\mu(p) - vp} dv \geq 0$ and δ_w is the Dirac measure centered in $w \in \mathrm{Arg}\mu(p) \cap V$. Here is an example where $\mathrm{Sing}(M) \neq \emptyset$:

Example 2.1. *Let $n > 1$ and $M = \omega_n^{-1} . \mathbb{1}_{\overline{B(0,1)}}$ where ω_n is the Lebesgue measure of the n-dimensional unit ball. Then,* $\mathrm{Sing}(M) = B\left(0, \frac{n}{n-1}\right)^c$. *Indeed, for $p = |p| \cdot e_1$, we have $\mu(p) = |p|$ and $v \cdot p = |p|\, v_1$ hence*

$$\int_V \frac{M(v)}{\mu(p) - v \cdot p} dv = \frac{1}{|p|\, \omega_n} \int_{B(0,1)} \frac{1}{1 - v_1} dv = \frac{\omega_{n-1}}{|p|\, \omega_n} \int_{-1}^{1} \frac{\left(1 - v_1^2\right)^{\frac{n-1}{2}}}{1 - v_1} dv_1 = \frac{1}{|p|} \times \frac{n}{n-1}.$$

By rotational invariance, we conclude that $\mathrm{Sing}(M) = B\left(0, \frac{n}{n-1}\right)^c$. *The Figure 1 gives illustrations of the hamiltonian and μ as functions of the radius of p, in the cases $n = 1$ and $n = 3$. In the cases $n = 3$ we can see the $\mathcal{C}^1$ singularity where $|p| = \frac{3}{2}$.*

Proposition 2.2. *The following properties hold :*

(i) The set $\mathrm{Sing}(M)^c$ *is convex.*

(ii) The function H is continuous and convex.

(iii) If $\mathrm{Sing}(M) \neq \emptyset$, *then H is not $\mathcal{C}^1$. More precisely, ∇H has a jump discontinuity at $\partial \mathrm{Sing} M$.*

Proof Let us first notice that μ is positively 1-homogeneous. Moreover, it is convex since it is a supremum of linear functions.

FIGURE 2.1 – **Hamiltonian in the one dimensional and in the multidimensional case**

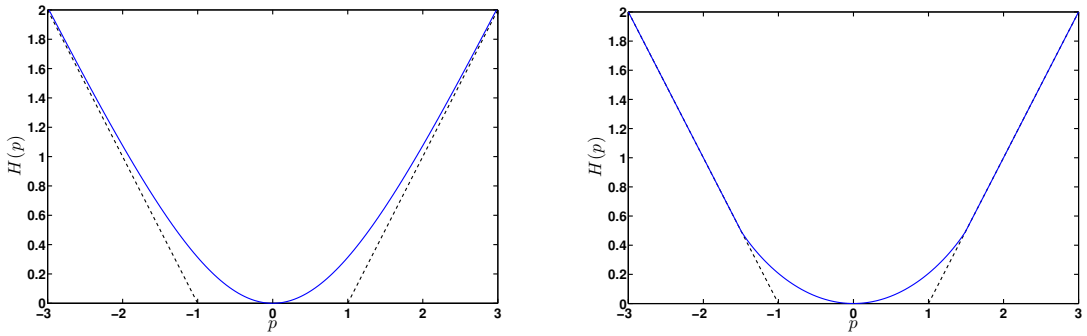

Blue plain lines : Hamiltonian for $n = 1, 3$ *and* $M = \omega_n^{-1}.\mathbb{1}_{\overline{B(0,1)}}$.
Black dotted lines : $|p| \mapsto \mu(p) - 1$.

(i) Let $p, q \in \text{Sing}(M)^c$ with $p \neq q$. Since μ is convex, we have for all $\tau \in [0,1]$

$$\begin{aligned} I(\tau) &:= \int_V \frac{M(v)}{\mu(p) - v \cdot p + \tau(\mu(q) - \mu(p) - v \cdot (q-p))} dv \\ &\leq \int_V \frac{M(v)}{\mu((1-\tau)p + \tau q) - v \cdot ((1-\tau)p + \tau q)} dv. \end{aligned}$$

Moreover, $I(0), I(1) > 1$ and I is differentiable on $[0,1]$ with

$$\partial_\tau I(\tau) = \int_V \frac{M(v)}{(\mu(p) - v \cdot p + \tau(\mu(q) - \mu(p) - v \cdot (q-p)))^2} (\mu(p) - \mu(q) - v \cdot (p-q)) dv.$$

It is clear that the sign of $\partial_\tau I$ does not change hence $I(\tau) > 1$, which proves (i).

(ii) We refer to [22], section 1, to prove that H is twice differentiable and strictly convex on $\text{Sing}(M)^c$ and that

$$\int_V \frac{M(v)}{(1 + H(q) - v \cdot q)^2} (\nabla H(q) - v) dv = 0, \quad \forall q \in \text{Sing}(M)^c. \tag{2.8}$$

In particular, $\nabla H(q) \in \text{Conv}(V)$ for all $q \in \text{Sing}(M)^c$. It is easy to see that H is continuous in the interior of $\text{Sing}(M)$. To show continuity of H on $\partial\text{Sing}(M)$, let $(p_m)_m$ converge to $p \in \partial\text{Sing}(M) \subset \text{Sing}(M)$. If we can extract a subsequence $(p_{m_l})_l \subset \text{Sing}(M)$, then $H(p_{m_l}) = \mu(p_{m_l}) - 1 \underset{l\to\infty}{\longrightarrow} \mu(p) - 1 = H(p)$. If not, then $p_m \in \text{Sing}(M)^c$ for m large enough and $1 = \int_V \frac{M(v)}{1+H(p_m)-v\cdot p_m} dv < \int_V \frac{M(v)}{\mu(p_m)-v\cdot p_m} dv$. Taking the limit, we get by dominated convergence $1 = \int_V \lim_{m\to\infty} \frac{M(v)}{1+H(p_m)-v\cdot p_m} dv \leq \int_V \frac{M(v)}{\mu(p)-v\cdot p} dv \leq 1$ hence $H(p_m) \underset{m\to\infty}{\longrightarrow} \mu(p) - 1 = H(p)$.

We now show that H is convex by proving that it is a maximum of convex functions :

$$H(p) = \max\left(\sup\left\{\nabla H(q) \cdot (p-q) + H(q) \mid q \in \text{Sing}(M)^c\right\}, \mu(p) - 1\right), \quad \forall p \in \mathbb{R}^n \tag{2.9}$$

In $\text{Sing}(M)^c$, (2.9) holds by convexity of H and $H(p) > \mu(p) - 1$. Let $p \in \text{Sing}(M)$ and $q \in \text{Sing}(M)^c$. By convexity of $\text{Sing}(M)^c \ni 0$, there exists a unique $\lambda \in (0,1]$ such that $\lambda p \in \partial\text{Sing}(M)$. For all $\tau \in [0,1]$, we set $\omega_1(\tau) := \mu(\tau p) - 1 = \tau\mu(p) - 1$ and $\omega_2(\tau) :=$

$\nabla H(q)\cdot(\tau p-q)+H(q)$. By continuity of H, $\mu(\lambda p)-1=H(\lambda p)\geq \nabla H(q)(\lambda p-q)+H(q)$ hence $\omega_1(\lambda)\geq\omega_2(\lambda)$. Moreover, ω_1 and ω_2 are both differentiable and $\partial_\tau\omega_1(\tau)=\mu(p)\geq \nabla H(q)\cdot p=\partial_\tau\omega_2(\tau)$ since $\nabla H(q)\in \mathrm{Conv}(V)$. Hence, $\omega_1(1)\geq\omega_2(1)$, which ends the proof of (ii).

(iii) Suppose $\mathrm{Sing}(M)\neq\emptyset$ and H is $\mathcal{C}^1$. Since $H+1=\mu$ is positive homogeneous of degree 1 on $\mathrm{Sing}(M)$ and since $\lambda p\in\mathrm{Sing}(M)$ for all $\lambda\geq 1$ and $p\in\mathrm{Sing}(M)$, we know that $\nabla H(p)\cdot p=H(p)+1=\mu(p)$ for all $p\in\mathrm{Sing}(M)\subset\mathrm{Sing}(M)$ hence $p\cdot(\nabla H(p)-v)\geq 0$, for all $v\in V$, the inequality being strict on a neighborhood of 0. Then,

$$p\cdot\int_V\frac{M(v)}{(1+H(p)-v\cdot p)^2}(\nabla H(p)-v)\,dv>0,\quad\forall p\in\partial\mathrm{Sing}(M). \tag{2.10}$$

By continuity, equations (2.8) and (2.10) are contradictory.

□

2.3 Proof of Theorem 2.1

Let $\varphi_0\in W^{1,\infty}(\mathbb{R}^n)$. We refer to Proposition 2.1 in [22] to prove that the Cauchy Problem (2.4) with initial condition φ_0 has a unique solution $\varphi^\varepsilon\in W^{1,\infty}$ which is locally (in t) uniformly (in ε, x and v) bounded in norm $W^{1,\infty}$. In particular, let us mention that

$$0\leq\varphi^\varepsilon(t,\cdot,\cdot)\leq\|\varphi_0\|_\infty,\quad\|\nabla_v\varphi^\varepsilon(t,\cdot,\cdot)\|_\infty\leq t\|\nabla_x\varphi_0\|_\infty. \tag{2.11}$$

Using the Arzelá-Ascoli theorem, we extract a locally uniformly converging subsequence. We denote by φ the limit. The function φ does not depend on v since $\int_V M(v')\,e^{\frac{\varphi^\varepsilon-\varphi'^\varepsilon}{\varepsilon}}dv'$ is uniformly bounded on $[0,T]\times\mathbb{R}^n\times V$ for all $T>0$. We use the perturbed test function method [57] to show that φ is a viscosity solution of (2.5). Theorem 2.1 will follow by uniqueness of the solution [42], thanks to the properties of H (see Proposition 2.2).

2.3.1 Subsolution procedure

Let $\psi\in\mathcal{C}^1(\mathbb{R}_+\times\mathbb{R}^n)$ be a test function such that $\varphi-\psi$ has a local strict maximum at (t^0,x^0). We want to show that ψ is a subsolution of (2.5). If $\nabla_x\psi(t^0,x^0)\in\mathrm{Sing}(M)^c$, then we refer to [22], section 2, step 2.

Suppose now that $\nabla_x\psi(t^0,x^0)\in\mathrm{Sing}(M)$. Let $w\in\mathrm{Arg}\mu(\nabla_x\psi(t^0,x^0))\cap V$. Then, $w\cdot\nabla_x\psi(t^0,x^0)=\mu(\nabla_x\psi(t^0,x^0))$. The uniform convergence of φ^ε toward φ ensures that the function $(t,x)\mapsto\varphi^\varepsilon(t,x,w)-\psi(t,x)$ has a local maximum at a point $(t^\varepsilon,x^\varepsilon)$ satisfying $(t^\varepsilon,x^\varepsilon)\to(t^0,x^0)$, as $\varepsilon\to 0$. We then have :

$$\begin{aligned}\partial_t\psi(t^\varepsilon,x^\varepsilon)+w\cdot\nabla_x\psi(t^\varepsilon,x^\varepsilon)&=\partial_t\varphi^\varepsilon(t^\varepsilon,x^\varepsilon)+w\cdot\nabla_x\varphi^\varepsilon(t^\varepsilon,x^\varepsilon)\\&=1-\int_V M(v')\,e^{\frac{\varphi^\varepsilon(t^\varepsilon,x^\varepsilon,w)-\varphi^\varepsilon(t^\varepsilon,x^\varepsilon,v')}{\varepsilon}}dv'\\&\leq 1.\end{aligned}$$

Passing to the limit $\varepsilon\to 0$, we get $\partial_t\psi(t^0,x^0)+\mu(\nabla_x\psi(t^0,x^0))\leq 1$. We conclude that φ is a viscosity subsolution of (2.5).

2.3.2 Supersolution procedure

Let $\psi \in \mathcal{C}^1(\mathbb{R}_+ \times \mathbb{R}^n)$ be a test function such that $\varphi - \psi$ has a local strict minimum at (t^0, x^0). We want to show that ψ is a supersolution of (2.5). If $\nabla_x \psi(t^0, x^0) \in \mathrm{Sing}(M)^c$, then we refer to [22], section 2, step 2.

Suppose now that $\nabla_x \psi(t^0, x^0) \in \mathrm{Sing}(M)$. Then, $\nabla_x \psi(t^0, x^0) \neq 0$ because $0 \in \mathrm{Sing}(M)^c$. We suppose without loss of generality that the minimum of $\varphi - \psi$ is global and that $\varphi(t^0, x^0) - \psi(t^0, x^0) = 0$. Let $\psi^\varepsilon := \psi - C(t - t^0)^2 + \varepsilon\eta$ with $C > 0$ yet to be determined and

$$\eta(v) := \ln\left(\mu\left(\nabla_x \psi(t^0, x^0)\right) - v \cdot \nabla_x \psi(t^0, x^0)\right).$$

Then, η is a continuous function on $D(\eta) = V \setminus \mathrm{Arg}\mu\left(\nabla_x \psi(t^0, x^0)\right)$ and, for all $w \in \mathrm{Arg}\mu\left(\nabla_x \psi(t^0, x^0)\right) \cap V$, we have $\lim_{v \to w} \eta(v) = -\infty$. Moreover, η is bounded from below on all compact sets yielding the uniform convergence $\psi^\varepsilon \to \psi$ on all compact sets of $D(\eta)$. Finally, $\int_V M(v') e^{-\eta(v')} dv' \leq 1$ since $\nabla_x \psi(t^0, x^0) \in \mathrm{Sing}(M)$.

The function $\varphi - \left(\psi - C(t - t^0)^2\right)$ has a global strict minimum at (t^0, x^0). The first inequality (2.11) ensures that the function $\varphi^\varepsilon - \psi^\varepsilon$ has a local minimum at a point $(t^\varepsilon, x^\varepsilon, v^\varepsilon) \in \mathbb{R}_+ \times \mathbb{R}^n \times D(\eta)$. As V compact, we can extract a subsequence $(v^\varepsilon)_\varepsilon$, without relabelling, such that $v^\varepsilon \to v^0$, as $\varepsilon \to 0$.

If $v^0 \in V \setminus \mathrm{Arg}\mu(p)$, then there exists a compact $A \subset D(\eta)$ such that $v^0 \in A$ and the uniform convergence of ψ^ε towards ψ on A guarantees that $(t^\varepsilon, x^\varepsilon) \to (t^0, x^0)$, as $\varepsilon \to 0$. We then get at point $(t^\varepsilon, x^\varepsilon, v^\varepsilon)$,

$$\begin{aligned}
\partial_t \psi - 2C\left(t^\varepsilon - t^0\right) + v^\varepsilon \cdot \nabla_x \psi &= \partial_t \psi^\varepsilon + v^\varepsilon \cdot \nabla_x \psi^\varepsilon \\
&= \partial_t \varphi^\varepsilon + v^\varepsilon \cdot \nabla_x \varphi^\varepsilon \\
&= 1 - \int_V M' e^{\frac{\varphi^\varepsilon - \varphi'^\varepsilon}{\varepsilon}} dv' \\
&\geq 1 - \int_V M(v') e^{\eta(v^\varepsilon) - \eta(v')} dv'.
\end{aligned}$$

We take the limit $\varepsilon \to 0$:

$$\partial_t \psi(t^0, x^0) + v^0 \cdot \nabla_x \psi(t^0, x^0) \geq 1 - e^{\eta(v^0)} \int_V M(v') e^{-\eta(v')} dv' \geq 1 - e^{\eta(v^0)}.$$

By construction, for all $v, v' \in D(\eta)$, we have $e^{\eta(v)} - e^{\eta(v')} = (v' - v) \cdot \nabla_x \psi(t^0, x^0)$ hence, for all $v \in D(\eta)$,we have $\partial_t \psi(t^0, x^0) + v \cdot \nabla_x \psi(t^0, x^0) \geq 1 - e^{\eta(v)}$. Let $w \in V \cap \mathrm{Arg}\mu\left(\nabla_x \psi(t^0, x^0)\right)$. Since $\mathrm{Arg}\mu\left(\nabla_x \psi(t^0, x^0)\right)$ is a null-set, V is dense in $\mathrm{Arg}\mu\left(\nabla_x \psi(t^0, x^0)\right)$. Taking the limit $v \to w$, we get : $\partial_t \psi(t^0, x^0) + \mu\left(\nabla_x \psi(t^0, x^0)\right) \geq 1$.

If $v^0 \in V \cap \mathrm{Arg}\mu(p)$, we still have $(t^\varepsilon, x^\varepsilon) \underset{\varepsilon \to 0}{\longrightarrow} (t^0, x^0)$ thanks to the following lemma :

Lemma 2.3. *For $C = 4\|\varphi_0\|_\infty$, we have $\lim_{\varepsilon \to 0} \varepsilon\eta(v^\varepsilon) = 0$.*

Proof of Lemma 2.3 We have $\varphi^\varepsilon(t, x, v) - \varphi(t, x) \geq -2\|\varphi_0\|_\infty$ by (2.11) and $\varphi(t, x) - \psi(t, x) \geq 0$ hence

$$\varphi^\varepsilon(t, x, v) - \psi^\varepsilon(t, x, v) \geq -2\|\varphi_0\|_\infty + C\left(t - t^0\right)^2 - \varepsilon\eta(v), \quad \forall \varepsilon > 0.$$

Moreover,

$$\varphi^\varepsilon\left(t^0,x^0,v\right)-\psi^\varepsilon\left(t^0,x^0,v\right) \;=\; \varphi^\varepsilon\left(t^0,x^0,v\right)-\varphi\left(t^0,x^0\right)-\varepsilon\eta\left(v\right)\leq 2\left\|\varphi_0\right\|_\infty-\varepsilon\eta\left(v\right).$$

Since $C=4\left\|\varphi_0\right\|_\infty$, we have $\varphi^\varepsilon\left(t,x,v\right)-\psi^\varepsilon\left(t,x,v\right)>\varphi^\varepsilon\left(t^0,x^0,v\right)-\psi^\varepsilon\left(t^0,x^0,v\right)$ for all $t>t^0+1$ and, thus, the minimum of $\varphi^\varepsilon-\psi^\varepsilon$ cannot be attained for $t>t^0+1$ hence $t^\varepsilon\leq t^0+1$ for all $\varepsilon>0$. At point $\left(t^\varepsilon,x^\varepsilon,v^\varepsilon\right)$ we have :

$$\nabla_v\varphi^\varepsilon\left(t^\varepsilon,x^\varepsilon,v^\varepsilon\right) \;=\; \nabla_v\psi^\varepsilon\left(t^\varepsilon,x^\varepsilon,v^\varepsilon\right)=\varepsilon\nabla_v\eta\left(v^\varepsilon\right)=-\frac{\varepsilon\nabla_x\psi\left(t^0,x^0\right)}{\mu\left(\nabla_x\psi\left(t^0,x^0\right)\right)-v^\varepsilon\cdot\nabla_x\psi\left(t^0,x^0\right)}.$$

The second estimation (2.11) yields $\left\|\nabla_v\varphi^\varepsilon\left(t^\varepsilon,\cdot,\cdot\right)\right\|_\infty\leq t^\varepsilon\left\|\nabla_x\varphi_0\right\|_\infty\leq\left(t^0+1\right)\left\|\nabla_x\varphi_0\right\|_\infty$ hence

$$\begin{aligned}\frac{\varepsilon}{\left(t^0+1\right)\left\|\nabla_x\varphi_0\right\|_\infty}\left|\nabla_x\psi\left(t^0,x^0\right)\right| \;&\leq\; \mu\left(\nabla_x\psi\left(t^0,x^0\right)\right)-v^\varepsilon\cdot\nabla_x\psi\left(t^0,x^0\right),\\ \Longrightarrow\; \varepsilon K\geq\varepsilon\eta\left(v^\varepsilon\right) \;&\geq\; \varepsilon\ln\left(\frac{\varepsilon}{\left(t^0+1\right)\left\|\nabla_x\varphi_0\right\|_\infty}\left|\nabla_x\psi\left(t^0,x^0\right)\right|\right),\end{aligned}$$

and $\varepsilon\eta\left(v^\varepsilon\right)\to 0$ as $\varepsilon\to 0$.

□

Thanks to Lemma 2.3, the function $(t,x)\mapsto\psi^\varepsilon\left(t,x,v^\varepsilon\right)=\psi\left(t,x\right)-4\left\|\varphi_0\right\|_\infty\left(t-t^0\right)^2+\varepsilon\eta\left(v^\varepsilon\right)$ converges uniformly towards $(t,x)\mapsto\psi\left(t,x\right)-4\left\|\varphi_0\right\|_\infty\left(t-t^0\right)^2$ and has a local minimum at $\left(t^\varepsilon,x^\varepsilon\right)$ satisfying $\left(t^\varepsilon,x^\varepsilon\right)\to\left(t^0,x^0\right)$, as $\varepsilon\to 0$. At point $\left(t^\varepsilon,x^\varepsilon,v^\varepsilon\right)$, we have :

$$\partial_t\psi^\varepsilon+v^\varepsilon\cdot\nabla_x\psi^\varepsilon=\partial_t\varphi^\varepsilon+v^\varepsilon\cdot\nabla_x\varphi^\varepsilon=1-\int_V M\left(v'\right)e^{\frac{\varphi^\varepsilon\left(t^\varepsilon,x^\varepsilon,v^\varepsilon\right)-\varphi^\varepsilon\left(t^\varepsilon,x^\varepsilon,v'\right)}{\varepsilon}}dv'.$$

The minimal property of $\left(t^\varepsilon,x^\varepsilon,v^\varepsilon\right)$ implies at this point :

$$\begin{aligned}\partial_t\psi\left(t^\varepsilon,x^\varepsilon\right)-8\left\|\varphi_0\right\|_\infty\left(t^\varepsilon-t^0\right)+v^\varepsilon\cdot\nabla_x\psi\left(t^\varepsilon,x^\varepsilon\right) \;&=\; \partial_t\psi^\varepsilon+v^\varepsilon\cdot\nabla_x\psi^\varepsilon\\ &\geq\; 1-\int_V M\left(v'\right)e^{\eta\left(v^\varepsilon\right)-\eta\left(v'\right)}dv'\\ &\geq\; 1-e^{\eta\left(v^\varepsilon\right)}.\end{aligned}$$

Passing to the limit $\varepsilon\to 0$, we get $\partial_t\psi\left(t^0,x^0\right)+\mu\left(\nabla_x\psi\left(t^0,x^0\right)\right)\geq 1$. We conclude that φ is a viscosity supersolution of (2.5).

□

Acknowledgements

This project has received funding from the European Research Council (ERC) under the European Union's Horizon 2020 research and innovation programme (grant agreement No 639638).

The author also wishes to thank Vincent Calvez and Julien Vovelle for their kind help.

Chapitre 3

Une limite Hamilton-Jacobi pour un processus à sauts de vitesse forcé

Nous étudions le mouvement de particules dans $\mathbb{R}^3$ suivant le processus de Markov déterministe par morceaux défini comme suit : une particule se déplace dans $\mathbb{R}^3$ et est soumise à un champ de forces Γ qui dépend uniquement de la vitesse de la particule. On suppose que l'espace des vitesses admissibles par la particule est la sphère de rayon 1. À des dates aléatoires exponentielles, la particule sélectionne une nouvelle vitesse uniformément sur la sphère. La densité des particules vérifie l'équation de Chapman-Kolmogorov du processus. Il s'agit d'une équation cinétique. Dans le but d'étudier des résultats de grandes déviations du processus, nous étudions l'équation cinétique après un rééchelonement hyperbolique. Conformément aux approches Hamilton-Jacobi déjà mises en place, on procède à un ansatz WKB qui nous donne une équation vérifiée par un potentiel. Nous démontrons que ce potentiel converge vers la solution de viscosité d'une équation de Hamilton-Jacobi. Notre résultat est valable pour un exemple précis du terme de force Γ pour lequel la preuve de la convergence est simplifiée.

Contents

3.1 Introduction

Recently, the study of propagation in kinetic equations has drawn a lot of interest. Among other motivations, one can cite the study of dispersal dynamics of biological populations as an example. The study of the *Escherichia Coli* bacterium's dispersal must be highlighted. In [98], the authors proved that the classically used diffusion approximation is not accurate to mathematically model the dispersion of bacteria and that one must stick to the mesoscopic scale to properly understand the expansion of the colony. Such an observation has lead mathematicians to look for spreading result in kinetic related models. For example, travelling waves for kinetic models have been investigates n [26, 99, 100].

One other way to study front propagation of a system of interacting particle is to use the Schrödinger WKB expansion [58, 65]. We refer to [22] where this technique was revisited to adapt to the context of a transport-reaction equation. In [18], it was successfully adapted to a more general set of reaction-transport equation. The aim of this technique is to perform a WKB ansatz at the hyperbolic scale of the kinetic equation. We then look for a limit of a potential u^ε, where ε is the rescaling factor. One can prove [62] that the population is contained in the null-set of $\lim_{\varepsilon\to 0} u^\varepsilon$ at the hyperbolic scale. In order to exhibit a limit and prove convergence, one needs to use the so-called "perturbed test-function method" [57]. The limit of the potential can sometimes be a viscosity solution to a Hamilton-Jacobi equation [22, 18]. In [34], the author proved that some care is in order while looking for a Hamilton-Jacobi limit, since C^1 singularities may occur in the multi-dimensional case.

The aim of this paper is to adapt the same methods for a kinetic forced equation. As of yet, the quest for a general result on this matter has been unsuccessful but some interesting results have been found in a particular case. We present those results here and discuss the possibility to generalize them in our last section.

We consider the motion dynamics of a velocity-jump process in $\mathbb{R}^3$. We call (e_1, e_2, e_3) the canonical orthonormal basis and we set from now on, $x_i := x \cdot e_i$, for all $x \in \mathbb{R}^3$. The set of admissible velocities V is the 2-dimensional sphere that we parametrize with the usual spherical coordinates :

$$V = \{(\theta, \varphi) \in [0, 2\pi] \times [0, \pi]\},$$

$$v(\theta,\varphi) := (\cos\theta\cdot\sin\varphi, \sin\theta\cdot\sin\varphi, \cos\varphi).$$

We consider the canonical measure on V : $d\nu(\theta,\varphi) = \frac{\sin\varphi}{4\pi} d\theta d\varphi$, such that $\nu(V) = 1$. We consider a probability density function M on (V,ν) that depends only on φ, hence $\int_V M(\varphi)\, d\nu(\theta,\varphi) = 1$ and a force term $\Gamma(\theta,\varphi) = (\sin(\varphi), 0)$.

We consider the following velocity-jump process : during its running phase, a particle moves in $\mathbb{R}^3$ under the influence of a force given by $\Gamma(\theta,\varphi)$, such that its position X_t at time t satisfies the ordinary differential equation

$$\frac{d}{dt}X_t = v(\Theta_t,\Phi_t), \quad \forall t > 0, \tag{3.1}$$

with

$$\begin{cases} \frac{d}{dt}\Theta_t = \sin(\Phi_t) \\ \frac{d}{dt}\Phi_t = 0 \end{cases}, \quad \forall t > 0.$$

At the ringing of an exponential clock of parameter 1, the particle changes its velocity and chooses a new one randomly on the sphere with probability law $M(\varphi)\, d\nu(\theta,\varphi)$. The forward-Kolmogorov equation satisfied by the density this process is

$$\begin{cases} \partial_t f + v(\theta,\varphi)\cdot\nabla_x f + \partial_\theta f = M\rho_f - f \\ \rho_f(t,x) = \int_V f(t,x,\theta,\varphi)\, d\nu(\theta,\varphi) \\ f(t,x,0,\varphi) = f(t,x,2\pi,\varphi) \\ \partial_\varphi f(t,x,\theta,0) = \partial_\varphi f(t,x,\theta,\pi) = 0 \end{cases}, \quad (t,x,\theta,\varphi) \in \mathbb{R}_+^* \times \mathbb{R}^3 \times V. \tag{3.2}$$

In order to study the propagation of this particle, we perform the hyperbolic scaling $(t,x,\theta,\varphi) \to \left(\frac{t}{\varepsilon}, \frac{x}{\varepsilon}, \theta, \varphi\right)$. The function $f^\varepsilon(t,x,\theta,\varphi) = f\left(\frac{t}{\varepsilon}, \frac{x}{\varepsilon}, \theta, \varphi\right)$ satisfies

$$\partial_t f^\varepsilon + v(\theta,\varphi)\cdot\nabla_x f^\varepsilon + \frac{\partial_\theta f^\varepsilon}{\varepsilon} = \frac{1}{\varepsilon}\left(M\rho_f^\varepsilon - f^\varepsilon\right), \quad (t,x,\theta,\varphi) \in \mathbb{R}_+^* \times \mathbb{R}^3 \times V. \tag{3.3}$$

Since the function f^ε relaxes to M, we perform the WKB ansatz $f^\varepsilon = Me^{-\frac{u^\varepsilon}{\varepsilon}}$. The function u^ε satisfies

$$\partial_t u^\varepsilon + v(\theta,\varphi)\cdot\nabla_x u^\varepsilon + \frac{\partial_\theta u^\varepsilon}{\varepsilon} = \int_V M'\left(1 - e^{\frac{u^\varepsilon - u'^\varepsilon}{\varepsilon}}\right) d\nu', \quad (t,x,\theta,\varphi) \in \mathbb{R}_+ \times \mathbb{R}^d \times V, \tag{3.4}$$

and

$$\begin{cases} u^\varepsilon(t,x,0,\varphi) = u^\varepsilon(t,x,2\pi,\varphi), \\ \partial_\varphi u^\varepsilon(t,x,\theta,0) = \partial_\varphi u^\varepsilon(t,x,\theta,\pi) = 0. \end{cases} \tag{3.5}$$

We suppose that the initial condition u_0 is well prepared :

$$u^\varepsilon(0,x,\theta,\varphi) = u_0(x) \geq 0, \tag{3.6}$$

and study the limit $\varepsilon \to 0$ of the function u^ε.

Such an issue has already been dealt with in [22, 34] in the case where no force term is involved. In that case, the authors have proven that u^ε converges uniformly locally to the

unique viscosity solution u of a Hamilton-Jacobi equation $\partial_t u + H(\nabla_x u) = 0$, where H is implicitly defined as the principle eigenvalue of a spectral problem in the set of positive measures : for all $p \in \mathbb{R}^3$, find $H(p)$ and Q a positive measure such that

$$(1 + H(p) - v(\varphi, \theta) \cdot p)\, Q = \int M' Q' dv'. \tag{3.7}$$

Actually, their result is more general since we can consider a more general compact set V and still keep their result. In [41], the author noticed that (3.7) may not have a solution Q in $L^1(V)$. The consequence is that one must look for solution associated to the eigenvalue $H(p) = \max\limits_{\theta,\varphi \in V} \{v(\theta, \varphi) \cdot p\} - 1$. The author also proved that such H is convex but not strictly convex, which was quite unseen in such problems. In [18], the author dealt with a similar equation, without the force term but with a reaction term and a more general setting of collision operators, such as elliptic operators or kernel operators. In the one-dimensional case, he proved convergence to a similar kind of Hamilton-Jacobi equation. In an ongoing work, Bouin and the author generalize this result to the multi-dimensional case with the same collision operator as the one considered in (3.2).

In this paper, we prove a similar result. In order to do so, we will need :

Definition 3.1. *We define the so-called singular set of M to be :*

$$\mathrm{Sing}(M) := \left\{ p \in \mathbb{R}^3, \quad \int_V M(\varphi) \int_0^\infty \exp\left(- \int_0^t (|p_3| - v(\theta - s, \varphi) \cdot p) ds \right) dt.dv(\theta, \varphi) \leq 1 \right\}, \tag{3.8}$$

where p_3 is the third cartesian coordinate of p.

Our result reads :

Theorem 3.2. *Under the previous assumptions, the solution u^ε of the Cauchy problem (3.4)-(3.6) converges uniformly locally towards u, where u does not on depend on (θ, φ). Moreover, u is the viscosity solution of the Hamilton-Jacobi equation*

$$\begin{cases} \partial_t u + H(\nabla_x u) = 0 \\ u(0, \cdot) = u_0 \end{cases}, \tag{3.9}$$

where H is defined as follows :

– *if $p \in \mathrm{Sing}^c(M)$, then $H(p)$ is implicitly given by*

$$\int_V M(\varphi) \int_0^\infty \exp\left(- \int_0^t (1 + H(p) - v(\theta - s, \varphi) \cdot p)\, ds \right) dt.dv(\theta, \varphi) \quad = \quad 1,$$

– *if $p \in \mathrm{Sing}(M)$, then $H(p) = |p_3| - 1$.*

Our paper is organized as follows : in section 3.2, we identify the limit of the sequence $(u^\varepsilon)_\varepsilon$. For this, we proceed to a WKB expansion

$$u^\varepsilon(t, x, \theta, \varphi) \quad = \quad u(t, x) + \varepsilon \eta(t, x, \theta, \varphi).$$

This ansatz leads us to the resolution of a spectral problem which will give us the necessary condition $\partial_t u + H(\nabla_x u) = 0$. We then prove sufficient properties on H such that the well-posedness of the Hamilton-Jacobi equation is guaranteed. Sections 3.3 and 3.4 consist of the proof of Theorem 3.2. In section 3.3, we first establish *a priori* estimates thanks to which we can extract a converging subsequence out of $(u^\varepsilon)_\varepsilon$. We then prove in section 3.4 that the limit is indeed the viscosity solution of the Hamilton-Jacobi equation. Section 3.5 is devoted to some perspectives for future work.

3.2 Identification of the limit

3.2.1 An eigenvalue problem

Let us recall the Cauchy-problem (3.4)-(3.6) :

$$\begin{cases} \partial_t u^\varepsilon + v(\theta,\varphi)\cdot\nabla_x u^\varepsilon + \frac{\partial_\theta u^\varepsilon}{\varepsilon} = \int_V M'\left(1 - e^{\frac{u^\varepsilon - u'^\varepsilon}{\varepsilon}}\right)dv' \\ u^\varepsilon(0,x,\theta,\varphi) = u_0(x) \\ u^\varepsilon(t,x,0,\varphi) = u^\varepsilon(t,x,2\pi,\varphi) \\ \partial_\varphi u^\varepsilon(t,x,\theta,0) = \partial_\varphi u^\varepsilon(t,x,\theta,\pi) = 0 \end{cases}, \forall (t,x,\theta,\varphi) \in \mathbb{R}_+^* \times \mathbb{R}^3 \times V.$$

Seeking a limit u not depending on (φ,θ), we perform the WKB expansion :

$$u^\varepsilon(t,x,\theta,\varphi) = u(t,x) + \varepsilon\eta(t,x,\theta,\varphi). \tag{3.10}$$

Plugging (3.10) into (3.4), we get at order 0 in ε :

$$\partial_t u + v(\theta,\varphi)\cdot\nabla_x u + \partial_\theta \eta = \int_V M'\left(1 - e^{\eta-\eta'}\right)dv',$$

In view of the expected Hamilton-Jacobi limit, we set $p = \nabla_x u$ and $H = -\partial_t u$, and we get :

$$1 + H - v(\theta,\varphi)\cdot p - \partial_\theta\eta = \int_V M' e^{\eta-\eta'}dv'.$$

Set $Q = e^{-\eta}$. The function Q satisfies

$$\begin{cases} HQ = (-1 + v(\theta,\varphi)\cdot p)Q - \partial_\theta Q + \int_V M'Q'dv' \\ Q > 0 \end{cases}, \tag{3.11}$$

which is an eigenvalue problem. As in [41, 34], this problem may not have a regular solution so we need to solve this problem on the set of positive measures, but then rewrite the last term in (3.11) as $\langle M, Q\rangle$. Let us first look for a regular solution, that is, a solution Q in $C^1(V)$. We solve the differential equation by the method of characteristics. We set :

$$\begin{cases} \dot{\phi}_\theta(s) = -1 \\ \phi_\theta(0) = \theta \end{cases},$$

thus

$$\phi_\theta(s) = \theta - s.$$

Following the method of characteristics, we set

$$E_{H,p}(t) := \exp\left(-\int_0^t (1 + H - v(\theta - s, \varphi)\cdot p)ds\right), \tag{3.12}$$

such that

$$\frac{d}{ds}\left(Q(\theta - s, \varphi)E_{H,p}(s)\right) = -E_{H,p}(s)\cdot\int_V M'Q'.$$

Integrating between 0 and $t > 0$ yields :

$$E_{H,p}(t)Q(\theta - t, \varphi) - Q(\theta, \varphi) = -\int_0^t E_{H,p}(t)dt\cdot\int_V M'Q'. \tag{3.13}$$

Let $H > |p_3| - 1$. Then,

$$\begin{aligned}
-\frac{1}{t}\int_0^t (1 + H - v(\theta - s, \varphi)\cdot p)d\sigma &< -\left(|p_3| - p\cdot\frac{1}{t}\int_0^t v(\theta - s, \varphi)ds\right)\\
&= -|p_3| + p_3\cdot\frac{1}{t}\int_0^t \cos(\varphi)ds\\
&\quad + p_1\cdot\frac{1}{t}\int_0^t \cos(\theta - s)\sin(\varphi)ds + p_2\cdot\frac{1}{t}\int_0^t \sin(\theta - s)\sin(\varphi)ds\\
&\underset{t\to\infty}{\longrightarrow} p_3\cos(\varphi) - |p_3| \le 0.
\end{aligned}$$

As a consequence, $E_{H,p}$ is integrable on $\mathbb{R}_+$, and taking the limit $t \to +\infty$ in (3.13), the eigenvector $Q \in C^1(V)$ necessarily satisfies :

$$Q(\theta, \varphi) = \int_0^{+\infty} \exp\left(-\int_0^t (1 + H - v(\theta - s, \varphi)\cdot p)ds\right)dt\cdot\int_V M'Q'dv'. \tag{3.14}$$

Integrating the previous equation against M yields :

$$\int_V M'Q'dv' = \int_V M'\int_0^{+\infty} \exp\left(-\int_0^t (1 + H - v(\theta' - s, \varphi')\cdot p)ds\right)dt.dv'\cdot\int_V M'Q'dv',$$

hence

$$\int_V M(\varphi)\int_0^{\infty} \exp\left(-\int_0^t (1 + H - v(\theta - s, \varphi)\cdot p)ds\right)dt.dv(\theta, \varphi) = 1. \tag{3.15}$$

It is straightforward to check that $H \mapsto \int_0^\infty E_{H,p}(t)dt$ is strictly monotone and that

$$\int_V M\int_0^\infty E_{H,p}(t)dt.dv \underset{H\to+\infty}{\longrightarrow} 0.$$

Moreover, by the monotone convergence theorem,

$$\int_V M \int_0^\infty E_{H,p}(t)dt.d\nu \underset{H\to|p_3|-1}{\longrightarrow} \int_V M \int_0^\infty E_{|p_3|-1,p}(t)dt.d\nu.$$

Thus, it is necessary and sufficient to prove that $\int_V M \int_0^\infty E_{|p_3|-1,p}(t)dt.d\nu > 1$ to get the existence of a unique $H(p)$ such that $\int_V M \int_0^\infty E_{H(p),p}(t)dt.d\nu = 1$. If this condition is not satisfied, then $p \in \mathrm{Sing}(M)$ by definition and a solution to (3.11) is the couple $(|p_3|-1, Q)$, where Q is a positive measure :

$$Q(\theta,\varphi) = \int_0^\infty \exp\left(-\int_0^t \left(|p_3| - v\left(\theta - s, \varphi\right)\cdot p\right) ds\right) dt \cdot d\nu(\theta,\varphi) + \alpha(p)\delta_N + \beta(p)\delta_S,$$

where δ_N and δ_S are the dirac-masses centered on the points $\varphi = 0$ and $\varphi = \pi$ (North and South poles) and $\alpha(p), \beta(p) \in [0,1]$ satisfy :

$$\int_V M' \int_0^\infty \exp\left(-\int_0^t \left(|p_3| - v\left(\theta' - s, \varphi'\right)\cdot p\right) ds\right) dt.d\nu' + \alpha(p) + \beta(p) = 1.$$

Moreover, $\alpha(p) = 0$ if $p \cdot e_3 < 0$ and $\beta(p) = 0$ if $p \cdot e_3 > 0$.

This motivates the introduction of hamiltonian defined in Theorem 3.2. From what we saw earlier, we get that $H(p) \geq |p_3| - 1$, with equality if and only if $p \in \mathrm{Sing}(M)$.

3.2.2 Properties of the hamiltonian

We now establish the properties on H that guarantee existence and uniqueness of the solution of (3.9). In order to do so, we need to define

$$F_T(H,p) := \int_V M' \int_0^T E_{H,p}(t)dtd\nu', \quad F_\infty(H,p) := \int_V M' \int_0^\infty E_{H,p}(t)dtd\nu'. \tag{3.16}$$

By construction, $F_T(H,p) \leq F_\infty(H,p)$ and $F_\infty(H(p),p) = 1$ for $p \in \mathrm{Sing}^c(M)$. By monotonicity and since

$$\lim_{H\to+\infty} F_T(H,p) = 0, \quad \lim_{H\to-\infty} F_T(H,p) = +\infty,$$

there exists a unique $H_T(p) \in \mathbb{R}$ such that $F_T(H,p) = 1$ for all $p \in \mathbb{R}^3$.

Proposition 3.3. *The following properties hold :*

1. *The set* $\mathrm{Sing}(M)^c$ *is convex and contains* $\{p \in \mathbb{R}^3 \mid p \cdot e_3 = 0\}$,
2. H_T *is continuous and convex,*
3. *For all* $p \in \mathbb{R}^3$, $\lim_{T\to+\infty} H_T(p) = H(p)$,
4. H *is continuous and convex,*

Démonstration. 1. Let $p, q \in \mathrm{Sing}(M)^c$. By definition,

$$\begin{aligned}\int_V M' \int_0^\infty E_{|p_3|-1,p}(t)dt.d\nu' &> 1,\\ \int_V M' \int_0^\infty E_{|q_3|-1,q}(t)dt.d\nu' &> 1.\end{aligned}$$

Let us prove that, for all $\tau \in [0,1]$, $(1-\tau)p + \tau q \in \mathrm{Sing}(M)^c$, which means

$$\int_V M \int_0^\infty E_{|(1-\tau)p_3+\tau q_3|-1,(1-\tau)p+\tau q}(t)dt.dv' > 1. \tag{3.17}$$

Clearly $H \mapsto E_{H,p}$ is decreasing. Thus, the inequality $|(1-\tau)p_3 + \tau q| \leq (1-\tau)|p_3| + \tau|q_3|$ implies

$$\begin{aligned} I(\tau) &:= \int_V M' \int_0^\infty E_{(1-\tau)|p_3|+\tau|q_3|,(1-\tau)p_3+\tau q_3} dt.dv' \\ &\leq \int_V M' \int_0^\infty E_{|(1-\tau)p_3+\tau q_3|,(1-\tau)p_3+\tau q_3} dt.dv'. \end{aligned}$$

Moreover, $I(0) > 1$ and $I(1) > 1$. Since the sign of $\partial_\tau I$ does not change, we have $I(\tau) > 1$ for all $\tau \in [0,1]$ hence inequality (3.17) holds, which proves our result.

Finally, $\left\{p \in \mathbb{R}^3 \mid p \cdot e_3 = 0\right\} \subset \mathrm{Sing}(M)^c$ since $E_{|0|-1,0} \equiv 1$, which is not integrable over $\mathbb{R}_+$.

2. Let $p \in \mathbb{R}^3$. The function $(H,p) \mapsto F_T(H,p) - 1$ is C^0. Thus, by the implicit function theorem, H_T is C^0. Let now $q \in \mathbb{R}^3$ and $\lambda \in [0,1]$. Since the exponential is convex,

$$E_{\lambda H_T(p)+(1-\lambda)H_T(q),\lambda p+(1-\lambda)q}(t) \leq \lambda E_{H_T(p),p} + (1-\lambda)E_{H_T(q),q}.$$

Integrating, this inequality gives :

$$F(\lambda H_T(p) + (1-\lambda)H_T(q), \lambda p + (1-\lambda)q) \leq \lambda + (1-\lambda) = 1.$$

Thus, by monotonicity,

$$\lambda H_T(p) + (1-\lambda)H_T(q) \geq H_T(\lambda p + (1-\lambda)q).$$

3. Since $F_T(H,p) \leq F_\infty(H,p)$ and $F_\infty(H_T(p),p) \geq F_T(H_T(p),p) = 1$, we have $H(p) \geq H_T(p)$. Besides, $H_T(p)$ is increasing with respect to T so the limit $H_*(p) := \lim_{T\to+\infty} H_T(p)$ exists and satisfies $H(p) \geq H_*(p)$. Suppose that there exists δ such that $H(p) \geq H_*(p) + \delta$.

If $p \in \mathrm{Sing}^c(M)$, we can assume that δ is small enough so that $F(p, H_*(p)) < +\infty$. Moreover, there exist δ' such that $F(H_*(p),p) \geq 1 + \delta'$. By dominated convergence, $F_T(H_T(p),p) \to F(H_*(p),p)$ hence $F_T(H_T(p),p) \geq 1 + \frac{\delta'}{2}$ for T large enough, which is absurd.

If $p \in \mathrm{Sing}(M)$, then

$$1 = F_T(H_T(p),p) \geq F_T(H(p)-\delta,p) \underset{T\to+\infty}{\longrightarrow} +\infty,$$

which is absurd.

4. After 2. and 3., H is convex as the limit of convex functions hence H is continuous.

□

Before going further, we point out what use we make of Proposition 3.3. The most important result is point 4. Using the fundamental theorems of viscosity solutions [44, 42], the convexity of H guarantees the existence and uniqueness of the viscosity solution of the Hamilton-Jacobi equation (3.9). We will use point 1 later on, and we established points 2 and 3 in order to get 4.

3.3 A priori estimates

In the following, we shall assume that equation (3.4) with initial condition (3.6) has a unique solution $u^\varepsilon \in W^{1,\infty}\left(\mathbb{R}_+ \times \mathbb{R}^3 \times V\right)$. Then, the following *a priori* estimates hold :

Proposition 3.4. *Assume $u_0 \in W^{1,\infty}\left(\mathbb{R}^d\right)$ and is nonnegative. Let u^ε be a solution of (3.4)-(3.6) in $[0,T] \times \mathbb{R}^2 \times V$. Then,*

$$\begin{aligned}
\left\|u^\varepsilon\left(t,\cdot,\cdot,\cdot\right)\right\|_\infty &\leq \left\|u_0\right\|_\infty, && (3.18)\\
\left\|\nabla_x u^\varepsilon\left(t,\cdot,\cdot,\cdot\right)\right\|_\infty &\leq \left\|\nabla_x u_0\right\|_\infty, && (3.19)\\
\left\|\partial_t u^\varepsilon\left(t,\cdot,\cdot,\cdot\right)\right\|_\infty &\leq \left\|\nabla_x u_0\right\|_\infty, && (3.20)\\
\left\|\partial_\theta u^\varepsilon\left(t,\cdot,\cdot,\cdot\right)\right\| &\leq \left\|\nabla_x u_0\right\|_\infty t, && (3.21)\\
\left\|\partial_\varphi u^\varepsilon\left(t,\cdot,\cdot,\cdot\right)\right\| &\leq \left\|\nabla_x u_0\right\|_\infty t. && (3.22)
\end{aligned}$$

Démonstration. Let us assume that there exists a solution u^ε. Then, u^ε necessarily satisfies the Duhamel formulation

$$\begin{aligned}
u^\varepsilon\left(t,x,\theta,\varphi\right) &= u_0\left(\mathcal{X}_t^\varepsilon\left(0\right)\right)\\
&+ \int_0^t \int_V M'\left(1-\exp\left(\frac{u^\varepsilon\left(s,\mathcal{X}_t^\varepsilon\left(s\right),\theta+(s-t)/\varepsilon,\varphi\right)-u^\varepsilon\left(s,\mathcal{X}_t^\varepsilon\left(s\right),\theta',\varphi'\right)}{\varepsilon}\right)\right) dv' ds,
\end{aligned}$$

where is the characteristic flow associated to (3.4) :

$$\begin{cases}
\frac{d}{ds}\mathcal{X}_t^\varepsilon\left(s\right) = v\left(\theta+(s-t)/\varepsilon,\varphi\right),\\
\mathcal{X}_t^\varepsilon\left(t\right) = x.
\end{cases}$$

We can explicitly compute $\mathcal{X}_t^\varepsilon$:

$$\begin{cases}
e_1 \cdot \mathcal{X}_t^\varepsilon(s) = x_1 + \sin\varphi\left(\sin(\theta+(s-t)/\varepsilon)-\sin\theta\right),\\
e_2 \cdot \mathcal{X}_t^\varepsilon(s) = x_2 - \sin\varphi\left(\cos(\theta+(s-t)/\varepsilon)-\cos\theta\right),\\
e_3 \cdot \mathcal{X}_t^\varepsilon(s) = x_3 + \frac{s-t}{\varepsilon}\cdot\cos\varphi.
\end{cases} \qquad (3.23)$$

From this formulation, is is easy to establish that $u^\varepsilon(t,x,\theta,\varphi) \leq \|u_0\|_\infty + t \leq \|u_0\|_\infty + T$, such that u^ε is uniformly bounded. To prove estimation (3.18), we use the same delta-correction argument as in [22]. We reproduce it here for the sake of self-containedness. Let $\psi_\delta^\varepsilon(t,x,\theta,\varphi) := u^\varepsilon(t,x,\theta,\varphi) - \delta t - \delta^4|x|^2$. Let $(t_\delta, x_\delta, \theta_\theta, \varphi_\delta)$ be the maximal point of ψ_δ^ε. Then, $t_\delta = 0$. Indeed, in the opposite case, we have at point $(t_\delta, x_\delta, \theta_\theta, \varphi_\delta)$:

$$\begin{aligned}\partial_t u^\varepsilon\left(t_\delta, x_\delta, \theta_\theta, \varphi_\delta\right) &\geq \delta,\\ \nabla_x u^\varepsilon\left(t_\delta, x_\delta, \theta_\theta, \varphi_\delta\right) &= 2\delta^4 x_\delta,\\ \partial_\theta u^\varepsilon\left(t_\delta, x_\delta, \theta_\theta, \varphi_\delta\right) &= 0.\end{aligned}$$

Since $u^\varepsilon(t,x,\theta,\varphi) - u^\varepsilon(t,x,\theta',\varphi') = \psi_\delta^\varepsilon(t,x,\theta,\varphi) - \psi_\delta^\varepsilon(t,x,\theta',\varphi')$, we have

$$0 \geq \int_V M(\varphi')\left(1 - e^{\frac{\psi_\delta^\varepsilon(t_\delta,x_\delta,\theta_\delta,\varphi_\delta)-\psi_\delta^\varepsilon(t_\delta,x_\delta,\theta',\varphi')}{\varepsilon}}\right) d\nu(\theta',\varphi') \geq \delta - 2\delta^4 x_\delta,$$

hence

$$x_\delta \geq \frac{\delta^{-3}}{2}. \tag{3.24}$$

Moreover, since $\psi_\delta^\varepsilon(0,0,0,0) = u_0(0) \geq 0$, we have $\|u^\varepsilon\|_\infty - \delta^4|x_\delta|^2 \geq u^\varepsilon(t_\delta, x_\delta, \theta_\delta, \varphi_\delta) - \delta t_\delta - \delta^4|x_\delta|^2 \geq 0$ and

$$\frac{\delta^{-6}}{4} \leq |x_\delta|^2 \leq \delta^{-4}, \tag{3.25}$$

which is absurd for δ small enough. We conclude that $t_\delta = 0$ and that $u^\varepsilon(t,x,\theta,\varphi) \leq \|u_0\|_\infty + \delta t + \delta^4|x|^2$, for all $(t,x,\theta,\varphi) \in [0,T]\times\mathbb{R}^3\times V$. We get (3.18) by taking the limit $\delta \to 0$.

We come now to the proof of estimation (3.19) : we set $u_h^\varepsilon(t,x,\theta,\varphi) := u^\varepsilon(t,x+h,\theta,\varphi) - u^\varepsilon(t,x,\theta,\varphi)$. Then, u_h^ε satisfies :

$$\partial_t u_h^\varepsilon + v(\theta,\varphi)\cdot\nabla_x u_h^\varepsilon + \frac{1}{\varepsilon}\partial_\varphi u_h^\varepsilon = \int_V M(\varphi') e^{\frac{u^\varepsilon - u'^\varepsilon}{\varepsilon}}\left(1 - e^{\frac{u_h^\varepsilon - u'^\varepsilon_h}{\varepsilon}}\right) d\nu(\theta',\varphi').$$

We then use the same delta-correction as earlier : we now set $\psi_\delta^\varepsilon(t,x,\theta,\varphi) := u_h^\varepsilon(t,x,\theta,\varphi) - \delta t - \delta^4|x|^2$. Suppose the maximal point $(t_\delta, x_\delta, \theta_\theta, \varphi_\delta)$ satisfies $t_\delta > 0$, the estimation (3.24) still holds by positivity of $\int_V M' e^{\frac{u^\varepsilon - u'^\varepsilon}{\varepsilon}}\left(1 - e^{\frac{u_h^\varepsilon - u'^\varepsilon_h}{\varepsilon}}\right) d\nu'$. Now, $\psi_\delta^\varepsilon(0,0,0,0) = u_0(h) - u_0(0) \geq -\|u_0\|$ so $2\|u_0\|_\infty - \delta^4|x_\delta|^2 \geq u_h^\varepsilon(t_\delta, x_\delta, \theta_\delta, \varphi_\delta) - \delta t_\delta - \delta^4|x_\delta|^2 \geq -\|u_0\|_\infty$ and Equation (3.25) becomes :

$$\frac{\delta^{-6}}{4} \leq |x_\delta|^2 \leq 3\delta^{-4}\|u_0\|,$$

hence, $t_\delta = 0$ and we get

$$u_h^\varepsilon(t,x,\theta,\varphi) \leq \sup_x |u_0(x+h) - u_0(x)|, \quad \forall (t,x,\theta,\varphi) \in [0,T]\times\mathbb{R}^3\times V.$$

The same argument holds for $-u_h^\varepsilon$ so that

$$-u_h^\varepsilon(t,x,\theta,\varphi) \geq -\sup_x |u_0(x+h) - u_0(x)|, \quad \forall (t,x,\theta,\varphi) \in [0,T]\times\mathbb{R}^3\times V.$$

Finally,

$$|u_h^\varepsilon(t,x,\theta,\varphi)| \leq \|\nabla_x u_0\|_\infty |h|, \quad \forall (t,x,\theta,\varphi) \in [0,T]\times\mathbb{R}^3\times V.$$

Taking $h \to 0$, we get (3.19).

For estimation (3.20), we use the same δ-correction argument as before on $u_s^\varepsilon(t,x,\theta,\varphi) = u^\varepsilon(t+s,x,\theta,\varphi) - u^\varepsilon(t,x,\theta,\varphi)$. We get

$$|u_s^\varepsilon(t,x,\theta,\varphi)| \leq \sup_{x,\theta,\varphi} |u^\varepsilon(s,x,\theta,\varphi) - u^\varepsilon(0,x,\theta,\varphi)|, \quad \forall (t,x,\theta,\varphi) \in [0,T]\times\mathbb{R}^3\times V.$$

We use the Duhamel formulation to see that

$$|u^\varepsilon(s,x,\theta,\varphi) - u^\varepsilon(0,x,\theta,\varphi)| \leq |u^\varepsilon(\mathcal{X}_s^\varepsilon(0)) - u^\varepsilon(0)| + o(s).$$

After (3.23), we know that $\|\partial_t \mathcal{X}_t^\varepsilon(0)\|_\infty \leq 1$. Estimation (3.19) follows for $s \to 0$.

For the (3.21) bound, let us derive (3.4) with respect to θ :

$$\left(\partial_t + v(\theta,\varphi)\cdot\nabla_x + \frac{1}{\varepsilon}\partial_\theta\right)\partial_\theta u^\varepsilon = -\partial_\theta v(\theta,\varphi)\cdot\nabla_x u^\varepsilon - \int_V \partial_\theta u'^\varepsilon e^{\frac{u^\varepsilon - u'^\varepsilon}{\varepsilon}} dv',$$

and then, multiply by $\frac{\partial_\theta u^\varepsilon}{|\partial_\theta u^\varepsilon|}$:

$$\begin{aligned}\left(\partial_t + v(\theta,\varphi)\cdot\nabla_x + \frac{1}{\varepsilon}\partial_\theta\right)|\partial_\theta u^\varepsilon| &= -\partial_\theta v(\theta,\varphi)\cdot\nabla_x u^\varepsilon \frac{\partial_\theta u^\varepsilon}{|\partial_\theta u^\varepsilon|} - \int_V |\partial_\theta u^\varepsilon| e^{\frac{u^\varepsilon - u'^\varepsilon}{\varepsilon}} dv', \\ &\leq -\partial_\theta v(\theta,\varphi)\cdot\nabla_x u^\varepsilon \frac{\partial_\theta u^\varepsilon}{|\partial_\theta u^\varepsilon|} \\ &\leq \|\nabla_x u_0\|.\end{aligned}$$

Integrating along the characteristics yields estimation (3.21). Estimation (3.22) is obtained similarly after a derivation with respect to φ.

□

3.4 Viscosity solution

The family $(u^\varepsilon)_\varepsilon$ is locally uniformly bounded in $W^{1,\infty}\left(\mathbb{R}_+\times\mathbb{R}^d\times V\right)$. Thanks to Arzelà-Ascoli theorem, there exists a subsequence, that we still denote $(u^\varepsilon)_\varepsilon$ for the sake of clarity, that converges toward a function u.

Lemma 3.5. *The function u does not depend on θ.*

Démonstration. Multiplying (3.4) by $\partial_\theta u^\varepsilon$ and integrating between 0 and 2π yields :

$$\begin{aligned}\int_0^{2\pi}\partial_\theta u^\varepsilon(\partial_t u^\varepsilon + v\cdot\nabla_x u^\varepsilon)d\theta + \frac{1}{\varepsilon}\int_0^{2\pi}|\partial_\theta u^\varepsilon|^2 d\theta &= \int_0^{2\pi}\partial_\theta u^\varepsilon\left(1 - e^{\frac{u^\varepsilon}{\varepsilon}}\int_V M' e^{-\frac{u'^\varepsilon}{\varepsilon}}dv'\right)d\theta \\ &= [u^\varepsilon]_0^{2\pi} - \left[\varepsilon e^{\frac{u^\varepsilon}{\varepsilon}}\right]_0^{2\pi}\int_V M' e^{-\frac{u'^\varepsilon}{\varepsilon}}dv' \\ &= 0.\end{aligned}$$

Thanks to the *a priori* bounds of Proposition 3.3, we get

$$\int_0^{2\pi} |\partial_\theta u^\varepsilon|^2 d\theta = \mathcal{O}(\varepsilon). \tag{3.26}$$

This shows that u is independent of θ. □

Lemma 3.6. *The function u does not depend on φ.*

Démonstration. For this, we use

$$\frac{u^\varepsilon - u'^\varepsilon}{\varepsilon} \leq e^{\frac{u^\varepsilon - u'^\varepsilon}{\varepsilon}}.$$

Let us define $\overline{u}^\varepsilon(t,x) := \int_V M' u'^\varepsilon dv'$. Integrating the latter expression against M' over $W \subset V$ and then integrating with respect to $\theta \in [0, 2\pi]$ yields :

$$\begin{aligned}\int_0^{2\pi} \left(\left(\int_W M' dv' \right) u^\varepsilon - \int_W M' u'^\varepsilon dv' \right) d\theta &\leq \varepsilon \int_0^{2\pi} \int_W M' e^{\frac{u^\varepsilon - u'^\varepsilon}{\varepsilon}} dv' d\theta \\ &\leq \varepsilon \int_0^{2\pi} \int_V M' e^{\frac{u^\varepsilon - u'^\varepsilon}{\varepsilon}} dv' d\theta = \mathcal{O}(\varepsilon).\end{aligned}$$

Indeed, integrating (3.4) with respect to $\theta \in [0, 2\pi]$ yields :

$$\begin{aligned}\int_0^{2\pi} \int_V M' e^{\frac{u^\varepsilon - u'^\varepsilon}{\varepsilon}} dv' d\theta &= 2\pi - \int_0^{2\pi} (\partial_t u^\varepsilon + v \cdot \nabla_x u^\varepsilon) d\theta - \frac{1}{\varepsilon} \int_0^{2\pi} \partial_\theta u^\varepsilon d\theta \\ &= 2\pi - \int_0^{2\pi} (\partial_t u^\varepsilon + v \cdot \nabla_x u^\varepsilon) d\theta = \mathcal{O}(1),\end{aligned}$$

thanks to Proposition 3.3. By dominated convergence, we get

$$\int_0^{2\pi} \left(\int_W M' dv' \right) u(t,x,\theta,\varphi) d\theta \leq 2\pi \int_W M' u' dv'.$$

After Lemma 3.5, we know that u is independent of θ hence

$$u(t,x,\varphi) \int_W M' dv' \leq \int_W M' u' dv'.$$

Since this relation is true for any $W \subset V$, we get $u(t,x,\varphi) \leq \inf_{\xi \in [0,\pi]} u(t,x,\xi)$, hence u is independent of the variable φ. □

We now show that u is the viscosity solution of our Hamilton-Jacobi equation in two steps.

3.4.1 Subsolution Procedure

Let us show that u is a viscosity subsolution of (3.9). Let $\psi \in C^1\left(\mathbb{R}_+ \times \mathbb{R}^d\right)$ be a test function such that $u - \psi$ has a local maximum in $\left(t^0, x^0\right) \in \mathbb{R}_+^* \times \mathbb{R}^d$. For the sake of readability, we set $p^0 := \nabla_x \psi\left(t^0, x^0\right)$. We seek to show that ψ is a subsolution of (3.9), which means :

$$\partial_t \psi\left(t^0, x^0\right) + H\left(p^0\right) \leq 0.$$

1st case : $p^0 \in \mathrm{Sing}\,(M)^c$**.**

We set $\psi^\varepsilon(t,x,v) = \psi(t,x) + \varepsilon\eta(v)$ where η is defined by :

$$\eta(\theta,\varphi) := -\ln\left(\int_0^{+\infty} \exp\left(-\int_0^t 1 + H(p^0) - v(\theta - s,\varphi)\cdot p^0 ds\right) dt\right) \tag{3.27}$$

Since $p^0 \in \mathrm{Sing}(M)^c$, we have $\int_V M' e^{-\eta'} dv' = 1$ and

$$Q\left(1 + H(p^0) - v(\theta,\varphi)\cdot p^0\right) + \partial_\theta Q = 1, \quad \forall(\theta,\varphi) \in V, \tag{3.28}$$

where $Q = e^{-\eta}$. Since $u^\varepsilon \to u$ and $\psi^\varepsilon \to \psi$ uniformly, the function $u^\varepsilon - \psi^\varepsilon$ has a maximum located at point $(t^\varepsilon, x^\varepsilon, \theta^\varepsilon, \varphi^\varepsilon)$, satisfying $(t^\varepsilon, x^\varepsilon) \to \left(t^0, x^0\right)$. Since V is compact, the sequence $(\theta^\varepsilon, \varphi^\varepsilon)_\varepsilon$ has an accumulation point in V we call (θ^*, φ^*). We still denote $\left((t^\varepsilon, x^\varepsilon, \theta^\varepsilon, \varphi^\varepsilon)\right)_\varepsilon$ the extracted sequence. At point $(t^\varepsilon, x^\varepsilon, \theta^\varepsilon, \varphi^\varepsilon)$, we have :

$$\begin{aligned} -1 + \partial_t\psi^\varepsilon + v(\theta^\varepsilon,\varphi^\varepsilon)\cdot\nabla_x\psi^\varepsilon + \frac{1}{\varepsilon}\partial_\theta\psi^\varepsilon &= -1 + \partial_t u^\varepsilon + v(\theta^\varepsilon,\varphi^\varepsilon)\cdot\nabla_x u^\varepsilon + \frac{1}{\varepsilon}\partial_\theta u^\varepsilon \\ &= -\int_V M' e^{\frac{u^\varepsilon - u'^\varepsilon}{\varepsilon}} dv'. \end{aligned}$$

The maximal property of $(t^\varepsilon, x^\varepsilon, \theta^\varepsilon, \varphi^\varepsilon)$ yields :

$$\int_V M' e^{\frac{u^\varepsilon - u'^\varepsilon}{\varepsilon}} dv' \geq \int_V M' e^{\frac{\psi^\varepsilon - \psi'^\varepsilon}{\varepsilon}} dv' = \int_V M\left(\varphi'\right) e^{\eta(\theta^\varepsilon,\varphi^\varepsilon) - \eta(\theta',\varphi')} dv' = e^{\eta(\theta^\varepsilon,\varphi^\varepsilon)}$$

Therefore, at point $(t^\varepsilon, x^\varepsilon, \theta^\varepsilon, \varphi^\varepsilon)$, we have :

$$\begin{aligned} -1 + \partial_t\psi + v(\theta^\varepsilon,\varphi^\varepsilon)\cdot\nabla_x\psi + \partial_\theta\eta &= -1 + \partial_t\psi^\varepsilon + v(\theta^\varepsilon,\varphi^\varepsilon)\cdot\nabla_x\psi^\varepsilon + \frac{1}{\varepsilon}\partial_\theta\psi^\varepsilon \\ &\leq -e^{\eta(\theta^\varepsilon,\varphi^\varepsilon)}, \end{aligned}$$

hence

$$e^{-\eta}\left(1 - \partial_t\psi - v(\theta^\varepsilon,\varphi^\varepsilon)\cdot\nabla_x\psi\right) + \partial_\theta\left(e^{-\eta}\right) \geq 1.$$

Passing to the limit $\varepsilon \to 0$, we get for $Q = e^{-\eta}$:

$$Q(\theta^*,\varphi^*)\left(1 - \partial_t\psi\left(t^0,x^0\right) - v(\theta^*,\varphi^*)\cdot p^0\right) + \partial_\theta Q(\theta^*,\varphi^*) \geq 1.$$

Evaluating (3.28) at (θ^*, φ^*), we get :

$$-Q(\theta^*,\varphi^*)\partial_t\psi\left(t^0,x^0\right) \geq Q(\theta^*,\varphi^*)H\left(p^0\right).$$

Since $Q > 0$, we have $\partial_t\psi\left(t^0,x^0\right) + H\left(\nabla_x\psi\left(t^0,x^0\right)\right) \leq 0$.

2nd case : $p^0 \in \text{Sing}\,(M)$**.**

We suppose without loss of generality that $p_3^0 \geq 0$. Then, $|p_3^0| = p_3^0 = \cos(0)p_3^0 = v\,(0,0) \cdot p^0$. The uniform convergence $u^\varepsilon \to u$ guarantees that $(t,x,\theta) \mapsto u^\varepsilon\,(t,x,\theta,0) - \psi\,(t,x)$ has a local maximum located at a point $(t^\varepsilon, x^\varepsilon, \theta^\varepsilon)$ such that $(t^\varepsilon, x^\varepsilon)$ converges toward $\left(t^0, x^0\right)$. At $(t^\varepsilon, x^\varepsilon, \theta^\varepsilon)$, we have $\partial_\theta u^\varepsilon = 0$ and

$$\begin{aligned}
\partial_t\psi + v\,(0,\theta^\varepsilon)\cdot\nabla_x\psi &= \partial_t u^\varepsilon + v\,(0,\theta^\varepsilon)\cdot\nabla_x u^\varepsilon \\
&= \partial_t u^\varepsilon + v\,(0,\theta^\varepsilon)\cdot\nabla_x u^\varepsilon + \frac{1}{\varepsilon}\partial_\theta u^\varepsilon(t^\varepsilon,x^\varepsilon,\theta^\varepsilon,0) \\
&= 1 - \int_V M' e^{\frac{u^\varepsilon - u'^\varepsilon}{\varepsilon}} dv' \\
&\leq 1.
\end{aligned}$$

Passing to the limit $\varepsilon \to 0$, we get $\partial_t\psi\left(t^0,x^0\right) + |p_3^0| \leq 1$.
We conclude that u is a viscosity subsolution of (3.9).

□

3.4.2 Supersolution Procedure

Let $\psi \in C^1\left(\mathbb{R}_+ \times \mathbb{R}^d\right)$ be a test function such that $u - \psi$ has a local minimum located at a point $\left(t^0,x^0\right) \in \mathbb{R}_+^* \times \mathbb{R}^d$. For the sake of readability, we set $p^0 := \nabla_x\psi\left(t^0,x^0\right)$. We seek to show that ψ is a supersolution of (3.9), which means

$$\partial_t\psi\left(t^0,x^0\right) + H\left(p^0\right) \geq 0.$$

We suppose without loss of generality that $p_3^0 \geq 0$ such that $|p_3^0| = v(0,0)\cdot p^0$.

1st case : $p^0 \in \text{Sing}\,(M)^c$**.**

Here, the proof works exactly as in the subsolution procedure 3.4.1.

2nd case : $p^0 \in \text{Sing}\,(M)$

Then, $\nabla_x\psi\left(t^0,x^0\right) \neq 0$ since $0 \in \text{Sing}\,(M)^c$. We define for all $\varphi \in (0,\pi]$ and $\theta \in [0,2\pi]$,

$$Q\,(\theta,\varphi) := \int_0^{+\infty} \exp\left(-\int_0^t (|p_3^0| - v\,(\theta - s,\varphi)\cdot p^0)ds\right)dt. \tag{3.29}$$

We set $\delta > 0$ and $\psi_\delta^\varepsilon := \psi + \varepsilon\eta_\delta$ where

$$\eta_\delta\,(\theta,\varphi) := -\ln\left(Q\,(\theta,\varphi)\right)\mathbb{1}_{Q\leq\frac{1}{\delta}} + \ln(\delta)\mathbb{1}_{Q>\frac{1}{\delta}} \tag{3.30}$$

By construction of η, we have

$$\int_V M' e^{-\eta'_\delta} dv' = \int_{\left\{Q\leq\frac{1}{\delta}\right\}} M'Q'dv' + \int_{\left\{Q>\frac{1}{\delta}\right\}} \frac{M'}{\delta}dv' \leq \int_V M'Q'dv' \leq 1,$$

the last inequality being true since $p^0 \in \mathrm{Sing}\,(M)$.

$$Q\left(|p_3^0| - v\,(\theta,\varphi)\cdot p^0\right) + \partial_\theta Q = 1. \tag{3.31}$$

The function $u^\varepsilon - \psi^\varepsilon$ has a local minimum located at a point $(t^\varepsilon, x^\varepsilon, \theta^\varepsilon, \varphi^\varepsilon) \in \mathbb{R}_+ \times \mathbb{R}^n \times V$. At point $(t^\varepsilon, x^\varepsilon, \theta^\varepsilon, \varphi^\varepsilon)$, we have :

$$\begin{aligned}
\partial_t\psi + v\,(\theta^\varepsilon,\varphi^\varepsilon)\cdot\nabla_x\psi + \partial_\theta\eta &= \partial_t\psi^\varepsilon + v\,(\theta^\varepsilon,\varphi^\varepsilon)\cdot\nabla_x\psi^\varepsilon + \frac{1}{\varepsilon}\partial_\theta\psi^\varepsilon \\
&= \partial_t u^\varepsilon + v\,(\theta^\varepsilon,\varphi^\varepsilon)\cdot\nabla_x u^\varepsilon + \frac{1}{\varepsilon}\partial_\theta u^\varepsilon \\
&= 1 - \int_V M' e^{\frac{u^\varepsilon - u'^\varepsilon}{\varepsilon}} dv'.
\end{aligned}$$

By the minimal property of $(t^\varepsilon, x^\varepsilon, \theta^\varepsilon, \varphi^\varepsilon)$, we can estimate the right-hand-side of the last equation such that

$$\partial_t\psi + v\,(\theta^\varepsilon,\varphi^\varepsilon)\cdot\nabla_x\psi + \partial_\theta\eta_\delta \geq 1 - \int_V M\left(\varphi'\right) e^{\eta_\delta(\theta^\varepsilon,\varphi^\varepsilon) - \eta_\delta(\theta',\varphi')} d\nu\left(\theta',\varphi'\right) \geq 1 - e^{\eta(\theta^\varepsilon,\varphi^\varepsilon)}. \tag{3.32}$$

Since V is compact, the sequence $\left(\theta^\varepsilon,\varphi^\varepsilon\right)_\varepsilon$ has an accumulation point in V we call $\left(\theta^\delta,\varphi^\delta\right)$. We still denote by $\left(\left(t^\varepsilon, x^\varepsilon, \theta^\varepsilon, \varphi^\varepsilon\right)\right)_\varepsilon$ the extracted subsequence.
If $(\theta^\delta,\varphi^\delta) \in \left\{Q \leq \frac{1}{\delta}\right\}$, then $e^{-\eta_\delta\left(\theta^\delta,\varphi^\delta\right)} = Q\left(\theta^\delta,\varphi^\delta\right)$ so, taking $\varepsilon \to 0$ in (3.32), we get :

$$\partial_t\psi\left(t^0,x^0\right) + v\left(\theta^\delta,\varphi^\delta\right)\cdot p^0 + \partial_\theta\eta_\delta\left(\theta^\delta,\varphi^\delta\right) \geq 1 - \frac{1}{Q\left(\theta^\delta,\varphi^\delta\right)},$$

and

$$Q\left(\theta^\delta,\varphi^\delta\right)\left(1 - \partial_t\psi\left(t^0,x^0\right) - v\left(\theta^\delta,\varphi^\delta\right)\cdot p^0\right) + \partial_\theta Q\left(\theta^\delta,\varphi^\delta\right) \leq 1,$$

Recalling (3.31), we have

$$Q\left(\theta^\delta,\varphi^\delta\right)\left(1 - \partial_t\psi\left(t^0,x^0\right)\right) \leq |p_3^0| Q\left(\theta^\delta,\varphi^\delta\right),$$

therefore

$$\partial_t\psi\left(t^0,x^0\right) + \left|\nabla_x\psi\left(t^0,x^0\right)\cdot e_3\right| \geq 1.$$

If $(\theta^\delta,\varphi^\delta) \in \left\{Q > \frac{1}{\delta}\right\}$, then $\partial_\theta\eta(\theta^\delta,\varphi^\delta) = 0$. As earlier, taking the limit $\varepsilon \to 0$ gives

$$\partial_t\psi\left(t^0,x^0\right) + v\left(\theta^\delta,\varphi^\delta\right)\cdot p^0 \geq 1 - \delta.$$

Since $Q \in C^0\left(V \setminus \{\varphi = 0\}\right)$, and $\left(\left\{Q > \frac{1}{\delta}\right\}\right)_\delta$ is a non-increasing sequence of sets, we have $\varphi^\delta \to 0$ hence $v\left(\theta^\delta,\varphi^\delta\right)\cdot p^0 \underset{\delta\to 0}{\longrightarrow} |p_3^0|$. Finally, as $\delta \to 0$,

$$\partial_t\psi\left(t^0,x^0\right) + \left|\nabla_x\psi\left(t^0,x^0\right)\cdot e_3\right| \geq 1,$$

and u is a viscosity supersolution of (3.9).

□

3.5 Perspectives

This work is a first attempt to produce a similar result to [18, 22, 34] with a force term. It has provided a particular example of a force term for which we can use a Hamilton-Jacobi at the hyperbolic scale, in order to study the Kolmogorov equation of a piecewise deterministic Markov process (PDMP). Yet, a similar result for a more general force term is, to our knowledge, an open question. The more general case we are interested in is the following framework. We consider the kinetic equation :

$$\partial_t g^\varepsilon + v \cdot \nabla_x g^\varepsilon + \mathrm{div}_v \left(\Gamma(\varepsilon x, v) g^\varepsilon\right) = M\rho_{g^\varepsilon} - g^\varepsilon, \quad (t, x, v) \in \mathbb{R}_+ \times \mathbb{R}^d \times V, \tag{3.33}$$

where V is a compact differentiable submanifold of $\mathbb{R}^d$. In the hyperbolic scale $f^\varepsilon(t, x, v) = g^\varepsilon(\frac{t}{\varepsilon}, \frac{x}{\varepsilon}, v)$, this equation reads

$$\partial_t f^\varepsilon + v \cdot \nabla_x f^\varepsilon + \frac{1}{\varepsilon}\mathrm{div}_v \left(\Gamma(x, v) f^\varepsilon\right) = \frac{1}{\varepsilon}\left(M\rho^\varepsilon - f^\varepsilon\right). \tag{3.34}$$

Let us detail what crucial assumptions we made in our paper to avoid certain problems. First of all, we assumed Γ to depend only on v and we chose the Maxwellian M such that $\mathrm{div}_v(\Gamma M) = 0$. This allowed to say that f^ε relaxed toward M. In the more general case, one need to solve $\mathrm{div}_v(\Gamma\overline{M}) = M\int \overline{M}' dv' - \overline{M}$ and perform the ansatz $f^\varepsilon = \overline{M}e^{-\frac{u^\varepsilon}{\varepsilon}}$, the function u^ε satisfies

$$\partial_t u^\varepsilon + v \cdot \nabla_x u^\varepsilon + \frac{\Gamma(x, v)}{\varepsilon}\nabla_v u^\varepsilon = \frac{M}{\overline{M}}\int_V \left(1 - \overline{M}e^{\frac{u^\varepsilon - u'^\varepsilon}{\varepsilon}}\right). \tag{3.35}$$

We do not think that this engenders much complication compared to what we have worked on. Our major assumption concerns the force term Γ. Our hypothesis is that $D_v\Gamma$ satisfies :

$$(D_v\Gamma(x, v)w) \cdot w = 0, \quad \forall (x, v) \in \mathbb{R}^d \times V,\ w \in \mathbb{R}^d. \tag{3.36}$$

Thanks to this hypothesis, we got the *a priori* bounds (3.21)-(3.22). Indeed, differentiating the kinetic equation (3.35) with respect to v engenders a term $-D_v\Gamma\nabla_v u^\varepsilon$ that we can control under the sufficient condition $(D_v\Gamma(x, v)w) \cdot w \geq 0$. Since this last inequation can not hold for all $v \in V$ since V is compact, we assumed (3.36) to be true. The examples of such a Γ are not numerous. One of them is obtained when V is the 2-dimensional sphere and Γ is a force that carries characteristics along the parallel lines of the sphere, this the example that was developed in the present paper. In this case, the cartesian coordinates are not easy to deal with so we used the spherical coordinates.

One way to overcome this issue could be to use the so-called superior and inferior half-relaxed limits, in the spirit of [9, 20]. This method spares us from establishing the *a priori* estimates since semi-limits always exist. Then, it only remains to show that both the superior and the inferior semi-limits are viscosity solutions of the Hamilton-Jacobi equation.

For these reasons, our result is not as general as it might be. It is our belief, however, that the viscosity solution procedures from Section 3.4 do not rely strongly on the hypothesis on Γ and that they can easily be adapted to a more general force term. As a matter of fact, we sacrificed the generality only to get easy *a priori* estimates and not to simplify the viscosity solution procedures.

In conclusion, we would like to emphasize that, provided that one can exhibit a limit of u^ε that is independent of v, this paper has already paved the way on finding the Hamilton-Jacobi limit. Thus, despite its obvious lack of generality, it might just prove useful for works to come.

Chapitre 4

Propagation dans des équations de transport-réaction à vitesses multidimensionnelles

Dans ce travail en commun avec Emeric Bouin, nous étendons et nous complétons des précédents travaux sur des phénomènes de propagation dans des équations de transport-réaction. Le modèle que nous étudions décrit des particules se déplaçant selon un processus à sauts de vitesse et qui prolifèrent grâce à un terme de réaction monostable. Nous nous plaçons dans le cas de vitesses bornées mais dans un espace à plusieurs dimensions, le cas unidimensionnel ayant déjà été traité par Bouin, Calvez et Nadin. Nous étudions la limite hyperbolique via une approche Hamilton-Jacobi et la méthode des semi-limites relaxées. Nous en déduisons des résultats de propagation ainsi que l'existence de solutions en ondes progressives. Une différence cruciale avec le cas unidimensionnel est que la résolution du problème spectral à l'avant du front engendre potentiellement des vecteurs propres singuliers.

Contents

4.1 Introduction

The model.

In this paper, we are interested in propagation phenomena occuring in the following reaction-transport equation

$$\begin{cases} \partial_t f + v \cdot \nabla_x f = M(v)\rho - f + r\rho\,(M(v) - f)\,, & (t,x,v) \in \mathbb{R}_+ \times \mathbb{R}^n \times V\,, \\ f(0,x,v) = f_0(x,v)\,, & (x,v) \in \mathbb{R}^n \times V\,. \end{cases} \tag{4.1}$$

The density f describes a population of individuals and $\rho(\cdot,\cdot) = \int_V f(\cdot,\cdot,v)\,dv$ is the macroscopic density. The subset $V \subset \mathbb{R}^n$ is the set of all possible velocities. From now on, we assume

(H0) The velocity set $V \subset \mathbb{R}^n$ is symmetric and compact.

For any given direction $e \in \mathbb{S}^{n-1}$, we define

$$\overline{v}(e) = \max\{v \cdot e, v \in V\}\,, \qquad \mu(p) = |p|\overline{v}\left(\frac{p}{|p|}\right), \quad \operatorname{Arg}\mu(p) = \{v \in V \mid v \cdot p = \mu(p)\}\,.$$

We set

$$v_{max} := \sup_{v \in V} |v|, \qquad |V| := \int_V dv.$$

Individuals move following a so-called velocity-jump process. That is, they alternate successively a run phase, with velocity $v \in V$, and a change of velocity at rate 1, which we call the tumbling. The new velocity is chosen according to the probability distribution M. Throughout the paper, we assume

(H1) $M \in L^1(V) \cap \mathcal{C}^0(V)$, and

$$\int_V M(v)dv = 1\,, \quad \int_V vM(v)dv = 0\,. \tag{4.2}$$

Note that it is challenging to replace the linear BGK operator $M\rho - f$ by a more general collision operator of the form $P(f) - \Sigma f$ where P is a positive operator. However, to keep our consistency with [26], we will stick to their framework and leave this question for future work.

The reproduction of individuals is taken into account through a reaction term of monostable type. The constant $r > 0$ is the growth rate in absence of any saturation. New individuals start with a velocity chosen at random with the same probability distribution M. The quadratic saturation term accounts for local competition between individuals, regardless of their speed.

We assume that initially $0 \leq f_0 \leq M$, so that this remains true for all times, see [26, 46].

Earlier works and related topics

It is realtively natural to address the question of spreading for (4.1) since there is a strong link between (4.1) and the classical Fisher-KPP equation [61, 78]. Indeed, a suitable parabolic rescaling

$$\varepsilon^2 \partial_t g_\varepsilon + \varepsilon v \cdot \nabla_x g_\varepsilon = \left(M(v)\rho_{g_\varepsilon} - g_\varepsilon\right) + \varepsilon^2 r \rho_{g_\varepsilon} \left(M(v) - g_\varepsilon\right) , \tag{4.3}$$

leads to the Fisher-KPP equation (see [46] for example) in the limit $\varepsilon \to 0$,

$$\begin{aligned} &\partial_t \rho_0 - \left(\int_V v^2 M(v) dv\right) \partial_{xx} \rho_0 = r\rho_0 \left(1 - \rho_0\right) , \\ &g_0 := \lim_{\varepsilon \to 0} g_\varepsilon = M\rho_0, \end{aligned} \tag{4.4}$$

assuming that the two following conditions on M hold :

$$\int_V v M(v) dv = 0, \quad D := \int_V v^2 M(v) dv > 0.$$

We recall that for nonincreasing initial data decaying sufficiently fast at $x = +\infty$, the solution of (4.4) behaves asymptotically as a travelling front moving at the minimal speed $c^* = 2\sqrt{rD}$ [78, 5]. However, even though the philosophy of the results will be the same in spirit, we emphasize that nothing related to this parabolic limit will be used of the present paper and that everything will be performed directly at the kinetic level. This will yield significant differences.

A short review of earlier results is now in order. Schwetlick has constructed in [99, 100] some travelling waves solutions to a very related model (a model sharing the same linearized equation as (4.1)). Morever, a similar type of result has been obtained by Cuesta, Hittmeir and Schmeiser [46] in the diffusive approximation of (4.1). Using a micro-macro decomposition, they construct possibly oscillatory travelling waves of speed $c \geq 2\sqrt{rD}$ for ε small enough (depending on c). In addition, when the set of admissible speeds V is bounded, $c > 2\sqrt{rD}$, and ε is small enough, they prove that the travelling wave constructed in this way is indeed nonnegative.

Propagation for the full kinetic model (4.1) has then been investigated by the first author with Calvez and Nadin in [26]. In one dimension of velocities, and when the velocities are bounded, they proved the existence and stability of travelling waves solutions to (4.1). Contrary to all previous works at that time, the minimal speed of propagation of the waves is purely coming from the kinetic structure of the model, and has nothing to do with the KPP speed. It is worth mentioning, even though this will not be discussed at all in this paper, that when velocities are unbounded, a front acceleration occurs. This phenomenon was newly appearing for this type of equations and unexpected from the macroscopic limit. One aim of this

paper is to extend the consturction of travelling waves solutions to any velocity dimension, which was left open after [26].

There is a strong link between this KPP type propagation phenomena and large deviations for the underlying velocity-jump process. Indeed, it is well known that fronts in Fisher-KPP equations are so-called *pulled fronts*, that is, are triggered by very small populations at the edge that are able to reproduce almost exponentially. Thus, studying large deviations for these type of processes at the kinetic level is an interesting problem in itself. In [22, 20], the authors have combined Hamilton-Jacobi equations and kinetic equations to study large deviations (and propgation) from a PDE point of view. These works show that it is necessary to stay at the kinetic level to understand the large deviation regime.

As a side note, the Hamilton-Jacobi technique (that will be described in the next subsection) has also much been used recently to study long time dynamics in all sorts of stuctured models. An interested reader could describe the evolution of dominant phenotypical traits in a given population reading [85, 29] and the references therein), study different adaptative dynamics issues [54], describe propagation in reaction-diffusion models of kinetic types [25] but also in age renewal equations[35]. This approach has also recently been used to study large deviations of velocity jump-processes[22, 24, 34] or slow-fast systems [32, 31, 59, 77, 92].

The Hamilton-Jacobi limit

After the seminal paper by Evans and Souganidis [65, 58], an important technique to derive the propagating behavior in reaction-diffusion equations is to revisit the WKB expansion to study hyperbolic limits. We will directly present the technique on our problem for conciseness but one can find the original framework for the Fisher-KPP equation in [58] and complements in [7, 8, 105, 43].

We perform the hyperbolic scaling $(t,x,v) \to \left(\frac{t}{\varepsilon}, \frac{x}{\varepsilon}, v\right)$ in (4.1). Importantly, the velocity variable is not rescaled (it may not be rescaled since it lies in a bounded set). The *kinetic Hopf-Cole transformation* (already used in [22, 34]) is written

$$\forall (t,x,v) \in \mathbb{R}^+ \times \mathbb{R}^n \times V, \qquad f^\varepsilon(t,x,v) = M(v) e^{-\frac{\varphi^\varepsilon(t,x,v)}{\varepsilon}}. \tag{4.5}$$

Thanks to the maximum principle [46], φ^ε is well defined and remains nonnegative for all times. Plugging (4.5) in (4.1), one obtains the following equation for φ^ε :

$$\partial_t \varphi^\varepsilon + v \cdot \nabla_x \varphi^\varepsilon + r = (1+r) \int_V M(v') \left(1 - e^{\frac{\varphi^\varepsilon(v) - \varphi^\varepsilon(v')}{\varepsilon}}\right) dv' + r\rho^\varepsilon. \tag{4.6}$$

Our aim is to pass to the limit in (4.6). To make the convergence result appear naturally, we shall start by providing formal arguments. Assuming Lipschitz bounds on φ^ε, and since ρ^ε is uniformly bounded, the boundedness of $\int_V M(v')(1 - \exp((\varphi^\varepsilon(v) - \varphi^\varepsilon(v'))/\varepsilon) dv'$ implies that we expect the limit φ^0 to be independent of v. To identify the limit φ^0, we shall thus perform the following expansion

$$\varphi^\varepsilon(t,x,v) = \varphi^0(t,x) + \varepsilon \eta(t,x,v). \tag{4.7}$$

Plugging the latter into (4.7) yields

$$\partial_t \varphi^0 + v \cdot \nabla_x \varphi^0 + r = (1+r) \int_V M(v') \left(1 - e^{\eta(v) - \eta(v')}\right) dv' + r e^{-\frac{\varphi^0}{\varepsilon}} \int_V e^{-\eta(v')} dv'.$$

As a consequence, for any $(t,x) \in \{\varphi^0 > 0\}$, we have

$$\partial_t \varphi^0 + v \cdot \nabla_x \varphi^0 = 1 - e^{\eta(v)}(1+r) \int_V M(v') e^{-\eta(v')} dv'. \tag{4.8}$$

One should read this equation as an eigenvalue problem in the velocity variable. Indeed, setting

$$p(t,x) = \nabla_x \varphi^0(t,x), \qquad \eta(t,x,v) := -\ln\left(\frac{Q_{p(t,x)}}{M(v)}\right), \qquad H(p(t,x)) := -\partial_t \varphi^0(t,x),$$

we see that (H,Q) are the principal eigenelements of the following spectral problem

$$(1+r)M(v) \int_V Q_p(v')\, dv' - (1 - v \cdot p)\, Q_p(v) = H(p) Q_p(v).$$

The dependency with respect to r can be identified by setting $p' := \frac{p}{1+r}$, $\mathcal{H}(\cdot) := \frac{H((1+r)\cdot) - r}{1+r}$ and $\widetilde{Q}_{p'} = Q_p$. Indeed, we have then that $\partial_t \varphi^0 + (r+1)\mathcal{H}(\frac{p}{r+1}) + r = 0$ and the Hamiltonian $\mathcal{H}$ is given by

$$\left(1 + \mathcal{H}\left(p'\right) - v \cdot p'\right) \widetilde{Q}_{p'}(v) = M(v) \int_V \widetilde{Q}_{p'}(v')\, dv'. \tag{4.9}$$

After these heuristics, we are now ready to define properly the Hamiltonian $\mathcal{H}$ involved.

Definition 4.1. *We define, for $e \in \mathbb{S}^{n-1}$,*

$$l(e) = \int_V \frac{M(v)}{\overline{v}(e) - v \cdot e} dv.$$

The so-called singular set is defined by

$$\mathrm{Sing}\,(M) := \left\{ p \in \mathbb{R}^n, \int_V \frac{M(v)}{\mu(p) - v \cdot p} dv \le 1 \right\} = \left\{ p \in \mathbb{R}^n,\, l\left(\frac{p}{|p|}\right) \le |p| \right\}. \tag{4.10}$$

Then, the Hamiltonian $\mathcal{H}$ involved in this paper is given as follows :

– *If $p \notin \mathrm{Sing}\,(M)$, then $\mathcal{H}$ is uniquely defined by the following implicit relation :*

$$\int_V \frac{M(v)}{1 + \mathcal{H}(p) - v \cdot p} dv = 1, \tag{4.11}$$

– *else, $\mathcal{H}(p) = \mu\,(p) - 1$.*

The relevancy of such a definition, *i.e.* the resolution of (4.9), will be discussed in Section 4.2 below. With this definition in hand, the convergence result for the sequence of functions φ^ε is as follows.

Theorem 4.2. *Suppose that (H0) and (H1) hold, and that the initial data satisfies*

$$\forall (x,v) \in \mathbb{R}^n \times V, \qquad \varphi^\varepsilon(0,x,v) = \varphi_0(x,v).$$

Then, $(\varphi^\varepsilon)_\varepsilon$ converges uniformly on all compacts of $\mathbb{R}_+^* \times \mathbb{R}^n \times V$ towards φ^0, where φ^0 does not depend on v. Moreover φ^0 is the unique viscosity solution of the following Hamilton-Jacobi equation :

$$\begin{cases} \min\left\{ \partial_t \varphi^0 + (1+r)\mathcal{H}\left(\frac{\nabla_x \varphi^0}{1+r}\right) + r, \varphi^0 \right\} = 0, & (t,x) \in \mathbb{R}_+^* \times \mathbb{R}^n, \\ \varphi^0(0,x) = \min\limits_{v \in V} \varphi_0(x,v), & x \in \mathbb{R}^n. \end{cases} \tag{4.12}$$

Let us now emphasize the differences between the result presented here and the very closely related works [22, 20, 34]. First, the results from [22] and [20] only hold for $n = 1$ and for $M > 0$. In [20], the first author successfully proved a convergence result in the case $r > 0$. It is worth mentioning that a much wider class of collision operators was considered in [20], but under the condition of existence of a L^1 eigenvector. We believe that the ideas of the present could be used there, but with technicalities inherent from the spectral problem that would require a special study.

As explained before, the multidimensional ($n > 1$) is more delicate since the relation (4.11) may not have a solution. We refer to our Example 4.9 for a situation where this happens. In [34], the second author generalized the convergence result of [22] in the multidimensional case, with no reaction term. However, the proof we design in this paper is simpler and more adaptable. For this we manage to use the half-relaxed limits of Barles and Perthame [9] in the spirit of [29].

We present the proof of Theorem 4.2 in Section 4.2 below.

Travelling wave solutions and spreading of planar like initial data

We then investigate the existence of travelling wave solutions of (4.1). As in the mono-dimensional case treated in [26], we will prove that there exists a minimal speed c^* for which travelling wave solutions exist. We will use the following definition throughout the paper.

Definition 4.3. *A function f is a smooth travelling wave solution of speed $c \in \mathbb{R}_+$ and direction $e \in \mathbb{S}^{n-1}$ of equation* (4.1) *if it can be written $f(t,x,v) = \tilde{f}(x \cdot e - ct, v)$, where the profile $\tilde{f} \in \mathcal{C}^2(\mathbb{R} \times V)$ solves*

$$(v \cdot e - c)\, \partial_\xi \tilde{f} = M(v)\tilde{\rho} - \tilde{f} + r\tilde{\rho}\left(M(v) - \tilde{f}\right) \tag{4.13}$$

and satisfies

$$\forall (z,v) \in \mathbb{R} \times V\,, \quad 0 \le \tilde{f}(z,v) \le M(v)\,, \quad \lim_{z \to -\infty} \tilde{f}(z,v) = M(v)\,, \quad \lim_{z \to +\infty} \tilde{f}(z,v) = 0\,. \tag{4.14}$$

It is well known for this kind of Fisher-KPP type problems that propagation fronts are so-called pulled fronts, that is the speed of propagation is given by seeking exponentially decaying solutions of the linearized problem in a moving frame. As a consequence, for any $\lambda > 0$, one can define $c(\lambda, e)$ using the spectral problem solved in Definition 4.1. Indeed, we set

$$c(\lambda, e) = (1+r)\mathcal{H}\left(\frac{\lambda e}{1+r}\right) + r. \tag{4.15}$$

Then we have the formula for the minimal speed in the direction $e \in \mathbb{S}^{n-1}$.

$$c^*(e) = \inf_{\lambda > 0} c(\lambda, e)\,.$$

We obtain the following existence result.

Theorem 4.4. *Let $e \in \mathbb{S}^{n-1}$. For all $c \in [c^*(e), \overline{v}(e))$, there exists a travelling wave solution of* (4.1) *with speed c and direction e. Moreover, there exists no positive travelling wave solution of speed $c \in [0, c^*(e))$.*

Following very closely the proof used in the mono-dimensional case, we shall prove this Theorem using sub and super-solution and a comparison principle satisfied by (4.1). We shall construct these sub- and super-solution using travelling wave solutions of the linearized problem. The main difference concerning the travelling wave result is the way we prove the minimality of the speed $c^*(e)$. Indeed, it might happen that $c(\lambda, e)$ is singular at its minimum λ^* so that one can not reproduce the same argument as for the mono-dimensional case used in [26], that was based on the Rouché Theorem. Using the Hamilton-Jacobi framework above, we prove the following result.

Proposition 4.5. *Let f_0 be a non-zero initial data, compactly supported in some direction e_0, such that there exists $\gamma < 1$ such that*

$$\gamma M(v)\mathbf{1}_{[-x_m,x_m]\cdot e_0+e_0^\perp}(x) \leq f_0(x,v) \leq M(v)\mathbf{1}_{[-x_M,x_M]\cdot e_0+e_0^\perp}(x),$$

for all $(x,v) \in \mathbb{R}^n \times V$. Let f be the solution of the Cauchy problem (4.1) *associated to this initial data. Then we have*

$$\lim_{t\to+\infty} \sup_{x\cdot e_0 > ct} \rho(t,x) = 0, \text{ if } c > c^*(e_0), \tag{4.16}$$

$$\lim_{t\to+\infty} f(t, e_0^\perp + cte_0, v) = M(v)\,, \text{ if } c < c^*(e_0), \tag{4.17}$$

uniformly in $v \in V$.

Spreading of compactly supported initial data

Finally, we also deduce from the Hamilton-Jacobi framework a spreading result for initial conditions that are compactly supported. To this aim, let us first define the speed $w^*(e_0)$ associated to any direction $e_0 \in \mathbb{S}^{n-1}$ via the following Freidlin-Gärtner formula (see [67] for its first derivation).

$$w^*(e_0) = \min_{\substack{e\in\mathbb{S}^{n-1}\\ e_0\cdot e>0}} \left(\frac{c^*(e)}{e_0\cdot e}\right).$$

We obtain the following result.

Proposition 4.6. *Let f^0 be a non-zero compactly supported initial data such that $0 \leq f_0(x,v) \leq M(v)$ for all $(x,v) \in \mathbb{R}^n \times V$. Let f be the solution of the Cauchy problem* (4.1) *associated to this initial data. Then for any $e_0 \in \mathbb{S}^{n-1}$ and all $x \in \mathbb{R}^n$, we have*

$$\lim_{t\to\infty} f(t, x+cte_0, v) = 0, \qquad \text{if } c > w^*(e_0), \tag{4.18}$$

and

$$\lim_{t\to\infty} f(t, cte_0, v) = M(v), \qquad \text{if } 0 \leq c \leq w^*(e_0), \tag{4.19}$$

for all $v \in V$.

This result is interesting since contrary to the case of the usual Fisher-KPP equation in heterogeneous domains, where the Freidlin-Gärtner formula holds, see [97], here there is no heterogeneity in space. The heterogeneity coming potentially from the velocity set, this would not be present in the macroscopic limit (the Fisher-KPP equation, see above). Of course, if V

is rotationally symmetric, the speed w^* is independent of the direction, and the propagation is radial.

We believe that our results remain true (when properly reformulated) when V is not symmetric. The proofs in this paper are not dramatically modified in this framework. Generalizing our results to a more general V, however, engenders additional notation and complexifies a bit the writing of the proofs without really adding much content. Note that a related paper [34] by the second author does not use this symmetry hypothesis.

The rest of this paper is organized as follows. In Section 4.2, we prove the Hamilton-Jacobi limit. We discuss the construction of travelling waves and the spreading results in Section 4.3.

4.2 The Hamilton-Jacobi limit

In this Section, we present the proof of the convergence result Theorem 4.2. We then prove a convergence result for ρ^ε in the region $\{\varphi^0 = 0\}$. This result will help us to show that the speed of propagation is still the minimal speed of existence of travelling waves, despite the singularity of $\mathcal{H}$.

4.2.1 The spectral problem

In this Section, we discuss the resolution of the spectral problem given by (4.9). We also provide examples for which the singular set of M is not empty.

The resolution

For any $p' > 0$, we look for an eigenvalue $\mathcal{H}(p')$ associated to a positive eigenvector $\widetilde{Q}_p$ such that

$$\left(1 + \mathcal{H}(p') - v \cdot p'\right) \widetilde{Q}_{p'}(v) = M(v) \int_V \widetilde{Q}_{p'}(v')\, dv', \qquad v \in V.$$

Note that it may happen that $\widetilde{Q}_{p'}$ is only a positive measure, that is, may happen to have a singular part. Since the problem is linear, one can always assume that $\widetilde{Q}_{p'}$ is a probability measure. We are thus led to find an eigenvalue $\mathcal{H}(p')$ such that there exists a probability measure $\widetilde{Q}_{p'}$ [1] such that

$$\left(1 + \mathcal{H}(p') - v \cdot p'\right) \widetilde{Q}_{p'}(v) = M(v), \qquad v \in V.$$

To make the singular set $\mathrm{Sing}\,(M)$ appear naturally, let us first investigate the case when $\widetilde{Q}_{p'} \in L^1(V)$. If a solution exists, then the profile $\widetilde{Q}_{p'}$ necessarily satisfies the following equation :

$$\widetilde{Q}_{p'}(v) = \frac{M(v)}{1 + \mathcal{H}(p') - v \cdot p'}, \qquad v \in V. \tag{4.20}$$

This is only possible if such an expression defines a probability measure. As a consequence, one shall look for conditions under which for any $p' \in \mathbb{R}^n$, there exists $\mathcal{H}(p')$ such that

$$I\left(\mathcal{H}(p'), p'\right) := \int_V \frac{M(v')}{1 + \mathcal{H}(p') - v' \cdot p'} dv' = 1,$$

1. To avoid too many notation, we identify $\widetilde{Q}_{p'}$ to its density when relevant.

with $1 + \mathcal{H}(p') - v' \cdot p > 0$ for all $v' \in V$, that is $\mathcal{H}(p') > \mu(p') - 1$.

For any $p' \notin \mathrm{Sing}(M)$, the function $\xi \mapsto I(\xi, p')$ is decreasing over $(\mu(p') - 1, +\infty)$. As such, $\mathcal{H}(p')$ exists and is unique in this interval since $I(\mu(p') - 1, p') > 1$, by the definition of p' not being in the singular set.

However, for any $p' \in \mathrm{Sing}(M)$, it is not possible to solve $I(\mathcal{H}(p'), p') = 1$ since $I(\mu(p') - 1, p') \leq 1$. After Theorem 1.2 in [41], there exists a solution to (4.9), given by the couple $(\mathcal{H}(p'), \widetilde{Q}_{p'})$ where $\mathcal{H}(p') = \mu(p') - 1$ and $\widetilde{Q}_{p'}$ is a positive measure given by :

$$\widetilde{Q}_{p'} := \frac{M(v)}{\mu(p') - v \cdot p'} dv + \left(1 - \int_V \frac{M(v)}{\mu(p') - v \cdot p'} dv\right) \delta_w,$$

where δ_w is the dirac mass located at $w \in \mathrm{Arg}\, \mu(p')$.

From [34], we know that the set $\mathrm{Sing}(M)^c$ is convex and contains 0. To identify the different cases where such a singularity set may occur, we detail three examples hereafter.

Examples

Example 4.7. *In the one-dimensional case ($n = 1$), we have* $\mathrm{Sing}(M) = \emptyset$ *when* $\inf_{v \in V} M(v) > 0$ *since*

$$\int_{-\overline{v}}^{\overline{v}} \frac{M(v')}{\mu(p') - vp'} dv = \int_{-\overline{v}}^{\overline{v}} \frac{M(v)}{|p'| v_{max} - vp'} dv \geq \frac{\inf M(v)}{|p'| \overline{v}} \cdot \int_{-1}^{1} \frac{dv}{1 - v} = +\infty. \tag{4.21}$$

By monotone convergence we have

$$\lim_{H \to \mu(p') - 1} \int_{-\overline{v}}^{\overline{v}} \frac{M(v)}{1 + H - vp'} dv = +\infty,$$

hence, for all $p' \in \mathbb{R}$, there exists a unique $\mathcal{H}(p')$ that solves the spectral problem in $L^1(V)$.

This latter framework is the one used in [26]. In fact, we can only require that M does not to cancel in a neighborhood of $v = \overline{v}$ in order to get $\mathrm{Sing}(M) = \emptyset$. Indeed, the integral in (4.21) will also diverge in that scenario. If $M(\overline{v}) = 0$, this argument may not work out. Consider for example :

Example 4.8. *Let $n = 1$, $V = [-1, 1]$ and $M(v) = \frac{3}{2}(1 - |v|)^2$. Then,*

$$\begin{aligned} l(1) = \int_{-1}^{1} \frac{M(v)}{1 - v} \, dv &= \frac{3}{2} \int_{-1}^{1} \frac{(1 - |v|)^2}{1 - v} \, dv = 3 \int_0^1 \frac{(1 - v)^2}{(1 - v)(1 + v)} \, dv \\ &= 3 \int_0^1 \frac{1 - v}{1 + v} \, dv = 3 \int_0^1 \frac{2 - (1 + v)}{1 + v} \, dv \\ &= 3 \left(\int_0^1 \frac{2}{1 + v} \, dv - 1 \right) = 3(2 \ln(2) - 1). \end{aligned}$$

Hence, $|p'| \geq 3(2 \ln(2) - 1)$ if and only if

$$\int_{-1}^{1} \frac{M(v)}{\mu(p') - vp'} dv = \frac{3}{2|p'|} \int_{-1}^{1} \frac{(1 - |v|)^2}{1 - v} dv \leq 1,$$

therefore, $\mathrm{Sing}(M) = (-3(2\ln(2)-1), 3(2\ln(2)-1))^c$. *Let us also notice that*

$$\begin{aligned}\int_V \frac{M(v)}{(\overline{v}(1)-v)^2}dv &= \frac{3}{2}\int_{-1}^1 \frac{(1-|v|)^2}{(1-v)^2}dv = 3\int_0^1 \frac{1+v^2}{(1+v)^2}dv \\ &= 3\int_0^1 \frac{(1+v)^2-2(1+v)+2}{(1+v)^2}dv \\ &= 3\int_0^1 \left(1-\frac{2}{1+v}+\frac{2}{(1+v)^2}\right)dv \\ &= 3(1-2\ln(2)+1) = 6(1-\ln(2)) < +\infty.\end{aligned}$$

We will make a use of this result later.

In the multi-dimensional case, we may encounter a singular set, even when $\inf_{v\in V} M(v) > 0$. These singularities can occur in the most simple cases.

Example 4.9. *Let $n \geq 1$, let $V = B(0,1)$ be the n-dimensional unit ball. Let $e = e_1$ and $M = \omega_n^{-1}.\mathbb{1}_{\overline{B(0,1)}}$, where ω_n is the Lebesgue measure of V. For $n = 1$, since $M > 0$ we have* $\mathrm{Sing}(M) = \emptyset$ *(recall Example 4.7). Suppose now that $n > 1$. Then,*

$$\begin{aligned} l(e_1) &= \int_{B(0,1)} \frac{M(v)}{\overline{v}(e_1) - v\cdot e_1}dv \\ &= \frac{1}{\omega_n}\int_{B(0,1)} \frac{1}{1-v_1}dv \\ &= \frac{1}{\omega_n}\int_{-1}^1 \frac{1}{1-v_1}\left(\int \mathbb{1}_{\{v_1^2+v_2^2+\ldots+v_n^2\leq 1\}}(v_2,\ldots,v_n)dv_2\ldots dv_n\right)dv_1.\end{aligned}$$

Now, for fixed v_1, the quantity $\int \mathbb{1}_{\{v_1^2+v_2^2+\ldots+v_n^2\leq 1\}}(v_2,\ldots,v_n)dv_2\ldots dv_n$ is the Lebesgue measure of the $(n-1)$-dimensional ball of radius $\sqrt{1-v_1^2}$, hence

$$\int \mathbb{1}_{\{v_1^2+v_2^2+\ldots+v_n^2\leq 1\}}(v_2,\ldots,v_n)dv_2\ldots dv_n = \omega_{n-1}\times\left(\sqrt{1-v_1^2}\right)^{n-1}.$$

Finally,

$$\begin{aligned} l(e_1) &= \frac{\omega_{n-1}}{\omega_n}\int_{-1}^1 \frac{\left(1-v_1^2\right)^{\frac{n-1}{2}}}{1-v_1}dv_1 \\ &= \frac{2\omega_{n-1}}{\omega_n}\int_0^1 \left(1-v_1^2\right)^{\frac{n-3}{2}}dv_1 \\ &= \frac{2\omega_{n-1}}{\omega_n}\int_0^{\frac{\pi}{2}} (\cos(\theta))^{n-2}\,d\theta, \\ &= \frac{n}{n-1}, \end{aligned}$$

where we have used, for example, the relationship between the volume of the unit ball and the Wallis integrals. By rotational invariance, $\mathrm{Sing}(M) = B\left(0, \frac{n-1}{n}\right)^c$.

4.2.2 Proof of Theorem 4.2

In this Section, we now prove Theorem 4.2. We will use the half-relaxed limits method of Barles and Perthame [9]. In addition to that, and similarly to the papers [22, 34], we need to use the perturbated test-function method. We emphasize that the correction test is defined thanks to the spectral problem (4.9), keeping only the regular part of the eigenfunction (recall that it may have singularities).

Since the sequence φ^ε is uniformly bounded by the maximum principle (check Proposition 5 in [20]), we can define its upper- and lower- semi continuous envelopes by the following formulas

$$\varphi^*(t,x,v) = \limsup_{\substack{\varepsilon\to 0\\ (s,y,w)\to(t,x,v)}} \varphi^\varepsilon(s,y,w), \qquad \varphi_*(t,x,v) = \liminf_{\substack{\varepsilon\to 0\\ (s,y,w)\to(t,x,v)}} \varphi^\varepsilon(s,y,w)$$

Recall that φ^* is upper semi-continuous, φ_* is lower semi-continuous and that from their definition, one has $\varphi_* \le \varphi^*$. We have the following :

Proposition 4.10. *Let φ^ε be a solution to* (4.6).

(i) The upper semi-limit φ^* is constant with respect to the velocity variable on $\mathbb{R}_+^* \times \mathbb{R}^n$.

(ii) The function $(t,x) \mapsto \varphi^*(t,x)$ is a viscosity sub-solution to (4.12) *on $\mathbb{R}_+^* \times \mathbb{R}^n$.*

(iii) The function $(t,x) \mapsto \min_{w\in V} \varphi_*(t,x,w)$ is a viscosity super-solution to (4.12) *on $\mathbb{R}_+^* \times \mathbb{R}^n$.*

We recall that for all (t,x), the minimum $\min_{w\in V} \varphi_*(t,x,w)$ is attained since V is bounded and φ_* is lower semi-continuous. We point out here that if $r = 0$, that is, the case of [22, 34], it is not necessary to prove that φ^* is constant in the velocity variable. One can replace this by proving that $\max_{w\in V} \varphi^*$ is a sub-solution to (4.12). The fact that φ^* is constant in the velocity variable is needed to control the limit of ρ^ε.

Proof of Proposition 4.10. We start with the proof of (i). Take $(t^0,x^0,v^0) \in \mathbb{R}_+^* \times \mathbb{R}^n \times V$. Let ψ be a test function such that $\varphi^* - \psi$ has a strict local maximum at (t^0,x^0,v^0). Then there exists a sequence $(t^\varepsilon,x^\varepsilon,v^\varepsilon)$ of maximum points of $\varphi^\varepsilon - \psi$ satisfying $(t^\varepsilon,x^\varepsilon,v^\varepsilon) \to (t^0,x^0,v^0)$. From this we deduce that $\lim_{\varepsilon\to 0} \varphi^\varepsilon(t^\varepsilon,x^\varepsilon,v^\varepsilon) = \varphi^*(t,x,v)$. Recalling (4.6), we have at $(t^\varepsilon,x^\varepsilon,v^\varepsilon)$:

$$\partial_t\psi + v^\varepsilon\cdot\nabla_x\psi + r = (1+r)\left(1 - \int_V M(v') e^{\frac{\varphi^\varepsilon - \varphi^{\varepsilon'}}{\varepsilon}} dv'\right) + r\rho^\varepsilon.$$

From this, we deduce that

$$\int_{V'} M(v') e^{\frac{\varphi^\varepsilon(t^\varepsilon,x^\varepsilon,v^\varepsilon) - \varphi^\varepsilon(t^\varepsilon,x^\varepsilon,v')}{\varepsilon}} dv'$$

is uniformly bounded for any $V' \subset V$. By the Jensen inequality,

$$\exp\left(\frac{1}{\varepsilon\,|V'|_M}\int_{V'}\left(\varphi^\varepsilon(t^\varepsilon,x^\varepsilon,v^\varepsilon) - \varphi^\varepsilon(t^\varepsilon,x^\varepsilon,v')\right) M(v')dv'\right) \le \frac{1}{|V'|_M}\int_{V'} M(v') e^{\frac{\varphi^\varepsilon(t^\varepsilon,x^\varepsilon,v^\varepsilon) - \varphi^\varepsilon(t^\varepsilon,x^\varepsilon,v')}{\varepsilon}} dv',$$

where $|V'|_M := \int_{V'} M(v)dv$. Thus,

$$\limsup_{\varepsilon\to 0}\left(\int_{V'}\left(\varphi^\varepsilon(t^\varepsilon,x^\varepsilon,v^\varepsilon) - \varphi^\varepsilon(t^\varepsilon,x^\varepsilon,v')\right) M(v')dv'\right) \le 0.$$

We write

$$\begin{aligned}\int_{V'} \left(\varphi^\varepsilon(v^\varepsilon) - \varphi^\varepsilon(v')\right) M(v')dv' &= \int_{V'} \left(\varphi^\varepsilon(v^\varepsilon) - \psi(v^\varepsilon)\right) - \left(\varphi^\varepsilon(v') - \psi(v')\right) + \left(\psi(v^\varepsilon) - \psi(v')\right) M(v')dv' \\ &= \int_{V'} \left[\left(\varphi^\varepsilon(v^\varepsilon) - \psi(v^\varepsilon)\right) - \left(\varphi^\varepsilon(v') - \psi(v')\right)\right] M(v')dv' \\ &+ \int_{V'} \left(\psi(v^\varepsilon) - \psi(v')\right) M(v')dv'\end{aligned}$$

We can thus use the Fatou Lemma, together with $-\limsup_{\varepsilon\to 0} \varphi^\varepsilon(t^\varepsilon, x^\varepsilon, v') \geq -\varphi^*(t^0, x^0, v')$ to get

$$\begin{aligned}\left(\int_{V'} M(v')dv'\right)\varphi^*(v^0) - \int_{V'} \varphi^*(v')M(v')dv' &= \int_{V'} \left(\varphi^*(v^0) - \varphi^*(v')\right) M(v')dv' \\ &\leq \int_{V'} \liminf_{\varepsilon\to 0} \left(\varphi^\varepsilon(v^\varepsilon) - \varphi^\varepsilon(v')\right) M(v')dv' \\ &\leq \liminf_{\varepsilon\to 0} \left(\int_{V'} \left(\varphi^\varepsilon(v^\varepsilon) - \varphi^\varepsilon(v')\right) M(v')dv'\right) \\ &\leq \limsup_{\varepsilon\to 0} \left(\int_{V'} \left(\varphi^\varepsilon(v^\varepsilon) - \varphi^\varepsilon(v')\right) M(v')dv'\right) \\ &\leq 0,\end{aligned}$$

We shall deduce, since the latter is true for any $|V'|$ that

$$\varphi^*(t^0, x^0, v^0) \leq \inf_V \varphi^*(t^0, x^0, \cdot)$$

and thus φ^* is constant in velocity.

We now continue with the proof of (ii). We have to prove that on $\{\varphi^* > 0\} \cap (\mathbb{R}_+^* \times \mathbb{R}^n)$, the function φ^* is a viscosity subsolution of (4.12). To this aim, let $\psi \in C^2(\mathbb{R}_+^* \times \mathbb{R}^n)$ be a test function such that $\varphi^* - \psi$ has a local maximum in $(t^0, x_0) \in (\mathbb{R}_+^* \times \mathbb{R}^n) \cap \{\varphi^* > 0\}$. We denote by $p^0(t^0, x_0) = \frac{\nabla_x \psi(t^0, x_0)}{1+r}$.

 # First case : $p^0(t^0, x^0) \notin \operatorname{Sing} M$.

We define a corrector η according to the following formula :

$$\eta(v) = \ln\left(1 + \mathcal{H}\left(p^0(t^0, x^0)\right) - v \cdot p^0(t^0, x^0)\right)$$

Let us define the perturbed test function $\psi^\varepsilon := \psi + \varepsilon\eta$. We recall the fact that in this case $\int_V M(v') \exp(-\eta(v'))dv' = 1$. The function ψ^ε converges uniformly to ψ since η is bounded on V. As a consequence, there exists a sequence $(t^\varepsilon, x^\varepsilon, v^\varepsilon)$ of maximum points of $\varphi^\varepsilon - \psi^\varepsilon$ satisfying $(t^\varepsilon, x^\varepsilon) \to (t^0, x^0)$ and such that $\lim_{\varepsilon\to 0} \varphi^\varepsilon(t^\varepsilon, x^\varepsilon, v^\varepsilon) = \varphi^*(t^0, x^0)$. Recalling (4.6), we have at $(t^\varepsilon, x^\varepsilon, v^\varepsilon)$:

$$\partial_t \psi^\varepsilon + v^\varepsilon \cdot \nabla_x \psi^\varepsilon + r = (1 + r)\left(1 - \int_V M(v') e^{\frac{\varphi^\varepsilon - \varphi^{\varepsilon'}}{\varepsilon}} dv'\right) + r\rho^\varepsilon.$$

Since $(t^\varepsilon, x^\varepsilon, v^\varepsilon)$ is a maximum point, we may rearrange the r.h.s. of the latter so that the

previous equation may be rewritten as follows

$$\begin{aligned}\partial_t\psi^\varepsilon + v^\varepsilon\cdot\nabla_x\psi^\varepsilon + r &\leq (1+r)\left(1-\int_V M(v')\exp\left(\eta(v^\varepsilon)-\eta(v')\right)dv'\right)+r\rho^\varepsilon,\\ &= (1+r)\left(1-\left(\int_V M(v')\exp\left(-\eta(v')\right)dv'\right)\exp\left(\eta(v^\varepsilon)\right)\right)+r\rho^\varepsilon,\\ &= (1+r)\left(1-\exp\left(\eta(v^\varepsilon)\right)\right)+r\rho^\varepsilon,\\ &= -(1+r)\mathcal{H}\left(p^0(t^0,x^0)\right)+v^\varepsilon\cdot\nabla_x\psi^0(t^0,x^0)+r\rho^\varepsilon.\end{aligned}$$

Since $(t^0,x^0)\in\{\varphi^*>0\}$ and $\lim_{\varepsilon\to 0}\varphi^\varepsilon(t^\varepsilon,x^\varepsilon,v^\varepsilon)=\varphi^*(t^0,x^0)$, we have that, eventually, $\varphi^\varepsilon(t^\varepsilon,x^\varepsilon,v^\varepsilon)>\varphi^*(t^0,x^0)/2>0$ for ε sufficiently small. Since

$$r\rho^\varepsilon\left(e^{\frac{\varphi^\varepsilon}{\varepsilon}}-1\right)=\left(1-\int_V M(v')e^{\frac{\varphi^\varepsilon-\varphi^{\varepsilon'}}{\varepsilon}}dv'\right)-\left(\partial_t\psi^\varepsilon+v^\varepsilon\cdot\nabla_x\psi^\varepsilon\right),$$

and the latter r.h.s. is uniformly bounded from above in ε, we deduce that $\lim_{\varepsilon\to 0}\rho^\varepsilon(t^\varepsilon,x^\varepsilon)=0$. Taking the limit $\varepsilon\to 0$, we get

$$\partial_t\psi\left(t^0,x^0\right)+(1+r)\mathcal{H}\left(\frac{\nabla_x\psi(t^0,x^0)}{1+r}\right)+r\leq 0.$$

 # Second case : $p^0(t^0,x^0)\in\operatorname{Sing}M$**.**

Let $v^*\in\operatorname{Arg}\mu(p^0(t^0,x^0))$. The function $(t,x)\mapsto\phi^\varepsilon(t,x,v^*)-\psi(t,x)$ has a local maximum at a point $(t^\varepsilon,x^\varepsilon)$ satisfying $(t^\varepsilon,x^\varepsilon)\to(t^0,x^0)$ as $\varepsilon\to 0$. We then have :

$$\begin{aligned}\partial_t\psi(t^\varepsilon,x^\varepsilon)+v^*\cdot\nabla_x\psi(t^\varepsilon,x^\varepsilon)+r &= \partial_t\phi^\varepsilon(t^\varepsilon,x^\varepsilon,v^*)+v^*\cdot\nabla_x\phi^\varepsilon(t^\varepsilon,x^\varepsilon,v^*)+r\\ &= (1+r)\int_V M(v')\left(1-e^{\frac{\varphi^\varepsilon(v^*)-\varphi^\varepsilon(v')}{\varepsilon}}\right)dv'+r\rho^\varepsilon\\ &\leq (1+r)+r\rho^\varepsilon.\end{aligned}$$

Since $(t^0,x^0)\in\{\varphi^*>0\}$, we have $\rho^\varepsilon(t^\varepsilon,x^\varepsilon)\to 0$. As a consequence, taking the limit $\varepsilon\to 0$, we get

$$\partial_t\psi(t^0,x^0)+\mu(\nabla_x\psi(t^0,x^0))\leq 1.$$

We finally turn to the proof of (iii). That is, the fact that on $\mathbb{R}^*_+\times\mathbb{R}^n$, the function $\min_{w\in V}\varphi_*(\cdot,w)$ is a viscosity supersolution of (4.12).

Let $\psi\in C^1(\mathbb{R}^*_+\times\mathbb{R}^n)$ be a test function such that $\min_{w\in V}\varphi_*-\psi$ has a local minimum in $(t^0,x^0)\in\mathbb{R}^*_+$. We denote by $p^0(t^0,x^0)=\frac{\nabla_x\psi(t^0,x^0)}{1+r}$. We define the truncated corrector η_δ,

$$\begin{aligned}\eta(v) &= \ln\left(1+\mathcal{H}\left(p^0(t,x)\right)-v\cdot p^0(t,x)\right),\\ \eta_\delta(v) &= \max\left(\eta(v),-\delta\right).\end{aligned}$$

Let us define the perturbed test function $\psi^\varepsilon:=\psi+\varepsilon\eta_\delta$. For any $\delta>0$, the function ψ^ε converges uniformly to ψ as $\varepsilon\to 0$ since η_δ is bounded on V. Since $\varphi_*(t^0,x^0,\cdot)$ attains its minimum at, say, v^0, we have, for all $v\in V$ and locally in the (t,x) variables,

$$\varphi_*(t^0,x^0,v^0)-\psi(t^0,x^0)=\min_{w\in V}\varphi_*(t^0,x^0)-\psi(t^0,x^0)\leq\min_{w\in V}\varphi_*(t,x)-\psi(t,x)\leq\varphi_*(t,x,v)-\psi(t,x),$$

and thus (t^0, x^0, v^0) is a local minimum of $\varphi_* - \psi$, strict in the (t, x) variables. By the definition of the lower semi-limit, there exists a sequence $\left(t^\varepsilon_\delta, x^\varepsilon_\delta, v^\varepsilon_\delta\right)$ of minimum points of $\varphi^\varepsilon - \psi^\varepsilon$ satisfying $(t^\varepsilon_\delta, x^\varepsilon_\delta) \to (t^0, x^0)$. We obtain, after (4.6), at the point $\left(t^\varepsilon_\delta, x^\varepsilon_\delta, v^\varepsilon_\delta\right)$,

$$\begin{aligned}\partial_t\psi^\varepsilon + v^\varepsilon_\delta \cdot \nabla_x\psi^\varepsilon + r &\geq (1+r)\left(1 - \int_V M(v')\exp\left(\eta_\delta(v^\varepsilon) - \eta_\delta(v')\right)dv'\right), \\ &= (1+r)\left(1 - \left(\int_V M(v')\exp\left(-\eta_\delta(v')\right)dv'\right)\exp\left(\eta_\delta(v^\varepsilon_\delta)\right)\right).\end{aligned}$$

Since the sequence v^ε_δ lies in a compact set, taking the limit $\varepsilon \to 0$ (up to extraction), we obtain v^0_δ such that

$$\partial_t\psi + v^0_\delta \cdot \nabla_x\psi + r \geq (1+r)\left(1 - \left(\int_V M(v')e^{-\eta_\delta(v')}dv'\right)e^{\eta_\delta(v^0_\delta)}\right).$$

By construction, $\eta_\delta \geq \eta$. As a consequence, $\int_V M(v')e^{-\eta_\delta(v')}dv' \leq \int_V M(v')e^{-\eta(v')}dv' \leq 1$. Thus,

$$\partial_t\psi + v^0_\delta \cdot \nabla_x\psi + r \geq (1+r)\left(1 - e^{\eta_\delta(v^0_\delta)}\right).$$

We now pass to the limit $\delta \to \infty$. By compactness of V, one can extract a converging subsequence from $(v^0_\delta)_\delta$, we denote by v^* the limit.

 # First case : $p^0(t^0, x^0) \notin \operatorname{Sing} M$**.**

In this case, since η is bounded, $\eta_\delta = \eta$ for δ sufficiently large (but finite). Thus, passing to the limit $\delta \to \infty$, one gets

$$\begin{aligned}\partial_t\psi + v^* \cdot \nabla_x\psi + r &\geq (1+r)\left(1 - \exp\left(\eta(v^*)\right)\right), \\ &= -(1+r)\mathcal{H}\left(p^0(t^0, x^0)\right) + v^* \cdot \nabla_x\psi(t^0, x^0),\end{aligned}$$

from which we deduce

$$\partial_t\psi\left(t^0, x^0\right) + (1+r)\mathcal{H}\left(\frac{\nabla_x\psi(t^0, x^0)}{1+r}\right) + r \geq 0.$$

 # Second case : $p^0(t^0, x^0) \in \operatorname{Sing} M$**.**

In this case, the corrector η_δ is

$$\eta_\delta(v) = \max\left(\ln\left(\mu\left(\nabla_x\psi(t^0, x^0)\right) - v \cdot \nabla_x\psi(t^0, x^0)\right), -\delta\right).$$

If $v^* \notin \operatorname{Arg}\mu(p^0(t^0, x^0))$, since η is bounded on all compacts of $V \setminus \operatorname{Arg}\mu(p^0(t^0, x^0))$, $\eta_\delta(v^0_\delta) = \eta(v^0_\delta)$ for δ sufficiently large and we recover the first case.

If $v^* \in \operatorname{Arg}\mu(p^0(t^0, x^0))$, then take $\delta' > 0$, one has when $\delta > \delta'$ is sufficiently large,

$$-\delta' = \eta_{\delta'}(v^0_\delta) \geq \eta_\delta(v^0_\delta),$$

and thus $\lim_{\delta \to +\infty} \eta_\delta(v^0_\delta) = -\infty$. From that we conclude

$$\partial_t\psi + \mu\left(\nabla_x\psi(t^0, x^0)\right) \geq 1.$$

□

We now conclude with the proof of the convergence result. For this, we need to input initial conditions. Obviously, one cannot get any uniqueness result for the Hamilton-Jacobi equation (4.12) without imposing any initial condition. We now check the initial condition of (4.12) in the viscosity sense.

Proposition 4.11. *If one assumes that $\varphi_0^\varepsilon = \varphi_0$, the sequence φ^ε converges uniformly on compact subsets of $\mathbb{R}_+^* \times \mathbb{R}^n$ to φ^0, the unique viscosity solution of*

$$\begin{cases} \min\left\{\partial_t\varphi^0 + (1+r)\mathcal{H}\left(\frac{\nabla_x\varphi^0}{1+r}\right) + r, \varphi^0\right\} = 0, & (t,x) \in \mathbb{R}_+^* \times \mathbb{R}^n, \\ \varphi^0(0,x) = \min\limits_{v\in V}\varphi_0(x,v), & x \in \mathbb{R}^n. \end{cases}$$

Proof of Proposition 4.11. We extend the definition of φ^* to $\{t=0\}\times\mathbb{R}^n$ by the formula

$$\varphi^*(0,x) = \limsup_{\substack{t\searrow 0^+ \\ x'\to x}} \varphi^*(t,x').$$

One has to prove the following

$$\min\left(\min\left\{\partial_t\varphi^* + (1+r)\mathcal{H}\left(\frac{\nabla_x\varphi^*}{1+r}\right) + r, \varphi^*\right\}, \varphi^* - \min_{v\in V}\varphi_0(\cdot,v)\right) \le 0, \tag{4.22}$$

on $\{t=0\}\times\mathbb{R}^n$ in the viscosity sense.

Let $\psi \in \mathcal{C}^1(\mathbb{R}^+\times\mathbb{R})$ be a test function such that $\varphi^* - \psi$ has a strict local maximum at $(t^0=0, x^0)$. We now prove that either

$$\varphi^*(0,x^0) \le \min_{v\in V}\varphi_0(x,v),$$

or

$$\partial_t\psi + (1+r)\mathcal{H}\left(\frac{\nabla_x\psi}{1+r}\right) + r \le 0 \qquad \text{when} \qquad \varphi^*(0,x^0) > 0.$$

Suppose then that

$$\varphi^*(0,x^0) > \min_{v\in V}\varphi_0(x,v).$$

We shall now prove that

$$\partial_t\psi + (1+r)\mathcal{H}\left(\frac{\nabla_x\psi}{1+r}\right) + r \le 0,$$

since then $\varphi^*(0,x^0) > 0$. We now go through the same steps as for the proof of Proposition 4.10, but with slight changes due to the present situation. We keep the same notations.

 # First case : $p^0(t^0,x^0) \notin \operatorname{Sing} M$**.**

The function ψ^ε converges uniformly to ψ since η is bounded on V. Adding this fact to the definition of $\varphi^*(0,x^0)$, we get the existence of a sequence $(t^\varepsilon,x^\varepsilon,v^\varepsilon)$ of maximum points of $\varphi^\varepsilon - \psi^\varepsilon$ satisfying $t^\varepsilon > 0$, $(t^\varepsilon,x^\varepsilon)\to(0,x^0)$ and such that $\lim_{\varepsilon\to 0}\varphi^\varepsilon(t^\varepsilon,x^\varepsilon,v^\varepsilon) = \varphi^*(0,x^0)$. The rest of the proof is similar.

 # Second case : $p^0(t^0,x^0) \in \operatorname{Sing} M$**.**

Let $v^* \in \operatorname{Arg}\mu(p^0(t^0,x^0))$. As for the previous case, due to the definition of φ^*, the function $(t,x) \mapsto \phi^\varepsilon(t,x,v^*) - \psi(t,x)$ has a local maximum at a point $(t^\varepsilon, x^\varepsilon)$ satisfying $(t^\varepsilon > 0, x^\varepsilon) \to (t^0, x^0)$ as $\varepsilon \to 0$. The end is the same.

We shall now prove that the initial condition for $\min_w \varphi_*$ is given by

$$\max\left(\min\left\{\partial_t\left(\min_w \varphi_*\right) + (1+r)\mathcal{H}\left(\frac{\nabla_x\left(\min_w \varphi_*\right)}{1+r}\right) + r, \min_w \varphi_*\right\}, \min_w \varphi_* - \min_{v\in V}\varphi_0\right) \geq 0, \tag{4.23}$$

on $\{t=0\}\times\mathbb{R}^n$ in the viscosity sense.

Let us prove (4.23). Let $\psi \in \mathcal{C}^1(\mathbb{R}^+\times\mathbb{R})$ be a test function such that $\min_{w\in V}\varphi_* - \psi$ has a strict local minimum at $(t^0=0, x^0)$. We now prove that either

$$\min_{w\in V}\varphi_*(0,x^0,w) \geq \min_{v\in V}\varphi_0(x^0,v),$$

or

$$\partial_t\psi + (1+r)\mathcal{H}\left(\frac{\nabla_x\psi}{1+r}\right) + r \geq 0 \qquad \text{and} \qquad \min_{w\in V}\varphi_*(0,x^0,w) \geq 0.$$

Suppose that $\min_{w\in V}\varphi_*(0,x^0,w) < \min_{v\in V}\varphi_0(x^0,v)$. The argument now starts similarly as in the proof above. Let us define the perturbed test function $\psi^\varepsilon := \psi + \varepsilon\eta_\delta$. For any $\delta > 0$, the function ψ^ε converges uniformly to ψ since η_δ is bounded on V. Since $\varphi_*(0,x^0,\cdot)$ attains its minimum at, say, v^0, we have, for all $v \in V$ and locally in the (t,x) variables,

$$\varphi_*(0,x^0,v_0) - \psi(0,x^0) \leq \min_{w\in V}\varphi_*(0,x^0,w) - \psi(0,x^0) \leq \min_{w\in V}\varphi_*(t,x,w) - \psi(t,x) \leq \varphi_*(t,x,v) - \psi(t,x),$$

and thus $(0,x^0,v^0)$ is a local minimum of $\varphi_* - \psi$, strict in the (t,x) variables. By the definition of the lower semi-limit, there exists a sequence $\left(t^\varepsilon_\delta, x^\varepsilon_\delta, v^\varepsilon_\delta\right)$ of minimum points of $\varphi^\varepsilon - \psi^\varepsilon$ satisfying $(t^\varepsilon_\delta, x^\varepsilon_\delta) \to (0,x^0)$. We first claim that there exists a subsequence $(t_{\varepsilon_k}, x_{\varepsilon_k}, v_{\varepsilon_k})_k$ of the above sequence, with $\varepsilon_k \to 0$ as $k\to\infty$, such that $t_{\varepsilon_k} > 0$, for all k.

Suppose that this is not true. Then, take a sequence $(x^{\varepsilon_{k'}}_\delta, v^{\varepsilon_{k'}}_\delta)_{k'}$ such that $(\varepsilon_{k'}, x^{\varepsilon_{k'}}_\delta) \to (0,x^0)$ and that $\varphi^{\varepsilon_{k'}} - \psi^{\varepsilon_{k'}}$ has a local minimum at $\left(0, x^{\varepsilon_{k'}}_\delta, v^{\varepsilon_{k'}}_\delta\right)$. It follows that, for all (t,x,v) in some neighborhood of $(0, x^{\varepsilon_{k'}}_\delta, v^{\varepsilon_{k'}}_\delta)$, we have

$$\begin{aligned}
\min_{v\in V}\varphi_0(x^{\varepsilon_{k'}}_\delta, v) - \psi^{\varepsilon_{k'}}\left(0, x^{\varepsilon_{k'}}_\delta, v^{\varepsilon_{k'}}_\delta\right) &\leq \varphi_0(x^{\varepsilon_{k'}}_\delta, v^{\varepsilon_{k'}}_\delta) - \psi^{\varepsilon_{k'}}\left(0, x^{\varepsilon_{k'}}_\delta, v^{\varepsilon_{k'}}_\delta\right) \\
&\leq \varphi^{\varepsilon_{k'}}\left(0, x^{\varepsilon_{k'}}_\delta, v^{\varepsilon_{k'}}_\delta\right) - \psi^{\varepsilon_{k'}}\left(0, x^{\varepsilon_{k'}}_\delta, v^{\varepsilon_{k'}}_\delta\right) \\
&\leq \varphi^{\varepsilon_{k'}}(t,x,v) - \psi^{\varepsilon_{k'}}(t,x,v).
\end{aligned}$$

Taking $\liminf_{\substack{k'\to\infty \\ (t,x,v)\to(0,x^0,v_0)}}$ at the both sides of the inequality, one obtains

$$\min_{v\in V}\varphi_0(x^0,v) - \psi\left(0,x^0\right) \leq \min_{w\in V}\varphi_*(0,x^0,w) - \psi\left(0,x^0\right).$$

However, this is in contradiction with $\min_{w\in V}\varphi_*(0,x^0,w) < \min_{v\in V}\varphi_0(x^0,v)$. Now having in hand that this sequence of times $t_{\varepsilon_n} > 0$, one can reproduce the same argument as from the proof above along the subsequence $(t_{\varepsilon_n}, x_{\varepsilon_n}, v_{\varepsilon_n})$.

By the strong uniqueness principle satisfied by (4.12) (that is, a comparison principle for discontinuous sub- and super- solutions), we deduce that for all $(t,x,v) \in \mathbb{R}_+^* \times \mathbb{R}^n \times V$,

$$\min_{w\in V} \varphi_*(t,x,w) \le \varphi_*(t,x,v) \le \varphi^*(t,x,v) = \varphi^*(t,x) \le \min_{w\in V} \varphi_*(t,x,w)$$

We deduce that necessarily all these inequalities are equalities, and thus that φ^ε converges locally uniformly towards φ^0, independent of v, on any subcompact of $\mathbb{R}_+^* \times \mathbb{R}^n$. □

4.2.3 Convergence of the macroscopic density ρ^ε

We prove a convergence result for ρ^ε in the region $\{\varphi^0 = 0\}$. Namely

Proposition 4.12. *Let φ^ε be the solution of* (4.6)*. Then, uniformly on compact subsets of Int $\{\varphi^0 = 0\}$,*

$$\lim_{\varepsilon\to 0} \rho^\varepsilon = 1, \qquad \lim_{\varepsilon\to 0} f^\varepsilon(\cdot, v) = M(v).$$

Proof of Proposition 4.12. We develop similar arguments as in [58]. Let K be a compact set of $\{\varphi^0 = 0\}$. Note that it suffices to prove the result when K is a cylinder. Let $(t^0,x^0) \in \mathrm{Int}\,(K)$ and the test function

$$\forall (t,x) \in K, \qquad \psi^0(t,x) = |x-x^0|^2 + \left(t-t^0\right)^2.$$

Since $\varphi^0 = 0$ on K, the function $\varphi^0 - \psi^0$ admits a strict maximum in (t^0,x^0). The locally uniform convergence of $\varphi^\varepsilon - \psi^0$ gives a sequence $(t^\varepsilon,x^\varepsilon,v^\varepsilon)$ of maximum points with $(t^\varepsilon,x^\varepsilon) \to (t^0,x^0)$ and a bounded sequence v^ε such that at the point $(t^\varepsilon,x^\varepsilon,v^\varepsilon)$ one has :

$$\partial_t \psi^0 + v^\varepsilon \cdot \nabla_x \psi^0 + r \le r\rho^\varepsilon. \tag{4.24}$$

As a consequence, one has, since $r > 0$,

$$\rho^\varepsilon(t^\varepsilon,x^\varepsilon) \ge 1 + o(1), \qquad \text{as } \varepsilon \to 0, \tag{4.25}$$

and then $\lim_{\varepsilon\to 0} \rho^\varepsilon(t^\varepsilon,x^\varepsilon) = 1$ if one recalls $\rho^\varepsilon \le 1$ (which, again, is a consequence of the maximum principle).

However, we need an extra argument to get $\lim_{\varepsilon\to 0} \rho^\varepsilon(t^0,x^0) = 1$. Since $(t^\varepsilon,x^\varepsilon,v^\varepsilon)$ maximizes $\varphi^\varepsilon - \psi^0$, we deduce that for all $v \in V$, we have

$$\varphi^\varepsilon\left(t^\varepsilon,x^\varepsilon,v^\varepsilon\right) - \psi^0(t^\varepsilon,x^\varepsilon) \ge \varphi^\varepsilon\left(t^0,x^0,v\right) - \psi^0(t^0,x^0).$$

Since $\psi^0(t^\varepsilon,x^\varepsilon) \ge 0$, $\psi^0(t^0,x^0) = 0$, we find

$$f^\varepsilon(t^0,x^0,v) = M(v) e^{-\frac{\varphi^\varepsilon(t^0,x^0,v)}{\varepsilon}} \ge M(v) e^{-\frac{\varphi^\varepsilon(t^\varepsilon,x^\varepsilon,v^\varepsilon)}{\varepsilon}}. \tag{4.26}$$

We shall now prove that $\lim_{\varepsilon\to 0} \varepsilon^{-1}\varphi^\varepsilon(t^\varepsilon,x^\varepsilon,v^\varepsilon) = 0$. Let us rewrite (4.6) at the point $(t^\varepsilon,x^\varepsilon,v^\varepsilon)$ in the form

$$r\rho^\varepsilon(t^\varepsilon,x^\varepsilon)\left(e^{\frac{\varphi^\varepsilon(t^\varepsilon,x^\varepsilon,v^\varepsilon)}{\varepsilon}} - 1\right) = \left(1 - \int_V M(v') e^{\frac{\varphi^\varepsilon(t^\varepsilon,x^\varepsilon,v^\varepsilon) - \varphi^\varepsilon(t^\varepsilon,x^\varepsilon,v')}{\varepsilon}} dv'\right) - \left(\partial_t\psi^0 + v\cdot\nabla_x\psi^0\right)(t^\varepsilon,x^\varepsilon,v^\varepsilon)$$

We finally deduce using the maximum principle in the latter r.h.s. that

$$0 \le r\rho^\varepsilon(t^\varepsilon,x^\varepsilon)\left(e^{\frac{\varphi^\varepsilon(t^\varepsilon,x^\varepsilon,v^\varepsilon)}{\varepsilon}} - 1\right) \le o_{\varepsilon\to 0}(1)$$

and thus $\lim_{\varepsilon\to 0}\left(\varepsilon^{-1}\varphi^\varepsilon(t^\varepsilon,x^\varepsilon,v^\varepsilon)\right) = 0$. This implies $\lim_{\varepsilon\to 0} f^\varepsilon(t,x,v) = M(v)$ locally uniformly on $K \times V$.

□

4.2.4 Speed of expansion

To be self-contained, we recall here how to study the propagation of the front after deriving the limit variational equation, in the case $r > 0$. From Evans and Souganidis [58], we are able to identify the solution of the variational Hamilton-Jacobi equation (4.12) using the Lagrangian duality. We emphasize that, in this context, one may assume that our initial condition is well-prepared, *i.e.* $\varphi(0,x,v) = \varphi_0(x)$. We recall the equation :

$$\begin{cases} \min\left\{\partial_t\varphi + (1+r)\mathcal{H}\left(\frac{\nabla_x\varphi}{1+r}\right) + r, \varphi\right\} = 0, \qquad \forall (t,x) \in \mathbb{R}_+^* \times \mathbb{R}^n, \\ \varphi(0,x) = \varphi_0(x). \end{cases}$$

We recall from [22, 34] that the Hamiltonian $\mathcal{H}$ is convex. For any $e_0 \in \mathbb{S}^{n-1}$, we define the minimal speed in that direction by the formula

$$c^*(e) = \inf_{\lambda>0} c(\lambda, e), \quad c(\lambda, e) = \frac{1}{\lambda}\left((1+r)\mathcal{H}\left(\frac{\lambda e}{1+r}\right) + r\right). \tag{4.27}$$

We first discuss the speed of propagation of a front-like initial data.

Proposition 4.13. *Assume that*

$$\varphi_0(x) := \begin{cases} 0 & x \in e_0^\perp \\ +\infty & else \end{cases}.$$

Then the nullset of φ propagates at speed $c^*(e_0)$:

$$\forall t \geq 0, \qquad \{\varphi(t,\cdot) = 0\} = e_0^\perp + c^*(e_0) t\, e_0.$$

Proof of Proposition 4.13. We first notice that since the initial data is invariant under any translation in $e_0^\perp$, and the the equation (4.12) invariant by translation, the solution φ depends only on $x \cdot e_0$. That is $\varphi(t,x) = \varphi(t,(x\cdot e_0)e_0) = \overline{\varphi}(t, x\cdot e_0)$. The function $\overline{\varphi}$ satisfies

$$\begin{cases} \min\left\{\partial_t\overline{\varphi} + (1+r)\mathcal{H}\left(\frac{\partial_\xi\overline{\varphi}}{1+r}e_0\right) + r, \varphi\right\} = 0, \qquad \forall (t,\xi) \in \mathbb{R}_+^* \times \mathbb{R}, \\ \overline{\varphi}(0,\xi) = \overline{\varphi}_0(\xi). \end{cases}$$

where

$$\overline{\varphi}_0(\xi) := \begin{cases} 0 & \xi = 0, \\ +\infty & \text{else} \end{cases}.$$

The Lagrangian associated to the latter Hamilton-Jacobi equation is by definition

$$\begin{aligned} \mathcal{L}(p) &= \sup_{q\in\mathbb{R}}\left(pq - (1+r)\mathcal{H}\left(\frac{q}{1+r}e_0\right) - r\right), \\ &= \sup_{q\in\mathbb{R}}\left(pq - (1+r)\mathcal{H}\left(\frac{|q|}{1+r}e_0\right) - r\right), \\ &= \sup_{q\in\mathbb{R}}\left(pq - |q|c(|q|,e_0)\right), \end{aligned}$$

To solve the variational Hamilton-Jacobi equation, let us define

$$J(x,t) = \inf_{x\in X}\left\{ \int_0^t [\mathcal{L}(\dot{x})]\, ds \,\middle|\, x(0) = x, x(t) = 0 \right\}$$

the minimizer of the action associated to the Lagrangian. Thanks to the so-called Freidlin condition, see [58, 65] we deduce that the solution of (4.12) is

$$\overline{\varphi}(t,\xi) = \max\left(J(t,\xi), 0\right).$$

The Hopf-Lax formula gives $J(t,\xi) = t\mathcal{L}\left(t^{-1}\xi\right)$ thanks to the assumption on the initial condition. Hence,

$$\begin{aligned}
\xi \in \{\overline{\varphi}(t,\cdot) = 0\} \Longleftrightarrow \mathcal{L}\left(t^{-1}\xi\right) \leq 0 \quad &\Longleftrightarrow \quad \sup_{q\in\mathbb{R}} \left(q\xi - |q| c(|q|, e_0)t\right) \leq 0, \\
&\Longleftrightarrow \quad \forall q \in \mathbb{R}, \quad q\xi - |q| c(|q|, e_0)t \leq 0, \\
&\Longleftrightarrow \quad |\xi| \leq c^*(e_0)t.
\end{aligned}$$

We deduce the result for φ by changing the variables back. □

For a compactly supported initial data, the issue of the speed of propagation in general is more involved, since different directions may have different speeds of propagation. Namely, the following Freidlin-Gärtner formula holds :

Proposition 4.14. *Assume that*

$$\varphi_0(x) := \begin{cases} 0 & x = 0 \\ +\infty & else \end{cases}.$$

Define

$$w^*(e_0) = \min_{\substack{e\in\mathbb{S}^{n-1} \\ e_0\cdot e>0}} \left(\frac{c^*(e)}{e_0\cdot e}\right).$$

Then the nullset of φ propagates at speed $w^*(e_0)$ in the direction e_0 :

$$\forall t \geq 0, \qquad \{x \in \mathbb{R},\ \varphi(t, x\, e_0) = 0\} = \{x \in \mathbb{R},\ |x| \leq w^*(e_0)t\}.$$

Proof of Proposition 4.14. The Lagrangian is by definition

$$\begin{aligned}
\mathcal{L}(p) &= \sup_{q\in\mathbb{R}^n} \left(p\cdot q - (1+r)\mathcal{H}\left(\frac{q}{1+r}\right) - r \right), \\
&= \sup_{e\in\mathbb{S}^{n-1}} \sup_{\lambda\in\mathbb{R}^+} \left(\lambda p\cdot e - \left[(1+r)\mathcal{H}\left(\frac{\lambda e}{1+r}\right) + r \right] \right), \\
&= \sup_{e\in\mathbb{S}^{n-1}} \sup_{\lambda\in\mathbb{R}^+} \left(\lambda \left[p\cdot e - c(\lambda, e) \right] \right),
\end{aligned}$$

To solve the variational Hamilton-Jacobi equation, let us define

$$J(x,t) = \inf_{x\in X}\left\{ \int_0^t [\mathcal{L}(\dot{x})]\, ds \,\middle|\, x(0) = x, x(t) = 0 \right\}$$

the minimizer of the action associated to the Lagrangian. Thanks to the so-called Freidlin condition, see [58, 65] we deduce that the solution of (4.12) is

$$\varphi(x,t) = \max\left(J(x,t), 0\right).$$

The Lax formula gives

$$J(x,t) = \min_{y\in\mathbb{R}^n}\left\{t\mathcal{L}\left(\frac{x-y}{t}\right) + \varphi_0(y)\right\} = t\mathcal{L}\left(\frac{x}{t}\right)$$

thanks to the assumption on the initial condition. Hence,

$$\begin{aligned}
\varphi(t, xe_0) = 0 \Longleftrightarrow \mathcal{L}\left(\frac{x}{t}e_0\right) \leq 0 \quad &\Longleftrightarrow \quad \sup_{e\in\mathbb{S}^{n-1}}\sup_{\lambda\in\mathbb{R}^+}\left(\lambda\left[x(e_0\cdot e) - c_e(\lambda)t\right]\right) \leq 0,\\
&\Longleftrightarrow \quad \forall\lambda\in\mathbb{R}^+, \forall e\in\mathbb{S}^{n-1}, \quad \lambda\left[(x\cdot e_0)(e_0\cdot e) - c_e(\lambda)t\right] \leq 0,\\
&\Longleftrightarrow \quad \forall e\in\mathbb{S}^{n-1}, \quad x(e_0\cdot e) \leq c^*(e)t\\
&\Longleftrightarrow \quad |x| \leq \min_{\substack{e\in\mathbb{S}^{n-1}\\ e_0\cdot e>0}}\left(\frac{c^*(e)}{e_0\cdot e}\right)t = w^*(e_0)t.
\end{aligned}$$

□

4.3 Existence of travelling waves and spreading result

In this Section, we now explain how to construct travelling wave solutions to (4.1). We will follow closely the construction in [26]. As is classical in this type of Fisher-KPP problems, the speeds of propagation are given by studying the linearised problem at infinity. As we will see later on, the main difference that has motivated this paper is the possible singularity of $c(\lambda, e)$ at $\lambda^*(e)$.

4.3.1 Travelling wave solutions

Given a direction $e \in \mathbb{S}^{n-1}$, looking for exponential solutions to the linearised problem of the form $e^{-\lambda(x\cdot e - c(\lambda,e)t)}F_{\lambda,e}(v)$ for any positive λ is exactly looking for solutions to

$$\left[1 + \lambda(c(\lambda,e) - v\cdot e)\right]F_{\lambda,e}(v) = (1+r)M(v)\int_V F_{\lambda,e}(v')dv', \qquad v\in V.$$

In view of earlier computations, it boils down to setting $c(\lambda,e)$ as in (4.27) and $F_{\lambda,e} := \tilde{Q}_{\frac{\lambda e}{1+r}}$ as in (4.20).

Recall that $\frac{\lambda e}{1+r} \in \mathrm{Sing}(M)$ if and only if $l(e) \leq \frac{\lambda}{1+r}$, that is $\lambda \geq \tilde{\lambda}(e) := (1+r)l(e)$. Thus, for $\lambda \leq \tilde{\lambda}(e)$, the function $c(\lambda,e)$ is convex and regular, and the profile is explicitly given by

$$F_{\lambda,e}(v) = \frac{(1+r)M(v)}{1+\lambda(c(\lambda,e) - v\cdot e)} > 0.$$

For $\lambda \geq \tilde{\lambda}(e)$, that is to say $\frac{\lambda e}{1+r} \in \mathrm{Sing}(M)$ one has $c(\lambda,e) = \overline{v}(e) - \frac{1}{\lambda}$ which is concave and increasing. As such, the infimum of $\lambda \mapsto c(\lambda,e)$ is attained for a $\lambda \leq \tilde{\lambda}(e)$, which we

denote $\lambda^*(e)$. As a consequence, the minimal speed $c^*(e)$ is always associated to an integrable eigenvector, since if $\lambda^*(e) = \tilde{\lambda}(e)$, one has

$$F_{\tilde{\lambda}(e),e}(v) = \frac{(1+r)M(v)}{\tilde{\lambda}(e)\left(\bar{v}(e) - v\cdot e\right)},$$

with $\int_V F_{\tilde{\lambda}(e),e}(v)\,dv = 1$ thanks to the definition of $\tilde{\lambda}(e)$.

Given a direction $e \in \mathbb{S}^{n-1}$, we shall now discuss the type of functions $\lambda \mapsto c(\lambda, e)$ that may arise from this problem. Qualitatively, four situations may happen. The first possibility is the one already appearing in [26] in the mono-dimensional case, that is $\tilde{\lambda}(e) = +\infty$ and thus $\mathrm{Sing}(M) = \emptyset$. We plot an example of this case in Figure 4.1, case 1. If $\tilde{\lambda}(e) < +\infty$, three supplementary situations can occur. Either the infimum of $\lambda \mapsto c(\lambda, e)$ is attained for $\lambda < \tilde{\lambda}(e)$, a shown in Figure 4.1, case 2, either it is attained for $\lambda = \tilde{\lambda}(e)$. In the latter case, the infimum can either be attained at a point where the left derivative of $c(\lambda, e)$ is zero (Figure 4.1, case 3), or where it is negative (Figure 4.1, case 4).

Remark 4.15. *One can get a criterion to check which case holds. The dispersion relation defining $c(\lambda, e)$ on $(0, \tilde{\lambda}(e))$ is*

$$\int_V \frac{(1+r)M(v)}{1+\lambda(c(\lambda,e) - v\cdot e)}dv = 1$$

Differentiating with respect to λ, we find

$$\int_V \frac{\lambda c'(\lambda,e)M(v)}{\left[1+\lambda(c(\lambda,e)-v\cdot e)\right]^2}dv + \int_V \frac{(c(\lambda,e)-v\cdot e)M(v)}{\left[1+\lambda(c(\lambda,e)-v\cdot e)\right]^2}dv = 0$$

Recalling $\int_V \frac{M(v)}{1+\lambda(c(\lambda,e)-v\cdot e)}dv = (1+r)^{-1}$ and defining

$$J(\lambda,e) = \int_V \frac{M(v)}{\left[1+\lambda(c(\lambda,e)-v\cdot e)\right]^2}dv,$$

we get

$$c'(\lambda,e) = \left(1 - \frac{(1+r)^{-1}}{J(\lambda,e)}\right)\frac{1}{\lambda^2}.$$

As such, computing the value of $\lim_{\lambda\to\tilde{\lambda}(e)^-} J(\lambda)$ allows to know in which case one falls. Indeed, the function $\lambda \mapsto c(\lambda)$ attains its minimum at $\tilde{\lambda}(e)$ if and only if $c'\left(\tilde{\lambda}^-(e)\right) \le 0$, which is equivalent to $J(\tilde{\lambda}(e)) \le (1+r)^{-1}$ which is in turn equivalent to

$$\int_V \frac{M(v)}{\left(\bar{v}(e)-v\cdot e\right)^2}dv \le (1+r)l(e)^2, \tag{4.28}$$

which can be checked case by case. Note that one has always, given the Cauchy-Schwarz inequality, $l(e)^2 \le \int_V \frac{M(v)}{\left(\bar{v}(e)-v\cdot e\right)^2}dv$.

Example 4.16. *Let us look back at Example 4.8. As was stated, $l(1) = 3(2\ln(2)-1)$ and $\int_V \frac{M(v)}{(1-v)^2}dv = 6(1-\ln(2)) < +\infty$. Thus, for $r > -1 + l(1)^{-2}\int \frac{M(v)}{(1-v)^2}dv > 0$, the condition (4.28) is satisfied so the minimum of $\lambda \mapsto c(\lambda, e)$ is attained at $\tilde{\lambda}(e)$. For $r = -1 + l(1)^{-2}\int_V \frac{M(v)}{(1-v)^2}dv$ the minimum has its left derivative equal to 0* (i.e. $\lambda^*(1) = \tilde{\lambda}(1)$)*. We illustrate those results in Figure 4.1, case 3 and 4.*

FIGURE 4.1 – **Various cases of speed functions** $\lambda \mapsto c(\lambda, e)$

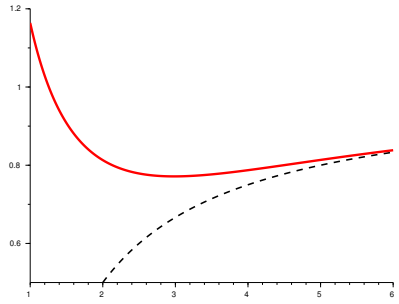

(a) Case 1

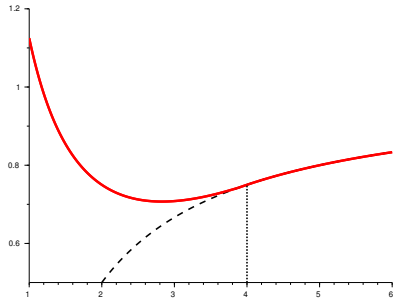

(b) Case 2

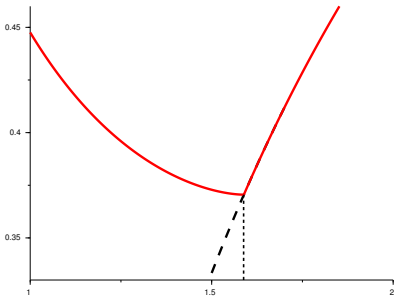

(c) Case 3

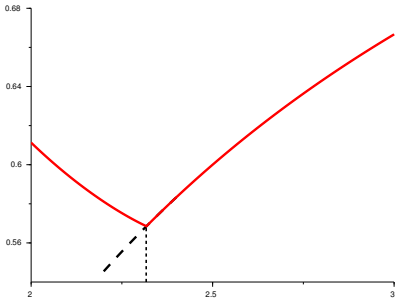

(d) Case 4

Red plain line : $\lambda \mapsto c(\lambda, e)$. *Black dotted line :* $\lambda \mapsto \bar{v}(e) - \frac{1}{\lambda}$.
(a) $n = 1$, $V = [-1, 1]$, $e = 1$, $M \equiv \frac{1}{2}$ *and* $r = 1$. *In this case,* $\mathrm{Sing}(M) = \emptyset$ *so that the function* $\lambda \mapsto c(\lambda, 1)$ *is regular. This is the case discussed in [26].*
(b) $n = 2$, $V = D(0, 1)$, $M \equiv \frac{1}{\pi}$ *and* $r = 1$. *In this case,* $\mathrm{Sing}(M) \neq \emptyset$ *but the minimum of* $c(\lambda, e_1)$ *is attained for* $\lambda < \tilde{\lambda}(e_1) = 4$.
(c) $n = 1$, $V = [-1, 1]$, $M(v) = \frac{3}{2}(1 - |v|)^2$ *and* $r = -1 + l(1)^{-2} \int_{-1}^{1} \frac{M(v)}{(1-v)^2} dv \approx 0.37$. *In this case, the minimum of* $c(\lambda, e_1)$ *is attained for* $\lambda = \tilde{\lambda}(e_1)$, *with a zero left derivative. Numerically* $\tilde{\lambda}(1) \approx 1.58$.
(d) $n = 1$, $V = [-1, 1]$, $M(v) = \frac{3}{2}(1 - |v|)^2$ *and* $r = 1$. *In this case, the minimum of* $c(\lambda, 1)$ *is attained for* $\lambda = \tilde{\lambda}(1)$, *with a negative left derivative. Numerically,* $\tilde{\lambda}(1) \approx 2.31$.

Since $c(\lambda, e)$ tends to infinity when λ tends to 0, for any $c \geq c^*(e)$ one can find $\lambda \in (0, \tilde{\lambda}(e)]$ such that $c(\lambda, e) = c$.

Fix $c \in (c^*(e), \overline{v}(e))$. Denote λ_c is the smallest solution in $(0, \tilde{\lambda}(e))$ of $c(\lambda_c, e) = c$. Notice that by construction it is possible to obtain $F_{\lambda_c, e}$ integrable and bounded (bounded since $c > c^*(e)$), the proof of [26], Section 3.2, that constructs sub and super solutions for (4.1) is unchanged. From the construction of a pair of sub- and super-solutions, we deduce the existence of travelling wave solutions exactly as in [26], by a monotonicity method when $c > c^*(e)$ and passing to the limit $c \to c^*(e)$ to get the case $c = c^*(e)$.

The main difference between the mono-dimensional case of [26] and the higher dimensional case comes here. It is rather non-standard and interesting that the function giving the speed of propagation could be singular at its minimum value.

To prove that c^* is still the minimal speed of propagation, the classical arguments involving the Rouché theorem (check [26], Lemma 3.10 for example) around λ^* are not applicable. We thus choose to use the Hamilton-Jacobi framework combined to the comparaison principle.

We now prove the following lemma.

Lemma 4.17. *Let f be a travelling wave solution to* (4.1) *in the direction $e \in \mathbb{S}^{n-1}$, with speed c. Then $c \geq c^*(e)$.*

Proof of Lemma 4.17. Let f be such a travelling wave solution. The solution of the Cauchy problem with initial data $\tilde{f}(x, v)$ is $f(x \cdot e - ct, v)$. After Proposition 4.12, we deduce that $f^\varepsilon(t, x, v) = f\left(\frac{1}{\varepsilon}(x \cdot e - ct), v\right)$ satisfies $\lim_{\varepsilon \to 0} f^\varepsilon = M$ on $x \cdot e - ct < 0$ and $\lim_{\varepsilon \to 0} f^\varepsilon = 0$ on $x \cdot e - ct > 0$. Take $0 < \gamma < 1$ and define $g(x, v) = \gamma M(v) \mathbf{1}_{[-1,1] \times \mathbb{R}^{n-1}}(x)$ and $g^\varepsilon(x, v) = g(x/\varepsilon, v)$. We have

$$\psi^\varepsilon(x) = -\varepsilon \ln(g(x/\varepsilon, v)/M) = \begin{cases} -\varepsilon \ln(\gamma) & x \in [-\varepsilon, \varepsilon] e_0 + e_0^\perp \\ +\infty & \text{else} \end{cases}.$$

Since $\lim_{z \to -\infty} \tilde{f}(z, v) = M$ uniformly in $v \in V$, one can shift the profile sufficiently enough so that $M \geq f \geq g \geq 0$. Thus, the comparison principle (see [26], Proposition 2.2 for a proof) yields that $f^\varepsilon \geq g^\varepsilon$. Passing to the limit $\varepsilon \to 0$, and recalling Theorem 4.2, Proposition 4.12 and Proposition 4.13, we deduce that

$$\left(e_0^\perp + c^*(e_0) t e_0\right) \cdot e_0 - ct \leq 0,$$

from which the result follows. □

From the Hamilton-Jacobi formalism, we may also deduce the following.

Proof of Proposition 4.5. We start by proving (4.16). For this, we use the the super-solution naturally provided by the linearised problem. We have

$$f(t, x, v) \leq \min\{M(v), e^{-\lambda^*(e_0)(x \cdot e_0 - c^*(e_0)t)} F_{\lambda^*(e_0), e_0}(v)\}$$

As a consequence,

$$\rho(t, x) \leq \min\{1, e^{-\lambda^*(e_0)(x \cdot e_0 - c^*(e_0)t)}\},$$

and thus one has $\lim_{t \to +\infty} \sup_{x \cdot e_0 > ct} \rho(t, x) = 0$.

For (4.17), we use the Hamilton-Jacobi results in the following way. We first notice that since the initial data is invariant under any translation in $e_0^\perp$, and the the equation (4.12) invariant by translation, the solution $f(t,x,v)$ depends only on $x \cdot e_0$. That is $f(t,x,v) = f(t,(x\cdot e_0)e_0,v) = \tilde{f}(t,x\cdot e_0,v)$. For any $c < c^*(e_0)$, recalling Theorem 4.2, Proposition4.12 and Proposition 4.13, we have

$$\lim_{t\to\infty} f(t,e_0^\perp + cte_0,v) = \lim_{t\to\infty} \tilde{f}(t,ct,v) = \lim_{\varepsilon\to 0} \tilde{f}^\varepsilon(1,c,v) = M(v),$$

since $c < c^*(e_0)$. □

4.3.2 Proof of Proposition 4.6 : spreading of a compactly supported initial data

We finally prove Proposition 4.6. The spreading result (4.18) goes as for the Fisher-KPP equation in an heterogeneous media. It can be found by using the super solution

$$\overline{f}(t,x,v) = \inf_{e\in\mathbb{S}^{n-1}} e^{-\lambda^*(e)(x\cdot e - c^*(e)t)} Q_{\lambda^*(e)e}(v)$$

By the comparison principle, and since the initial data is compactly supported, the function $\overline{f}$ lies above f (multiplying $\overline{f}$ by a big constant if necessary). We deduce that for any given $e_0 \in \mathbb{S}^{n-1}$, and any fixed $x \in \mathbb{R}^n$,

$$f(t,x+ce_0t,v) \le \inf_{e\in\mathbb{S}^{n-1}} e^{-\lambda^*(e)((x+ce_0t)\cdot e - c^*(e)t)} Q_{\lambda^*(e)e}(v) = \inf_{e\in\mathbb{S}^{n-1}} e^{-\lambda^*(e)(x\cdot e + ce_0\cdot et - c^*(e)t)} Q_{\lambda^*(e)e}(v).$$

Moreover, the domain of $Q_{\lambda^*(e)e}$ contains $V\setminus\{v_{max}e\}$ and $Q_{\lambda^*(e)e}$ is bounded on all compact sets of $V\setminus\{v_{max}e\}$. Hence, for fixed $v \in V$, we can choose $e \in \mathbb{S}^{n-1}$ such that $v \in V\setminus\{v_{max}e\}$. Then, as soon as $c > w^*(e_0)$, we have $c(e\cdot e_0) > c^*(e)$ for any e, and thus $\lim_{t\to\infty} f(t,x+ce_0t,v) = 0$.

Moreover, we shall prove (4.19) as follows. For any $c < c^*(e_0)$, recalling Theorem 4.2, Proposition 4.12 and Proposition 4.14, we have

$$\lim_{t\to\infty} f(t,cte_0,v) = \lim_{t\to\infty} \tilde{f}(t,ct,v) = \lim_{\varepsilon\to 0} \tilde{f}^\varepsilon(1,ce_0,v) = M(v),$$

since $c < w^*(e_0)$.

□

Acknowledgement

The authors thank warmly Vincent Calvez for early discussions about this problem, and for a careful reading of the manuscript. This work has benefited of an invaluable insight from Guy Barles, which, while originally meant for another manuscript, found a direct application in the present one. The authors are more that deeply grateful to Guy Barles for this. Emeric Bouin acknowledges the green hospitality of the University of Cambridge during the second semester of the academic year 2015-2016. Emeric Bouin and Nils Caillerie acknowledge the support of the ERC Grant MATKIT (ERC-2011-StG). Nils Caillerie thanks the University of Cambridge for its hospitality during his three week stay over Spring 2016. In addition, Nils Caillerie has received funding from the European Research Council (ERC) under the European Unions Horizon 2020 research and innovation programme (grant agreement No 639638).

Troisième partie

Approximation-diffusion dans les équations cinétiques avec termes aléatoires

Chapitre 5

Approximation-diffusion d'une équation cinétique aléatoire

Dans ce travail en collaboration avec Julien Vovelle, nous étudions une équation cinétique avec un terme source aléatoire après un réechlonnemet parabolique. Nous étudions la limite de cette équation lorsque le facteur du réechelonnement tend vers zéro. Nous utilisons une adaptation de la méthode de la fonction test perturbée pour établir la convergence vers la solution d'une équation de diffusion stochastique.

Contents

5.1 Introduction

Kinetic models with small parameters appear in many situations and it is challenging to understand the limiting equations since they are much easier to simulate numerically. For deterministic equations, such problems have been widely studied. In the following paper, we consider the following kinetic random equation :

$$\partial_t f^\varepsilon + \frac{v}{\varepsilon} \cdot \nabla_x f^\varepsilon = \frac{\lambda}{\varepsilon^2} \left(M\rho^\varepsilon - f^\varepsilon \right) + \frac{1}{\varepsilon^2} \rho^\varepsilon v \cdot \nabla_x \overline{m}_t^\varepsilon, \quad (t, x, v) \in \mathbb{R}_+ \times \mathbb{T}^d \times V, \tag{5.1}$$

with initial condition

$$f^\varepsilon(0) = f_0^\varepsilon \in L^2(\mathbb{T}^d \times \mathbb{T}^d), \tag{5.2}$$

where, $\lambda, \varepsilon > 0$ and $V \subset \mathbb{T}^d$. We assume furthermore that

$$\sup_{\varepsilon > 0} \| f_0^\varepsilon \|_{L^2(\mathbb{T}^d \times \mathbb{T}^d)} < +\infty. \tag{5.3}$$

Here, $\mathbb{T}^d$ is the d-dimensional torus. The function M is a probability density function and the density ρ^ε is defined by :

$$\rho^\varepsilon(t, x) := \int_V f^\varepsilon(t, x, v) dv. \tag{5.4}$$

$\overline{m}^\varepsilon$ is a defined by

$$\overline{m}^\varepsilon_t(x) := \overline{m}_{t/\varepsilon^2}(x), \tag{5.5}$$

where $\overline{m}$ is a stationary Markov process.

Equation (5.1) is obtained from the rescaling $f^\varepsilon(t,x,v) = f(\varepsilon^2 t, x, v)$, where f is solution to

$$\partial_t f + \varepsilon v \cdot \nabla_x f = \lambda\left(M\rho - f\right) + \rho v \cdot \nabla_x \overline{m}_t, \quad (t,x,v) \in \mathbb{R}_+ \times \mathbb{T}^d \times V. \tag{5.6}$$

Our aim is to study the behavior in the limit $\varepsilon \to 0$. We will give details about our supplementary assumptions and state our main result in the next section.

In the deterministic case ($\overline{m}^\varepsilon \equiv 0$), the sequence $(\rho^\varepsilon)_\varepsilon$ converges in $L^2_{t,x}$ to ρ the solution of the diffusion equation

$$\partial_t \rho - \operatorname{div}\left(K \nabla_x \rho\right) = 0,$$

with initial condition $\rho(0) = \rho_0$, where $K = \int_V v \otimes v M(v) dv$. One can check [53] for a proof of this result.

We should also mention that such an issue has been dealt with in the case of ordinary differential equations with random terms. In that case, a stochastic differential equation with white noise is obtained at the limit [56, 64, 75, 76, 79].

The study of stochastic partial differential equations is more recent. Diffusion limits have been found for stochastic PDEs modeling radiative transfer equation perturbed by small random processes [49, 50]. The case of a kinetic equation with a random source term was already studied in [51]. Using the so-called perturbed test function method, the authors have established a converging result to a stochastic diffusion equation. Their equation is very similar to ours but the source term is of order ε^{-1}, contrary to us. This makes our work a little more complicated since the limit equation is harder to identify. Moreover, in the scaling we consider, the stochastic terms have an effect on the diffusion term of the limit equation. However, our method will be very similar to theirs and we will often refer to their paper when our proofs are not significantly different from theirs. Following their lead, we will organize our paper as follows.

The Section 5.2 is devoted to the statement of our main result. For this, we will need to specify some notations that will be used throughout this paper and state the assumptions that we need to prove our result. In Section 5.3, we will look for invariant solution and a generator of our equation, that will be very useful to find the limit equation. In Section 5.4, we will detail the first step of our perturbed test function method. In this step, we will identify the limit generator of our equation by formal considerations. In Section 5.5, we will identify the diffusion stochastic equation associated with this limit generator. We prove that this equation is indeed the limit we look for equation (5.1) in Section 5.6. For this, we first establish *a priori* estimate in L^2 for $(\rho^\varepsilon)_\varepsilon$, then we use the perturbed function method to prove a tightness result for $(\rho^\varepsilon)_\varepsilon$ and to identify the accumulation points for convergence in law of $(\rho^\varepsilon)_\varepsilon$ as solution of the diffusion equation. By uniqueness of the solution, we will prove that the complete sequence $(\rho^\varepsilon)_\varepsilon$ converges in law.

5.2 Preliminaries and main result

5.2.1 Notations

We give here a list of notation and assumptions that we will use throughout this paper. We will consider all our assumptions to be true from now on. First of all, we assume that

$$\int_V v dv = 0. \tag{5.7}$$

We suppose that M satisfies :

$$\int_V M(v)dv = 1, \quad \int_V vM(v)dv = 0. \tag{5.8}$$

For readability reasons, we introduce the following operators :

$$\begin{aligned} Tf &:= v \cdot \nabla_x f, \\ Lf &:= \lambda\left(M\rho - f\right), \\ R\left(f,m\right) &:= Lf + \rho Tm, \\ \widehat{f} &:= \int_V f(v)dv, \\ J(f) &:= \int vf(v)dv \\ K(f) &:= \int_V v \otimes vf(v)dv. \end{aligned}$$

We denote $K := K(\mathbb{1}_V)$ and we assume furthermore that

$$K = \int_V v \otimes v dv > 0, \tag{5.9}$$

and that

$$K(v) = \int_V v \otimes v \cdot v dv = 0. \tag{5.10}$$

For two matrices $\mathrm{A} = (a_{ij})_{ij}, \mathrm{B} = (b_{ij})_{ij} \in M_d(\mathbb{R})$ we will denote $\mathrm{A} : \mathrm{B}$ the canonical scalar product : $(\mathrm{A} : \mathrm{B})_{ij} = a_{ij} \times b_{ij}$.

Throughout this paper, we will prove results in some functional spaces. The domain of an operator F will be denoted $\mathcal{D}(F)$. For a Banach space $\mathcal{X}$ we will denote by $\mathcal{X}^*$ its dual space. For simplicity, we will denote $L^2_{x,v}$ the space $L^2(\mathbb{T}^d \times V, dx \otimes dv)$ and, in the same spirit, we will use L^2_x instead of $L^2(\mathbb{T}^d, dx)$ and L^2_v instead of $L^2(V, dv)$. From now on, the variable f will only be used for functions in subsets of $L^2_{x,v}$ and ρ for functions in subsets of L^2_x. Hence, when there is no ambiguity, we will denote L^2 instead of $L^2_{x,v}$, L^2_x and L^2_v indistinctly.

We denote by $(\cdot,\cdot)$ all inner scalar products of the L^2 spaces described earlier and by $\|\cdot\|_{L^2}$ their norm. For $\gamma \in \mathbb{N}$, we denote by $H^\gamma(\mathbb{T}^d)$ the Sobolev space of functions $\rho \in L^2(\mathbb{T}^d)$ whose derivative up to order γ exists and belongs to $L^2(\mathbb{T}^d)$. For a general $\gamma \geq 0$, one can find generalization in [1]. For $\gamma > 0$ we will denote $H^{-\gamma}(\mathbb{T}^d) := (H^\gamma(\mathbb{T}^d))^*$ the dual of $H^\gamma(\mathbb{T}^d)$. We emphasize that, for $\gamma_1 > \gamma_2$ the injection of $H^{\gamma_1}(\mathbb{T}^d)$ in $H^{\gamma_2}(\mathbb{T}^d)$ is compact.

5.2.2 The driving random term

Let $(\Omega, \mathcal{F}, \mathbb{P})$ be a probability space. The random process $(\overline{m}_t)_t$ is a stationary Markov process taking values in $E \subset C^1$, where E is a fixed ball of $\left(C^1, \|\cdot\|\right)$, *i.e.* there exists $C^* > 0$ such that for all $t \in \mathbb{R}$,

$$\|m_t\| := \sup_{x \in \mathbb{T}^d} |m_t| + |\nabla_x m_t| \leq C^*. \tag{5.11}$$

We denote by ν the stationary law of $(\overline{m}_t)_t$. For all $t \in \mathbb{R}$, we set $\mathcal{F}_t := \sigma(\overline{m}_t)$ the sigma-field generated by $\overline{m}_t$. Naturally, $(\mathcal{F}_t)_t$ is a filtration and $(\overline{m}_t)_t$ is adapted to $(\mathcal{F}_t)_t$ and $(\overline{m}^\varepsilon_t)_t$ is adapted to $(\mathcal{F}^\varepsilon_t)_t := (\mathcal{F}_{\varepsilon^{-}2t})_t$.

We suppose that $\overline{m}$ is centered :

$$\mathbb{E}\overline{m}_t = \int_E n d\nu(n) = 0, \forall t \in \mathbb{R}. \tag{5.12}$$

We denote by $(P_s)_s$ the semi-group and by A the infinitesimal generator of $\overline{m}_t$:

$$A\varphi(n) := \lim_{t \to 0} \frac{1}{t}(\mathbb{E}_n \varphi(\overline{m}_t) - \varphi(n)), \quad \varphi \in \mathcal{D}(A),$$

where $\mathbb{E}_n$ is the expectation with respect to $\mathbb{P}(\cdot \mid \overline{m}_0 = n)$. For all $n \in E$ and $t_0 \in \mathbb{R}$, we denote by $m_{t_0,t}(n)$ the Markov process with generator A, such that $m_{t_0,t_0}(n) = n$. We will assume that m has some ergodic mixing properties, namely, there exists a random process $(\eta_t)_t$ such that : for all n, $\mathbb{P}$-almost-surely,

$$\lim_{t_0 \to -\infty} m_{t_0,t}(n) = \eta_t \quad \text{in } W^{1,\infty}(\mathbb{T}^d), \tag{5.13}$$

and

$$\text{Law}(\eta_t) = \nu, \quad \forall t \in \mathbb{R}. \tag{5.14}$$

For simplicity, we denote $m_t(n) := m_{0,t}(n)$. We set

$$\tilde{\eta}_t := \int_{-\infty}^t e^{\lambda s} \eta_s ds, \tag{5.15}$$

and we suppose that there exists $\theta > 0$ such that $\mathbb{P}$-almost-surely,

$$1 - \frac{1}{2} \cdot \frac{v \cdot \nabla_x(\eta_t - \lambda\tilde{\eta}_t)}{\lambda(M + v \cdot \nabla_x \tilde{\eta}_t)} \geq \theta, \quad \forall (t, x, v) \in \mathbb{R} \times \mathbb{T}^d \times V. \tag{5.16}$$

Finally, since η is a bounded stationary process, we have

$$\mathbb{E}\,\|\eta_t\|_{L^2} = \mathbb{E}\,\|\eta_0\|_{L^2} < +\infty. \tag{5.17}$$

5.2.3 Main result

Our main result reads

Theorem 5.1. *Let $(f^\varepsilon)_\varepsilon$ be a mild solution of (5.1)-(5.2). Assume that, f_0^ε satisfies (5.3), that V and M satisfy (5.7),(5.8), (5.9) and (5.10) and that $(\overline{m}_t)_t$, $(\eta_t)_t$ and $(\tilde{\eta}_t)_t$ satisfy (5.11), (5.12) (5.13) and (5.16). We define furthermore*

$$\chi(n) := K \cdot \nabla_x \int_0^\infty P_s \mathrm{Id}(n) ds, \quad \forall n \in E,$$

$$R(n) := \int_0^\infty \frac{1}{\lambda} P_s \mathrm{Id}(n) ds, \quad \forall n \in E,$$

$$\mathcal{K}(x,y) := \mathbb{E}[(\tilde{\eta}_0 + R(\eta_0)(x))\tilde{\eta}_0(y)],$$

$$\eta_0' := \int_0^{+\infty} \left(1 - e^{-\lambda\sigma}\right) P_\sigma \mathrm{Id}(\eta_0) d\sigma$$

and

$$\Sigma\theta(x) := \int_{\mathbb{T}^d} \mathcal{K}(x,y)\theta(y) dy, \quad \forall \theta \in L^2_x.$$

Then, Σ is self-adjoint positive and trace-class.

If we assume furthermore that

$$\rho_0^\varepsilon := \int_V f_0^\varepsilon(v) dv \to \rho_0 \in L^2_v, \tag{5.18}$$

and that

$$\lambda K(M) - \mathbb{E} K \nabla_x \eta_0' \cdot K \nabla_x \eta_0 > 0, \tag{5.19}$$

then, for all $\delta > 0$, the density ρ^ε converges in law on $C([0,\tau]; H^{-\delta}(\mathbb{T}^d))$ to the solution ρ of the stochastic diffusion equation :

$$\begin{aligned} d\rho &= \frac{1}{\lambda^2} \mathrm{div}\left(\left(\lambda K(M) - \mathbb{E} K \nabla_x \eta_0' \cdot K \nabla_x \eta_0\right) \nabla_x \rho\right) dt \\ &- \frac{1}{\lambda^2} \mathrm{div}\left(\rho \cdot \mathbb{E} K \nabla_x \eta_0' \mathrm{div}\left(K \nabla_x \eta_0\right)\right) dt \\ &+ P(\rho) \Sigma^{1/2} \circ dW_t, \quad \text{in } \mathbb{R}_+ \times \mathbb{T}^d, \end{aligned}$$

with initial condition

$$\rho(0,x) = \rho_0(x), \quad \text{in } \times \mathbb{T}^d,$$

where W is a cylindrical Wiener process on L^2_x and $P(\rho)$ is the linear operator in $H^1(\mathbb{T}^d)$ defined by

$$P(\rho)\, p = \sqrt{\frac{2}{\lambda}} \mathrm{div}_x \left[\rho K \nabla_x p\right], \quad \forall p \in H^1(\mathbb{T}^d). \tag{5.20}$$

We prove the properties of Σ in Section 5.5 and the convergence result in Section 5.6.

5.3 Semi-group and generator

5.3.1 Invariant solution

In order to pass to the limit $\varepsilon \to 0$ in (5.1) and considering only the term ε of highest order, we look for invariant solutions of

$$\begin{cases} \frac{d}{dt} g_t = \lambda L g_t + \widehat{g_t} v \cdot \nabla_x m_{t_0,t}(n) \\ g_{t_0} = f_0, \end{cases} \tag{5.21}$$

First, we notice that, since $\widehat{Lg_t} = 0$ and (5.7) hold, we have $\frac{d}{dt}\widehat{g_t} = 0$ hence $\widehat{g_t} = \widehat{f_0}$. Thus,

$$\partial_t g_t + \lambda g_t = \lambda M \widehat{f_0} + \widehat{f_0} v \cdot \nabla_x m_{t_0,t}.$$

This gives

$$\begin{aligned} g_t &= e^{-\lambda(t-t_0)} f_0 + \int_{t_0}^t e^{-\lambda(t-s)} \left(\lambda M \widehat{f_0} + \widehat{f_0} v \cdot \nabla_x m_{t_0,s} \right) ds \\ &= e^{-\lambda(t-t_0)} f_0 + M \widehat{f_0} \left(1 - e^{-\lambda(t-t_0)} \right) + \widehat{f_0} T \int_{t_0}^t m_{t_0,s} e^{-\lambda(t-s)} ds. \end{aligned}$$

Taking the limit $t_0 \to -\infty$, one gets $g_t \to \overline{g}_t$, where

$$\begin{cases} \overline{g}_t := \widehat{f_0}(M + T\tilde{\eta}_t), \\ \tilde{\eta}_t := \int_{-\infty}^t e^{-\lambda(t-s)} \eta_s ds. \end{cases} \tag{5.22}$$

We define the following stationary solution :

$$\overline{M}_t := M + T\tilde{\eta}_t. \tag{5.23}$$

The random process $\overline{M}^\varepsilon_t := \overline{M}_{t/\varepsilon^2}$ will be our reference solution. Note that $\widehat{\overline{M}_t} = \widehat{M} = 1$.

5.3.2 Generator

The process f^ε is not Markov but $(f^\varepsilon, \overline{m}^\varepsilon)$ is. Its generator is

$$\mathscr{L}^\varepsilon \varphi = \frac{1}{\varepsilon} \mathscr{L}_{T*} \varphi + \frac{1}{\varepsilon^2} \mathscr{L}_{R*} \varphi, \tag{5.24}$$

where

$$\begin{aligned} \mathscr{L}_{T*} \varphi(f,n) &= -\left(Tf, D\varphi(f,n) \right), \\ \mathscr{L}_{R*} \varphi(f,n) &= \left(R(f,n), D\varphi(f,n) \right) + A\varphi(f,n). \end{aligned}$$

These are differential operators with respect to the variable $f \in L^2_{x,v}$ and $n \in E$. The operator D denotes differentiation with respect to f. For a C^2 function on $L^2_{x,v}$, we use the second differential operator $D^2\varphi$ with respect to f, which is a bilinear form on $L^2_{x,v}$ that we identify with a bilinear operator with the formula

$$D^2\varphi(f)(h,k) = (D^2\varphi(f)h,k).$$

We define a set of test functions associated to the martingale problem associated to the generator $\mathscr{L}^\varepsilon$.

Definition 5.2. *Let $\varphi \in L^2(V;H^1(\mathbb{T}^d)) \times E \to \mathbb{R}$. We denote by f the first variable of φ and by n the second. We say that φ is a good test function if*

- *φ is differentiable with respect to f*
- *$(f,n) \mapsto D\varphi(f,n)$ is continuous from $L^2(V;H^1(\mathbb{T}^d)) \times E$ to $L^2_{x,v}$ and maps bounded sets onto bounded sets*
- *$(f,n) \mapsto A\varphi(f,n)$ is continuous from $L^2(V;H^1(\mathbb{T}^d)) \times E$ to $\mathbb{R}$ and maps bounded sets onto bounded sets*
- *for any $f \in L^2(V;H^1(\mathbb{T}^d))$, $\varphi(f,\cdot) \in \mathcal{D}(A)$.*

Proposition 5.3. *Let φ be a good test function. Let $f_0^\varepsilon \in L^2(V;H^1(\mathbb{T}^d))$ and let f^ε be a solution to (5.1)-(5.2). Then,*

$$\mathcal{M}^\varepsilon_\varphi(t) := \varphi(f^\varepsilon(t),\overline{m}^\varepsilon(t)) - \int_0^t \mathscr{L}^\varepsilon\varphi(f^\varepsilon(s),\overline{m}^\varepsilon(s))ds$$

is a continuous and integrable $(\mathcal{F}^\varepsilon_t)$-martingale with quadratic variation

$$\langle \mathcal{M}^\varepsilon_\varphi, \mathcal{M}^\varepsilon_\varphi\rangle(t) = \int_0^t \left(\mathscr{L}^\varepsilon|\varphi|^2 - 2\varphi\mathscr{L}^\varepsilon\varphi\right)(f^\varepsilon(s),\overline{m}^\varepsilon(s))ds. \tag{5.25}$$

We refer to [51] for a proof of this result.

5.4 The perturbed test-function method

To prove the convergence of $(\rho^\varepsilon)_\varepsilon$, we use the so-called "method of the perturbed test function method" [90]. The idea is that we know how the generator $\mathscr{L}^\varepsilon$ acts on test functions φ. To identify the limit generator, we construct a corrector φ^ε to φ (we "perturb" the test function) so that $\mathscr{L}^\varepsilon\varphi^\varepsilon$ is controlled. This will exhibit necessary conditions that $\mathscr{L}$ needs to satisfy. We can use Itô's representation formula to write this condition in terms of a stochastic PDE (this will be done in Section 5.5). We then show the tightness of the measures sequence associated with $(\rho^\varepsilon)_\varepsilon$. This allow us to extract a converging (in law) subsequence. We then prove that the limit is solution of the martingale problem associated to this stochastic PDE. This will be done in Section 5.6. In the present section, we identify the limit generator.

We will restrict ourselves to a certain class of test functions. Namely, we will consider maps φ from $L^2(\mathbb{R}^d)$. As such, we may see φ as a function from $\mathbb{T}^d \times E$ to $\mathbb{R}$ defined by

$$(f,n) \mapsto \varphi\left(\widehat{f}\right). \tag{5.26}$$

We will require (5.26) to define a good test function in the sense of Definition 5.2. Moreover, we will need a regularity result on $D^2\varphi$. Namely,

Definition 5.4. *We say that $\varphi \in C^2(L^2_x)$ is regularizing and subquadratic if there exists a constant $C_\varphi \geq 0$ such that*

$$\begin{cases} |\varphi(\rho)| \leq C_\varphi(1+\|\rho\|_{L^2})^2, \\ \|\mathrm{div} J\left(D\varphi(\rho)\right)\|_{L^2} \leq C_\varphi(1+\|\rho\|_{L^2}), \\ \left|D^2\varphi(f)\cdot(\mathrm{div} J(h),k)\right| \leq C_\varphi \|h\|_{L^2}\|k\|_{L^2}, \\ \|\mathrm{div}\left(D\varphi(\rho)\chi(n)\right)\|_{L^2} \leq C_\varphi(1+\|\rho\|_{L^2}\|n\|_{L^2}), \end{cases} \tag{5.27}$$

for all $\rho, h, k, n \in L^2$.

5.4.1 Main generator

The generator $\mathscr{L}_{R*}$ is the generator of a semi-group (P_t), given by

$$P_{t-t_0}\varphi(f,n) = \mathbb{E}\varphi(g_t, m_t(n)), \tag{5.28}$$

where

$$\begin{cases} \frac{d}{dt}g_t = \lambda L g_t + \widehat{g_t} v\cdot\nabla_x m_{t_0,t}(n) \\ g_{t_0} = f, \end{cases} \tag{5.29}$$

We recall that $m_t(n)$ is a Markov process of generator A such that $m_{t_0,t_0}(n) = n$. We already solved this equation in Section 5.3.1 :

$$g_t = e^{-\lambda(t-t_0)}f + M\widehat{f}\left(1-e^{-\lambda(t-t_0)}\right) + \widehat{f}T\int_{t_0}^t m_s(n)\, e^{-\lambda(t-s)}ds.$$

Consequently,

$$P_{t-t_0}\varphi(f,n) = Q_t\psi_f(0,n),$$

where

$$\psi_f(r,n) := \varphi\left(e^{-\lambda(t-t_0)}f + (1-e^{-\lambda(t-t_0)})\widehat{f}M + \widehat{f}Tr, n\right),$$

and

$$Q_t\psi(r,n) = \mathbb{E}\psi(r_t(r,n), m_t(n)),$$

with

$$r_t(r,n) := e^{-\lambda(t-t_0)}r + \int_{t_0}^t m_{t_0,s}(n)e^{-\lambda(t-s)}ds,$$

i.e.

$$\begin{cases} \partial_t r_t + \lambda r_t = m_{t_0,t}, \\ r_{t_0} = r. \end{cases}$$

Thanks to (5.13), we deduce that, $\mathbb{P}$-almost-surely,

$$r_t(r,n) \underset{t_0\to-\infty}{\longrightarrow} \tilde{\eta}_t,$$

and $Q_t\psi(r,n) \to \mathbb{E}\psi(\tilde{\eta}_t, \eta_t)$. Consequently,

$$P_{t-t_0}\varphi(f,n) \to \mathbb{E}\varphi\left(\widehat{fM}_t, \eta_t\right) =: \int \varphi(f,n) d\mu_{\widehat{f}}(f,n). \tag{5.30}$$

Since the law of $(\tilde{\eta}_t, \eta_t)$ does not depend on t, neither does $\mu_{\widehat{f}}$.

5.4.2 Perturbed test function

To find a candidate for the limit operator $\mathscr{L} = \lim_{\varepsilon\to 0} \mathscr{L}^\varepsilon$, we use the so-called perturbed test function method. Let $\varphi \in C^2(L^2_{x,v})$ be a test function and let $\varphi^\varepsilon = \varphi + \varepsilon\varphi_1 + \varepsilon^2\varphi_2$. We want to find $\mathscr{L}$, φ_1 and φ_2 such that

$$\mathscr{L}^\varepsilon\varphi^\varepsilon = \mathscr{L}\varphi + o(1). \tag{5.31}$$

By identification of the powers of ε, the Equation (5.31) gives

$$\begin{aligned} \mathscr{L}_{R*}\varphi &= 0, & (5.32)\\ \mathscr{L}_{R*}\varphi_1 + \mathscr{L}_{T*}\varphi &= 0, & (5.33)\\ \mathscr{L}_{R*}\varphi_2 + \mathscr{L}_{T*}\varphi_1 &= \mathscr{L}\varphi. & (5.34) \end{aligned}$$

Order ε^{-2}

Suppose that (5.32) holds. By construction, $\frac{d}{dt}\mathbb{E}\left[\varphi\left(g_t\left(f,n\right), m_{t_0,t}\left(n\right)\right)\right] = 0$ hence

$$\varphi(f,n) = \langle \varphi, \mu_{\widehat{f}} \rangle, \tag{5.35}$$

hence φ is a function of $\rho = \widehat{f}$ only, as expected at the limit.

Order ε^{-1}

Assume

$$\mathscr{L}_{R*}\varphi_1 + \mathscr{L}_{T*}\varphi = 0. \tag{5.36}$$

We look for solutions of (5.36) given by

$$\begin{aligned} \varphi_1\left(f,n\right) &= \int_0^\infty P_t \mathscr{L}_{T*}\varphi\left(f,n\right) dt\\ &= \int_0^\infty \mathbb{E}\left[\left(-\widehat{Tg_t\left(f,n\right)}, D\varphi\left(\widehat{g_t\left(f,n\right)}\right)\right)\right] dt\\ &= \int_0^\infty \mathbb{E}\left[\left(-\mathrm{div}_x J(g_t(f,n)), D\varphi\left(\widehat{f}\right)\right)\right] dt. \end{aligned}$$

Using (5.29), we have

$$J(g_t(f,n)) = e^{-\lambda t}J(f) + 0 + \widehat{f}K \cdot \nabla_x r_t(0,n),$$

since $J(M) = \widehat{vM} = 0$. Hence,

$$\begin{aligned}\varphi_1(f,n) &= -\frac{1}{\lambda}\left(\mathrm{div}J\left(f\right), D\varphi\left(\widehat{f}\right)\right)\\ &- \left(\mathrm{div}_x\left(\widehat{f}K\cdot\nabla_x\int_0^\infty \mathbb{E}r_t(0,n)dt\right), D\varphi\left(\widehat{f}\right)\right).\end{aligned}$$

Moreover,

$$\begin{aligned}\int_0^\infty \mathbb{E}r_t(0,n)dt &= \int_{s=0}^\infty\int_{t=s}^\infty e^{-\lambda(t-s)}dtP_s\mathrm{Id}(n)ds\\ &= \int_{s=0}^\infty \frac{1}{\lambda}P_s\mathrm{Id}(n)ds\\ &= -\frac{1}{\lambda}A^{-1}\mathrm{Id}(n).\end{aligned}$$

Therefore, setting

$$\chi(n) := K\cdot\nabla_x A^{-1}\mathrm{Id}(n), \tag{5.37}$$

we have

$$\varphi_1(f,n) = -\frac{1}{\lambda}\left(\mathrm{div}J\left(f\right), D\varphi\left(\widehat{f}\right)\right) + \frac{1}{\lambda}\left(\mathrm{div}_x\left(\widehat{f}\chi(n)\right), D\varphi\left(\widehat{f}\right)\right). \tag{5.38}$$

The last computations are formal but it easy to check that φ_1 satisfies the following property.

Proposition 5.5. *Let φ be regularizing and subquadratic (Definition 5.4). Then, the function φ_1 defined by (5.38) is a good test function that satisfies (5.33). Moreover, there exists C such that*

$$|\varphi_1(f,n)| \le C\left(1+\left\|\widehat{f}\right\|_{L^2}\right), \tag{5.39}$$

for all $f\in L^2(\mathbb{T}^d\times\mathbb{T}^d)$.

Order ε^0

Averaging (5.34) with respect to μ_ρ gives :

$$\mathscr{L}\varphi(\rho) = \langle\mathscr{L}_{R*}\varphi_2(\rho,n),\mu_\rho\rangle + \langle\mathscr{L}_{T*}\varphi_1(\rho,n),\mu_\rho\rangle.$$

The first term vanishes since

$$\begin{aligned}\langle\mathscr{L}_{R*}\varphi_2(\rho,n),\mu_\rho\rangle &= -\mathbb{E}\left(\mathrm{div}_x J(\widehat{f}\tilde{M}_0), D\varphi_2\right)\\ &= -\widehat{f}\mathbb{E}\left(\mathrm{div}_x J(M) + \mathrm{div}_x\left(K\cdot\nabla_x\tilde{\eta}_0\right), D\varphi_2\right)\\ &= 0,\end{aligned}$$

since $J(M)=0$ and $\mathbb{E}\tilde{\eta}_0=0$. Let us now compute $\mathscr{L}_{T*}\varphi_1$. First, we compute

$$
\begin{aligned}
(h, D\varphi_1(f,n)) &= -\frac{1}{\lambda}\left(\mathrm{div}_x J(h), D\varphi(\widehat{f})\right) \\
&\quad +\frac{1}{\lambda}\left(\mathrm{div}_x(\widehat{h}\chi(n)), D\varphi(\widehat{f})\right) \\
&\quad -\frac{1}{\lambda}D^2\varphi(\widehat{f})\cdot\left(\mathrm{div}_x J(f), \widehat{h}\right). \\
&\quad +\frac{1}{\lambda}D^2\varphi(\widehat{f})\cdot\left(\mathrm{div}_x(\widehat{f}\chi(n)), \widehat{h}\right).
\end{aligned}
$$

We now take $h = Tf$ with $f = \rho\tilde{M}_0$ and $n = \eta_0$. Then,

$$
\begin{aligned}
\widehat{h} &= \mathrm{div}_x\left(J(\rho\tilde{M}_0)\right) \\
&= \mathrm{div}_x(\rho J(v)\cdot\nabla_x\tilde{\eta}_0) \\
&= \mathrm{div}_x(\rho K\cdot\nabla_x\tilde{\eta}_0),
\end{aligned}
$$

and

$$
\begin{aligned}
J(h) &= -\mathrm{div}_x(K(\rho\tilde{M}_0)) \\
&= -\mathrm{div}_x(\rho K(M)) - \mathrm{div}_x(\rho K(T\tilde{\eta}_0)) \\
&= -\mathrm{div}_x(\rho K(M)) - \mathrm{div}_x(\rho K(v)\cdot\nabla_x\tilde{\eta}_0) \\
&= -\mathrm{div}_x(\rho K(M)),
\end{aligned}
$$

thanks to (5.10). We obtain :

$$
\begin{aligned}
\mathscr{L}_{T*}\varphi_1(\rho\tilde{M}_0,\eta_0) &= \frac{1}{\lambda}\left(\mathrm{div}_x(\mathrm{div}_x(\rho K(M))), D\varphi(\rho)\right) \\
&- \frac{1}{\lambda}\left(\mathrm{div}_x\left(\chi(\eta_0)\mathrm{div}_x(\rho K\cdot\nabla_x\tilde{\eta}_0)\right), D\varphi(\rho)\right) \\
&+ \frac{1}{\lambda}D^2\varphi(\rho)\cdot\left(\mathrm{div}_x(\rho K\cdot\nabla_x\tilde{\eta}_0), \mathrm{div}_x(\rho K\cdot\nabla_x\tilde{\eta}_0)\right) \\
&- \frac{1}{\lambda}D^2\varphi(\rho)\cdot\left(\mathrm{div}_x(\rho\chi(\eta_0)), \mathrm{div}_x(\rho K\cdot\nabla_x\tilde{\eta}_0)\right).
\end{aligned}
$$

Taking the expectation yields :

$$
\begin{aligned}
\mathscr{L}\varphi(\rho) &= \frac{1}{\lambda}\left(\mathrm{div}_x(K(M)\cdot\nabla_x\rho), D\varphi(\rho)\right) && (5.40)\\
&- \frac{1}{\lambda}\mathbb{E}\left(\mathrm{div}_x\left(\chi(\eta_0)\mathrm{div}_x(\rho K\cdot\nabla_x\tilde{\eta}_0)\right), D\varphi(\rho)\right) && (5.41)\\
&+ \frac{1}{\lambda}\mathbb{E}D^2\varphi(\rho)\cdot\left(\mathrm{div}_x(\rho(K\cdot\nabla_x\tilde{\eta}_0 - \chi(\eta_0))), \mathrm{div}_x(\rho K\cdot\nabla_x\tilde{\eta}_0)\right). && (5.42)
\end{aligned}
$$

Finally, we will make a use of the following fact :

Proposition 5.6. *Let $\varphi \in C^2(L^2_x)$ be regularizing and subquadratic and $\varphi^\varepsilon = \varphi + \varepsilon\varphi_1$, where φ is defined by (5.38). Then, there exists $C > 0$ depending on C^* and C_φ such that*

$$|\mathscr{L}^\varepsilon \varphi^\varepsilon(f, n) - \mathscr{L}\left(\widehat{f}\right)| \leq C\varepsilon(1 + \|f\|^2_{L^2}). \tag{5.43}$$

Moreover,

$$\mathcal{M}^\varepsilon(t) := \varphi^\varepsilon(f^\varepsilon(t), \overline{m}^\varepsilon_t) - \int_0^t \mathscr{L}^\varepsilon \varphi^\varepsilon\left(f^\varepsilon(s), \overline{m}^\varepsilon_s\right) ds,$$

is a continuous martingale for the filtration $(\mathcal{F}^\varepsilon_t)$ generated by $\overline{m}^\varepsilon$ with quadratic variation

$$\langle \mathcal{M}^\varepsilon, \mathcal{M}^\varepsilon\rangle(t) = \int_0^t \left(\left(A|\varphi_1|^2 - 2\varphi_1 A\varphi_1\right)\left(f^\varepsilon(s), \overline{m}^\varepsilon_s\right) + a_\varepsilon(s)\right) ds, \tag{5.44}$$

where

$$|a_\varepsilon(t)| \leq C\varepsilon \int_0^t (1 + \|\rho^\varepsilon(s)\|^4_{L^2}) ds, \tag{5.45}$$

for a constant C depending on C^* and C_φ. Moreover, for $0 \leq s_1 \leq \cdots \leq s_k \leq s \leq t$ and $\psi \in C_b((L^2)^k)$,

$$\begin{aligned}&\left|\mathbb{E}\left(\varphi(\rho^\varepsilon(t)) - \varphi(\rho^\varepsilon(s)) - \int_s^t \mathscr{L}\varphi(\rho^\varepsilon(\sigma))d\sigma\right)\psi\left(\rho^\varepsilon(s_1), ..., \rho^\varepsilon(s_k)\right)\right| \\ \leq& C\varepsilon\left(1 + \sup_{\sigma\in[0,t]} \mathbb{E}\,\|f^\varepsilon(\sigma)\|^2_{L^2}\right),\end{aligned} \tag{5.46}$$

where C is another constant depending on C_* and C_φ and the supremum of φ.

We will not prove this Proposition but a proof of a similar result can be found in [51], Corollary 9.

5.5 The limit equation

In this section, we identify the limit of ρ^ε. For this, we identify first the contribution of the first order terms and then, the contribution of the second order terms of the operator $\mathcal{L}$.

5.5.1 First order terms

We recognize that the first term (5.40) corresponds to the diffusion term

$$\frac{1}{\lambda}\mathrm{div}_x(K(M)\cdot\nabla_x\rho). \tag{5.47}$$

In order to identify the contribution of (5.41), we compute $\mathbb{E}\mathrm{div}_x\left(\chi(\eta_0)\mathrm{div}_x(\rho K\cdot\nabla_x\tilde{\eta}_0)\right)$. Let us recall that

$$\chi(\eta_0) = K\nabla_x \int_0^\infty \frac{1}{\lambda} P_s\mathrm{Id}(\eta_0) ds. \tag{5.48}$$

For readability, we set

$$R(\eta_0) := \int_0^\infty \frac{1}{\lambda} P_s\mathrm{Id}(\eta_0) ds. \tag{5.49}$$

We now compute

$$\begin{aligned}\mathbb{E}\mathrm{div}_x\left(\chi(\eta_0)\mathrm{div}_x(\rho K\cdot\nabla_x\tilde{\eta}_0)\right) &= \mathrm{div}_x\left(\mathbb{E}\chi(\eta_0)K\cdot\nabla_x\tilde{\eta}_0\nabla_x\rho\right)+\mathrm{div}_x\left(\mathbb{E}\chi(\eta_0)\mathrm{div}_x(K\cdot\nabla_x\tilde{\eta}_0)\rho\right)\\ &= \mathrm{div}\left(\mathbb{E}K\nabla_x\int_0^\infty P_s\mathrm{Id}(\eta_0)dsK\nabla_x\int_{-\infty}^0\eta_\sigma e^{\lambda\sigma}d\sigma\nabla_x\rho\right)\\ &+ \mathrm{div}\left(\mathbb{E}K\nabla_x\int_0^\infty P_s\mathrm{Id}(\eta_0)ds\mathrm{div}\left(K\nabla_x\int_{-\infty}^0\eta_\sigma e^{\lambda\sigma}d\sigma\right)\rho\right)\end{aligned}$$

Let us compute both term separately. Hereafter, we use the convention of summation over repeated indices :

$$\begin{aligned}&\mathrm{div}\left(\mathbb{E}K\nabla_xR\left(\eta_0\right)K\nabla_x\int_{-\infty}^0\eta_\sigma e^{\lambda\sigma}d\sigma\nabla_x\rho\right)\\ =&\partial_i\left(K_{ij}K_{lk}\int_{\sigma=-\infty}^0e^{\lambda\sigma}\int_{s=0}^{+\infty}\mathbb{E}\partial_j(P_s\mathrm{Id}\left(\eta_0\right))\partial_k\eta_\sigma\partial_l\rho.dsd\sigma\right)\\ =&\partial_i\left(K_{ij}K_{lk}\int_{\sigma=-\infty}^0\int_{s=0}^{+\infty}e^{\lambda\sigma}\mathbb{E}\partial_j(P_s\mathrm{Id}\left(\eta_{-\sigma}\right))\partial_k\eta_0\partial_l\rho.dsd\sigma\right),\end{aligned}$$

since $(\eta_\sigma)_\sigma$ is a stationary process. We go on with the computation :

$$\begin{aligned}&\mathrm{div}\left(\mathbb{E}K\nabla_xR\left(\eta_0\right)K\nabla_x\int_{-\infty}^0\eta_\sigma e^{\lambda\sigma}d\sigma\nabla_x\rho\right)\\ =&\partial_i\left(K_{ij}K_{lk}\int_{\sigma=0}^{+\infty}\int_{s=0}^{+\infty}e^{-\lambda\sigma}\mathbb{E}\partial_j(P_{s+\sigma}\mathrm{Id}\left(\eta_0\right))\partial_k\eta_0\partial_l\rho.dsd\sigma\right)\\ =&\partial_i\left(K_{ij}K_{lk}\int_{s=0}^{+\infty}\int_{\sigma=s}^{+\infty}e^{\lambda(s-\sigma)}\mathbb{E}\partial_j(P_\sigma\mathrm{Id}\left(\eta_0\right))\partial_k\eta_0\partial_l\rho.d\sigma ds\right)\\ =&\partial_i\left(K_{ij}K_{lk}\int_0^{+\infty}e^{-\lambda\sigma}\mathbb{E}\partial_j(P_\sigma\mathrm{Id}\left(\eta_0\right))\partial_k\eta_0\partial_l\rho.d\sigma\int_0^\sigma e^{\lambda s}ds\right)\\ =&\partial_i\left(K_{ij}K_{lk}\int_0^{+\infty}\left(\frac{1-e^{-\lambda\sigma}}{\lambda}\right)\mathbb{E}\partial_j(P_\sigma\mathrm{Id}\left(\eta_0\right))\partial_k\eta_0\partial_l\rho.d\sigma\right)\\ =&\frac{1}{\lambda}\mathbb{E}\mathrm{div}\left(K\nabla_x\int_0^{+\infty}\left(1-e^{-\lambda\sigma}\right)P_\sigma\mathrm{Id}(\eta_0)d\sigma K\nabla_x\eta_0\nabla_x\rho\right).\end{aligned}$$

For the second term, the computation is similar hence we simplify a bit :

$$\begin{aligned}&\mathrm{div}\left(\mathbb{E}K\nabla_x\int_0^\infty P_s\mathrm{Id}(\eta_0)ds\mathrm{div}\left(K\nabla_x\int_{-\infty}^0\eta_\sigma e^{\lambda\sigma}d\sigma\right)\rho\right)\\ =&\partial_i\left(K_{ij}K_{lk}\int_{\sigma=-\infty}^0e^{\lambda\sigma}\int_{s=0}^{+\infty}\mathbb{E}\partial_j(P_s\mathrm{Id}\left(\eta_0\right))\partial^2_{kl}\eta_\sigma\rho.dsd\sigma\right)\\ =&\partial_i\left(K_{ij}K_{lk}\int_0^{+\infty}\left(\frac{1-e^{-\lambda\sigma}}{\lambda}\right)\mathbb{E}\partial_j(P_\sigma\mathrm{Id}\left(\eta_0\right))\partial^2_{kl}\eta_0\rho.d\sigma\right)\\ =&\frac{1}{\lambda}\mathbb{E}\mathrm{div}\left(K\nabla_x\int_0^{+\infty}\left(1-e^{-\lambda\sigma}\right)P_\sigma\mathrm{Id}(\eta_0)d\sigma\mathrm{div}\left(K\nabla_x\eta_0\right)\rho\right).\end{aligned}$$

Setting $\eta_0' := \int_0^{+\infty} \left(1 - e^{-\lambda\sigma}\right) P_\sigma \mathrm{Id}(\eta_0) d\sigma$, we have

$$\begin{aligned} \mathbb{E}\mathrm{div}_x \left(\chi(\eta_0)\mathrm{div}_x(\rho K \cdot \nabla_x \tilde{\eta}_0)\right) &= \frac{1}{\lambda}\mathbb{E}\mathrm{div}\left(K\nabla_x\eta_0' K\nabla_x\eta_0\nabla_x\rho\right) \quad (5.50) \\ &+ \frac{1}{\lambda}\mathbb{E}\mathrm{div}\left(K\nabla_x\eta_0'\mathrm{div}\left(K\nabla_x\eta_0\right)\rho\right). \quad (5.51) \end{aligned}$$

5.5.2 Second order terms

To determine the contribution of the second order terms in the limit equation associated to the generator $\mathscr{L}$, we compute $\mathscr{L}\psi$ with ψ quadratic with kernel $\Phi \in C^1$:

$$\psi(\rho) = \int_{\mathbb{T}^d}\int_{\mathbb{T}^d} \Phi(x,y)\rho(x)\rho(y)\,dxdy,$$

where Φ is symmetric $\Phi(x,y) = \Phi(y,x)$. Then,

$$\begin{aligned} D^2\psi(\rho)(\mathrm{div}_x h, \mathrm{div}_x k) &= \int_{\mathbb{T}^d}\int_{\mathbb{T}^d} \Phi(x,y)\,\mathrm{div}_x h(x)\,\mathrm{div}_y k(y)\,dxdy \\ &+ \int_{\mathbb{T}^d}\int_{\mathbb{T}^d} \Phi(x,y)\,\mathrm{div}_x k(x)\,\mathrm{div}_y h(y)\,dxdy \\ &= 2\int_{\mathbb{T}^d}\int_{\mathbb{T}^d} \partial^2_{x_i,y_j}\Phi(x,y)h_i(x)k_j(y)dxdy. \end{aligned}$$

Consequently,

$$\begin{aligned} &\frac{D^2\psi(\rho)}{\lambda}\mathbb{E}\left(\mathrm{div}_x(\rho(K\nabla_x\tilde{\eta}_0 - \chi(\eta_0))), \mathrm{div}_x(\rho K\nabla_x\tilde{\eta}_0)\right) \\ =&\frac{2}{\lambda}\int\int \partial^2_{x_i,y_j}\Phi(x,y)\rho(x)\rho(y)\mathbb{E}(K\nabla_x\tilde{\eta}_0 - \chi(\eta_0))_i(K\nabla_x\tilde{\eta}_0)_j. \end{aligned}$$

To find the limit equation, we will use the following lemma :

Proposition 5.1. *Let Σ be the operator*

$$\Sigma\theta(x) = \int \mathcal{K}(x,y)\,\theta(y)\,dy$$

where the kernel $\mathcal{K}$ is defined by :

$$\mathcal{K}(x,y) = \mathbb{E}\left[\left(\tilde{\eta}_0 + R(\eta_0)(x)\right)\tilde{\eta}_0(y)\right].$$

Then, Σ is self-adjoint, positive and trace-class.

We will prove this proposition later on. For now, let us assume that it is true. Then, $\Sigma^{1/2}$ is well defined. Denote by (μ_k, p_k) the spectral elements associated to Σ : for all $\rho \in L^2$,

$$\Sigma\rho = \sum_k \mu_k \langle \rho, p_k\rangle p_k$$

hence

$$\mathcal{K}(x,y) = \sum_k \mu_k p_k(x)\,p_k(y).$$

And, if we let $\mathtt{k}$ be the kernel of $\Sigma^{1/2}$:

$$\mathtt{k}(x,y) \quad = \quad \sum_k \mu_k^{1/2} p_k(x)\, p_k(y)\,.$$

Finally,

$$\begin{aligned}
&\frac{D^2\psi(\rho)}{\lambda}\mathbb{E}\left(\operatorname{div}\left(\rho\left(K\cdot\nabla_x\tilde{\eta}_0-\chi(\eta_0)\right)\right),\operatorname{div}\left(\rho K\cdot\nabla_x\tilde{\eta}_0\right)\right)\\
=&\frac{2}{\lambda}\int\int\partial^2_{x_iy_j}\Phi(x,y)\,\rho(x)\,\rho(y)\,\mathbb{E}\left(\left(K\cdot\nabla_x\tilde{\eta}_0-\chi(\eta_0)\right)_i(x)\left(K\cdot\nabla_x\tilde{\eta}_0\right)_j(y)\right)dxdy\\
=&\frac{2}{\lambda}\int\int\partial^2_{x_iy_j}\Phi(x,y)\,\rho(x)\,\rho(y)\,K_{il}K_{jm}\partial_{x_l}\partial_{y_m}\mathbb{E}\left[\left(\tilde{\eta}_0-R(\eta_0)\right)(x)\,\tilde{\eta}_0(y)\right]dxdy\\
=&\frac{2}{\lambda}\sum_k\int\int\partial^2_{x_iy_j}\Phi(x,y)\,\rho(x)\,\rho(y)\,\mu_kK_{il}K_{jm}\partial_{x_l}p_k(x)\,\partial_{y_m}p_k(y)\,dxdy.\\
=&\sum_k\int\int\Phi(x,y)\,\mu_k\partial_{x_i}\left(\sqrt{\frac{2}{\lambda}}\rho K\nabla_x p_k\right)\partial_{y_j}\left(\sqrt{\frac{2}{\lambda}}\rho K\nabla_x p_k\right)dxdy
\end{aligned}$$

Introducing the linear operator (recall 5.20)

$$P(\rho):p \quad\mapsto\quad \sqrt{\frac{2}{\lambda}}\operatorname{div}_x\left[\rho K\nabla_x p\right],$$

we get

$$\frac{D^2\psi(\rho)}{\lambda}\mathbb{E}\left(\operatorname{div}\left(\rho\left(K\cdot\nabla_x\tilde{\eta}_0-\chi(\eta_0)\right)\right),\operatorname{div}\left(\rho K\cdot\nabla_x\tilde{\eta}_0\right)\right)=\operatorname{Trace}\left(P(\rho)\,\Sigma^{1/2}D^2\psi(\rho)\,P(\rho)\,\Sigma^{1/2}\right). \tag{5.52}$$

We now prove Proposition 5.1. To do so, let us decompose our kernel in two parts. First,

$$\mathbb{E}\left[\tilde{\eta}_0(x)\,\tilde{\eta}_0(y)\right]=\mathbb{E}\left[\int_{-\infty}^0\int_{-\infty}^0\eta_\sigma(x)\,\eta_s(y)\,e^{\lambda(\sigma+s)}d\sigma ds\right].$$

Hereafter, we will denote

$$\mathcal{R}(\sigma-s)(x,y):=\mathbb{E}\left[\eta_\sigma(x)\eta_s(y)\right]. \tag{5.53}$$

Then,

$$\begin{aligned}
\mathbb{E}\left[\tilde{\eta}_0\tilde{\eta}_0\right] &= \int_{-\infty}^{0}\int_{-\infty}^{0}\mathcal{R}\left(\sigma-s\right)e^{\lambda(\sigma+s)}d\sigma ds \\
&= \int_{\sigma=-\infty}^{0}\int_{s=\sigma}^{\infty}\mathcal{R}\left(s\right)e^{\lambda\sigma}e^{\lambda(\sigma-s)}dsd\sigma \\
&= \int_{\sigma=-\infty}^{0}\int_{s=\sigma}^{0}\mathcal{R}\left(s\right)e^{\lambda\sigma}e^{\lambda(\sigma-s)}dsd\sigma \\
&+ \int_{\sigma=-\infty}^{0}\int_{s=0}^{\infty}\mathcal{R}\left(s\right)e^{\lambda\sigma}e^{\lambda(\sigma-s)}dsd\sigma \\
&= \int_{s=-\infty}^{0}\mathcal{R}\left(s\right)e^{-\lambda s}\int_{\sigma=-\infty}^{s}e^{2\lambda\sigma}dsd\sigma+\int_{0}^{\infty}\mathcal{R}(s)e^{-\lambda s}ds \\
&= \int_{-\infty}^{0}\frac{1}{2\lambda}\mathcal{R}\left(s\right)e^{\lambda s}ds+\int_{0}^{\infty}\frac{1}{2\lambda}\mathcal{R}\left(s\right)e^{-\lambda s}ds \\
&= \frac{1}{2\lambda}\int_{\mathbb{R}}\mathcal{R}\left(s\right)e^{-\lambda|s|}ds
\end{aligned}$$

To conduct a similar analysis on the second part of the kernel, we will use the following lemma :

Lemma 5.2. $\mathbb{E}\left[P_s\mathrm{Id}\left(\eta_0\right)\eta_\sigma\right]=\mathcal{R}\left(s-\sigma\right)$

Démonstration. We have

$$\begin{aligned}
\mathbb{E}\left[P_s\mathrm{Id}\left(\eta_0\right)\eta_\sigma\right] &= \mathbb{E}\left[\mathbb{E}\left[P_s\mathrm{Id}\left(\eta_0\right)\eta_\sigma\mid\eta_\sigma\right]\right] \\
&= \mathbb{E}\left[\mathbb{E}\left[P_s\mathrm{Id}\left(\eta_0\right)\mid\eta_\sigma\right]\eta_\sigma\right] \\
&= \mathbb{E}\left[P_{s-\sigma}\mathrm{Id}\left(\eta_\sigma\right)\mid\eta_\sigma\right] \\
&= \mathbb{E}\left[\mathbb{E}\left[\eta_s\mid\eta_\sigma\right]\eta_\sigma\right] \\
&= \mathbb{E}\left[\eta_s\eta_\sigma\right] \\
&= \mathcal{R}\left(s-\sigma\right).
\end{aligned}$$

□

$$\begin{aligned}
\mathbb{E}\left[R\left(\eta_0\right)\tilde{\eta}_0\right] &= \int_{-\infty}^{0}\int_{-\infty}^{0}e^{\lambda\sigma}\mathbb{E}\left[P_s\mathrm{Id}\left(\eta_0\right)\eta_\sigma\right]dsd\sigma \\
&= \int_{-\infty}^{0}\int_{-\infty}^{0}e^{\lambda\sigma}\mathcal{R}\left(s-\sigma\right)dsd\sigma \\
&= \int_{s=-\infty}^{0}\int_{\sigma=-\infty}^{s}e^{\lambda\sigma}\mathcal{R}\left(s\right)dsd\sigma \\
&= \frac{1}{\lambda}\int_{-\infty}^{0}\mathcal{R}\left(s\right)ds \\
&= \frac{1}{2\lambda}\int_{\mathbb{R}}\mathcal{R}\left(s\right)ds
\end{aligned}$$

Thanks to this decomposition, we can write Σ in a much nicer form :

$$\left\langle\Sigma\theta,\theta\right\rangle=\int_{\mathbb{R}}\frac{1+e^{-\lambda|s|}}{2\lambda^2}\left(\int\int\mathcal{R}\left(s\right)\left(x,y\right)\theta\left(x\right)\theta\left(y\right)dxdy\right)ds \tag{5.54}$$

Since $\mathcal{R}$ is symmetric, Σ is self-adjoint. Hence, it only remains to prove that Σ is positive. In order to do so, we will prove the two following lemmas :

Lemma 5.3. *Let* $\gamma_\mu(s) = \left(\sqrt{\frac{1}{\lambda}}e^{-\lambda s} + \frac{\sqrt{\mu}}{\lambda}e^{-\mu s}\right)\mathbb{1}_{\mathbb{R}_+}(s)$. *Then,* $\gamma_\mu \in L^2(\mathbb{R})$ *and*

$$\lim_{\mu\to 0}\left\|\gamma_\mu\right\|^2_{L^2(\mathbb{R})} = \frac{1}{\lambda^2}. \tag{5.55}$$

Moreover,

$$\frac{1+e^{-\lambda|s|}}{2\lambda^2} = \lim_{\mu\to 0}\gamma_\mu * \check{\gamma}_\mu(s), \tag{5.56}$$

where $\check{\gamma}_\mu(s) = \gamma_\mu(-s)$.

Lemma 5.4. *For all* $\Psi \in C_b(\mathbb{R}^n, \mathbb{R})$, *we have*

$$\int_{\mathbb{R}} \gamma_\mu * \check{\gamma}_\mu(s)\,\mathbb{E}\left[\Psi(\eta_s)\Psi(\eta_0)\right]ds = \mathbb{E}\left|\int_{\mathbb{R}_+}\gamma_\mu(s)\Psi(\eta_s)\,ds\right|^2.$$

Proof of Lemma 5.3. We have

$$\begin{aligned}\int_{\mathbb{R}}|\gamma_\mu(s)|^2 ds &= \int_0^{+\infty}\left(\frac{1}{\lambda}e^{-2\lambda s} + \frac{2\sqrt{\mu}}{\lambda\sqrt{\lambda}}e^{-(\lambda+\mu)s} + \frac{\mu}{\lambda^2}e^{-2\mu s}\right)ds\\ &= \frac{1}{\lambda^2} + \frac{2\sqrt{\mu}}{\lambda\sqrt{\lambda}(\lambda+\mu)} \underset{\mu\to 0}{\longrightarrow} \frac{1}{\lambda^2}.\end{aligned}$$

which proves (5.55).

Let now $t > 0$,

$$\begin{aligned}\gamma_\mu * \check{\gamma}_\mu(t) &= \int \gamma_\mu(s)\gamma_\mu(s-t)\,ds\\ &= \int_t^{+\infty}\left(\frac{1}{\lambda}e^{-2\lambda s+\lambda t} + \frac{\sqrt{\mu}}{\lambda\sqrt{\lambda}}\left(e^{-\lambda s-\mu(s-t)} + e^{-\mu s-\lambda(s-t)}\right) + \frac{\mu}{\lambda^2}e^{-2\mu s+\mu t}\right)ds\\ &= \frac{e^{-\lambda t}}{2\lambda^2} + \frac{\sqrt{\mu}}{\lambda\sqrt{\lambda}(\lambda+\mu)}\left(e^{-\lambda t} + e^{-\mu t}\right) + \frac{1}{2\lambda^2}e^{-\mu t}\\ &\underset{\mu\to 0}{\longrightarrow} \frac{e^{-\lambda t}+1}{2\lambda^2}.\end{aligned}$$

Let now $t \le 0$. Then,

$$\begin{aligned}\gamma_\mu * \check{\gamma}_\mu(t) &= \int_0^{+\infty}\left(\frac{1}{\lambda}e^{-2\lambda s+\lambda t} + \frac{\sqrt{\mu}}{\lambda\sqrt{\lambda}}\left(e^{-\lambda s-\mu(s-t)} + e^{-\mu s-\lambda(s-t)}\right) + \frac{\mu}{\lambda^2}e^{-2\mu s+\mu t}\right)ds\\ &= \frac{e^{\lambda t}}{2\lambda^2} + \frac{\sqrt{\mu}}{\lambda\sqrt{\lambda}(\lambda+\mu)}\left(e^{\mu t} + e^{\mu s}\right) + \frac{1}{2\lambda^2}e^{\mu t}\\ &\underset{\mu\to 0}{\longrightarrow} \frac{e^{\lambda t}+1}{2\lambda^2},\end{aligned}$$

which proves (5.56). □

Proof of Lemma 5.4. Using Fubini's theorem and the fact that $(\eta_t)_t$ is stationary, we compute

$$\begin{aligned}
\int_{\mathbb{R}} \gamma_\mu * \check{\gamma}_\mu (s)\, \mathbb{E}\left[\Psi(\eta_s)\Psi(\eta_0)\right] ds &= \int_{\mathbb{R}}\int_{\mathbb{R}} \gamma_\mu(t)\gamma_\mu(t-s)\,\mathbb{E}\left[\Psi(\eta_s)\Psi(\eta_0)\right] dsdt \\
&= \mathbb{E}\int_{\mathbb{R}}\int_{\mathbb{R}} \gamma_\mu(t)\gamma_\mu(t-s)\Psi(\eta_s)\Psi(\eta_0)\, dsdt \\
&= \mathbb{E}\int_{\mathbb{R}}\int_{\mathbb{R}} \gamma_\mu(t)\gamma_\mu(t-s)\Psi(\eta_t)\Psi(\eta_{t-s})\, dsdt \\
&= \mathbb{E}\int_{\mathbb{R}} \gamma_\mu(t)\gamma_\mu(\sigma)\Psi(\eta_t)\Psi(\eta_\sigma)\, dtd\sigma \\
&= \mathbb{E}\left|\int_{\mathbb{R}} \gamma_\mu(s)\Psi(\eta_s)\, ds\right|^2 \\
&= \mathbb{E}\left|\int_{\mathbb{R}_+} \gamma_\mu(s)\Psi(\eta_s)\, ds\right|^2.
\end{aligned}$$

□

Proof of Proposition 5.1. Thanks to (5.54), since $\mathcal{R}$ is symmetric, Σ is self adjoint. Moreover, thanks to Lemma 5.3 and Lemma 5.4, we get by dominated convergence,

$$\begin{aligned}
\langle \Sigma\theta, \theta\rangle &= \lim_{\mu\to 0}\int_{\mathbb{R}} \gamma_\mu * \check{\gamma}_\mu(s)\,\mathbb{E}\left[\int\int \eta_s(x)\theta(x)\eta_0(y)\theta(y)\,dxdy\right] ds \\
&= \lim_{\mu\to 0}\mathbb{E}\left|\int_{\mathbb{R}_+} \gamma_\mu(s)\langle \eta_s, \theta\rangle_{L^2}\, ds\right|^2.
\end{aligned}$$

Hence, Σ is positive. Moreover, if we let $(\theta_k)_{k\in\mathbb{N}}$ be an orthonormal basis of $L^2(\mathbb{T}^d)$, we have by Bessel's estimate

$$\begin{aligned}
\sum_{k\le N}\langle \Sigma\theta_k, \theta_k\rangle &= \lim_{\mu\to 0}\sum_{k\le N}\mathbb{E}\left|\int_{\mathbb{R}_+} \gamma_\mu(s)\langle \eta_s, \theta_k\rangle_{L^2}\, ds\right|^2 \\
&\le \lim_{\mu\to 0}\mathbb{E}\left\|\int_{\mathbb{R}_+} \gamma_\mu(s)\eta_s ds\right\|_{L^2}^2.
\end{aligned}$$

By Jensen's estimate

$$\begin{aligned}
\lim_{\mu\to 0}\mathbb{E}\left\|\int_{\mathbb{R}_+} \gamma_\mu(s)\eta_s ds\right\|_{L^2}^2 &\le \lim_{\mu\to 0}\int_{\mathbb{R}_+}|\gamma_\mu(s)|^2\mathbb{E}\left[\|\eta_s\|_{L^2}^2\right] ds \\
&\le \lim_{\mu\to 0}\int_{\mathbb{R}_+}|\gamma_\mu(s)|^2\mathbb{E}\left[\|\eta_0\|_{L^2}^2\right] ds \\
&= \mathbb{E}\left[\|\eta_0\|_{L^2}^2\right]\lim_{\mu\to 0}\|\gamma_\mu\|_{L^2(\mathbb{R})}^2.
\end{aligned}$$

by stationary of $(\eta_s)_s$. We now use Lemma 5.3 and the positivity of Σ to conclude that

$$\sum_{k\in\mathbb{N}}\langle \Sigma\theta_k, \theta_k\rangle < +\infty,$$

hence, Σ is trace-class. □

5.5.3 Stratonovitch formulation

Let us now conclude our identification of the limit equation. We recall that our limit generator is given as the sum of (5.40), (5.41) and(5.42). Gathering formulas (5.47), (5.51), (5.50) and (5.52), the Stratonovitch formulation associated to the generator $\mathscr{L}$ is :

$$\begin{aligned} d\rho &= \frac{1}{\lambda^2}\mathrm{div}\left(\left(\lambda K(M) - \mathbb{E}K\nabla_x\eta_0' K\nabla\eta_0\right)\nabla_x\rho\right)dt \\ &- \frac{1}{\lambda^2}\mathrm{div}\left(\rho\cdot\mathbb{E}K\nabla_x\eta_0'\mathrm{div}\left(K\nabla\eta_0\right)\right)dt \\ &+ P(\rho)\Sigma^{1/2}\circ dW_t, \end{aligned} \tag{5.57}$$

where W_t is a cylindrical Wiener process on $L^2(\mathbb{T}^d)$:

$$W_t = \sum_k \beta_k(t)p_k.$$

5.6 Diffusive limit

5.6.1 L^2 bound

Proposition 5.5. *Assume (5.16). Then, for all $\tau > 0$, for all $p \geq 2$ there exists $C > 0$ such that, for all $\varepsilon > 0$,*

$$\mathbb{E}\sup_{t\in[0,\tau]} \|f^\varepsilon(t)\|^p_{L^2((\overline{M}_{t/\varepsilon^2})^{-1})} \leq C,$$

where

$$\|f\|^2_{L^2((\overline{M}_{t/\varepsilon^2})^{-1})} := \int_{\mathbb{T}^d}\int_V \frac{|f(t,x,v)|^2}{\overline{M}_{t/\varepsilon^2}}dxdv, \tag{5.58}$$

and

$$\begin{aligned} \overline{M}_{t/\varepsilon^2} &= M + v\cdot\nabla_x\bar{r}^\varepsilon_t, \\ \bar{r}^\varepsilon_t &= \int_{-\infty}^{t/\varepsilon^2} e^{-\lambda(\varepsilon^{-2}t-s)}\overline{m}_s ds. \end{aligned}$$

In the proof of Proposition 5.5, we will often use the following Lemma :

Lemma 5.7. *For all $\varepsilon > 0$,*

$$\left\|\widehat{f}(t)\right\|_{L^2(\mathbb{T}^d)} \leq \|f(t)\|_{L^2((M(r)^{-1})}, \tag{5.59}$$

where $M(r) := M + v\cdot\nabla_x r$.

Démonstration. This is easily obtained since

$$\begin{aligned} \left\|\widehat{f}(t)\right\|^2_{L^2(\mathbb{T}^d)} &= \int\left|\int f(t)dv\right|^2 dx \\ &= \int\left|\int \frac{f(t)}{\sqrt{M(r)}}\times\sqrt{M(r)}dv\right|^2 dx \\ &\leq \int\left(\int\frac{|f^\varepsilon(t)|^2}{M(r)}dv\times\widehat{M(r)}\right)dx \end{aligned}$$

and since $\widehat{M(r)} = \widehat{M} = 1$. □

In the following, we will denote by C any constant that depends on C^*, τ and p but not on ε.

Proof of Proposition 5.5. Note that

$$\begin{aligned} \|f^\varepsilon(t)\|^2_{L^2((\overline{M}_{t/\varepsilon^2})^{-1})} &= \varphi(f^\varepsilon(t), r^\varepsilon_t(\tilde{\eta}_0, \eta_0), m^\varepsilon_t(\eta_0)) \\ &= \mathcal{P}^\varepsilon_t \varphi(f_0, \tilde{\eta}_0, \eta_0), \end{aligned}$$

with

$$\varphi(f, r, n) := \int\int \frac{|f|^2}{M + v \cdot \nabla_x r} dx dv. \tag{5.60}$$

For simplicity, let us denote

$$M(r) := M + v \cdot \nabla_x r. \tag{5.61}$$

$$L(r) := M(r)\rho - f. \tag{5.62}$$

We have

$$\mathcal{P}^\varepsilon_t \varphi(f_0, \tilde{\eta}_0, \eta_0) = \varphi(f_0, \tilde{\eta}_0, \eta_0) + \int_0^t \mathcal{L}^\varepsilon \varphi(f^\varepsilon(s), \tilde{\eta}_s, \eta_s) ds, \tag{5.63}$$

where $\mathcal{L}^\varepsilon$ is the generator associated to $\mathcal{P}^\varepsilon_t$:

$$\mathcal{L}^\varepsilon = \frac{1}{\varepsilon^2}\mathcal{L}_\# + \frac{1}{\varepsilon}\mathcal{L}_{T*} \tag{5.64}$$

$$\mathcal{L}_\# \varphi(f, r, n) = \left(\lambda L f + \widehat{f} v \cdot \nabla_x n, D_f \varphi\right) + (n - \lambda r, D_r \varphi) + A\varphi, \tag{5.65}$$

$$\mathcal{L}_{T*} \varphi(f, r, n) = -\left(Tf, D_f \varphi\right). \tag{5.66}$$

Here, D_f denotes differentiation with respect to the variable f and D_r differentiation with respect to r. Hence,

$$\begin{aligned} D_f \varphi(f, r, n) &= 2\frac{f}{M(r)}, \\ D_r \varphi(f, r, n) &= -\frac{|f|^2}{M(r)^2} v \cdot \nabla_x. \end{aligned}$$

To estimate the first term (5.65), let us compute

$$\begin{aligned} \mathcal{L}_\# \varphi(f, r, n) &= 2\int\int \frac{f \cdot (\lambda L(r) f + \widehat{f} v \cdot \nabla_x (n - \lambda r))}{M(r)} dx dv - \int\int \frac{|f|^2}{M(r)^2} v \cdot \nabla_x (n - \lambda r) dx dv \\ &= 2\lambda \int\int \frac{f L(r) f}{M(r)} dx dv + \int\int v \cdot \nabla_x (n - \lambda r) \left(\frac{2\widehat{f} f}{M(r)} - \frac{|f|^2}{M(r)^2}\right) dx dv \\ &= -2\lambda \int\int \frac{|L(r) f|^2}{M(r)} dx dv + \int\int \frac{v \cdot \nabla_x (n - \lambda r)}{M(r)^2} \left(-|L(r) f|^2 + \left(M(r)\widehat{f}\right)^2\right) dx dv \\ &= -2\lambda \int\int \frac{|L(r) f|^2}{M(r)} \left(1 - \frac{1}{2} \cdot \frac{v \cdot \nabla_x (n - \lambda r)}{M(r)}\right) dx dv + \int\int \widehat{f}^2 v \cdot \nabla_x (n - \lambda r) dx dv \end{aligned}$$

Since $\int_V v dv = 0$, we have

$$\int\int \left|\widehat{f_0}\right|^2 v \cdot \nabla_x(\tilde{\eta}_s - \lambda\eta_s) = 0.$$

Furthermore, since we assume (5.16), we get

$$\mathcal{L}_{\#}\varphi(f^\varepsilon(s), \tilde{\eta}_s, \eta_s) \leq -2\lambda\theta \int\int \frac{|L(\tilde{\eta}_s)f^\varepsilon(s)|^2}{M(\tilde{\eta}_s)} dxdv. \tag{5.67}$$

Let us now estimate the second term :

$$\begin{aligned}
\mathcal{L}_{T*}\varphi &= -\langle Tf, D_f\varphi\rangle \\
&= -2\int\int \frac{f(v\cdot\nabla_x f)}{M(r)} dxdv \\
&= -\int\int \frac{v\cdot\nabla_x |f|^2}{M(r)} dxdv \\
&= -\int\int \frac{|f|^2}{M(r)^2} v\cdot\nabla_x M(r) dxdv \\
&= -\int\int \frac{|f|^2}{M(r)^2} v\otimes v\colon D_x^2 r,
\end{aligned}$$

where A : B is the canonical scalar product of A and B in the set of matrices (check Section 5.2.1). Decomposing $f = \widehat{f}M(r) - L(r)f$, we get

$$\begin{aligned}
\mathcal{L}_{T*}\varphi &= -\int\int \left|\widehat{f}\right|^2 v\otimes v\colon D_x^2 r dxdv \\
&\quad +2\int\int \frac{\widehat{f}L(r)f}{M(r)} v\otimes v\colon D_x^2 r dxdv \\
&\quad -\int\int \frac{|L(r)f|^2}{M(r)^2} v\otimes v\colon D_x^2 r dxdv.
\end{aligned} \tag{5.68}$$

For the second and the third terms, we have :

$$\begin{aligned}
\frac{2}{\varepsilon}\int\int \frac{\widehat{f}L(r)f}{M(r)} v\otimes v\colon D^2 r &\leq \frac{C}{\varepsilon}\int\int \frac{\left|\widehat{f}\right| |L(r)f|}{M(r)} \\
&\leq \frac{\alpha}{\varepsilon^2}\int\int \frac{|L(r)f|^2}{M(r)} dxdv + \frac{C^2}{4\alpha}\int\int \frac{\left|\widehat{f}\right|^2}{M(r)} dxdv \\
&\leq \frac{\alpha}{\varepsilon^2}\int\int \frac{|L(r)f|^2}{M(r)} dxdv + \tilde{C}_\alpha \int\int \frac{|f|^2}{M(r)} dxdv,
\end{aligned} \tag{5.69}$$

and

$$-\frac{1}{\varepsilon}\int\int \frac{|f|^2}{M(r)^2} v\otimes v\colon D_x^2 r \leq \frac{\varepsilon C}{\varepsilon^2}\int\int \frac{|L(r)f|^2}{M(r)} dxdv \tag{5.70}$$

To deal with the first term in (5.68), we use a perturbed test function argument again. We look for φ_1 such that

$$\mathscr{L}_{\#}\varphi_1(f,r,n) = -\int\int \left|\widehat{f}\right|^2 v\otimes v\colon D_x^2 r dv dx.$$

Let us look for φ_1 of the form $\varphi_1(f,r,n) = \varphi_1(\widehat{f},r,n)$. In that case,

$$\mathscr{L}_{\#}\varphi_1(\widehat{f},r,n) = 0 + (n-\lambda r, D_r\varphi_1) + A\varphi_1,$$

hence, we need to inverse

$$A\varphi_1 + (n-\lambda r, D_r\varphi_1) = -\int\int \left|\widehat{f}\right|^2 v\otimes v\colon D_x^2 r dv dx.$$

This gives

$$\frac{d}{dt}\mathbb{E}\varphi_1(\widehat{f}, r_t(r,n), m_t(n)) = -\mathbb{E}\int\int \left|\widehat{f}\right|^2 v\otimes v\colon D_x^2 r_t(r,n) dv dx. \tag{5.71}$$

We set

$$\begin{aligned}\varphi_1(\rho,r,n) &:= \mathbb{E}\int_0^{+\infty}\int\int \rho^2 v\otimes v\colon D_x^2 r_t(r,n) dx dv dt\\ &= \int\int \rho^2 v\otimes v\colon D_x^2\left(\frac{r_t(r,n)}{\lambda} + R(n)\right) dx dv.\end{aligned}$$

By linearity, $\mathbb{E}\varphi_1(\rho, r_t(r,n), m_t(n)) = 0$ and (5.71) holds. Moreover,

$$|\varphi_1(\widehat{f},r,n)| \leq C\left\|\widehat{f}\right\|_{L^2}^2 \leq C\left\|\widehat{f}\right\|_{L^2(M(r)^{-1})}^2, \tag{5.72}$$

$$|A\varphi_1(\widehat{f},r,n)| \leq C\left\|\widehat{f}\right\|_{L^2}^2 \leq C\left\|\widehat{f}\right\|_{L^2(M(r)^{-1})}^2, \tag{5.73}$$

thanks to Lemma 5.7. Finally, thanks to (5.10),

$$\mathscr{L}_T * \varphi_(\rho,r,n) = (T\rho, D\varphi_1(\rho,r,n)) = 0. \tag{5.74}$$

We now set $\varphi^\varepsilon(f,r,n) := \varphi(f,r,n) + \varepsilon\varphi_1(\widehat{f},r,n)$. By construction of φ_1, choosing α and ε small enough such that $2\lambda\theta - \alpha - \varepsilon C > \lambda\theta$, we get, using (5.74) and the estimates (5.67), (5.69) and (5.70),

$$\mathscr{L}^\varepsilon\varphi^\varepsilon(f^\varepsilon(s),\tilde{\eta}_s,\eta_s) \leq \tilde{C}_\alpha \left\|f^\varepsilon(s)\right\|^2_{L^2((\overline{M}_{t/\varepsilon^2})^{-1})}. \tag{5.75}$$

Let us define

$$\mathcal{M}_t^\varepsilon := \mathcal{P}_t^\varepsilon\varphi^\varepsilon(f_0,\tilde{\eta}_0,\eta_0) - \varphi^\varepsilon(f_0,\tilde{\eta}_0,\eta_0) - \int_0^t \mathcal{L}^\varepsilon\varphi^\varepsilon(f^\varepsilon(s),\tilde{\eta}_s,\eta_s) ds.$$

Then, thanks to (5.75), we obtain for ε small enough,

$$\mathcal{P}_t^\varepsilon\varphi^\varepsilon(f_0,\tilde{\eta}_0,\eta_0) \leq C + \tilde{C}_\alpha\int_0^t \left\|f^\varepsilon(s)\right\|^2_{L^2((\overline{M}_{t/\varepsilon^2})^{-1})} ds + \sup_{s\in[0,t]}|\mathcal{M}_s^\varepsilon|.$$

We deduce in particular that

$$\mathcal{P}_t^\varepsilon\varphi^\varepsilon(f_0,\tilde{\eta}_0,\eta_0) \leq C_p + C_p\int_0^t \left\|f^\varepsilon(s)\right\|^{2p}_{L^2((\overline{M}_{t/\varepsilon^2})^{-1})} ds + \sup_{s\in[0,t]}|\mathcal{M}_s^\varepsilon|^p. \tag{5.76}$$

Thanks to (5.44) in Proposition 5.6, $(\mathcal{M}_t^\varepsilon)_t$ is a martingale with quadratic variation

$$\langle \mathcal{M}^\varepsilon, \mathcal{M}^\varepsilon \rangle_t = \int_0^t \left(\mathscr{L}^\varepsilon |\varphi^\varepsilon|^2 - 2\varphi^\varepsilon \mathscr{L}^\varepsilon \varphi^\varepsilon \right) (f^\varepsilon(s), \overline{r}_s^\varepsilon, \overline{m}_s^\varepsilon)\, ds.$$

In particular, $\mathbb{E}\mathcal{M}_t^\varepsilon = \mathbb{E}\mathcal{M}_0^\varepsilon = 0$.

Since $D_f|\varphi^\varepsilon| - 2\varphi^\varepsilon D_f \varphi^\varepsilon = 0$ and $A|\varphi^\varepsilon|^2 = 0$, $A\varphi^\varepsilon = 0$ (since φ^ε does not depend on n), we obtain

$$\langle \mathcal{M}^\varepsilon, \mathcal{M}^\varepsilon \rangle_t = \int_0^t \left(A|\varphi_1|^2 - 2\varphi_1 A\varphi_1 \right) (f^\varepsilon(s), \overline{r}_s^\varepsilon, \overline{m}_s^\varepsilon)\, ds.$$

Thanks to (5.72) and (5.73), we have

$$\left| A|\varphi_1|^2 - 2\varphi_1 A\varphi_1 \right| (f, r, n) \leq C \|f\|^4_{L^2(M(r)^{-1})}.$$

By the Hölder inequality, we have for $q \geq 1$,

$$\mathbb{E}\, |\langle \mathcal{M}^\varepsilon, \mathcal{M}^\varepsilon \rangle_t|^q \leq C \int_0^t \mathbb{E}\, \|f^\varepsilon(s)\|^{4q}_{L^2(M(r)^{-1})}\, ds.$$

Since $\mathcal{M}^\varepsilon$ is a martingale with $\mathbb{E}\mathcal{M}_t^\varepsilon = 0$, the Burkholder-Davis-Gundy inequality yields

$$\mathbb{E} \sup_{s\in[0,t]} |\mathcal{M}_s^\varepsilon|^p \leq C\mathbb{E} \langle \mathcal{M}^\varepsilon, \mathcal{M}^\varepsilon \rangle_t^{p/2} \leq C \int_0^t \mathbb{E}\, \|f^\varepsilon(s)\|^{2p}_{L^2(M(r)^{-1})}\, ds. \tag{5.77}$$

Gathering (5.76) and (5.77), we get

$$\mathbb{E}\, \|f^\varepsilon(t)\|^{2p}_{L^2((\overline{M}_{t/\varepsilon^2})^{-1})} \leq C + C\mathbb{E} \int_0^t \|f^\varepsilon(s)\|^{2p}_{L^2((\overline{M}_{t/\varepsilon^2})^{-1})}\, ds$$

Thanks to Grönwall's Lemma, there exists $C > 0$ such that

$$\mathbb{E} \sup_{t\in[0,\tau]} \|f^\varepsilon(t)\|^{2p}_{L^2((\overline{M}_{t/\varepsilon^2})^{-1})} \leq C.$$

By monotonicity of $t \mapsto \int_0^t \|f^\varepsilon(s)\|^{2p}_{L^2((\overline{M}_{t/\varepsilon^2})^{-1})}\, ds$, we get

$$\mathbb{E} \sup_{t\in[0,\tau]} \int_0^t \|f^\varepsilon(s)\|^{2p}_{L^2((\overline{M}_{t/\varepsilon^2})^{-1})}\, ds \leq \mathbb{E} \int_0^T \|f^\varepsilon(s)\|^{2p}_{L^2((\overline{M}_{t/\varepsilon^2})^{-1})}\, ds \leq C. \tag{5.78}$$

Plugging (5.78) and (5.77) back into (5.76), we get the bound

$$\mathbb{E} \sup_{s\in[0,\tau]} \|f^\varepsilon(s)\|^{2p}_{L^2((\overline{M}_{t/\varepsilon^2})^{-1})} \leq C,$$

which proves the proposition.

□

Corollary 5.8. *Assume (5.16). Then, for all $T > 0$, there exists $C > 0$ such that, for all $\varepsilon > 0$,*

$$\mathbb{E} \sup_{t\in[0,T]} \|\rho^\varepsilon(t)\|_{L^2(\mathbb{T}^d)} \leq C. \tag{5.79}$$

Démonstration. Using the same argument as in the proof of Lemma 5.7, we get (5.79) thanks to Proposition 5.5. □

5.6.2 Tightness

Proposition 5.9. *Let $\tau > 0$ and $\delta > 0$. Assume that (5.3), (5.8), (5.9), (5.11) and (5.12) hold. Then, the sequence $(\rho^\varepsilon)_\varepsilon$ is tight in $C([0,\tau]; H^{-\delta}(\mathbb{T}^d))$.*

Démonstration. Let $(p_j)_{j\geq 1}$ be a complete orthonormal system in $L^2(\mathbb{T}^d)$, let $\gamma > \max(2,d)$ and let

$$\Xi_\gamma = (\mathrm{Id} - \Delta_x)^{-\gamma/2}.$$

Then, Ξ_γ is Hilbert-Schmidt on $L^2(\mathbb{T}^d)$ and satisfies $\|\rho\|_{H^{-\gamma}(\mathbb{T}^d)} = \|\Xi_\gamma \rho\|_{L^2(\mathbb{T}^d)}$ since $\gamma > d$. We set

$$\varphi_j(\rho) := (\Xi_\gamma \rho, p_j).$$

Then, φ_j is linear (hence subquadratic) and regularizing as in Definition 5.4. Let $\varphi_{j,1}$ be the good test function defined by (5.38).

We set $\varphi_j^\varepsilon(f,n) := \varphi\left(\widehat{f}\right) + \varepsilon\varphi_1(f,n)$,

$$M_j^\varepsilon(t) = \varphi_j^\varepsilon(f^\varepsilon(t), \overline{m}_t^\varepsilon) - \varphi_j^\varepsilon(f_0^\varepsilon, \overline{m}_0^\varepsilon) - \int_0^t \mathscr{L}^\varepsilon \varphi_j^\varepsilon\left(f^\varepsilon(s), \overline{m}_s^\varepsilon\right) ds$$

and

$$\begin{aligned}\Theta_j^\varepsilon(t) &:= \varphi_j(\rho_0^\varepsilon) + \int_0^t \mathscr{L}^\varepsilon \varphi_j^\varepsilon\left(f^\varepsilon(s), \overline{m}_s^\varepsilon\right) ds + M_j^\varepsilon(t) \\ &= \varphi_j(\rho_0^\varepsilon) + \varphi_j^\varepsilon\left(f^\varepsilon(t), \overline{m}_t^\varepsilon\right) - \varphi_j^\varepsilon\left(f_0^\varepsilon, \overline{m}_0^\varepsilon\right).\end{aligned}$$

Then,

$$\begin{aligned}\varphi_j^\varepsilon\left(\rho^\varepsilon(t)\right) - \Theta_j^\varepsilon(t) &= \left[\varphi_j^\varepsilon\left(\rho^\varepsilon(t)\right) - \varphi_j^\varepsilon\left(f^\varepsilon(t), \overline{m}_t^\varepsilon\right)\right] - \left[\varphi_j^\varepsilon\left(\rho_0^\varepsilon\right) - \varphi_j^\varepsilon\left(f_0^\varepsilon, \overline{m}_0^\varepsilon\right)\right]. \\ &= \varepsilon\left(\varphi_{1,j}^\varepsilon\left(\rho^\varepsilon(t)\right) + \varphi_{1,j}^\varepsilon\left(\rho_0^\varepsilon\right)\right).\end{aligned}$$

By the estimates (5.39) and the L^2-bounds of Corollary 5.8, we get

$$\mathbb{E}\sup_{t\in[0,\tau]} \left|\varphi_j(\rho^\varepsilon(t)) - \Theta_j^\varepsilon(t)\right| = \mathcal{O}(\varepsilon). \tag{5.80}$$

Moreover, $\mathbb{E}\sup_{t\in[0,\tau]} \left|\Theta_j^\varepsilon(t)\right| = \mathcal{O}(1)$. Since Ξ_γ is Hilbert-Schmidt the function

$$\Theta^\varepsilon(t) := \Xi_\gamma^{-1} \sum_{j\geq 1} \Theta_j^\varepsilon(t) \Xi_\gamma p_j$$

is almost surely well defined in $H^{-\gamma}(\mathbb{T}^d)$ for all $t \in [0,\tau]$. By (5.80), we obtain

$$\mathbb{E}\sup_{t\in[0,\tau]} \|\rho^\varepsilon(t) - \Theta^\varepsilon(t)\|_{H^{-\gamma}(\mathbb{T}^d)} = \mathcal{O}(\varepsilon). \tag{5.81}$$

We define

$$w(\rho,\sigma) := \sup_{|t-s|<\sigma} \|\rho(t) - \rho(s)\|_{H^{-\gamma}(\mathbb{T}^d)}$$

the modulus of continuity of $\rho \in C([0,\tau];H^{-\sigma}(\mathbb{T}^d))$. By the compact injection $L^2(\mathbb{T}^d) \subset H^{-\gamma}(\mathbb{T}^d)$, the following set is compact in $C([0,\tau];H^{-\gamma}(\mathbb{T}^d))$:

$$\left\{ \rho \in C([0,\tau];H^{-\sigma}(\mathbb{T}^d)) \mid \sup_{t\in[0,\tau]} \|\rho(t)\|_{L^2(\mathbb{T}^d)} \leq \mathcal{C}, \quad w(\rho,\sigma) \leq g(\sigma) \right\},$$

where $\mathcal{C} > 0$ and g satisfies $\lim_{\sigma\to 0} g(\sigma) = 0$, thanks to Ascoli's Theorem. By Prokhorov's Theorem, the tightness of $(\rho^\varepsilon)_\varepsilon$ will follow if, for all $\alpha > 0$, there exists $\mathcal{C} > 0$, such that

$$\mathbb{P}\left(\sup_{t\in[0,\tau]} \|\rho^\varepsilon(t)\|_{L^2} \leq C \right) < \alpha, \tag{5.82}$$

and

$$\lim_{\delta\to 0} \limsup_{\varepsilon\to 0} \mathbb{P}(w(\rho^\varepsilon,\sigma) > \alpha) = 0. \tag{5.83}$$

The estimate (5.82) is straight-forward by the Markov inequality

$$\mathbb{P}\left(\sup_{t\in[0,\tau]} \|\rho^\varepsilon(t)\|_{L^2} > \mathcal{C} \right) \leq \frac{1}{\mathcal{C}} \mathbb{E} \sup_{t\in[0,\tau]} \|\rho^\varepsilon(t)\|_{L^2},$$

and by Corollary 5.8.

We now prove estimate (5.83), which will conclude the proof. Once again, the Markov inequality yields

$$\mathbb{P}\left(w(\rho^\varepsilon,\sigma) > \alpha\right) \leq \frac{1}{\alpha} \mathbb{E} w(\rho^\varepsilon,\sigma). \tag{5.84}$$

To control this last term, we use Corollary 5.8 and use interpolation to check that, for all $\delta_2 > \delta_1 > 0$, there exists ι such that

$$\mathbb{E} w(\rho^\varepsilon,\sigma) = \mathbb{E} \sup_{|t-s|<\sigma} \|\rho^\varepsilon(t) - \rho^\varepsilon(s)\|_{H^{-\delta_1}(\mathbb{T}^d)} \leq C \mathbb{E} \sup_{|t-s|<\sigma} \|\rho^\varepsilon(t) - \rho^\varepsilon(s)\|^\iota_{H^{-\delta_2}(\mathbb{T}^d)},$$

where C is a constant depending on the constant in Corollary 5.8. Therefore, it is sufficient to work with $\delta = \gamma$ since we will recover the result for $\delta > \gamma$. Moreover,

$$\begin{aligned} w(\rho^\varepsilon,\sigma) &= \sup_{t\in[0,\tau]} \|\rho^\varepsilon(t) - \Theta^\varepsilon(t)\|_{H^{-\gamma}(\mathbb{T}^d)} \\ &+ \sup_{|t-s|<\sigma} \|\Theta^\varepsilon(t) - \Theta^\varepsilon(s)\|_{H^{-\gamma}(\mathbb{T}^d)} \\ &+ \sup_{s\in[0,\tau]} \|\rho^\varepsilon(s) - \Theta^\varepsilon(s)\|_{H^{-\gamma}(\mathbb{T}^d)} \\ &= \mathcal{O}(\varepsilon) + w(\Theta^\varepsilon,\sigma). \end{aligned} \tag{5.85}$$

By construction,

$$\Theta^\varepsilon_j(t) - \Theta^\varepsilon_j(s) = \int_s^t \mathscr{L}^\varepsilon_j(f^\varepsilon(s'),\overline{m}^\varepsilon_{s'})ds' + \mathcal{M}^\varepsilon_j(t) - \mathcal{M}^\varepsilon_j(s),$$

for $0 \leq s \leq t \leq \tau$. By Corollary 5.8 and by (5.43), we have

$$\mathbb{E}\left| \int_s^t \mathscr{L}^\varepsilon_j(f^\varepsilon(s'),\overline{m}^\varepsilon_{s'})ds' \right|^4 = \mathcal{O}(|t-s|^4).$$

By Burkholder-Davis-Gundy inequality,

$$\mathbb{E}|\mathcal{M}_j^\varepsilon(t) - \mathcal{M}_j^\varepsilon(s)|^4 = \mathcal{O}\left(\mathbb{E}|\langle \mathcal{M}_j^\varepsilon, \mathcal{M}_j^\varepsilon\rangle(t) - \langle \mathcal{M}_j^\varepsilon, \mathcal{M}_j^\varepsilon\rangle(s)|^2\right).$$

By (5.25) and Corollary 5.8, we obtain

$$\mathbb{E}|\mathcal{M}_j^\varepsilon(t) - \mathcal{M}_j^\varepsilon(s)|^4 = \mathcal{O}(|t-s|^2).$$

The Kolmogorov's criterion hence yields that, for $\alpha < 1/2$,

$$\mathbb{E}\,\|\Theta^\varepsilon\|^4_{W^{\alpha,4}([0,\tau],H^{-\gamma}(\mathbb{T}^d))} = \mathcal{O}(1).$$

Thanks to the embedding

$$W^{\alpha,4}\left([0,\tau];H^{-\gamma}(\mathbb{T}^d)\right) \subset C^{0,\mu}\left([0,\tau];H^{-\gamma}(\mathbb{T}^d)\right), \quad \mu < \alpha - \frac{1}{4},$$

we obtain $\mathbb{E}w(\Theta^\varepsilon, \sigma) = \mathcal{O}(\sigma^\mu)$ for a certain positive μ. Plugging this result in (5.85), and then (5.85) back into (5.84), the equality (5.83) follows.

□

5.6.3 Convergence

We now conclude the proof of Theorem 5.1. Let $\delta > 0$. By Proposition 5.9, we can extract a subsequence, still denoted $(\rho^\varepsilon)_\varepsilon$ and a probability measure $\mathcal{P}$ on $C([0,\tau];H^{-\gamma}(\mathbb{T}^d))$ such that the law $\mathcal{P}^\varepsilon$ satisfies

$$\mathcal{P}^\varepsilon \rightharpoonup \mathcal{P} \quad \text{ on } C([0,\tau];H^{-\gamma}(\mathbb{T}^d)).$$

Let us now prove that $\mathcal{P}$ is a solution of the martingale problem associated to the limit equation (5.57).

By Skohorod representation Theorem [14], since $C([0,\tau];H^{-\gamma}(\mathbb{T}^d))$ is separable, there exists a probability space $(\tilde\Omega, \tilde{\mathcal{F}}, \tilde{\mathbb{P}})$ and some new random variables $\tilde\rho^\varepsilon, \tilde\rho$ with law $\mathcal{P}^\varepsilon$ and $\mathcal{P}$ such that $\tilde\rho^\varepsilon \to \tilde\rho$ in $C([0,\tau];H^{-\gamma}(\mathbb{T}^d))$, $\tilde{\mathbb{P}}$-almost surely.

Let $\varphi \in C^2(L^2(\mathbb{T}^d))$ be regularizing and subquadratic. Let $(\varphi^j)_j$ be a sequence of subquadratic and regularizing functions in $C_b(H^{-\delta}(\mathbb{T}^d))$ converging pointwise to φ. Thanks to Corollary 5.8, the estimate (5.27) still holds, replacing $\|\cdot\|_{L^2_x}$ by $\|\cdot\|_{H^{-\delta}_x}$. By (5.46) and Corollary 5.8, and since ρ^ε and $\tilde\rho^\varepsilon$ have the same law, we have for $0 \le s_1 \le \cdots \le s_k \le s \le t$ and $\psi \in C_b((L^2))$,

$$\left|\tilde{\mathbb{E}}\left(\varphi_j(\tilde\rho^\varepsilon(t)) - \varphi_j(\tilde\rho^\varepsilon(s)) - \int_s^t \mathscr{L}\varphi_j(\tilde\rho^\varepsilon(\sigma))d\sigma\right)\psi\left(\tilde\rho^\varepsilon(s_1),...,\tilde\rho^\varepsilon(s_k)\right)\right| \le C\varepsilon. \tag{5.86}$$

By Vitali's Theorem [15], we can take the limit $\varepsilon \to 0$ in (5.86) and get

$$\left|\tilde{\mathbb{E}}\left(\varphi_j(\tilde\rho(t)) - \varphi_j(\tilde\rho(s)) - \int_s^t \mathscr{L}\varphi_j(\tilde\rho(\sigma))d\sigma\right)\psi\left(\tilde\rho(s_1),...,\tilde\rho^(s_k)\right)\right| = 0.$$

Taking now the limit $j \to \infty$, we have

$$\left|\tilde{\mathbb{E}}\left(\varphi(\tilde\rho(t)) - \varphi(\tilde\rho(s)) - \int_s^t \mathscr{L}\varphi(\tilde\rho(\sigma))d\sigma\right)\psi\left(\tilde\rho(s_1),...,\tilde\rho^(s_k)\right)\right| = 0,$$

thus, $\mathcal{P}$ solves the martingale problem associated to $\mathscr{L}$ with subquadratic and regularizing test functions.

For such a function φ, by (5.25), the $(\mathcal{F}_s)_s$ martingale

$$\mathcal{M}_\varphi(t) := \varphi(\rho(t)) - \int_0^t \mathscr{L}\varphi(\rho(s))ds,$$

has quadratic variation given by

$$\langle \mathcal{M}_\varphi, \mathcal{M}_\varphi \rangle(t) = \mathscr{L}|\varphi|^2 - 2\varphi\mathscr{L}\varphi.$$

From (5.52), we have

$$\begin{aligned}\mathscr{L}|\varphi(\rho(s))|^2 - 2\varphi(\rho(s))\mathscr{L}\varphi(\rho(s)) &= \text{Trace}\left(\left(P\left(\rho(s)\right)\Sigma^{1/2}\right) D\varphi(\rho(s)) \otimes D\varphi(\rho(s)) \left(P\left(\rho(s)\right)\Sigma^{1/2}\right)^*\right) \\ &= \left\| P\left(\rho\right)\Sigma^{1/2} D\varphi(\rho)\right\|_{L^2}^2.\end{aligned}$$

Hence,

$$\begin{aligned}\mathcal{M}(t) = \rho(t) - \rho(0) \quad - \quad \int_0^t \Bigg(&\frac{1}{\lambda^2}\text{div}\left(\left(\lambda K(M) - \mathbb{E}K\nabla_x\eta_0 K\nabla\eta_0\right)\nabla_x\rho(s)\right) \\ &- \frac{1}{\lambda^2}\text{div}\left(\rho(s)\mathbb{E}K\nabla_x\eta_0\text{div}\left(K\nabla\eta_0\right)\right)\Bigg) ds, \end{aligned} \tag{5.87}$$

(check 5.57) is a martingale with quadratic variation $\int_0^t P\left(\rho(s)\right)\Sigma^{1/2}\left(P\left(\rho(s)\right)\Sigma^{1/2}\right)^* ds$. Thanks to martingale representation results, there exists a new probability space and a cylindrical Wiener process W such that

$$\mathcal{M}(t) = \int_0^t P(\rho(s))\Sigma^{1/2} dW(s). \tag{5.88}$$

Pathwise uniqueness of solutions of (5.87)-(5.88) in the space $C([0,\tau], H^{-\delta}(\mathbb{T}^d))$ is a classical result, if we assume (5.19). Hence, the law $\mathcal{P}$ of this solution is uniquely determined. Thus, by uniqueness, the whole sequence $\mathcal{P}^{\uparrow}{}_\varepsilon$ converges to $\mathcal{P}$ weakly in the space of probability measures on $C([0,\tau], H^{-\delta}(\mathbb{T}^d))$.

Annexe A

Données trajectorielles

Dans cette annexe, nous présentons les données dont nous nous servons dans le Chapitre 1. Nous représentons les trajectoires des 22 crapauds constituant nos données, le déplacement quadratique moyen moyenné en temps (TAMSD) correspondant et l'histogramme des déplacements journaliers. Les données présentées dans cette annexe sont issues d'une étude statistique conduite par Gregory Brown, Benjamin Phillips et Richard Shine.

The following annex presents the data set that was used in Chapter 1. Cane toads were radio tracked on a daily basis on the Adelaide River flood plain in tropical Australia during wet season (November to March) 2005, just when the first toads arrived in the area. The dataset we are using is the daily position in UTM coordinates (UTM zone 52L) of 22 toads tracked for a period of time that lasted between 6 and 65 days. All telemetry procedures were carried out under approval of the University of Sydney Animal Ethics Committee (permit L04/11-2005/3/4252).

The toads were given a number between 1 and 21 and one toad has number 49. For all 22 toads we represent hereafter three Figures.

The first Figure is the "raw" data. The data we used is the daily position of the toad in UTM coordinates. In the first figure, we simply represent those position as a point with the corresponding day. We draw a line between consecutive days. When the data of the n-th is missing (the GPS belt on the toad may disfunction), two possibilities occur : either the last and the next location is the same and then we suppose that the toad did not move hence we replace the missing data by this position, or the last and next location are different. In that case, we do not represent the position at the n-th day.
The first position is marked by a black diamond and the number 1. All other positions are marked with a white diamond and the number of the corresponding day.

The second figure represents the TAMSD (check Chapter 1 for a definition) of the trajectory in a log-log scale.

The third figure is a histogram of the daily displacement sorted in classes of size 100 meters. For every toad, we computed the distance travelled between two consecutive days. When one data was missing, we computed the displacement between the last existent data and the next and divided by the number of days between those two positions. There are toads which did not relocate from one day to the next. We represent the number of such events by a blue line on the histogram.

FIGURE A.1 – Toad 1

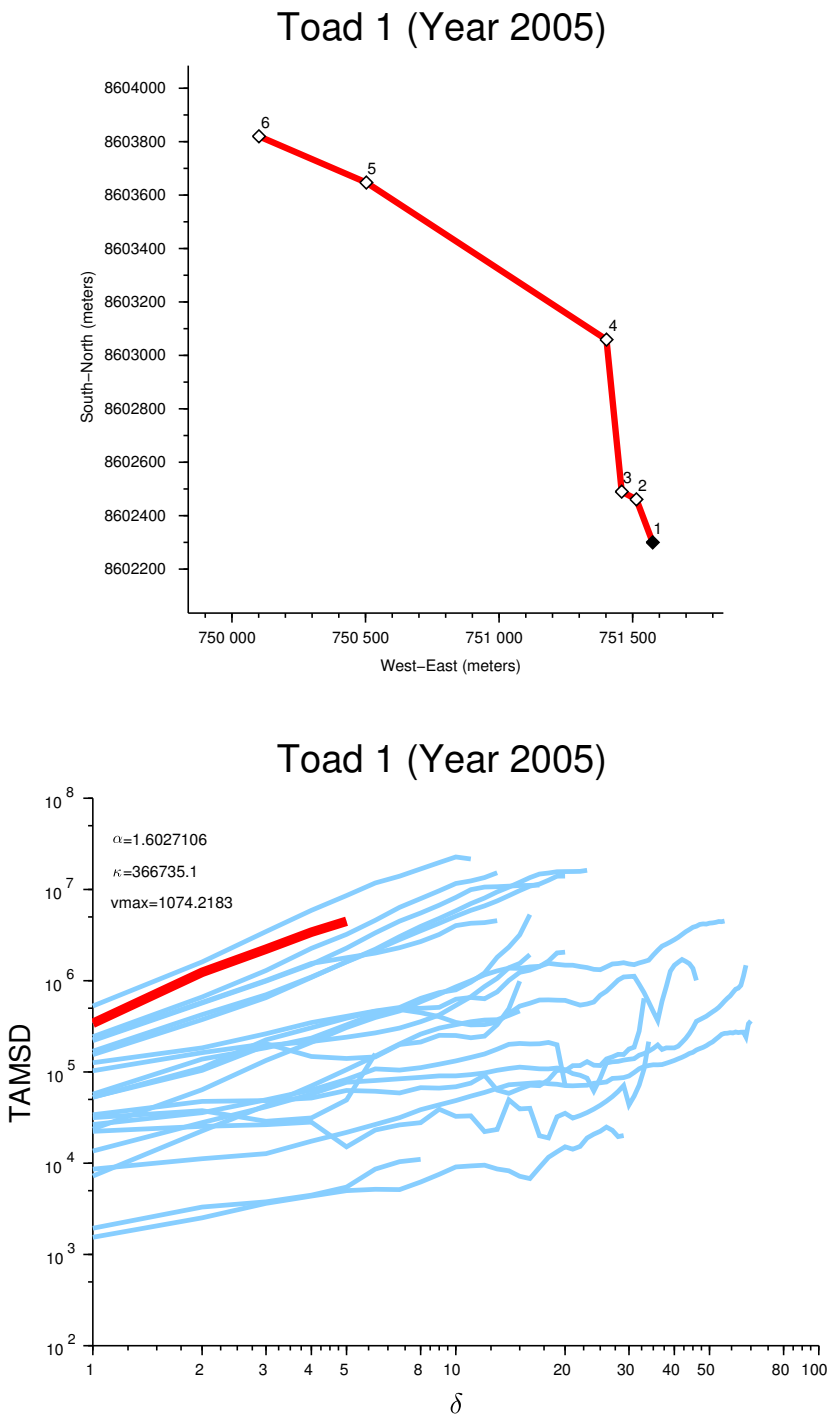

Trajectory and TAMSD of Toad number 1, radio tracked during wet season 2005.
Red line : function $\delta \mapsto \ln(TAMSD(\delta))$.
Light-blue lines : TAMSD of the other radio tracked toads from 2005.
Units : δ (days), $TAMSD(\delta)$ (m^2/day).

FIGURE A.2 – Toad 1

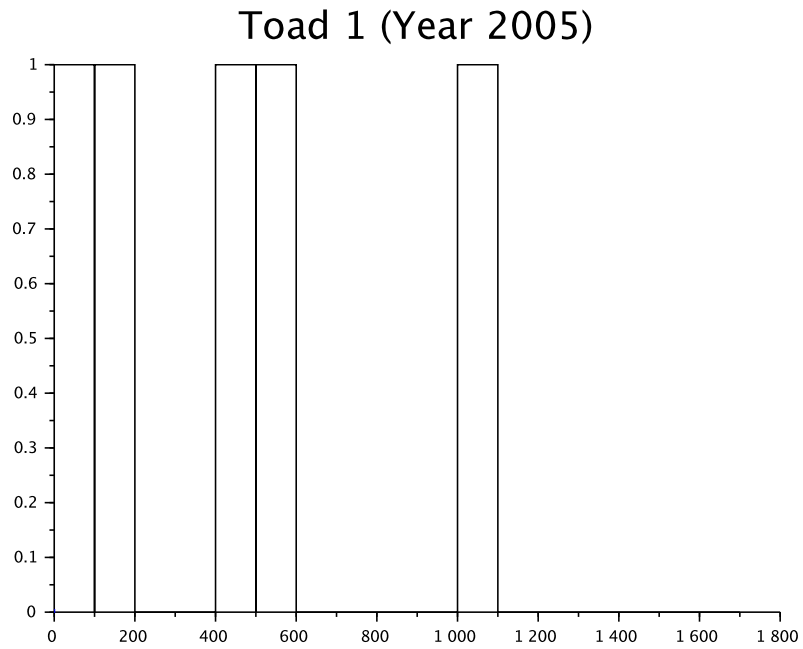

Histogram of the daily displacement of Toad 1. x-axis : velocity (m/day), y-axis : number of data in the class.

FIGURE A.3 – Toad 2

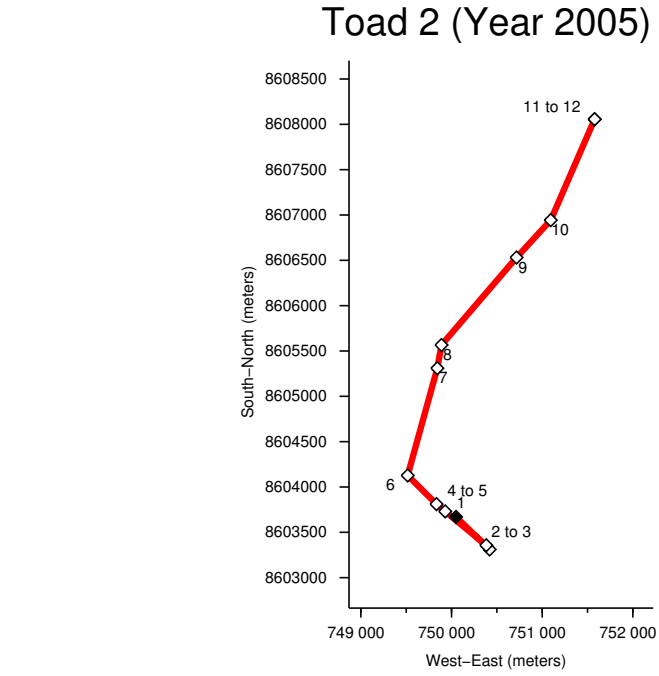

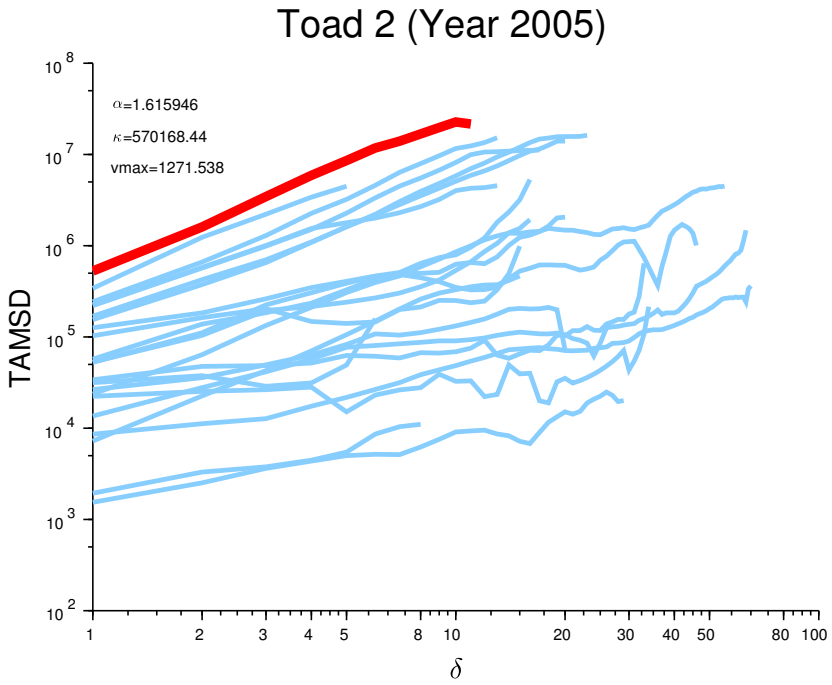

Trajectory and TAMSD of Toad number 2, radio tracked during wet season 2005.
Red line : function $\delta \mapsto \ln(TAMSD(\delta))$.
Light-blue lines : TAMSD of the other radio tracked toads from 2005.
Units : δ (days), $TAMSD(\delta)$ (m^2/day).

FIGURE A.4 – Toad 2

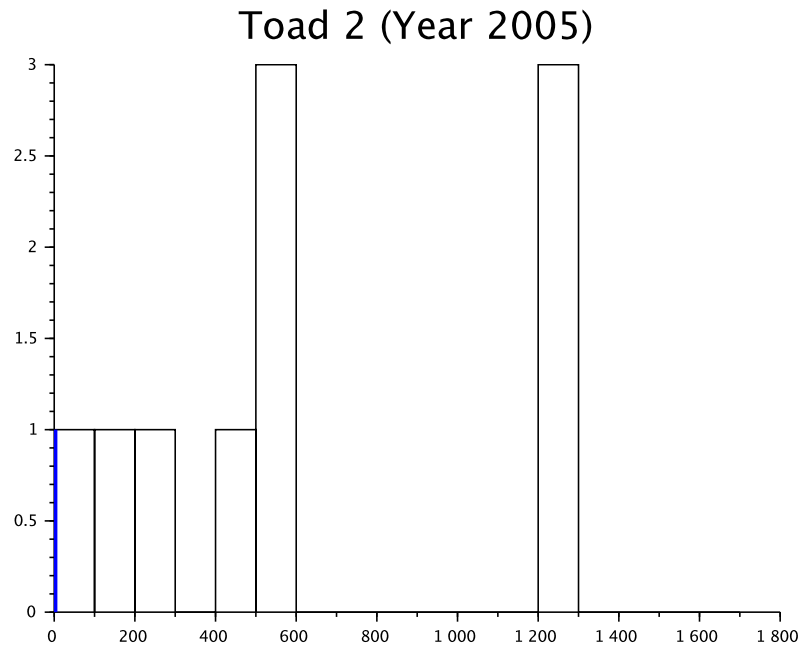

Histogram of the daily displacement of Toad 2. x-axis : velocity (m/day), y-axis : number of data in the class.

FIGURE A.5 – Toad 3

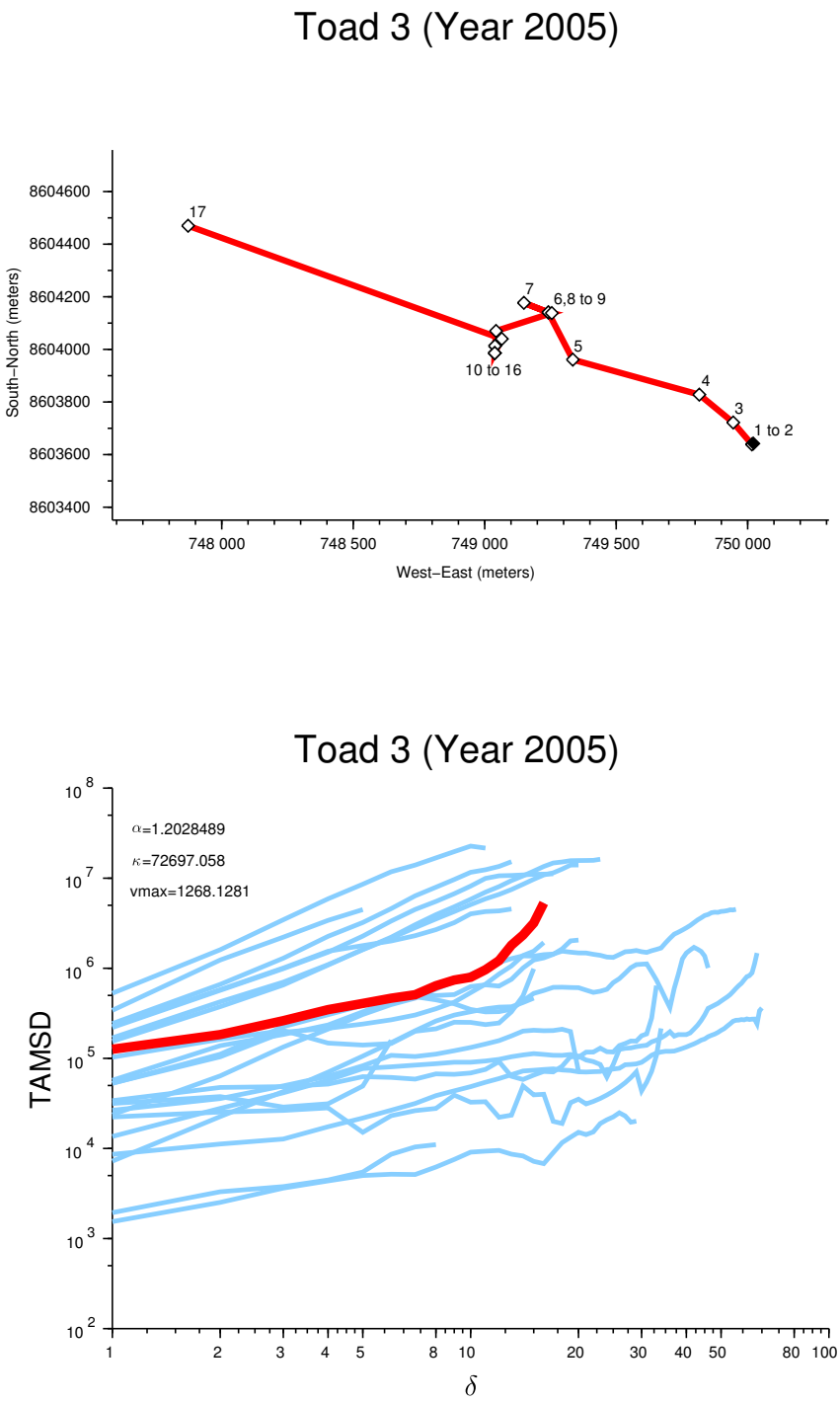

Trajectory and TAMSD of Toad number 3, radio tracked during wet season 2005.
Red line : function $\delta \mapsto \ln(TAMSD(\delta))$.
Light-blue lines : TAMSD of the other radio tracked toads from 2005.
Units : δ (days), $TAMSD(\delta)$ (m^3/day).

FIGURE A.6 – Toad 3

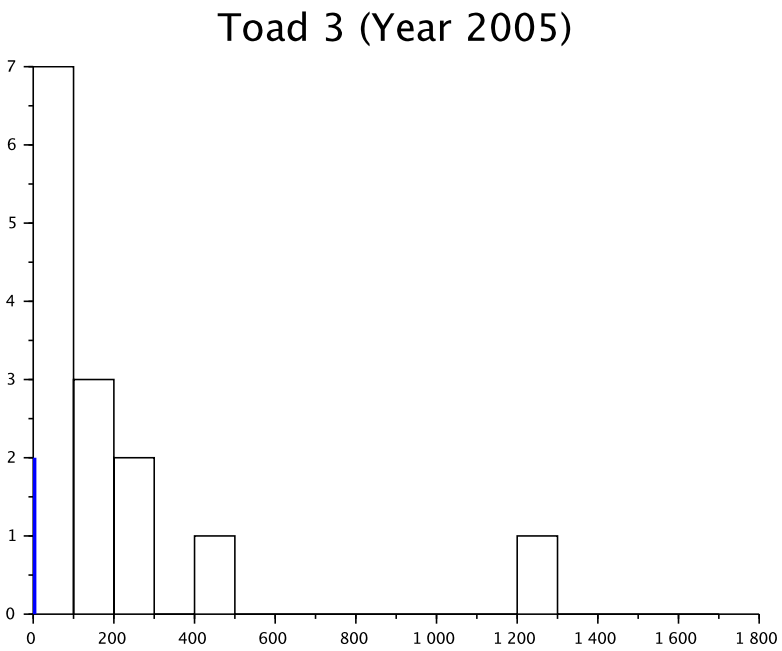

Histogram of the daily displacement of Toad 3. x-axis : velocity (m/day), y-axis : number of data in the class.

FIGURE A.7 – Toad 4

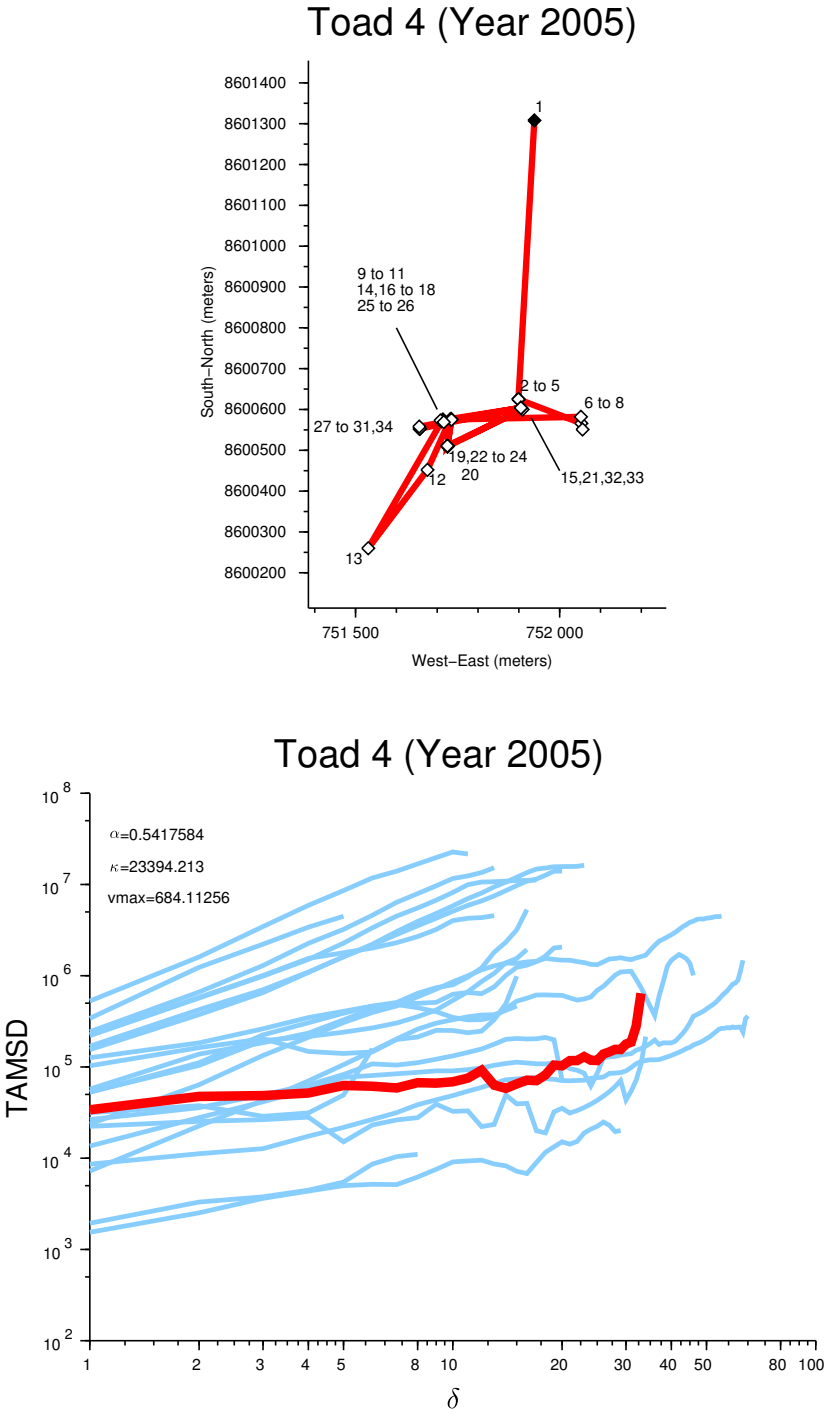

Trajectory and TAMSD of Toad number 4, radio tracked during wet season 2005.
Red line : function $\delta \mapsto \ln(TAMSD(\delta))$.
Light-blue lines : TAMSD of the other radio tracked toads from 2005.
Units : δ (days), $TAMSD(\delta)$ (m^4/day).

FIGURE A.8 – Toad 4

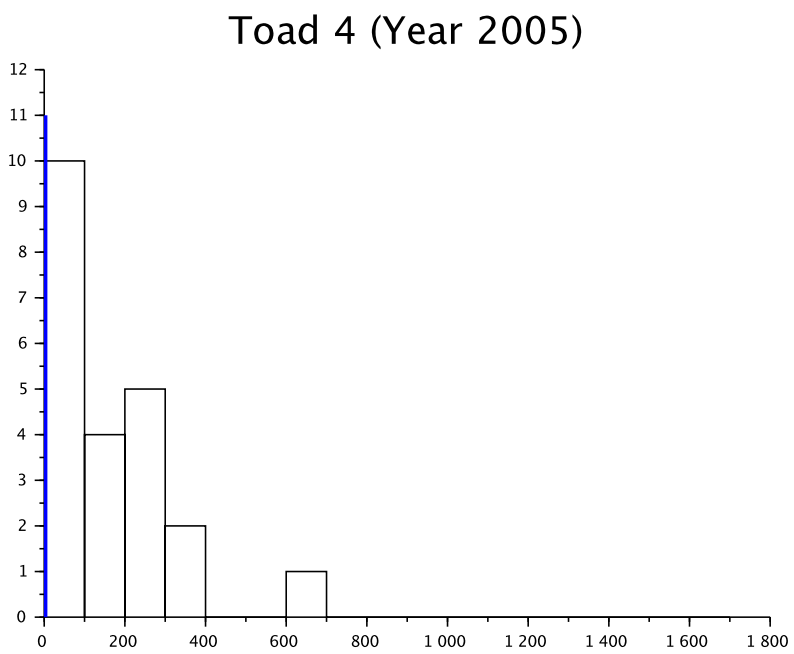

Histogram of the daily displacement of Toad 4. x-axis : velocity (m/day), y-axis : number of data in the class.

FIGURE A.9 – Toad 5

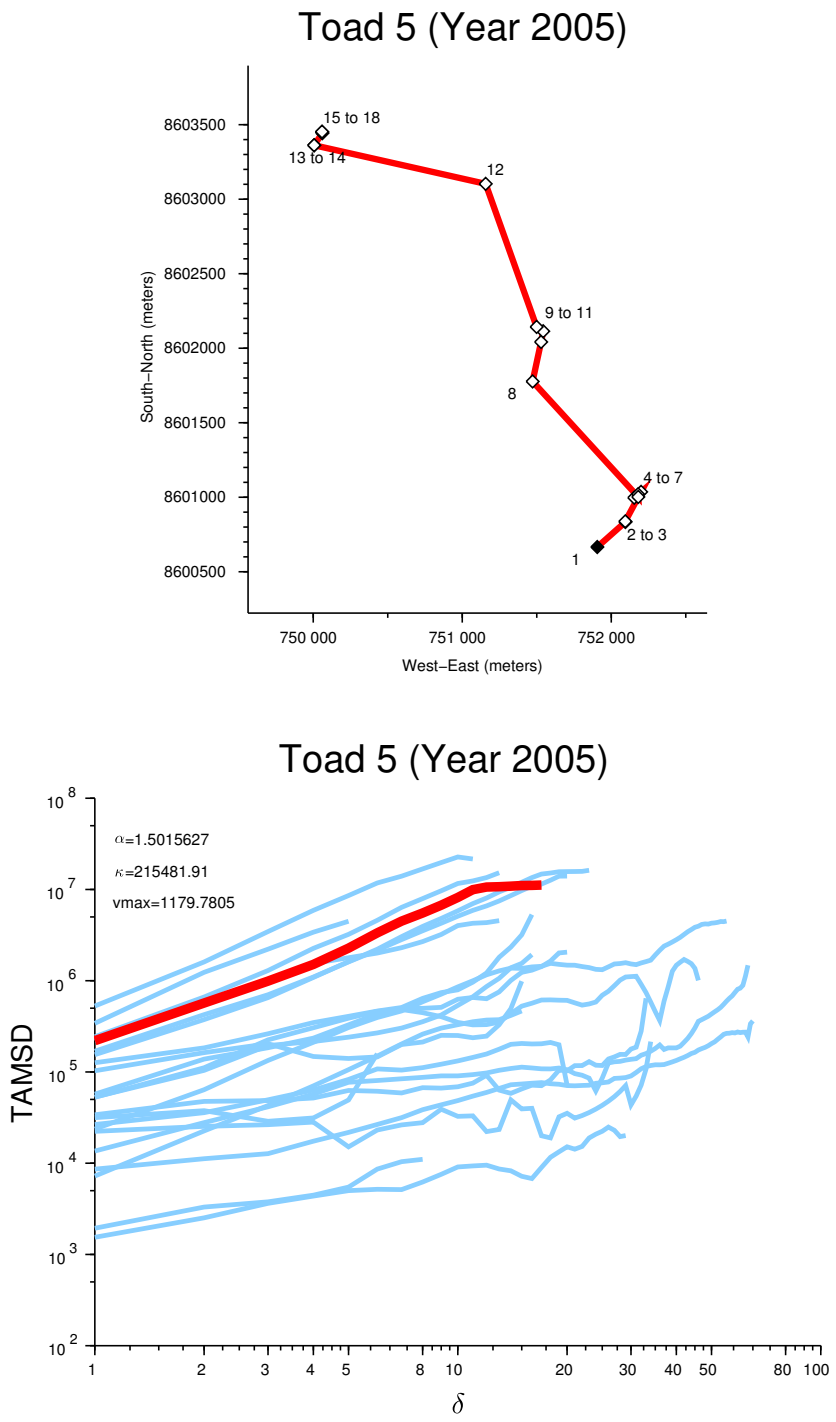

Trajectory and TAMSD of Toad number 5, radio tracked during wet season 2005.
Red line : function $\delta \mapsto \ln(TAMSD(\delta))$.
Light-blue lines : TAMSD of the other radio tracked toads from 2005.
Units : δ (days), $TAMSD(\delta)$ (m^5/day).

FIGURE A.10 – Toad 5

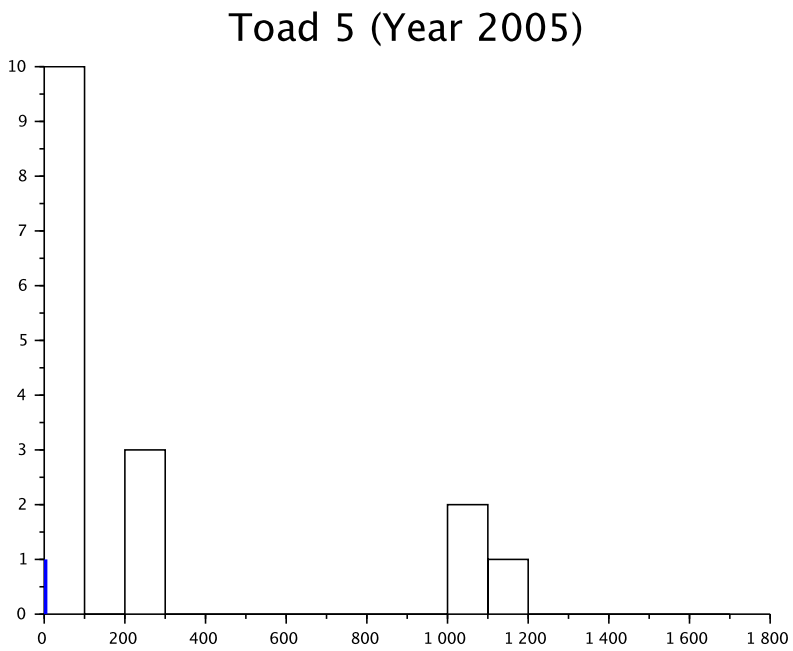

Histogram of the daily displacement of Toad 5. x-axis : velocity (m/day), y-axis : number of data in the class.

FIGURE A.11 – Toad 6

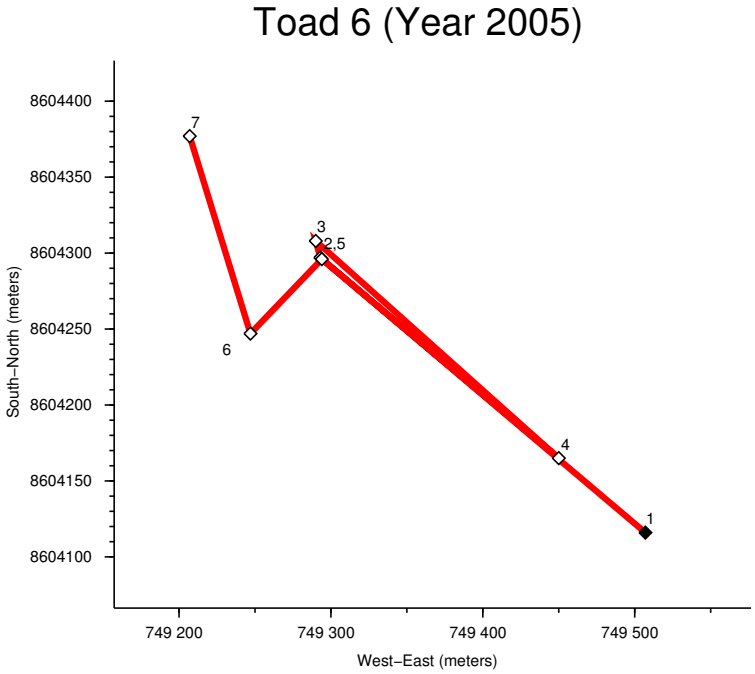

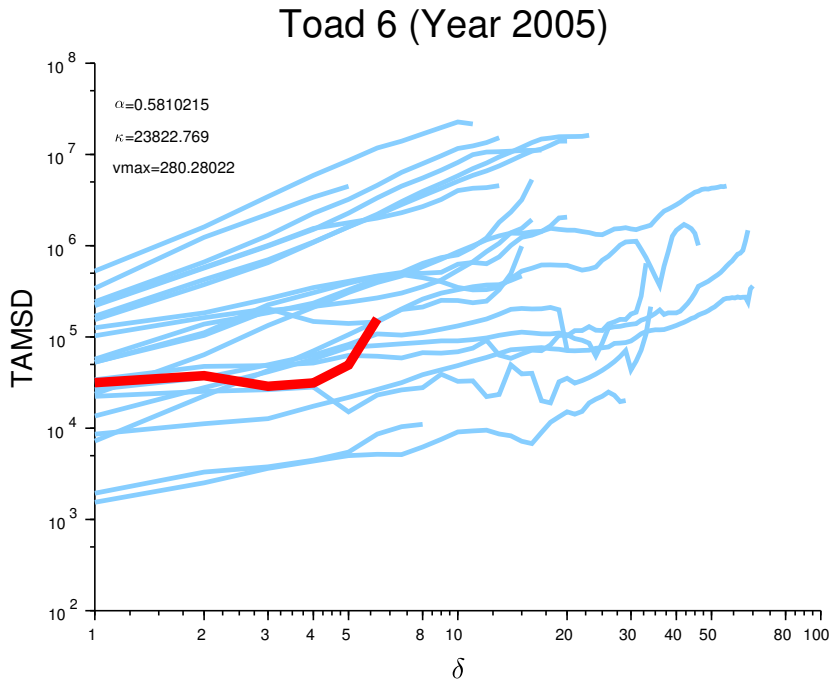

Trajectory and TAMSD of Toad number 6, radio tracked during wet season 2005.
Red line : function $\delta \mapsto \ln(TAMSD(\delta))$.
Light-blue lines : TAMSD of the other radio tracked toads from 2005.
Units : δ (days), $TAMSD(\delta)$ (m^6/day).

FIGURE A.12 – Toad 6

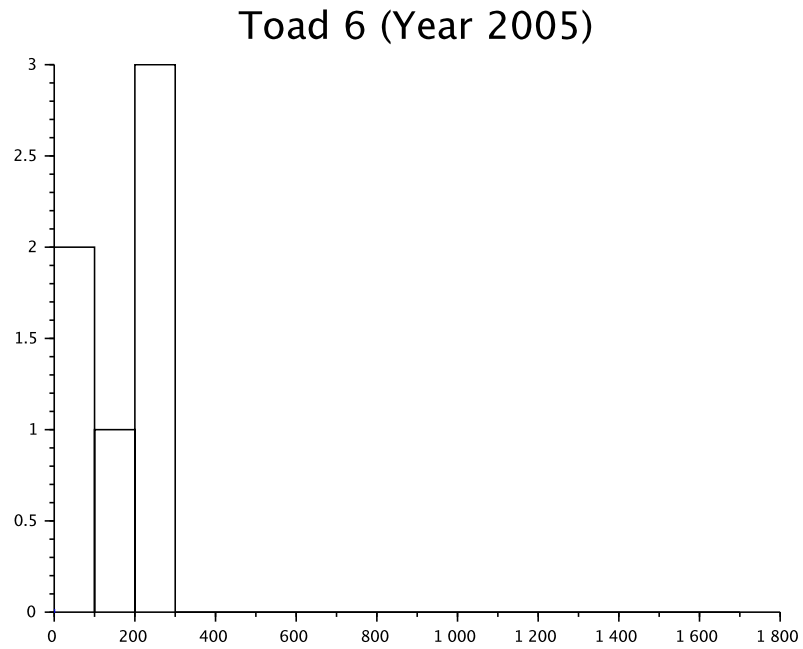

Histogram of the daily displacement of Toad 6. x-axis : velocity (m/day), y-axis : number of data in the class.

FIGURE A.13 – Toad 7

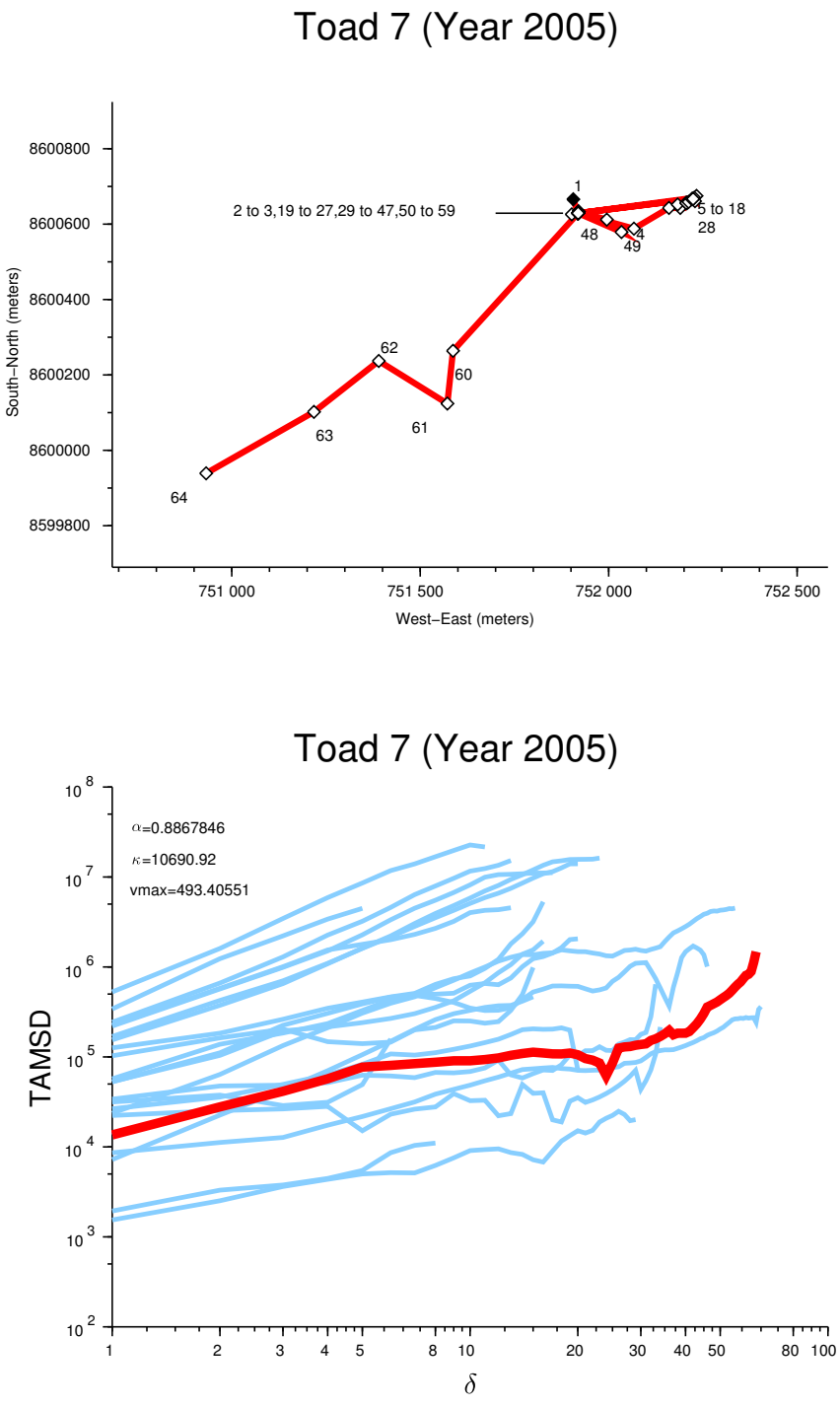

Trajectory and TAMSD of Toad number 7, radio tracked during wet season 2005.
Red line : function $\delta \mapsto \ln(TAMSD(\delta))$.
Light-blue lines : TAMSD of the other radio tracked toads from 2005.
Units : δ (days), $TAMSD(\delta)$ (m^7/day).

FIGURE A.14 – Toad 7

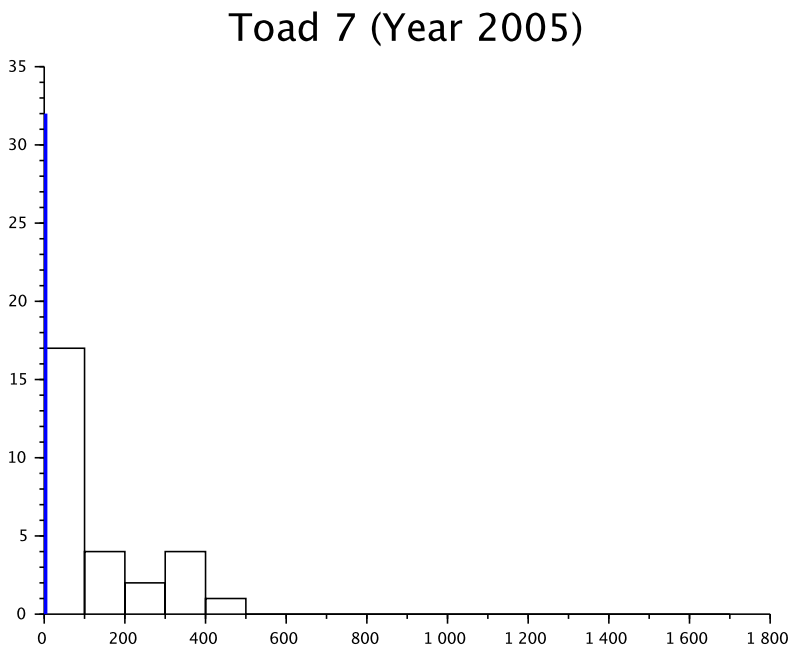

Histogram of the daily displacement of Toad 7. *x*-axis : velocity (m/day), *y*-axis : number of data in the class.

FIGURE A.15 – Toad 8

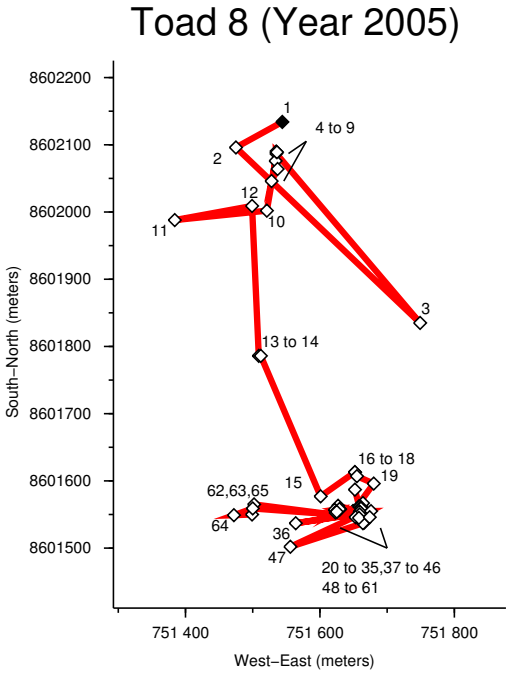

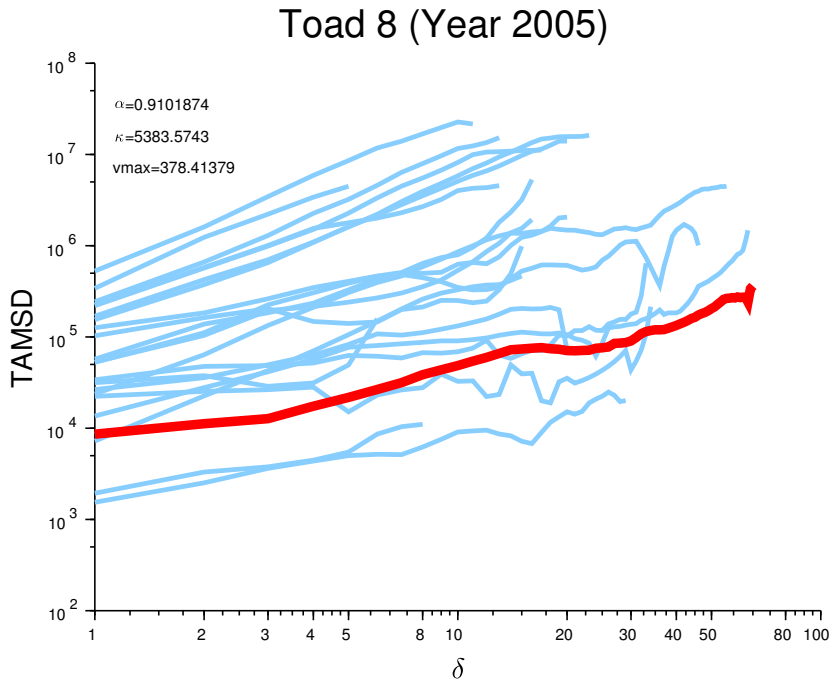

Trajectory and TAMSD of Toad number 8, radio tracked during wet season 2005.
Red line : function $\delta \mapsto \ln(TAMSD(\delta))$.
Light-blue lines : TAMSD of the other radio tracked toads from 2005.
Units : δ (days), $TAMSD(\delta)$ (m^8/day).

FIGURE A.16 – Toad 8

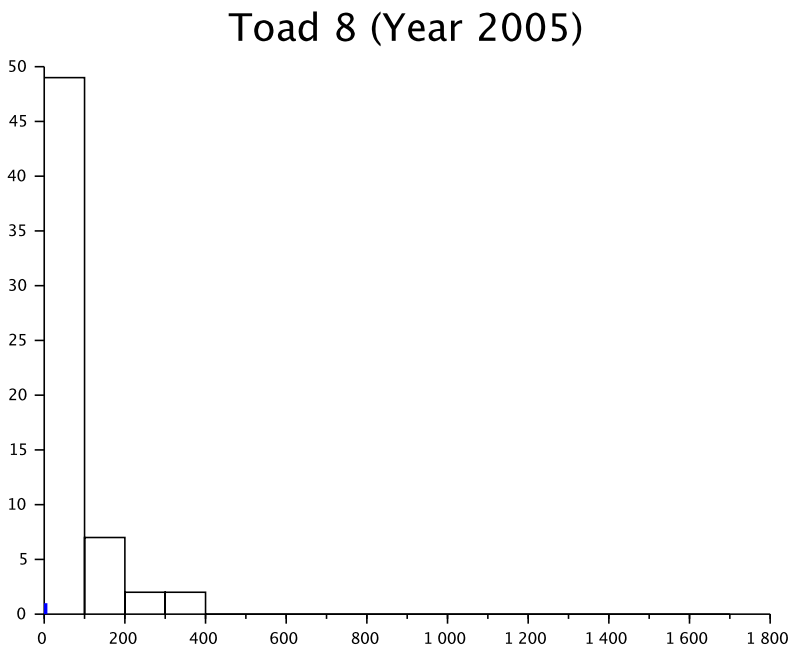

Histogram of the daily displacement of Toad 8. x-axis : velocity (m/day), y-axis : number of data in the class.

FIGURE A.17 – Toad 9

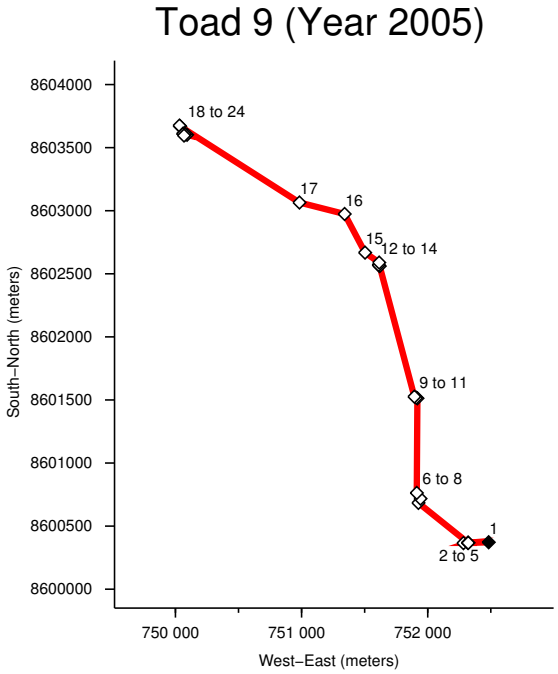

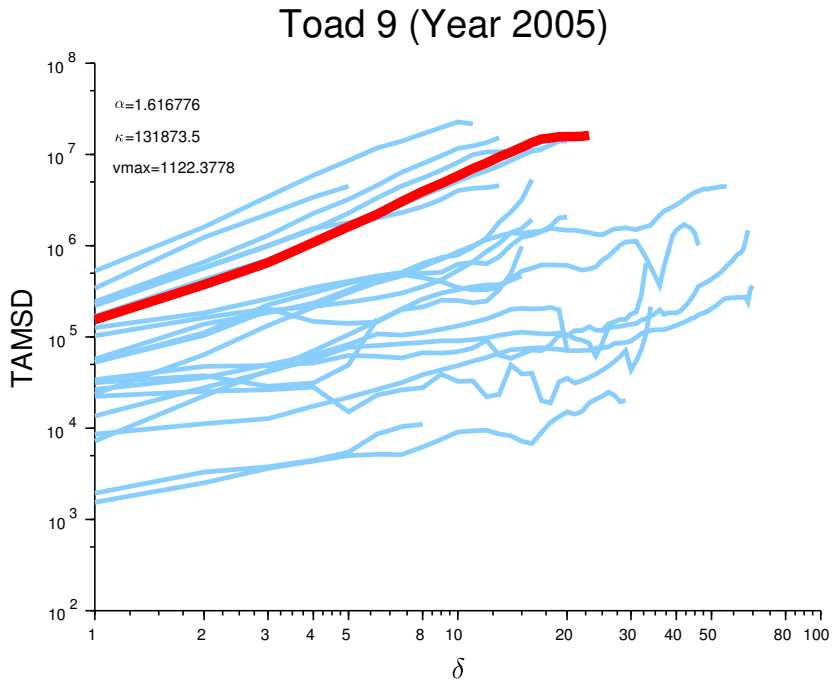

Trajectory and TAMSD of Toad number 9, radio tracked during wet season 2005.
Red line : function $\delta \mapsto \ln(TAMSD(\delta))$.
Light-blue lines : TAMSD of the other radio tracked toads from 2005.
Units : δ (days), $TAMSD(\delta)$ (m^9/day).

FIGURE A.18 – Toad 9

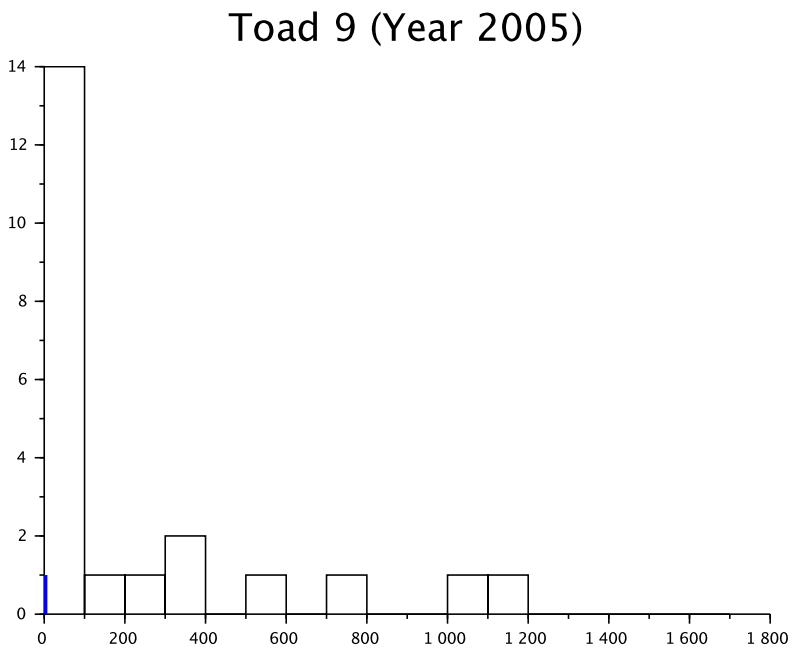

Histogram of the daily displacement of Toad 9. x-axis : velocity (m/day), y-axis : number of data in the class.

FIGURE A.19 – Toad 10

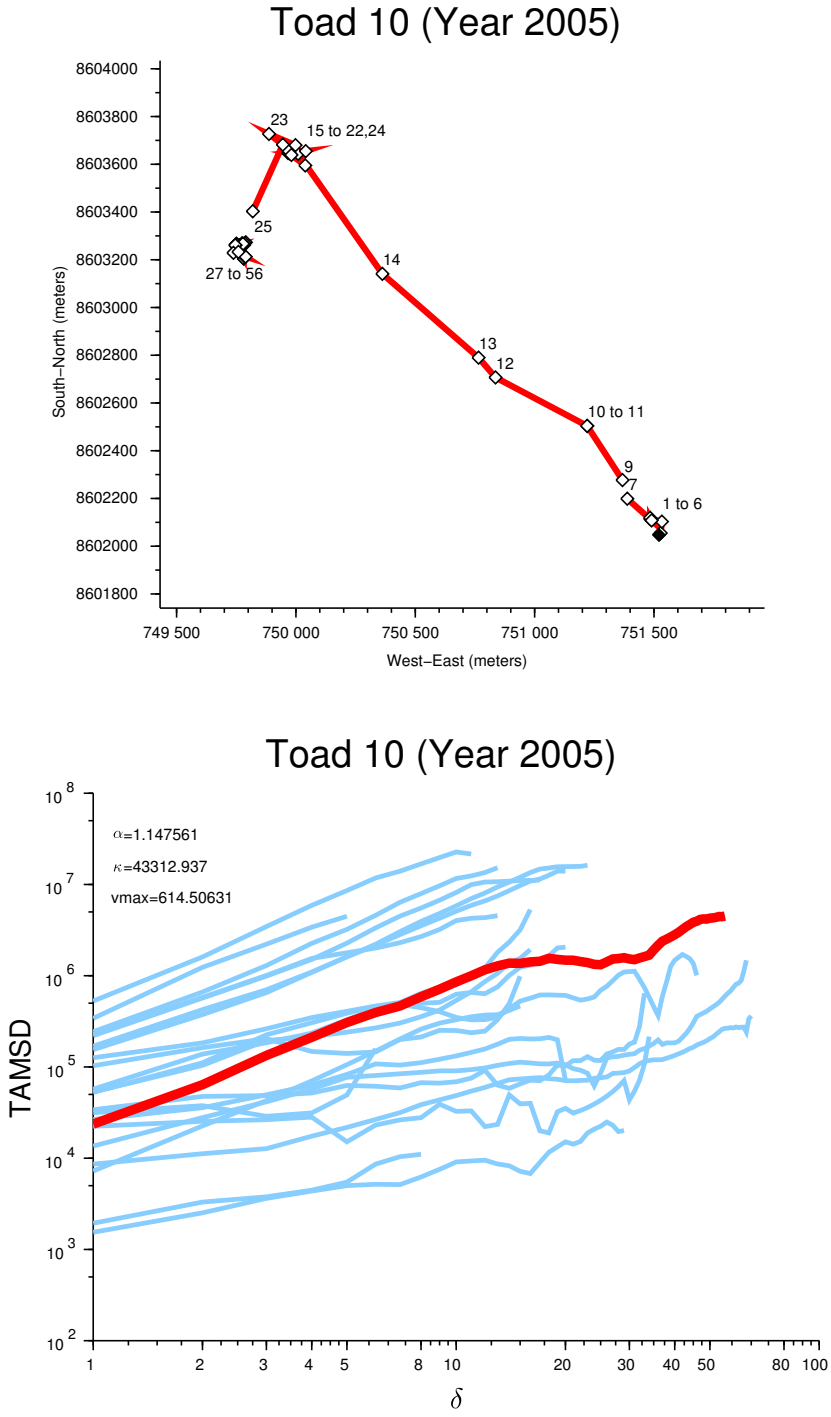

Trajectory and TAMSD of Toad number 10, radio tracked during wet season 2005.
Red line : function $\delta \mapsto \ln(TAMSD(\delta))$.
Light-blue lines : TAMSD of the other radio tracked toads from 2005.
Units : δ (days), $TAMSD(\delta)$ (m^10/day).

Figure A.20 – Toad 10

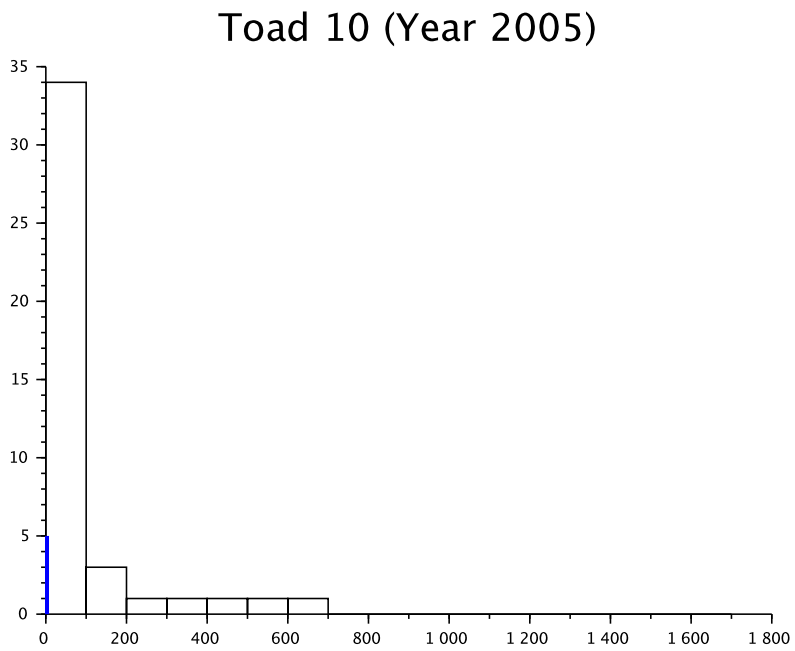

Histogram of the daily displacement of Toad 10. x-axis : velocity (m/day), y-axis : number of data in the class.

FIGURE A.21 – Toad 11

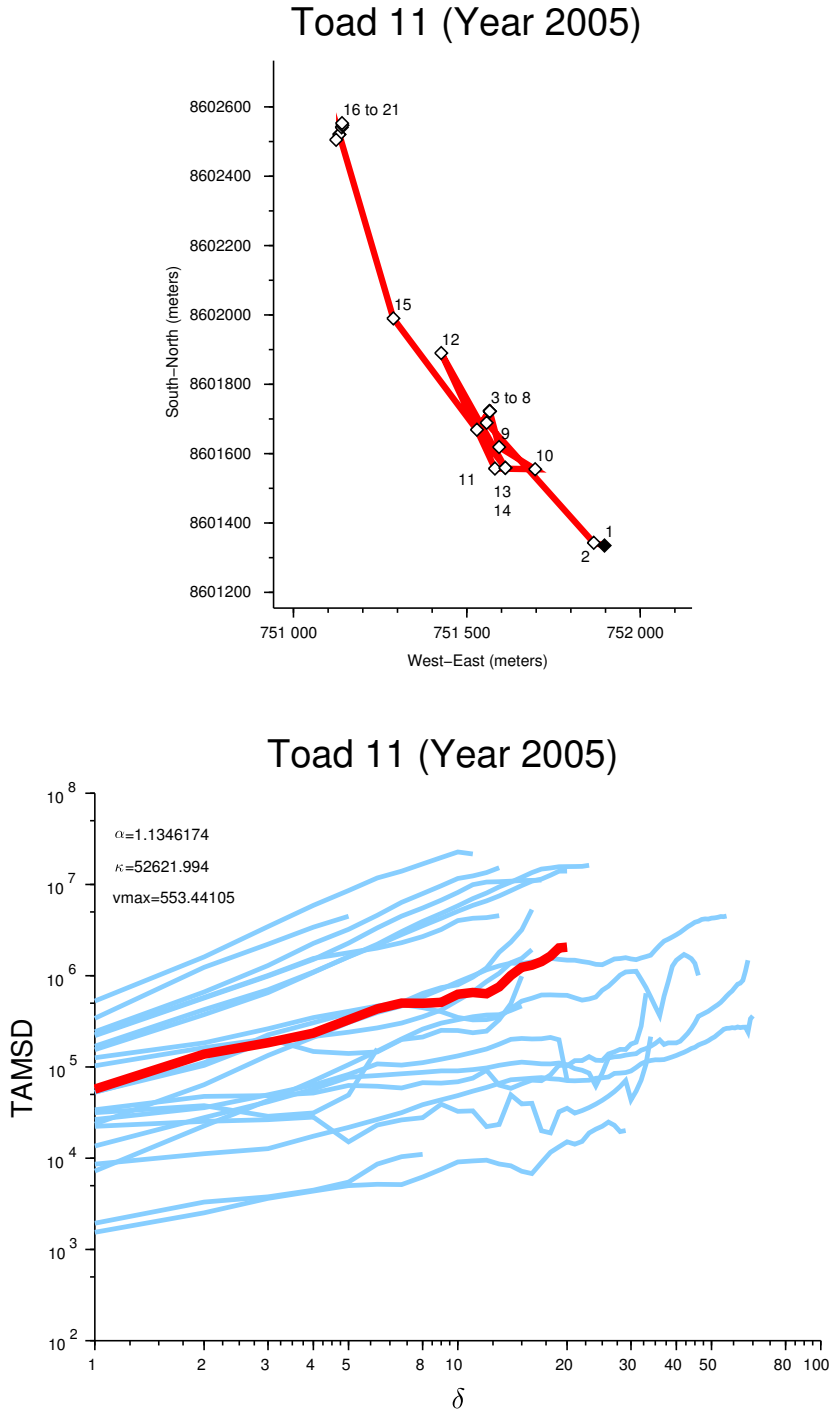

Trajectory and TAMSD of Toad number 11, radio tracked during wet season 2005.
Red line : function $\delta \mapsto \ln(TAMSD(\delta))$.
Light-blue lines : TAMSD of the other radio tracked toads from 2005.
Units : δ (days), $TAMSD(\delta)$ ($m^1 1/day$).

FIGURE A.22 – Toad 11

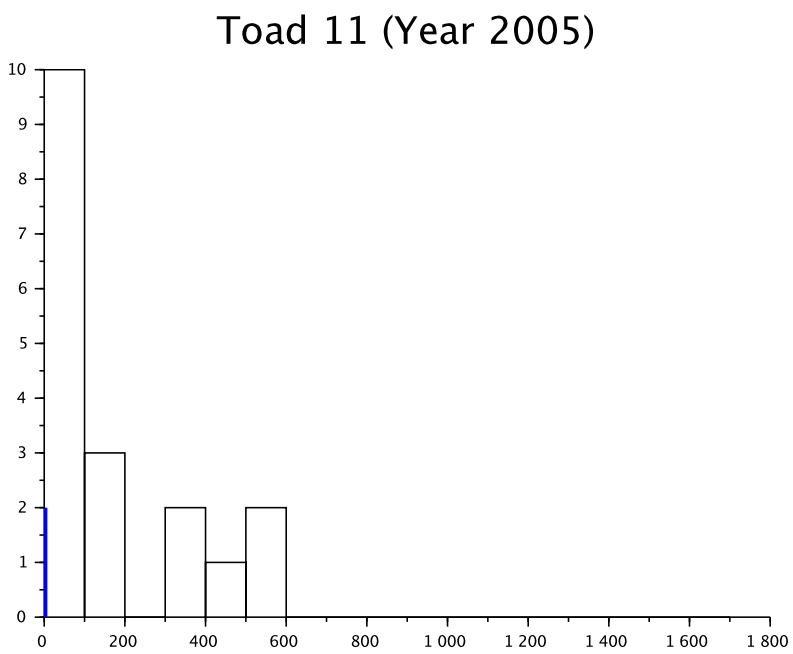

Histogram of the daily displacement of Toad 11. x-axis : velocity (m/day), y-axis : number of data in the class.

FIGURE A.23 – Toad 12

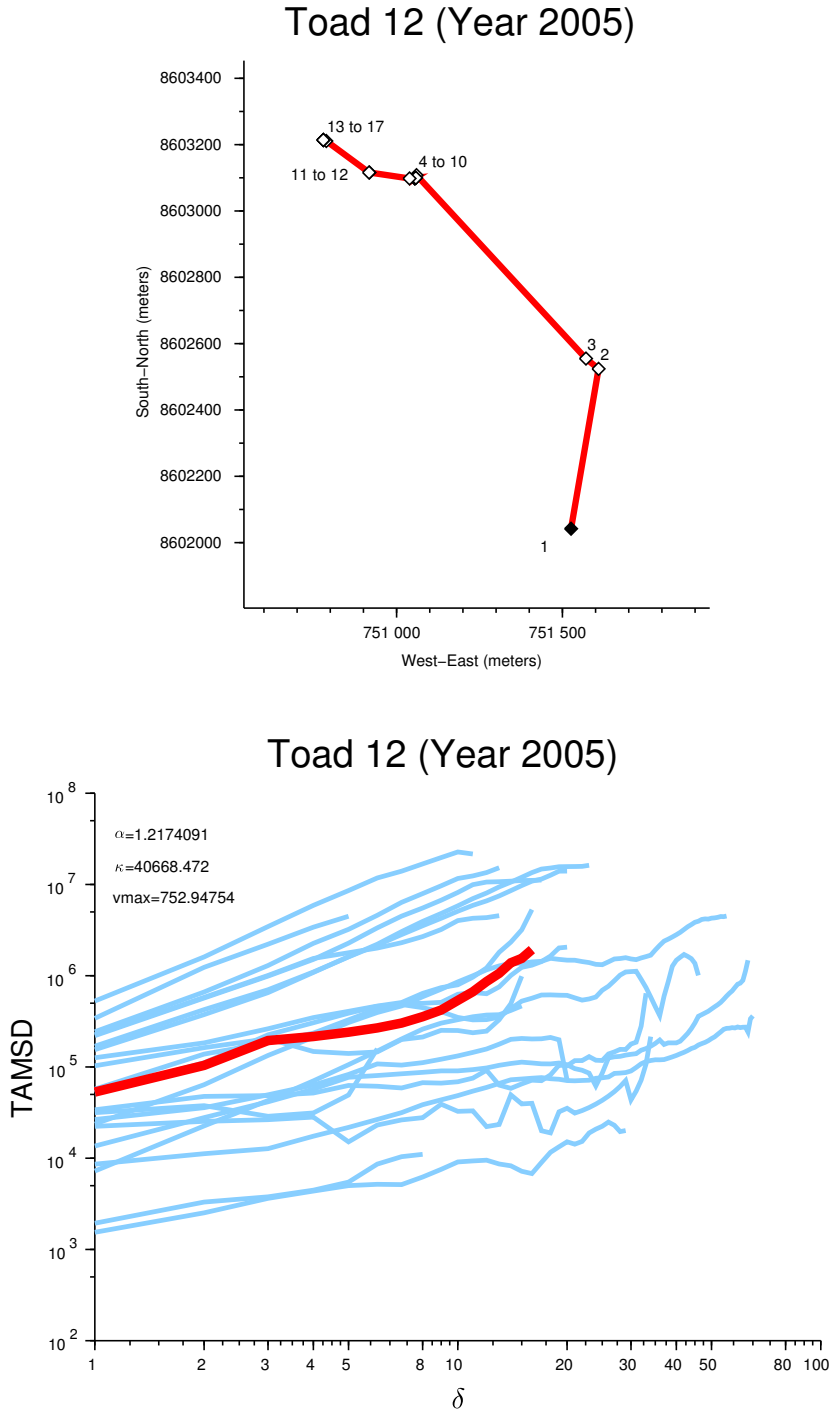

Trajectory and TAMSD of Toad number 12, radio tracked during wet season 2005.
Red line : function $\delta \mapsto \ln(TAMSD(\delta))$.
Light-blue lines : TAMSD of the other radio tracked toads from 2005.
Units : δ (days), $TAMSD(\delta)$ (m^12/day).

FIGURE A.24 – Toad 12

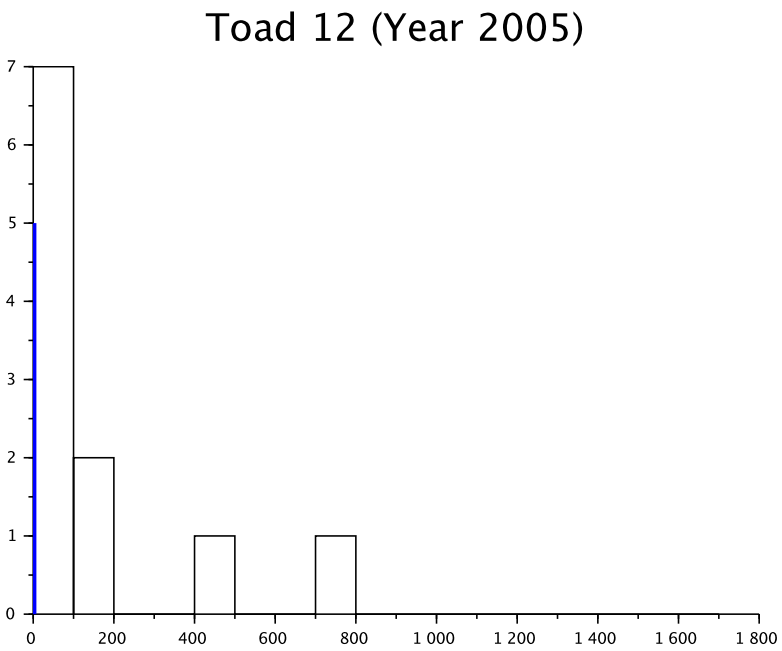

Histogram of the daily displacement of Toad 12. x-axis : velocity (m/day), y-axis : number of data in the class.

FIGURE A.25 – Toad 13

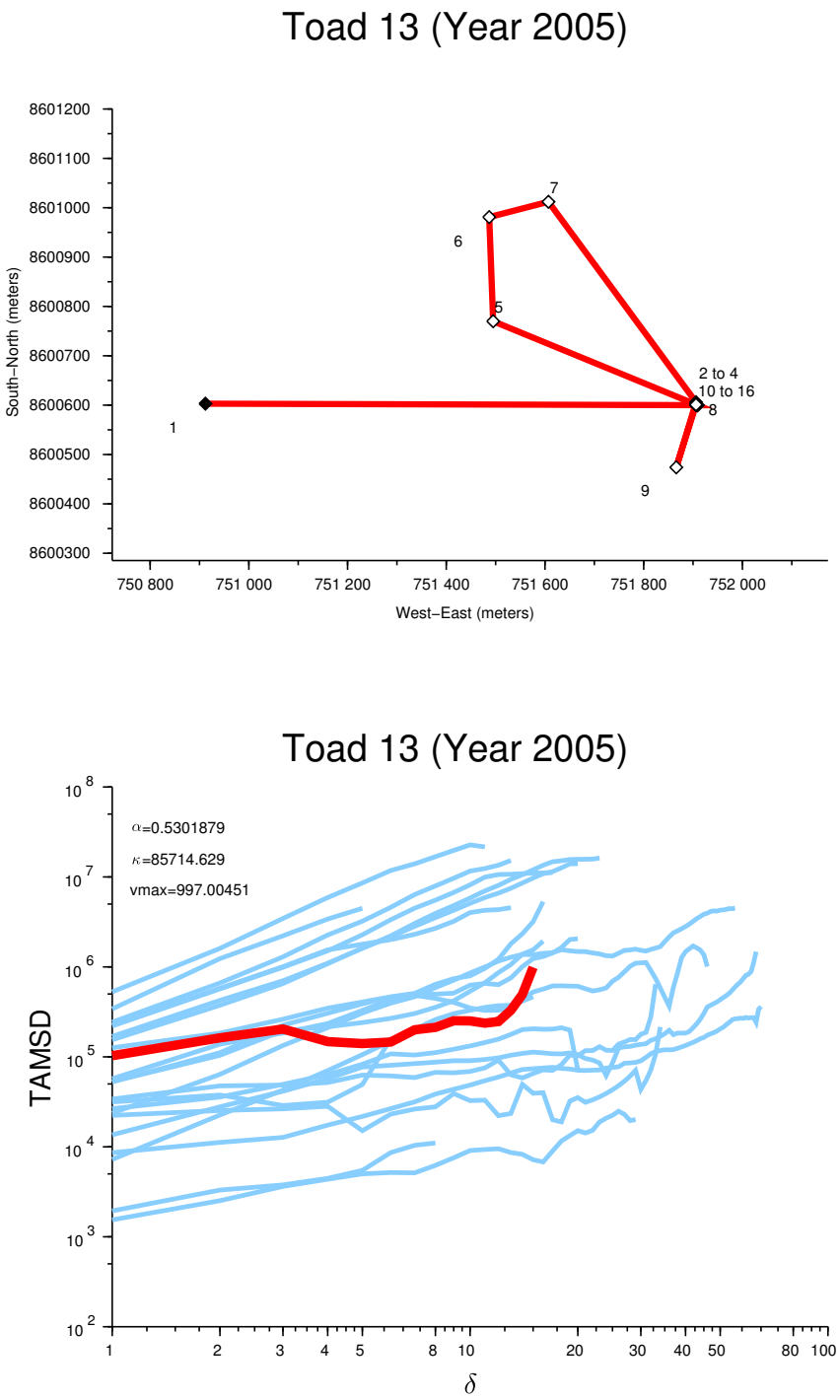

Trajectory and TAMSD of Toad number 13, radio tracked during wet season 2005.
Red line : function $\delta \mapsto \ln(TAMSD(\delta))$.
Light-blue lines : TAMSD of the other radio tracked toads from 2005.
Units : δ (days), $TAMSD(\delta)$ ($m^1 3/day$).

FIGURE A.26 – Toad 13

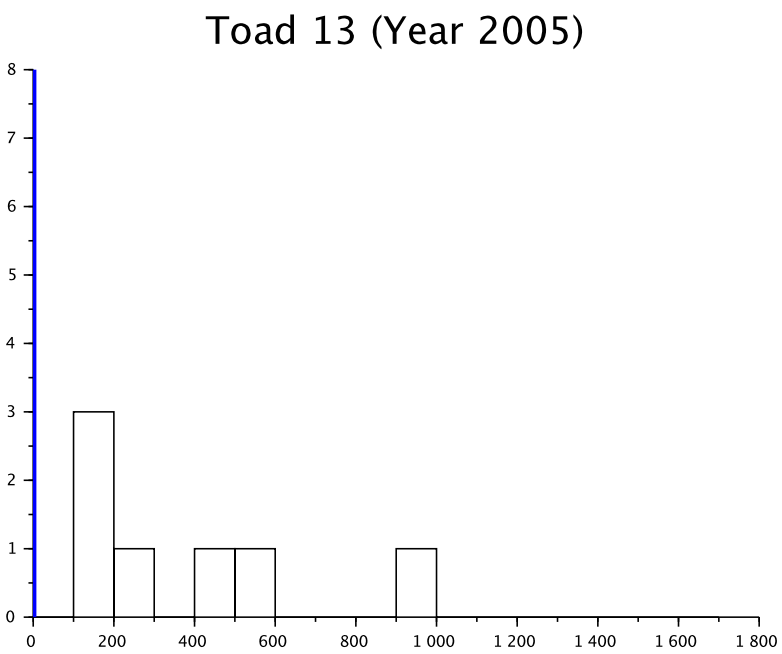

Histogram of the daily displacement of Toad 13. x-axis : velocity (m/day), y-axis : number of data in the class.

FIGURE A.27 – Toad 14

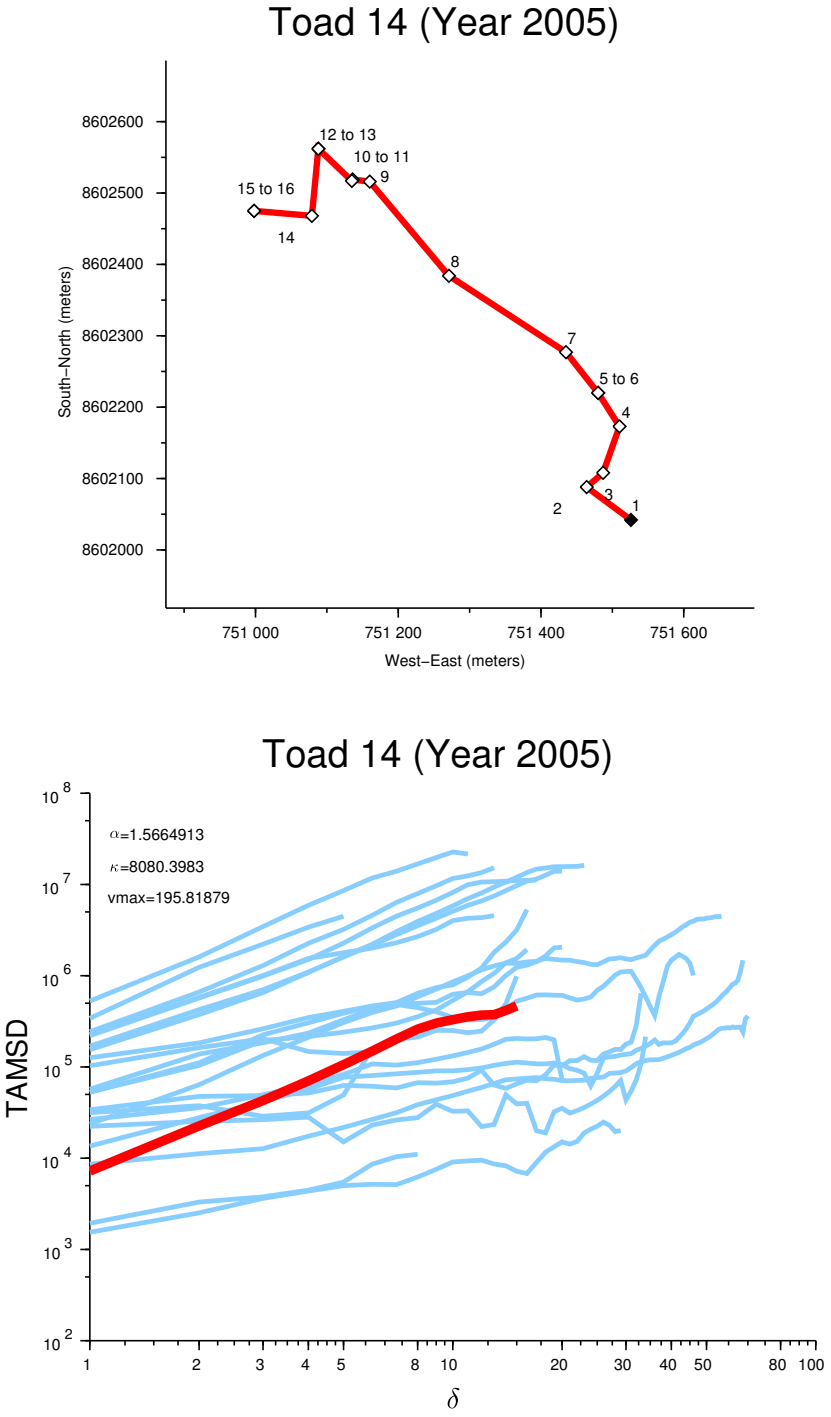

Trajectory and TAMSD of Toad number 14, radio tracked during wet season 2005.
Red line : function $\delta \mapsto \ln(TAMSD(\delta))$.
Light-blue lines : TAMSD of the other radio tracked toads from 2005.
Units : δ (days), $TAMSD(\delta)$ ($m^1 4/day$).

FIGURE A.28 – Toad 14

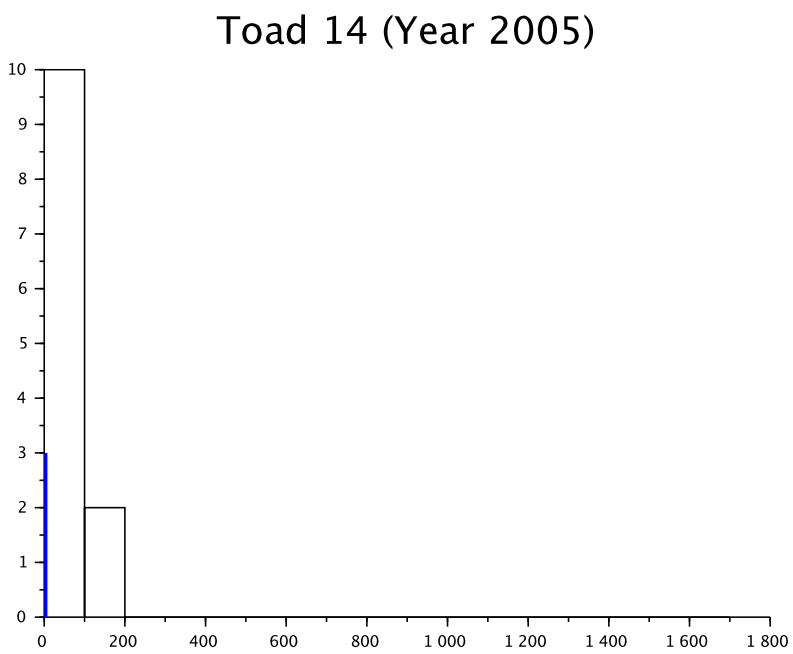

Histogram of the daily displacement of Toad 14. x-axis : velocity (m/day), y-axis : number of data in the class.

FIGURE A.29 – Toad 15

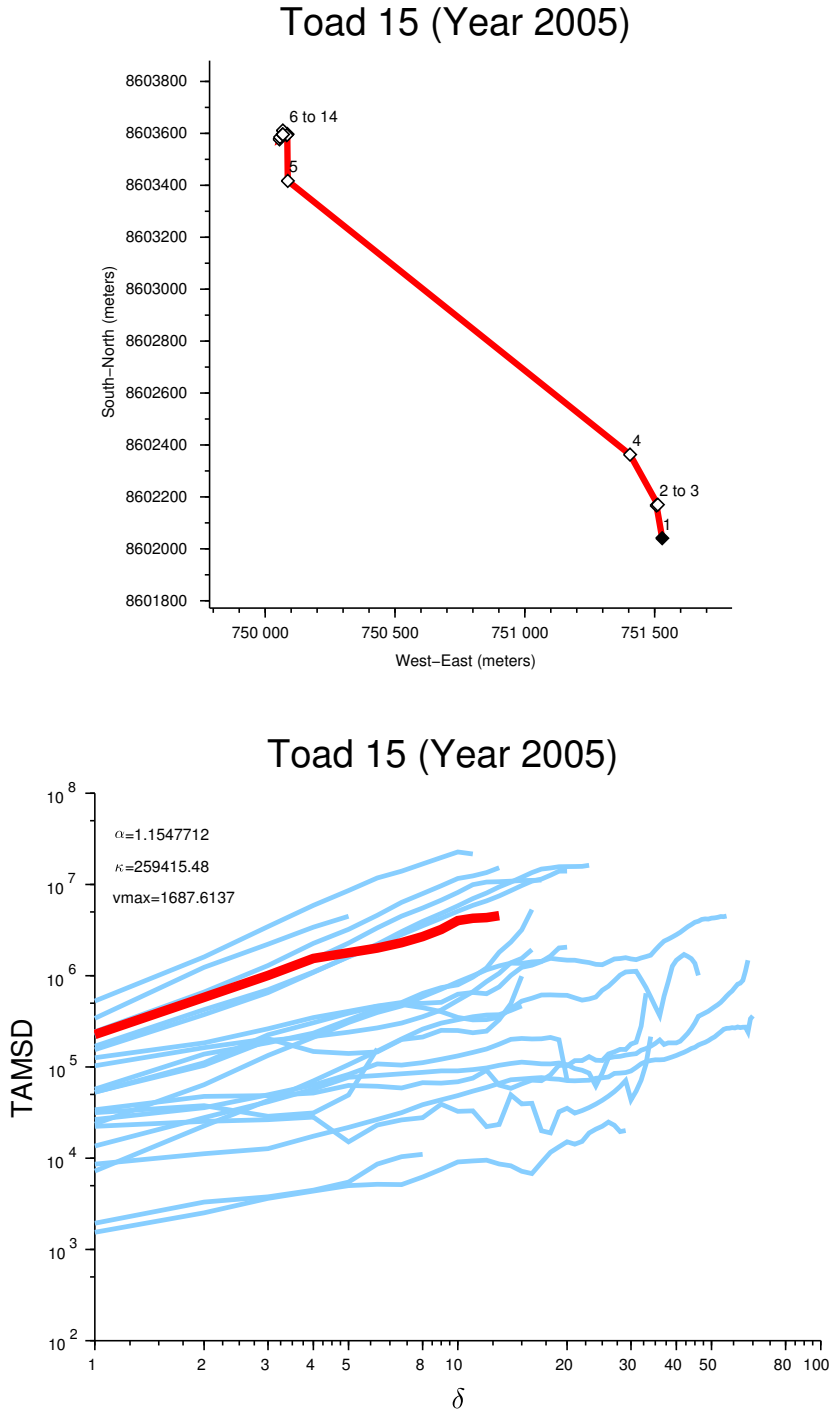

Trajectory and TAMSD of Toad number 15, radio tracked during wet season 2005.
Red line : function $\delta \mapsto \ln(TAMSD(\delta))$.
Light-blue lines : TAMSD of the other radio tracked toads from 2005.
Units : δ (days), $TAMSD(\delta)$ (m^15/day).

FIGURE A.30 – Toad 15

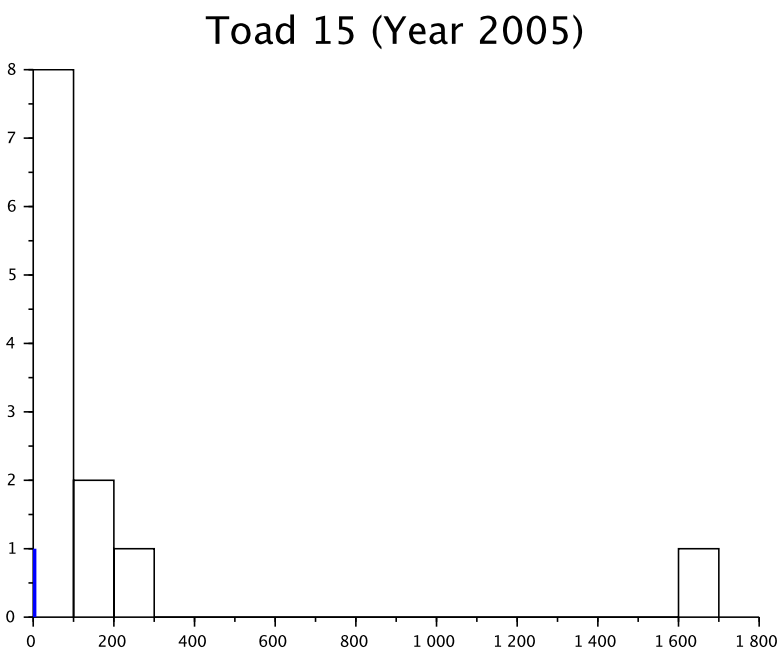

Histogram of the daily displacement of Toad 15. x-axis : velocity (m/day), y-axis : number of data in the class.

FIGURE A.31 – Toad 16

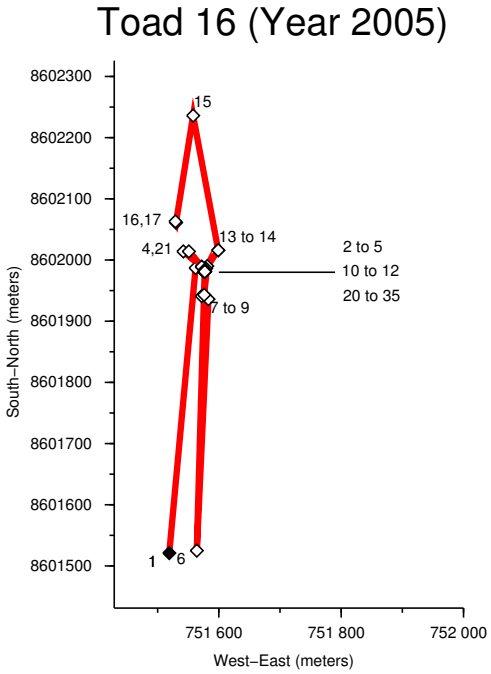

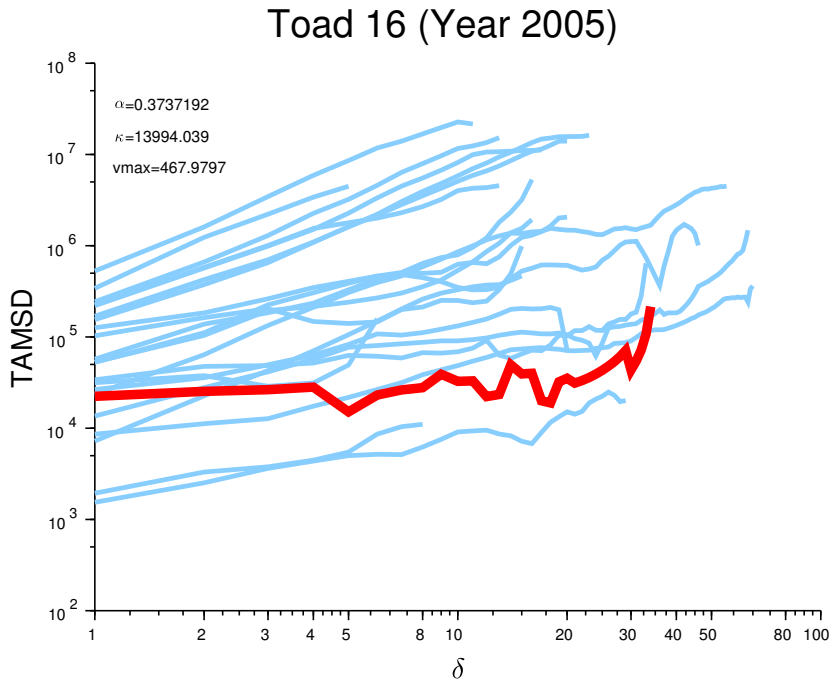

Trajectory and TAMSD of Toad number 16, radio tracked during wet season 2005.
Red line : function $\delta \mapsto \ln(TAMSD(\delta))$.
Light-blue lines : TAMSD of the other radio tracked toads from 2005.
Units : δ (days), $TAMSD(\delta)$ (m^16/day).

FIGURE A.32 – Toad 16

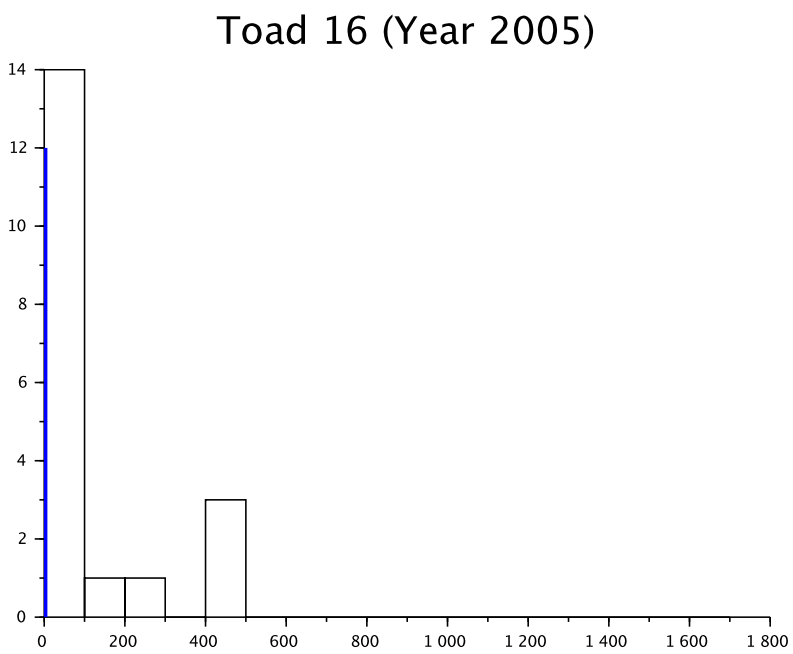

Histogram of the daily displacement of Toad 16. x-axis : velocity (m/day), y-axis : number of data in the class.

FIGURE A.33 – Toad 17

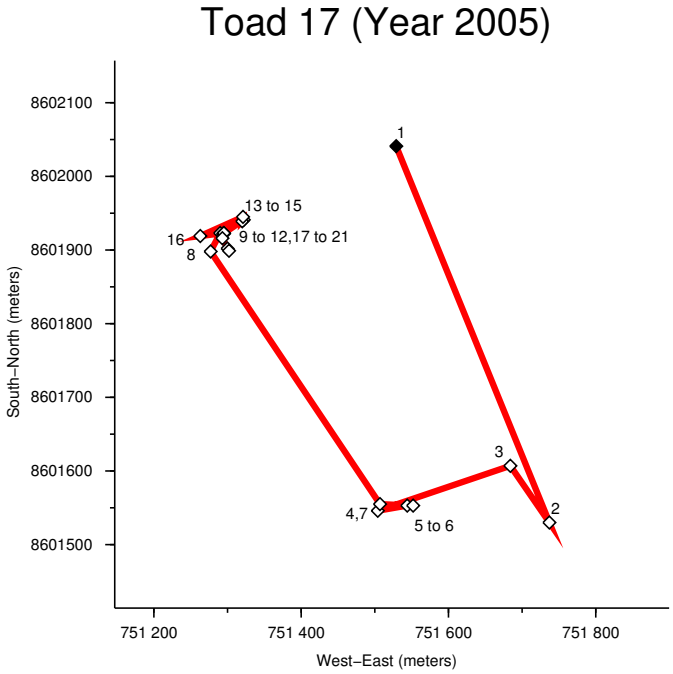

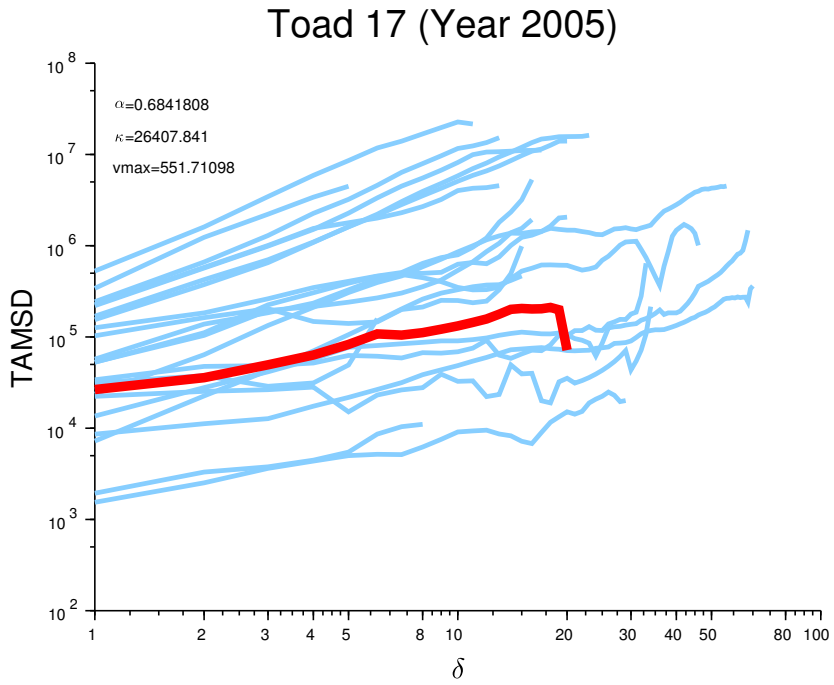

Trajectory and TAMSD of Toad number 17, radio tracked during wet season 2005.
Red line : function $\delta \mapsto \ln(TAMSD(\delta))$.
Light-blue lines : TAMSD of the other radio tracked toads from 2005.
Units : δ (days), $TAMSD(\delta)$ (m^17/day).

FIGURE A.34 – Toad 17

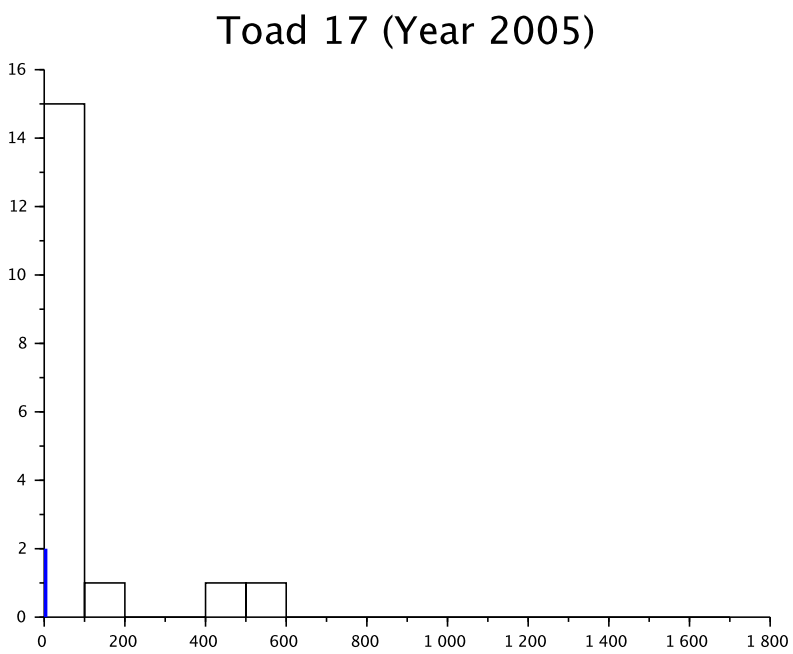

Histogram of the daily displacement of Toad 17. x-axis : velocity (m/day), y-axis : number of data in the class.

FIGURE A.35 – Toad 18

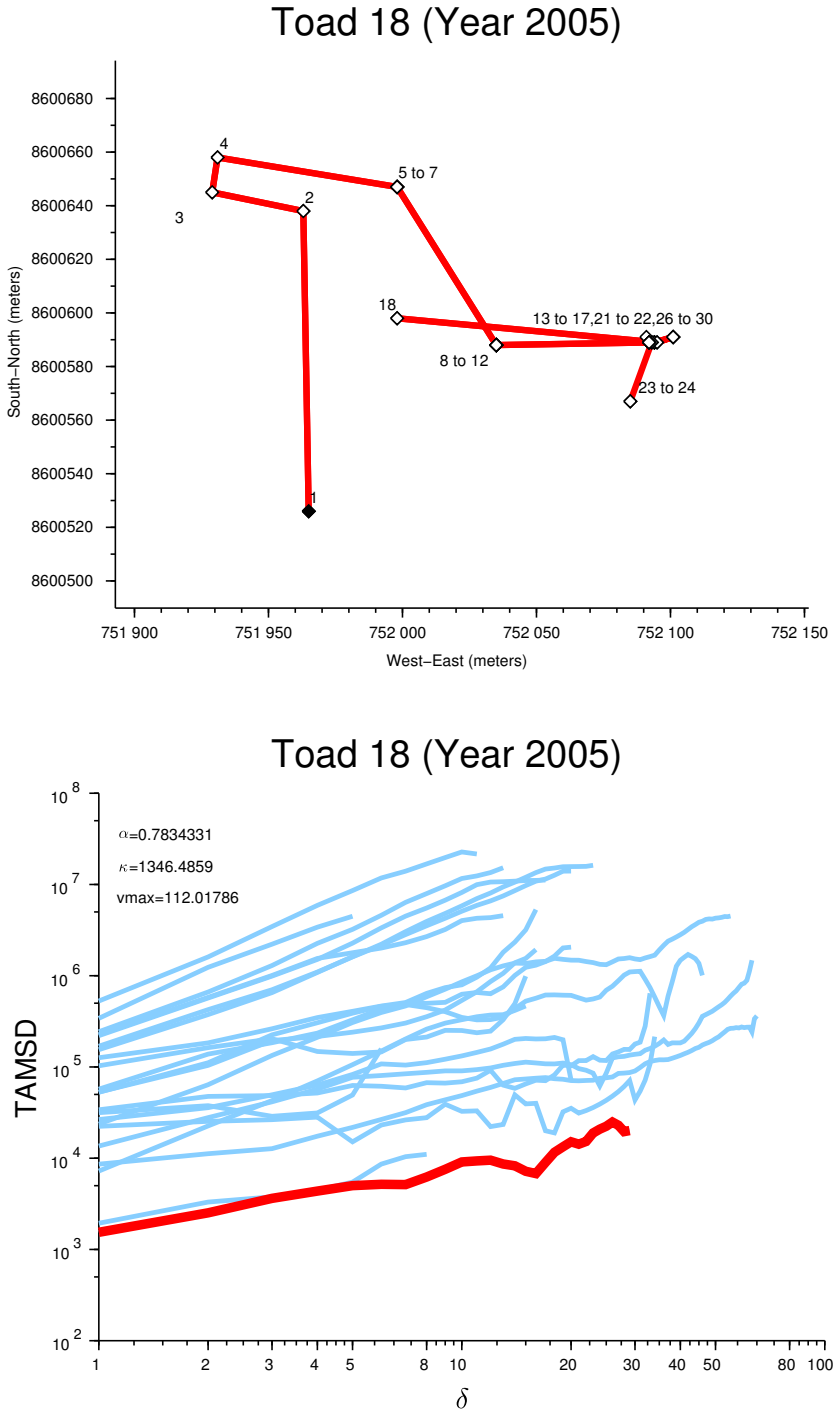

Trajectory and TAMSD of Toad number 18, radio tracked during wet season 2005.
Red line : function $\delta \mapsto \ln(TAMSD(\delta))$.
Light-blue lines : TAMSD of the other radio tracked toads from 2005.
Units : δ (days), $TAMSD(\delta)$ ($m^1 8/day$).

FIGURE A.36 – Toad 18

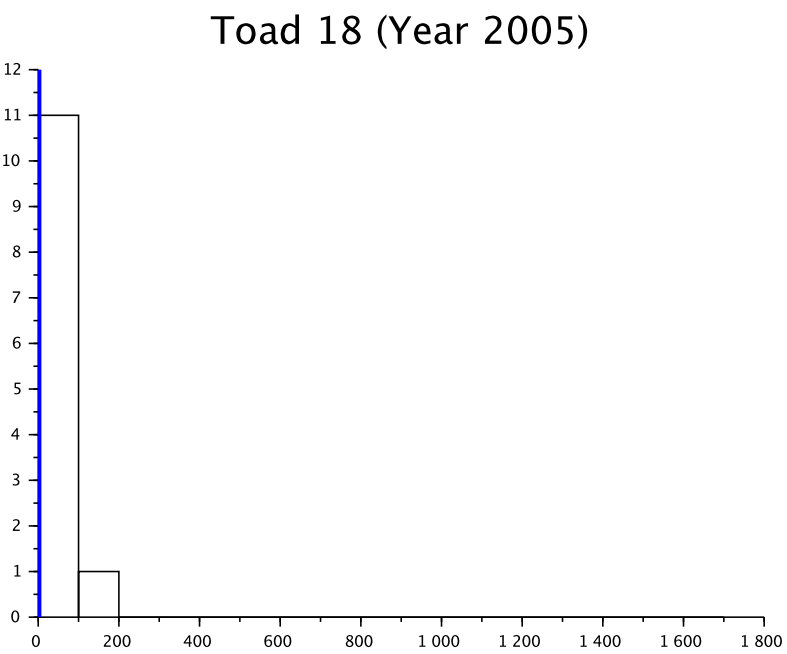

Histogram of the daily displacement of Toad 18. x-axis : velocity (m/day), y-axis : number of data in the class.

FIGURE A.37 – Toad 19

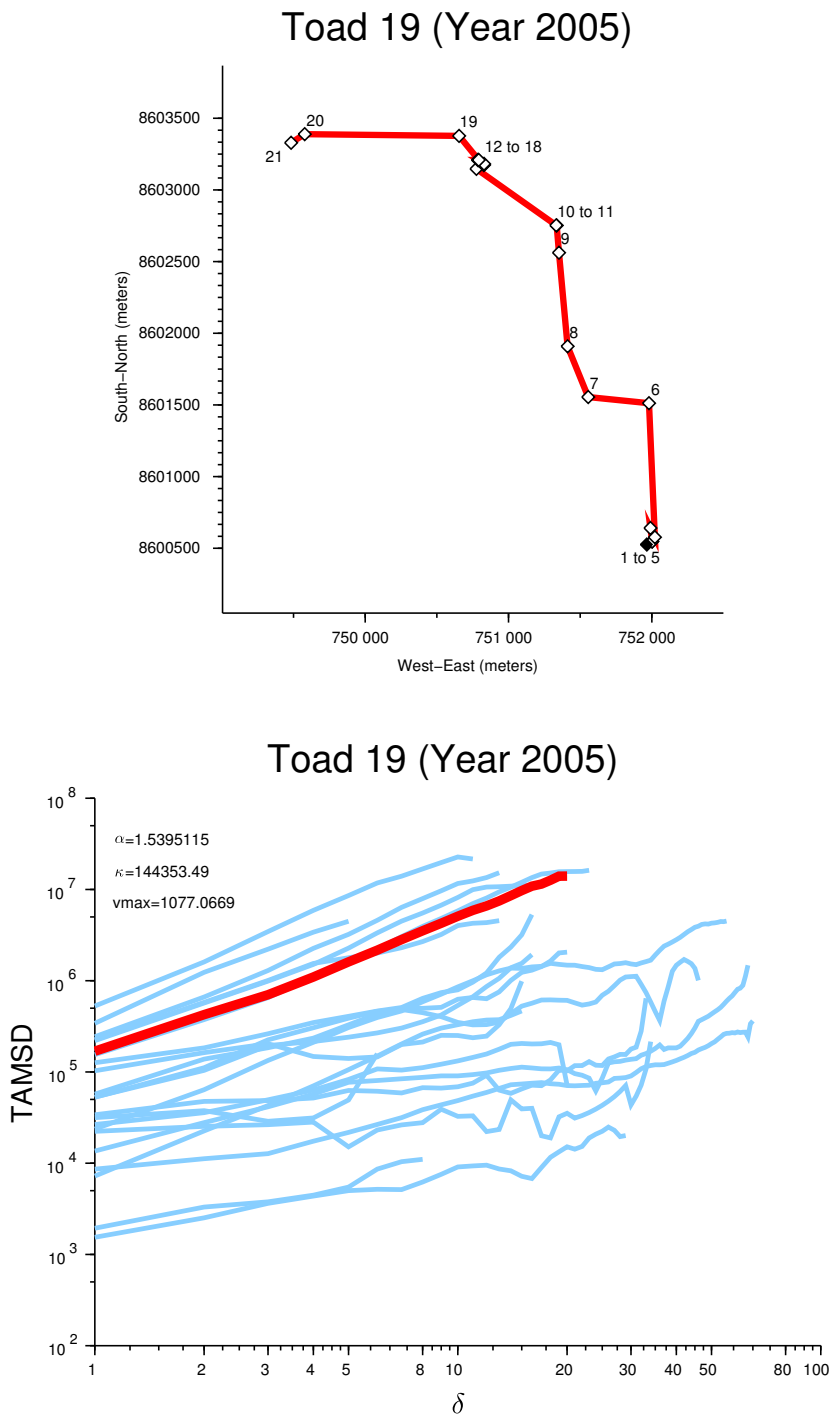

Trajectory and TAMSD of Toad number 19, radio tracked during wet season 2005.
Red line : function $\delta \mapsto \ln(TAMSD(\delta))$.
Light-blue lines : TAMSD of the other radio tracked toads from 2005.
Units : δ (days), $TAMSD(\delta)$ (m^19/day).

FIGURE A.38 – Toad 19

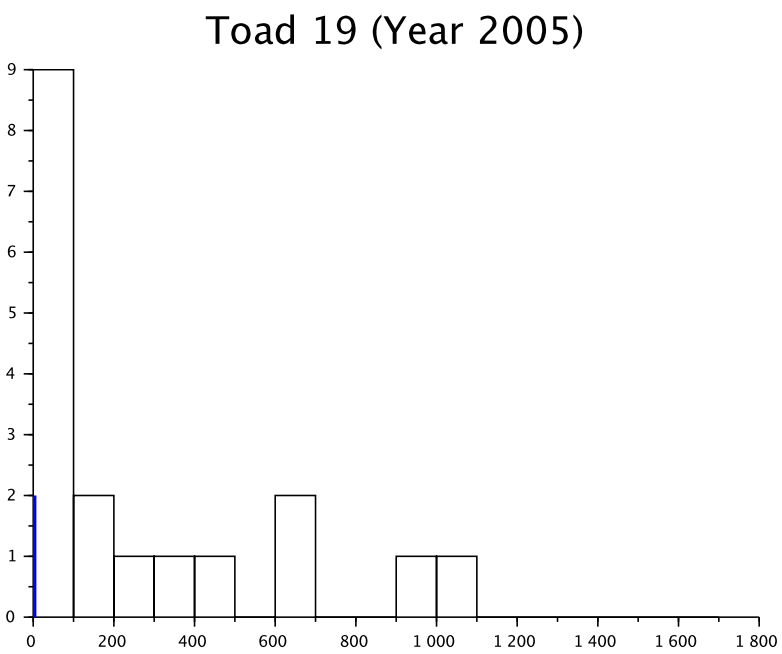

Histogram of the daily displacement of Toad 19. x-axis : velocity (m/day), y-axis : number of data in the class.

FIGURE A.39 – Toad 20

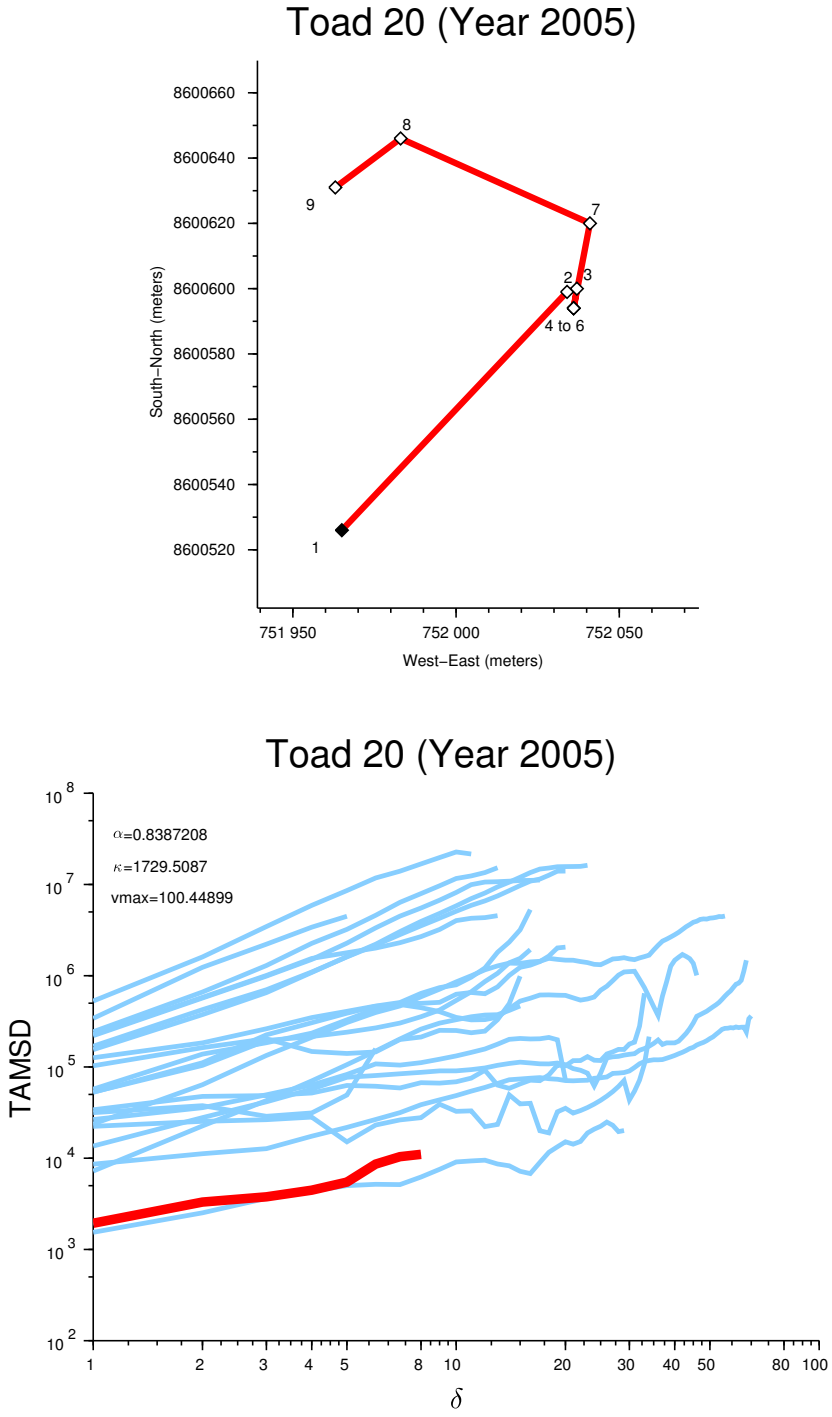

Trajectory and TAMSD of Toad number 20, radio tracked during wet season 2005.
Red line : function $\delta \mapsto \ln(TAMSD(\delta))$.
Light-blue lines : TAMSD of the other radio tracked toads from 2005.
Units : δ (days), $TAMSD(\delta)$ (m^20/day).

Figure A.40 – Toad 20

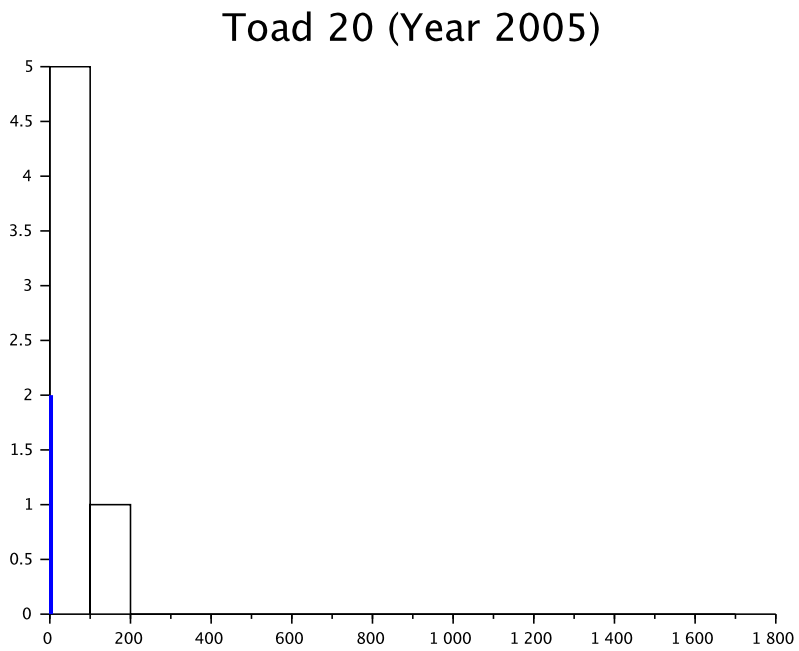

Histogram of the daily displacement of Toad 20. x-axis : velocity (m/day), y-axis : number of data in the class.

FIGURE A.41 – Toad 21

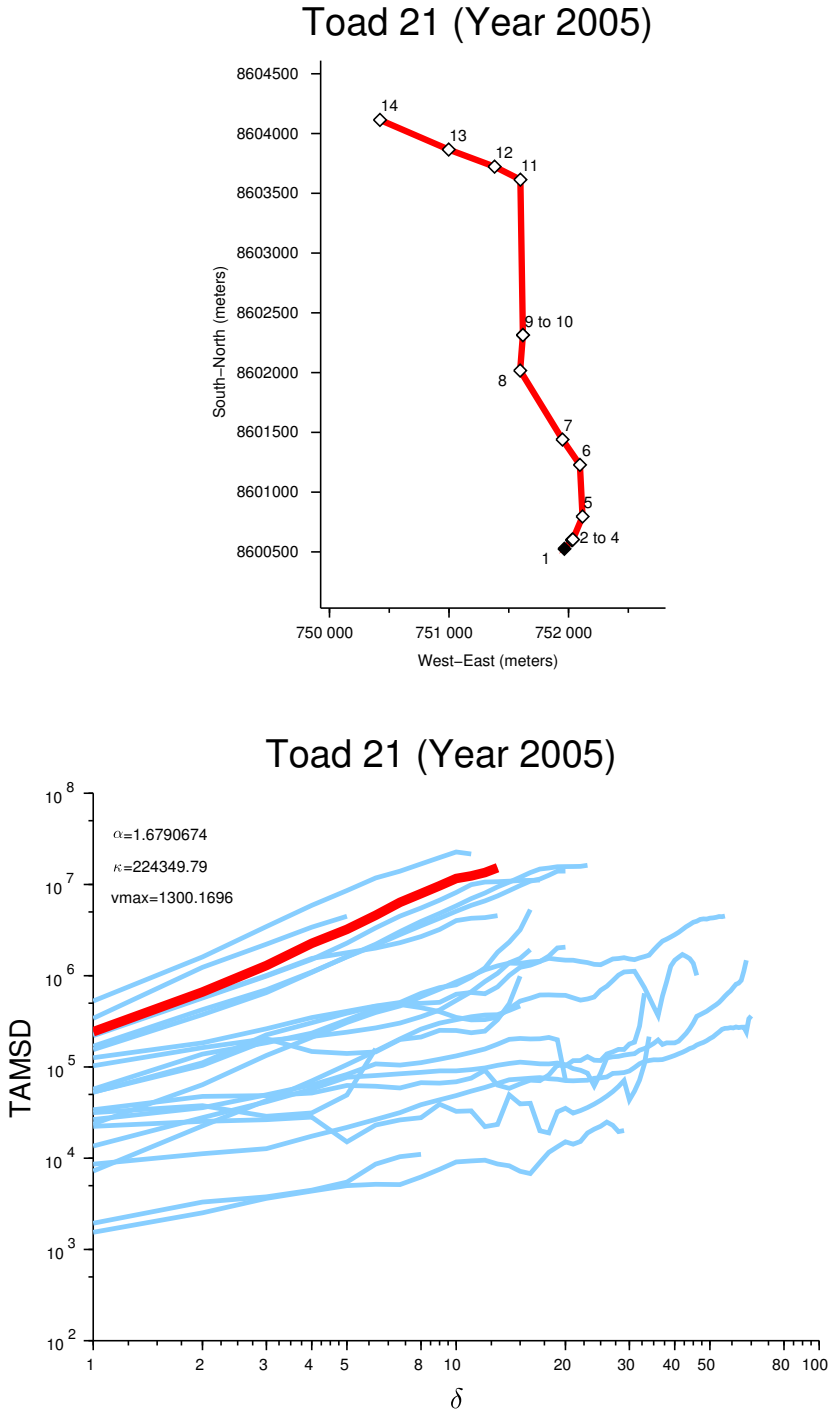

Trajectory and TAMSD of Toad number 21, radio tracked during wet season 2005.
Red line : function $\delta \mapsto \ln(TAMSD(\delta))$.
Light-blue lines : TAMSD of the other radio tracked toads from 2005.
Units : δ (days), $TAMSD(\delta)$ ($m^2 1/day$).

Figure A.42 – Toad 21

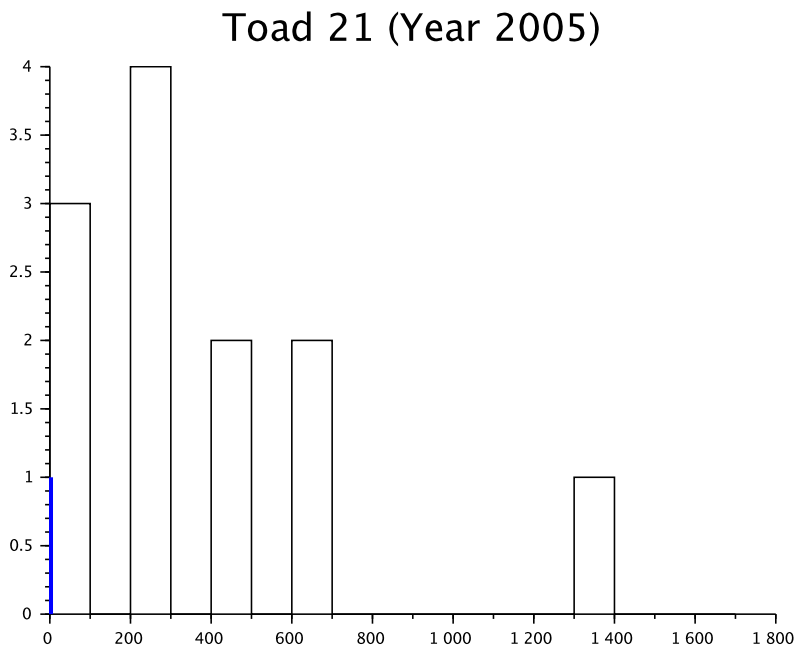

Histogram of the daily displacement of Toad 21. x-axis : velocity (m/day), y-axis : number of data in the class.

FIGURE A.43 – Toad 49

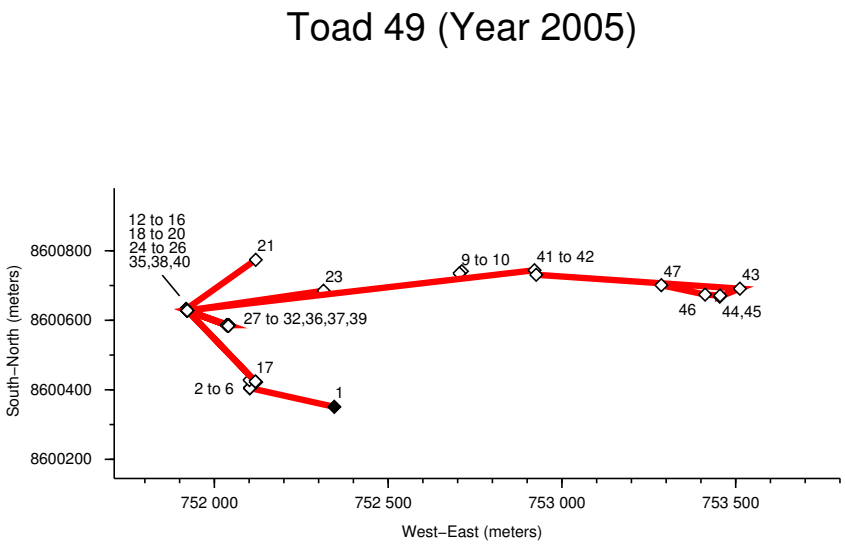

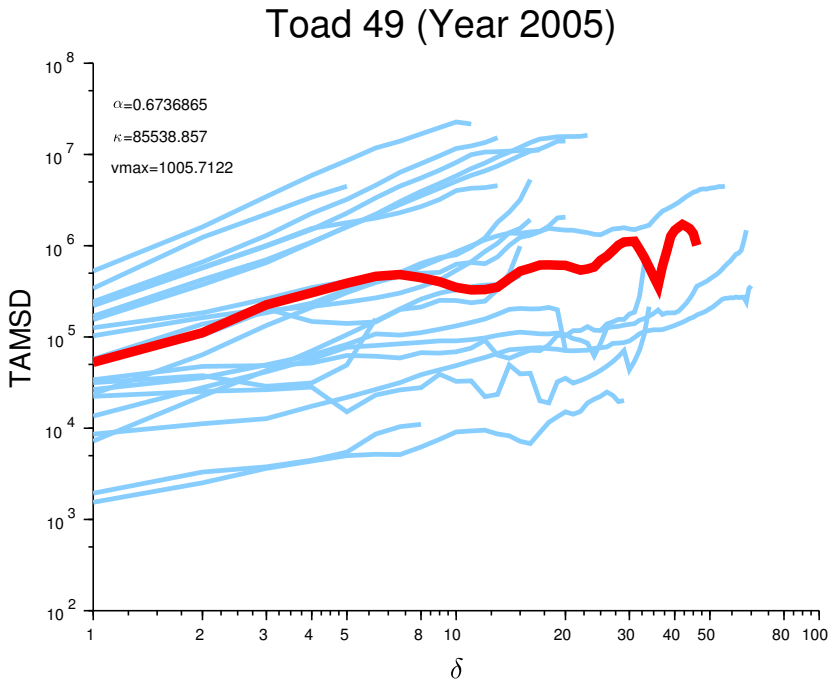

Trajectory and TAMSD of Toad number 49, radio tracked during wet season 2005.
Red line : function $\delta \mapsto \ln(TAMSD(\delta))$.
Light-blue lines : TAMSD of the other radio tracked toads from 2005.
Units : δ (days), $TAMSD(\delta)$ ($m^4 9/day$).

Figure A.44 – Toad 49

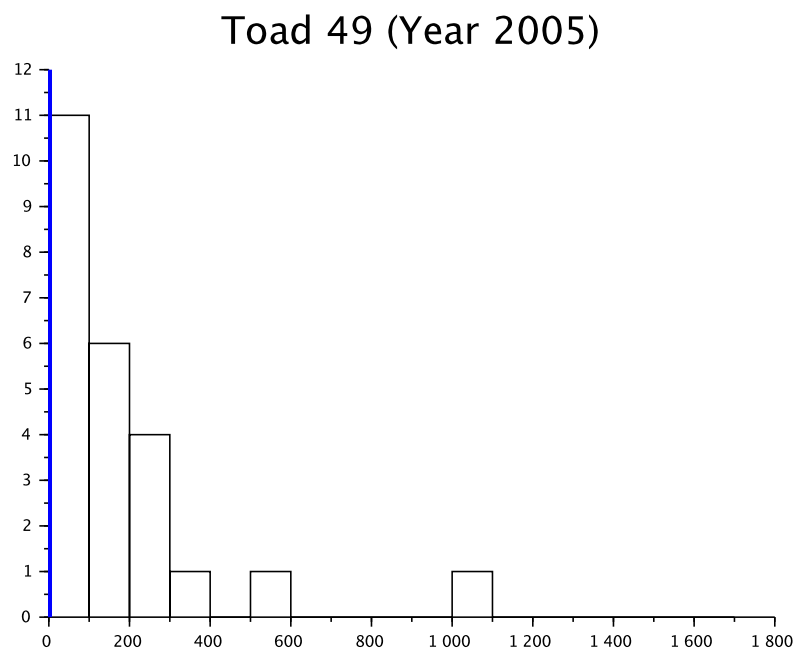

Histogram of the daily displacement of Toad 49. x-axis : velocity (m/day), y-axis : number of data in the class.

Bibliographie

[1] Robert A. Adams and John J. F. Fournier. *Sobolev space*. Pure and applied mathematics edition, 2003.

[2] Ross A. Alford, Gregory P. Brown, Lin Schwarzkopf, Benjamin L. Phillips, and Richard Shine. Comparisons through time and space suggest rapid evolution of dispersal behaviour in an invasive species. *Wildlife Research*, 36(1) :23, 2009.

[3] Ross A. Alford, Martin P. Cohen, Michael R. Crossland, M. N. Hearnden, and Lin Schwarzkopz. Population biology of Bufo marinus in northern Australia. In *Wetland research in the wet-dry tropics of Australia : workshop, Jabiru, NT, 22-24*, number 101 in Supervising Scientists Report, pages 173–181. C.M. Finlayson, Office of the supervising Scientist, Canberra., March 1995.

[4] Alexei Andreanov and Denis S. Grebenkov. Time-averaged MSD of Brownian motion. *Journal of Statistical Mechanics : Theory and Experiment*, 2012(07) :P07001, 2012.

[5] D. G Aronson and H. F Weinberger. Multidimensional nonlinear diffusion arising in population genetics. *Advances in Mathematics*, 30(1) :33–76, October 1978.

[6] Donald G. Aronson and Hans F. Weinberger. Nonlinear diffusion in population genetics, combustion, and nerve pulse propagation. In Jerome A. Goldstein, editor, *Partial Differential Equations and Related Topics*, volume 446, pages 5–49. Springer Berlin Heidelberg, Berlin, Heidelberg, 1975. DOI : 10.1007/BFb0070595.

[7] Guy Barles. *Solutions de viscosité des équations de Hamilton-Jacobi*. Number 17 in Mathématiques & applications. Springer-Verlag, Paris ; New York, 1994.

[8] Guy Barles, Lawrence C. Evans, and Panagiotis E. Souganidis. Wavefront propagation for reaction-diffusion systems of PDE. *Duke Mathematical Journal*, 61(3) :835–858, December 1990.

[9] Guy Barles and Benoît Perthame. Exit Time Problems in Optimal Control and Vanishing Viscosity Method. *SIAM Journal on Control and Optimization*, 26(5) :1133–1148, September 1988.

[10] Peter Bayliss. *The Ecology of post metamorphic Bufo marinus in Central Amazonian savanna, Brazil /*. PhD thesis, University of Queensland, 1995.

[11] M A Beaumont. Approximate bayesian computation in evolution and ecology. *Annual Review of Ecology, Evolution and Systematics*, 41 :379–406, 2010.

[12] Olivier Bénichou, Vincent Calvez, Nicolas Meunier, and Raphael Voituriez. Front acceleration by dynamic selection in Fisher population waves. *Physical Review E*, 86(4) :041908, October 2012.

[13] Nathanaël Berestycki, Clément Mouhot, and Gaël Raoul. Existence of self-accelerating fronts for a non-local reaction-diffusion equations. *arXiv :1512.00903 [math]*, December 2015. arXiv : 1512.00903.

[14] Patrick Billingsley. *Convergence of probability measures*. Wiley series in probability and statistics. Probability and statistics section. Wiley, New York, 2nd ed edition, 1999.

[15] Vladimir I. Bogachev. *Measure Theory*. Springer-Verlag Berlin Heidelberg, Berlin, Heidelberg, 2007. OCLC : 929013641.

[16] Emmanuel Boissard, Pierre Degond, and Sébastien Motsch. Trail formation based on directed pheromone deposition. *Journal of Mathematical Biology*, 66(6) :1267–1301, May 2013. arXiv : 1108.3495.

[17] Ludwig Boltzmann. Weitere Studien über das Wärmegleichgewicht unter Gasmolekülen. In S. G. Brush, editor, *Kinetische Theorie II : Irreversible Prozesse Einführung und Originaltexte*, pages 115–225. Vieweg+Teubner Verlag, Wiesbaden, 1970. DOI : 10.1007/978-3-322-84986-1_3.

[18] Emeric Bouin. A Hamilton-Jacobi approach for front propagation in kinetic equations. working paper or preprint, 2014.

[19] Emeric Bouin. *Propagation de fronts structurés en biologie : modélisation et analyse mathématique*. PhD thesis, ENS, Lyon, 2014.

[20] Emeric Bouin. A Hamilton-Jacobi approach for front propagation in kinetic equations. *Kinetic and Related Models*, 8(2) :255–280, March 2015.

[21] Emeric Bouin and Nils Caillerie. Reaction-transport travelling waves in velocity dimensions higher than one. *(work in progress)*, 2017.

[22] Emeric Bouin and Vincent Calvez. A kinetic eikonal equation. *Comptes Rendus Mathematique*, 350(5) :243–248, March 2012.

[23] Emeric Bouin and Vincent Calvez. Travelling waves for the cane toads equation with bounded traits. *Nonlinearity*, 27(9) :2233, 2014.

[24] Emeric Bouin, Vincent Calvez, Emmanuel Grenier, and Grégoire Nadin. Large deviations for velocity-jump processes and non-local Hamilton-Jacobi equations. *arXiv :1607.03676*, 2016.

[25] Emeric Bouin, Vincent Calvez, Nicolas Meunier, Sepideh Mirrahimi, Benoît Perthame, Gaël Raoul, and Raphaël Voituriez. Invasion fronts with variable motility : Phenotype selection, spatial sorting and wave acceleration. *Comptes Rendus Mathematique*, 350(15) :761 – 766, 2012.

[26] Emeric Bouin, Vincent Calvez, and Grégoire Nadin. Propagation in a Kinetic Reaction-Transport Equation : Travelling Waves And Accelerating Fronts. *Archive for Rational Mechanics and Analysis*, 217(2) :571–617, August 2015.

[27] Emeric Bouin and Christopher Henderson. Super-linear spreading in local bistable cane toads equations. *Nonlinearity*, 30(4) :1356, 2017.

[28] Emeric Bouin, Christopher Henderson, and Lenya Ryzhik. Super-linear spreading in local and non-local cane toads equations. *arXiv :1512.07793 [math]*, December 2015. arXiv : 1512.07793.

[29] Emeric Bouin and Sepideh Mirrahimi. A Hamilton–Jacobi approach for a model of population structured by space and trait. *Communications in Mathematical Sciences*, 13(6) :1431–1452, 2015.

[30] Maury Bramson. Convergence of solutions of the Kolmogorov equation to travelling waves. *Memoirs of the American Mathematical Society*, 44(285) :0–0, 1983.

[31] Paul C. Bressloff and Olivier Faugeras. On the Hamiltonian structure of large deviations in stochastic hybrid systems. *arXiv :1410.2152 [math, q-bio]*, October 2014. arXiv : 1410.2152.

[32] Paul C. Bressloff and Jay M. Newby. Path integrals and large deviations in stochastic hybrid systems. *Physical Review E*, 89(4), April 2014.

[33] Gregory P. Brown, Benjamin L. Phillips, and Richard Shine. The straight and narrow path : the evolution of straight-line dispersal at a cane toad invasion front. *Proceedings. Biological Sciences*, 281(1795), November 2014.

[34] Nils Caillerie. Large deviations of a velocity jump process with a Hamilton–Jacobi approach. *Comptes Rendus Mathematique*, February 2017.

[35] Vincent Calvez, Pierre Gabriel, and Álvaro Mateos González. Limiting Hamilton-Jacobi equation for the large scale asymptotics of a subdiffusion jump-renewal equation. *arXiv :1609.06933 [math]*, September 2016. arXiv : 1609.06933.

[36] Nicolas Champagnat, Régis Ferrière, and Sylvie Méléard. Unifying evolutionary dynamics : From individual stochastic processes to macroscopic models. *Theoretical Population Biology*, 69(3) :297–321, May 2006.

[37] Nicolas Champagnat, Régis Ferrière, and Sylvie Méléard. From Individual Stochastic Processes to Macroscopic Models in Adaptive Evolution. *Stochastic Models*, 24(sup1) :2–44, November 2008.

[38] Nicolas Champagnat and Sylvie Méléard. Invasion and adaptive evolution for individual-based spatially structured populations. *Journal of Mathematical Biology*, 55(2) :147–188, July 2007.

[39] Young-Pil Choi, Seung-Yeal Ha, and Zhuchun Li. Emergent dynamics of the Cucker-Smale flocking model and its variants, 2016.

[40] Sarah Cooper. *Animal Life : In The Sea and On The Land*. New York : Harper & Brothers (from http ://etc.usf.edu/clipart/), 1887.

[41] Jerome Coville. Singular measure as principal eigenfunction of some nonlocal operators. *arXiv :1302.0949 [math]*, February 2013. arXiv : 1302.0949.

[42] Michael G. Crandall, Lawrence C. Evans, and Pierre-Louis Lions. Some properties of viscosity solutions of Hamilton-Jacobi equations. *Transactions of the American Mathematical Society*, 282(2) :487–502, 1984.

[43] Michael G. Crandall, Hitoshi Ishii, and Pierre-Louis Lions. User's guide to viscosity solutions of second order partial differential equations. *Bulletin of the American Mathematical Society*, 27(1) :1–68, November 1992.

[44] Michael G. Crandall and Pierre-Louis Lions. Viscosity solutions of Hamilton-Jacobi equations. *Transactions of the American Mathematical Society*, 277(1) :1–42, 1983.

[45] Katalin Csilléry, Michael G. B. Blum, Oscar E. Gaggiotti, and Olivier François. Approximate Bayesian Computation (ABC) in practice. *Trends in Ecology and Evolution*, 25 :410–418, 2010.

[46] Carlota M. Cuesta, Sabine Hittmeir, and Christian Schmeiser. Traveling Waves of a Kinetic Transport Model for the KPP-Fisher Equation. *SIAM Journal on Mathematical Analysis*, 44(6) :4128–4146, January 2012.

[47] Les C. Cwynar and Glen M. MacDonald. Geographical Variation of Lodgepole Pine in Relation to Population History. *The American Naturalist*, 129(3) :463–469, 1987.

[48] Charles Darwin. *The Origin of Species*. John Murray, London, 1859.

[49] Arnaud Debussche, Sylvain de Moor, and Julien Vovelle. Diffusion limit for the radiative transfer equation perturbed by a Wiener process. *Kinetic and Related Models*, 8(3) :467–492, 2015.

[50] Arnaud Debussche, Sylvain de Moor, and Julien Vovelle. Diffusion limit for the radiative transfer equation perturbed by a Markovian process. *Asymptotic Analysis*, 98(1-2) :31–58, May 2016.

[51] Arnaud Debussche and Julien Vovelle. Diffusion limit for a stochastic kinetic problem. *Communications on Pure and Applied Analysis*, 11(6) :2305–2326, April 2011.

[52] Pierre Degond, Amic Frouvelle, and Jian-Guo Liu. Macroscopic Limits and Phase Transition in a System of Self-propelled Particles. *Journal of Nonlinear Science*, 23(3) :427–456, June 2013.

[53] Pierre Degond, Thierry Goudon, and Frédéric Popaud. Diffusion limit for nonhomogeneous and non-micro reversible processes. *Indiana University Mathematics Journal*, 49(3) :1175–1198, 2000.

[54] Odo Diekmann, Pierre-Emmanuel Jabin, Stéphane Mischler, and Benoît Perthame. The dynamics of adaptation : An illuminating example and a Hamilton–Jacobi approach. *Theoretical Population Biology*, 67(4) :257–271, June 2005.

[55] A Estoup, M A Beaumont, F Sennedot, C Moritz, and J M Cornuet. Genetic analysis of complex demographic scenarios : spatially expanding populations of the cane toad, ıt \uppercaseBufo marinus. *Evolution*, 58 :2021–2036, 2004.

[56] Stewart N. Ethier and Thomas G. Kurtz. *Markov processes : characterization and convergence*. Wiley series in probability and statistics. Wiley Interscience, Hoboken, 2005. OCLC : ocm62724166.

[57] Lawrence C. Evans. The perturbed test function method for viscosity solutions of nonlinear PDE. *Proceedings of the Royal Society of Edinburgh Section A : Mathematics*, 111(3-4) :359–375, January 1989.

[58] Lawrence C. Evans and Panagiotis E. Souganidis. *A PDE Approach to Geometric Optics for Certain Semilinear Parabolic Equations*. Lefschetz Center for Dynamical Systems. Division of Appl. Math., Brown Univ., 1987.

[59] Alessandra Faggionato, Davide Gabrielli, and Marco Ribezzi Crivellari. Averaging and Large Deviation Principles for Fully-Coupled Piecewise Deterministic Markov Processes and Applications to Molecular Motors. *Markov Processes Relat. Fields*, 16(3) :497–548, 2010.

[60] Paul C. Fife and John B. McLeod. The approach of solutions of nonlinear diffusion equations to travelling front solutions. *Archive for Rational Mechanics and Analysis*, 65(4), 1977.

[61] Ronald A. Fisher. The Wave of Advance of Advantageous Genes. *Annals of Eugenics*, 7(4) :355–369, 1937.

[62] Wendell H. Fleming and Panagiotis E. Souganidis. PDE-viscosity solution approach to some problems of large deviations. *Annali della Scuola Normale Superiore di Pisa - Classe di Scienze*, 13(2) :171–192, 1986.

[63] Anders Forsman, Juha Merilä, and Torbjörn Ebenhard. Phenotypic evolution of dispersal-enhancing traits in insular voles. *Proceedings of the Royal Society B : Biological Sciences*, 278(1703) :225–232, January 2011.

[64] Jean-Pierre Fouque, Josselin Garnier, George C. Papanicolaou, and Knut Solna, editors. *Wave propagation and time reversal in randomly layered media*. Number 56 in Stochastic modelling and applied probability. Springer, New York, NY, 2007. OCLC : 728118192.

[65] Mark Freidlin. *Functional Integration and Partial Differential Equations. (AM-109)*. Princeton University Press, 1985.

[66] Mark I. Freidlin. Geometric Optics Approach to Reaction-Diffusion Equations. *SIAM Journal on Applied Mathematics*, 46(2) :222–232, April 1986.

[67] Mark I. Freidlin and Jürgen Gärtner. On the propagation of concentration waves in periodic and random media. *Sov. Math. Dokl.*, 20 :1282–1286, 1979.

[68] Mark I. Freidlin and Alexander D. Wentzell. *Random Perturbations of Dynamical Systems. Second Edition.* Number 260 in Grundlehren der Mathematischen Wissenschaften. Springer-Verlag, New York, 1998.

[69] Denis S. Grebenkov. Probability distribution of the time-averaged mean-square displacement of a Gaussian process. *Phys. Rev. E*, 84(3) :031124, September 2011.

[70] Denis S. Grebenkov. Time-averaged quadratic functionals of a Gaussian process. *Phys. Rev. E*, 83(6) :061117, June 2011.

[71] Karl P. Hadeler. Reaction transport equations in biological modeling. *Mathematical and Computer Modelling*, 31(4-5) :75–81, February 2000.

[72] François Hamel, James Nolen, Jean-Michel Roquejoffre, and Lenya Ryzhik. A short proof of the logarithmic Bramson correction in Fisher-KPP equations. *Networks and Heterogeneous Media*, 8(1) :275–289, April 2013.

[73] Mark N. Hearnden. *The reproductive and larval ecology of Bufo marinus (Anura : Bufonidae)*. PhD thesis, James Cook University of North Queensland, 1991.

[74] Raymond B. Huey, George W. Gilchrist, Margen L. Carlson, David Berrigan, and Luis Serra. Rapid Evolution of a Geographic Cline in Size in an Introduced Fly. *Science*, 287(5451) :308–309, 2000.

[75] Rafail Z. Khas'minskii. A Limit Theorem for the Solutions of Differential Equations with Random Right-Hand Sides. *Theory of Probability & Its Applications*, 11(3) :390–406, January 1966.

[76] Rafail Z. Khas'minskii. On Stochastic Processes Defined by Differential Equations with a Small Parameter. *Theory of Probability & Its Applications*, 11(2) :211–228, January 1966.

[77] Yuri Kifer. *Large deviations and adiabatic transitions for dynamical systems and Markov processes in fully coupled averaging*. Number no. 944 in Memoirs of the American Mathematical Society. American Mathematical Society, Providence, R.I, 2009. OCLC : ocn321047153.

[78] Andreï N. Kolmogorov, Ivan G. Petrovsky, and Nikolaï S. Piskunov. Etude de l'équation de la diffusion avec croissance de la quantité de matière et son application à un problème biologique. *Moskow Univ. Math. Bull.*, 1 :1–25, 1937.

[79] Harold J. Kushner. *Approximation and weak convergence methods for random processes, with applications to stochastic systems theory*. Number 6 in The MIT Press series in signal processing, optimization, and control. MIT Press, Cambridge, Mass, 1984.

[80] Margarita Lampo and Giulio A. de Leo. The Invasion Ecology of the Toad Bufo marinus : From South America to Australia. *Ecological Applications*, 8(2) :388–396, 1998.

[81] Margarita Lampo and Victoria Medialdea. Energy Allocation Patterns in Bufo marinus from Two Habitats in Venezuela. *Journal of Tropical Ecology*, 12(3) :321–331, 1996.

[82] Guillaume Léotard, Gabriel Debout, Ambroise Dalecky, Sylvain Guillot, Laurence Gaume, Doyle McKey, and Finn Kjellberg. Range Expansion Drives Dispersal Evolution In An Equatorial Three-Species Symbiosis. *PLoS ONE*, 4(7), July 2009.

[83] Tom Lindström, Gregory P. Brown, Scott A. Sisson, Benjamin L. Phillips, and Richard Shine. Rapid shifts in dispersal behavior on an expanding range edge. *Proceedings of the National Academy of Sciences*, 110(33) :13452–13456, August 2013.

[84] John Llewelyn, Benjamin L. Phillips, Ross A. Alford, Lin Schwarzkopf, and Richard Shine. Locomotor performance in an invasive species : cane toads from the invasion front have greater endurance, but not speed, compared to conspecifics from a long-colonised area. *Oecologia*, 162(2) :343–348, February 2010.

[85] Alexander Lorz, Sepideh Mirrahimi, and Benoît Perthame. Dirac Mass Dynamics in Multidimensional Nonlocal Parabolic Equations. *Communications in Partial Differential Equations*, 36(6) :1071–1098, January 2011.

[86] Jean-Michel Marin, Pierre Pudlo, Christian P Robert, and Robin J Ryder. Approximate Bayesian computational methods. *Statistics and Computing*, 22 :1167–1180, 2012.

[87] P Marjoram, V Plagnol, and S Tavaré. Markov chain \uppercaseMonte \uppercaseCarlo without likelihoods. *PNAS*, 100 :15324–15328, 2003.

[88] Paul A. Orlando, Robert A. Gatenby, and Joel S. Brown. Tumor Evolution in Space : The Effects of Competition Colonization Tradeoffs on Tumor Invasion Dynamics. *Frontiers in Oncology*, 3, 2013.

[89] Leonard S. Ornstein and George E. Uhlenbeck. On the Theory of the Brownian Motion. *Physical Review*, 36(5) :823–841, September 1930.

[90] George C. Papanicolaou, Daniel Stroock, and Sathamangalam R.S. Varadhan. Martingale approach to some limit theorems. *Papers from the Duke Turbulence Conference, Paper No. 6, Duke Univ. Duke Univ. Math. Ser., Vol. III.*, 1976.

[91] T. Alex Perkins, Benjamin L. Phillips, Marissa L. Baskett, and Alan Hastings. Evolution of dispersal and life history interact to drive accelerating spread of an invasive species. *Ecology Letters*, 16(8) :1079–1087, August 2013.

[92] Benoît Perthame and Panagiotis E. Souganidis. Asymmetric potentials and motor effect : a homogenization approach. *Annales de l'Institut Henri Poincare (C) Non Linear Analysis*, 26(6) :2055–2071, November 2009.

[93] Benjamin L. Phillips, Gregory P. Brown, Jonathan K. Webb, and Richard Shine. Invasion and the evolution of speed in toads. *Nature*, 439(7078) :803–803, February 2006.

[94] Céline Prévost, Laurent Desvillettes, and Anton Arnold. Existence of nontrivial steady states for populations structured with respect to space and a continuous trait. *Communications on Pure and Applied Analysis*, 11(1) :83–96, September 2011.

[95] Hong Qian, Michael P. Sheetz, and Elliot L. Elson. Single particle tracking. Analysis of diffusion and flow in two-dimensional systems. *Biophysical Journal*, 60(4) :910–921, October 1991.

[96] Ophelie Ronce. How Does It Feel to Be Like a Rolling Stone ? Ten Questions About Dispersal Evolution. *Annual Review of Ecology, Evolution, and Systematics*, 38 :231–253, 2007.

[97] Luca Rossi. The Freidlin-Gartner formula for general reaction terms. *arXiv :1503.09010v3*, 2015.

[98] Jonathan Saragosti, Vincent Calvez, Nikolaos Bournaveas, Benoît Perthame, Axel Buguin, and Pascal Silberzan. Directional persistence of chemotactic bacteria in a traveling concentration wave. *Proceedings of the National Academy of Sciences of the United States of America*, 108(39) :16235–16240, September 2011.

[99] Hartmut R. Schwetlick. Travelling fronts for multidimensional nonlinear transport equations. *Annales de l'Institut Henri Poincare (C) Non Linear Analysis*, 17(4) :523–550, July 2000.

[100] Hartmut R. Schwetlick. Limit Sets for Multidimensional Nonlinear Transport Equations. *Journal of Differential Equations*, 179(1) :356–368, February 2002.

[101] Nanako Shigesada. Spatial distribution of dispersing animals. *Journal of Mathematical Biology*, 9(1) :85–96, 1980.

[102] Richard Shine, Gregory P. Brown, and Benjamin L. Phillips. An evolutionary process that assembles phenotypes through space rather than through time. *Proceedings of the National Academy of Sciences of the United States of America*, 108(14) :5708–5711, April 2011.

[103] Adam D. Simmons and Chris D. Thomas. Changes in dispersal during species' range expansions. *The American Naturalist*, 164(3) :378–395, September 2004.

[104] Samuel Soubeyrand, Florence Carpentier, François Guiton, and Etienne K. Klein. Approximate Bayesian computation with functional statistics. *Statistical Applications in Genetics and Molecular Biology*, 12 :17–37, 2013.

[105] Panagiotis E. Souganidis. Front propagation : Theory and applications. In *Viscosity Solutions and Applications*, pages 186–242. Springer Berlin Heidelberg, Berlin, Heidelberg, 1997. DOI : 10.1007/BFb0094298.

[106] Chris D. Thomas, E. J. Bodsworth, Robert J. Wilson, Adam D. Simmons, Zoe G. Davies, Martin Musche, and Larissa Conradt. Ecological and evolutionary processes at expanding range margins. *Nature*, 411(6837) :577–581, May 2001.

[107] Olga Turanova. On a model of a population with variable motility. *Mathematical Models and Methods in Applied Sciences*, 25(10) :1961–2014, September 2015.

[108] James W. Tutt. *British Moths*. George Routledge & Sons Ltd., London, 1896.

[109] Michael J. Tyler. *Australian frogs*. Viking O'Neil, Ringwood, 1989. OCLC : 488136435.

[110] Mark C. Urban, Ben L. Phillips, David K. Skelly, and Richard Shine. A toad more traveled : the heterogeneous invasion dynamics of cane toads in Australia. *The American Naturalist*, 171(3) :E134–148, March 2008.

[111] Cédric Villani. A Review of Mathematical Topics in Collisional Kinetic Theory. In *Handbook of Mathematical Fluid Dynamics*, volume 1, pages 71–74. Elsevier, 2002. DOI : 10.1016/S1874-5792(02)80004-0.

[112] Anatoly Vlasov. The vibrational properties of an electron gas. *Soviet Physics Uspekhi*, 10(6) :721, 1968.

Abstract

In this thesis, we study some biology inspired mathematical models. More precisely, we focus on kinetic partial differential equations. The fields of application of such equations are numerous but we focus here on propagation phenomena for invasive species, the *Escherichia coli*bacterium and the cane toad *Rhinella marina*, for example.

The first part of this this does not establish any mathematical result. We build several models for the dispersion of the cane toad in Australia. We confront those very models to multiple statistical data (birth rate, survival rate, dispersal behaviors) to test their validity. Those models are based on velocity-jump processes and kinetic equations.

In the second part, we study propagation phenomena on simpler kinetic models. We illustrate several methods to mathematically establish propagation speed in this models. This part leads us to establish convergence results of kinetic equations to Hamilton-Jacobi equations by the perturbed test function method. We also show how to use the Hamilton-Jacobi framework to establish spreading results et finally, we build travelling wave solutions for reaction-transport model.

In the last part, we establish a stochastic diffusion limit result for a kinetic equation with a random term. To do so, we adapt the perturbed test function method on the formulation of a stochastic PDE in term of infinitesimal generators.

The thesis also contains an annex which presents the data on toads' trajectories used in the first part.

Keywords: Kinetic equations, Hamilton-Jacobi equation, Front propagation, Modelling, Stochastic partial differential equations, Perturbed test function method.

Équations cinétiques stochastiques et déterministes dans le contexte des mathématiques appliquées à la biologie

Résumé : Cette thèse étudie des modèles mathématiques inspirés par la biologie. Plus précisément, nous nous concentrons sur des équations aux dérivées partielles cinétiques. Les champs d'application des équations cinétiques sont nombreux mais nous nous concentrons ici sur des phénomènes de propagation d'espèces invasives, notamment la bactérie *Escherichia coli* et le crapaud buffle *Rhinella marina*.
La première partie de la thèse ne présente pas de résultats mathématiques. Nous construisons plusieurs modélisations pour la dispersion à grande échelle du crapaud buffle en Australie. Nous confrontons ces mêmes modèles à des données statistiques multiples (taux de fécondité, taux de survie, comportements dispersifs) pour mesurer leur pertinence. Ces modèles font intervenir des processus à sauts de vitesses et des équations cinétiques.
Dans la seconde partie, nous étudions des phénomènes de propagation dans des modèles cinétiques plus simples. Nous illustrons plusieurs méthodes pour établir mathématiquement des formules de vitesse de propagation dans ces modèles. Cette partie nous amène à établir des résultats de convergence d'équations cinétiques vers des équations de Hamilton-Jacobi par la méthode de la fonction test perturbée. Nous montrons également comment le formalisme Hamilton-Jacobi permet de trouver des résultats de propagation et enfin, nous construisons des solutions en ondes progressives pour un modèle de transport-réaction.
Dans la dernière partie, nous établissons un résultat de limite de diffusion stochastique pour une équation cinétique aléatoire. Pour ce faire, nous adaptons la méthode de la fonction test perturbée sur la formulation d'une EDP stochastique en terme de générateurs infinitésimaux.
La thèse comporte également une annexe qui expose les données trajectorielles des crapauds dont nous nous servons en première partie.

Mots clés : Équations cinétiques, Équations de Hamilton-Jacobi, Propagation de fronts, Modélisation, Équations aux dérivées partielles stochastiques, Méthode de la fonction test perturbée.

Crédit image : Stacey Jessop *via* iStock by Getty Images.

ED 512 INFOMATHS Ecole doctorale

UNIVERSITÉ DE LYON